

The Influence of Neurotrophins on Traumatic Brain Injury, Fracture Healing and  
Bone Metabolism

*A thesis submitted in total fulfillment  
of the requirements for the degree of  
Doctor of Philosophy*

**Maddison Rosina Johnstone**  
**Bachelor of Biomedical Science (Honours), 2013 La Trobe University**

Department of Physiology, Anatomy and Microbiology  
School of Life Sciences  
College of Science, Health and Engineering

La Trobe University  
Victoria, Australia

December 2020



## **Statement of Authorship**

Except where reference is made in the text of the thesis, this thesis contains no material published elsewhere or extracted in whole or in part from a thesis accepted for the award of any other degree or diploma. No other person's work has been used without due acknowledgment in the main text of the thesis. This thesis has not been submitted for the award of any degree or diploma in any other tertiary institution.

All research from this thesis was approved by either the La Trobe or the Florey Institute of Neuroscience and Mental Health Animal Ethics Committees.

This work was supported by an Australian Government Research Training Program Scholarship and a La Trobe University Postgraduate Research Scholarship.

Maddison Rosina Johnstone

4<sup>th</sup> December 2020

### **Publications emanating from this thesis**

**Johnstone M. R.**, Brady R. D., Church J. E., Orr D., McDonald S. J., Grills B. L. The TrkB agonist, 7,8-dihydroxyflavone, impairs fracture healing in mice. *Journal of Musculoskeletal and Neuronal Interactions*. **Accepted for publication 9<sup>th</sup> November 2020.**

**Johnstone M. R.**, Brady R. D., Schuijers J. A., Church J. E., Orr D., Quinn J. M. W., McDonald S. J., Grills B. L., The selective TrkA agonist, gambogic amide, promotes osteoblastic differentiation and improves fracture healing in mice. *Journal of Musculoskeletal and Neuronal Interactions*. 2019 19(1) 94-103.

**Johnstone M. R.**, Sun M., Taylor C. J., Brady R. D., Grills B. L., Church J. E., Shultz S. R., and McDonald S. J., Gambogic amide, selective TrkA agonist, does not improve outcomes from traumatic brain injury in mice. *Brain Injury*. 2018 32(2) 257-268.

### **Conferences, Presentations and Awards**

**Johnstone M. R.**, Brady R. D., Church J. E., Orr D., McDonald S. J., Grills B. L. (February 2020). The TrkB agonist, 7,8-DHF, impairs fracture healing in mice. 9<sup>th</sup> Clare Valley Bone Conference, Clare Valley Country Club, Clare, South Australia.

**Johnstone M. R.**, Sun M., Grills B. L., Shultz S. R., McDonald S. J. (December 2016). The effect of a specific tropomyosin kinase receptor A (TrkA) agonist, gambogic amide, on traumatic brain injury. 7<sup>th</sup> Australian Neurotrauma Symposium: Hobart, Australia.

**Johnstone M. R.**, Brady R. D., Schuijers J. A., Quinn J. M. W., McDonald S. J., Grills B. L. (September 2016). The effects of TrkA agonist, gambogic amide, on osteoblasts and bone fracture healing. The American Society for Bone and Mineral Research (ASBMR): Atlanta, USA.

**Johnstone M. R.**, Brady R. D., Schuijers J. A., McDonald S. J., Grills B. L. (September 2016). The effects of TrkA agonist, gambogic amide, on bone fracture healing. Graduate Researchers Showcase: Bundoora, Australia.

**Johnstone M. R.**, Brady R. D., Schuijers J. A., McDonald S. J., Grills B. L. (November 2015). Effects of specific TrkA agonist, gambogic amide, on fracture healing in mice: a pilot study. Australian and New Zealand Bone and Mineral Society (ANZBMS): Hobart, Australia.

### **Conferences, Presentations and Awards (cont.)**

Awarded the Student Travel Grant (\$150) to attend the 2015 Australian and New Zealand Bone and Mineral Society (ANZBMS) Annual Scientific Meeting, Hobart, November 2015.

Attended the 6<sup>th</sup> Australian Neurotrauma Symposium: Adelaide, Australia (October 2015).

Attended the 2014 ANZBMS Annual Scientific Meeting, Queenstown, New Zealand, September 2014.

La Trobe University Postgraduate Research Scholarship (LTUPRS): (August 2014 – December 2017).

Golden Key International Honour Society Recipient – La Trobe University 2015.

## Acknowledgements

Foremost, I would like to express my sincerest gratitude to my two supervisors Brian Grills and Stuart McDonald, thank you for allowing me to be your PhD student. I am grateful for your ongoing encouragement and patience throughout these years and allowing me to put a pause on this thesis to begin medicine. You have always made time for me and opened many doors for new opportunities throughout the years. You both have taught me many skills and the meaning of hard work in research, so thank you.

An immense thank you to Karen Griggs, whom without your assistance throughout my experiments, ongoing reassurance, and love, this thesis may not have been finished. Thank you for always being there for me in both the easy and hard times these past years.

Besides my supervisors and Karen, I would like to thank the last member of my research committee Andrew Bendrups for his guidance and support, as well as the many staff of La Trobe University in Human Biosciences and LARFT who have helped me successfully complete my experiments.

I would also like to say thank you to the researchers from the Melbourne Brain Centre, Sandy and Mujun; Garvin Institute, Julian; and Van der Buuse Laboratory; Maarten and Emily, who granted me the opportunities to work and publish with them.

Thank you to all my fellow PhD students who have come and gone throughout the years and have passed onto me little gems of knowledge. These people include Kristina, Karlene, Rhys, Stuart, Yeukai, and Michael. I take with me some friendships that will last a lifetime.

Finally, to my family. My parents Trish and Ross, I am indebted to your undying support, praise, and encouragement in my endless pursuit of knowledge. I am proud to be your daughter. To my sisters, Carlin, Mallory and Tennille, I did it!

Por Santiago, te amo todo el mundo.

## Table of Contents

<b>Statement of Authorship.....</b>	<b>i</b>
<b>Publications emanating from this thesis .....</b>	<b>ii</b>
<b>Acknowledgements.....</b>	<b>iv</b>
<b>List of Tables .....</b>	<b>x</b>
<b>List of Figures .....</b>	<b>xi</b>
<b>List of Abbreviations .....</b>	<b>xii</b>
<b>Thesis Summary .....</b>	<b>xvi</b>
<b>Chapter 1. Literature review .....</b>	<b>1</b>
General introduction .....	1
1.1. Neurotrophins .....	1
1.2. Nerve growth factor (NGF).....	2
1.2.1. NGF expression.....	3
1.3. NGF receptor function and distribution.....	3
1.3.1. TrkA.....	3
1.3.2. p75NTR.....	4
1.4. Brain derived neurotropic factor (BDNF) .....	5
1.4.1. BDNF expression.....	6
1.5. BDNF receptor function and distribution.....	6
1.5.1. TrkB.....	6
1.5.2. p75NTR.....	6
1.6. Traumatic brain injury.....	7
1.6.1. Mechanisms of TBI.....	8
1.6.2. NGF and TBI.....	10
1.6.3. Therapies for TBI.....	11
1.6.4. Animal models of TBI .....	13
1.7. Fracture healing.....	15
1.7.1. Osseous cell types in fracture healing .....	15
1.7.2. Mechanisms of fracture healing .....	16
1.7.3. NGF and fracture healing .....	19
1.7.4. BDNF and fracture healing .....	21
1.7.5. Therapies for fracture healing.....	22
1.7.6. Animal models of fracture healing .....	24

1.8. Trk receptor ligands as possible therapeutic agents for TBI and fracture healing .....	26
1.8.1. GA as a therapeutic drug.....	26
1.8.2. 7,8-DHF as a therapeutic drug.....	27
1.9. BDNF polymorphisms.....	27
1.9.1. BDNF polymorphism and BMD.....	27
1.10. Research aims and hypotheses .....	29
1.11. References.....	30
<b>Chapter 2. General Methods .....</b>	<b>52</b>
2.1. Animals.....	52
2.1.1. Ethics.....	52
2.1.2. Housing .....	52
2.2. Drugs and reagents.....	52
2.3. Microcomputed tomography ( $\mu$ CT).....	53
2.4. Biomechanics.....	53
2.4.1 Cross-sectional area of calluses.....	54
2.4.2. Mechanical properties analysis .....	54
2.5. Histology.....	55
2.5.1 Tissue preparation and embedding.....	55
2.5.2. Sectioning tissue.....	56
2.5.3. Tissue section staining .....	56
2.6. Cell Culture .....	56
2.6.1. Cell storage and maintenance.....	57
2.6.2. Cell subculture and freezing process .....	57
2.6.3. Western blotting.....	57
2.6.4. Proliferation Assays .....	59
2.6.5. Gene expression analysis by reverse transcription-polymerase chain reaction (RT-PCR) .....	59
2.6.6. Mineralization assays.....	60
2.7. Statistical analysis.....	60
2.8. References.....	61
<b>Chapter 3. The effects of the selective TrkA agonist, gambogic amide, on the outcomes of traumatic brain injury in mice .....</b>	<b>63</b>
3.1. Introduction.....	63
3.2. Materials and methods.....	64
3.2.1. Subjects .....	64



3.2.2. Experimental groups.....	64
3.2.3. Lateral fluid percussion injury .....	65
3.2.4. Acute injury severity .....	65
3.2.5. Behavioural testing .....	65
3.2.6. Oedema.....	67
3.2.7. Brain tissue preparation.....	67
3.2.8. RNA extraction and RT-PCR.....	67
3.2.9. Western blot analysis.....	69
3.2.10. Statistical analysis .....	69
3.3. Results.....	70
3.3.1. Acute injury severity measures .....	70
3.3.2. Behavioural outcomes .....	70
3.3.3. Brain water content .....	72
3.3.4. TrkA expression and phosphorylation .....	72
3.3.5. Neuroinflammation .....	73
3.3.6. Apoptosis.....	74
3.3.7. Neurite sprouting and synaptogenesis .....	75
3.4. Discussion.....	77
3.5. Conclusions.....	81
3.6. References.....	82
<b>Chapter 4. The effects of the selective TrkA agonist, gambogic amide, on fracture healing in mice and osteoblasts <i>in vitro</i> .....</b>	<b>90</b>
4.1. Introduction.....	90
4.2. Materials and methods .....	91
4.2.1. Solubility and delivery of GA .....	91
4.2.2. Experimental groups.....	92
4.2.3. Bilateral fibular osteotomy and pump insertion .....	92
4.2.4. Region of interest and grayscale thresholds used in $\mu$ CT callus reconstruction .....	92
4.2.5. Callus position during biomechanical testing.....	93
4.2.6. Histological assessment .....	93
4.2.7. Cell culture .....	93
4.2.8. Statistical analysis.....	95
4.3. Results.....	95
4.3.1. Calluses are structurally smaller when treated with GA.....	95
4.3.2. Biomechanical analyses .....	97
4.3.3. Histological Assessment.....	97

4.3.4. Cell Culture .....	99
4.4. Discussion .....	101
4.5. Conclusions.....	104
4.6. References.....	105
<b>Chapter 5. The effects of BDNF signalling and polymorphisms on bone. A. The effects of the TrkB agonist, 7,8-dihydroxyflavone on tibial fracture healing in mice. B. BDNF polymorphism in mice and their influence on bone.....</b>	<b>109</b>
5.1. Introduction.....	109
5.2. Materials and methods .....	111
5.2.1. Solubility and delivery of 7,8-DHF .....	112
5.2.2. Experimental groups.....	112
5.2.3. Closed tibial fracture model .....	112
5.2.4. Regions of interest and grayscale thresholds $\mu$ CT callus reconstruction .....	113
5.2.5. Callus position during biomechanical testing.....	113
5.2.6. Histological assessment .....	113
5.2.7. Cell culture .....	114
5.2.8. Peripheral quantitative computed tomography (pQCT).....	115
5.2.9. BDNF polymorphic (hBDNFVal66Met) mice.....	115
5.2.10. Statistical analysis .....	116
5.3. Results.....	116
5.3.1. 7,8-DHF reduces callus size .....	116
5.3.2. 7,8-DHF reduces peak force to failure in fracture calluses .....	118
5.3.3. 7,8-DHF treatment has no discernible effects on either callus histomorphometry or osteoclastic density in callus.....	118
5.3.4. Cell culture .....	118
5.3.5. 7,8-DHF treatment did not affect intact bone.....	120
5.3.6. hBDNF <sup>Val66Met</sup> polymorphism does not influence bone.....	122
5.4. Discussion.....	123
5.5. References.....	127
<b>Chapter 6. Discussion and Future Directions .....</b>	<b>135</b>
<b>6.1. Conclusions .....</b>	<b>143</b>
<b>6.2. References.....</b>	<b>144</b>
<b>Appendix A.....</b>	<b>150</b>
<b>Appendix B.....</b>	<b>151</b>

<b>Appendix C.....</b>	<b>164</b>
<b>Appendix D .....</b>	<b>175</b>
<b>Appendix E.....</b>	<b>176</b>

## List of Tables

	Page
<b>Table 3.1.</b> RT-PCR oligonucleotide name and sequence (5'-3').....	85
<b>Table 3.2.</b> Acute injury severity outcomes in mice given SHAM or TBI and assigned to a VEH or GA treatment group.....	87
<b>Table 4.1.</b> Oligonucleotide name and sequence (5'-3') used in Real-Time PCR.....	111
<b>Table 4.2.</b> Mechanical properties of vehicle and GA-treated calluses at 42 days post-fracture..	114
<b>Table 5.1.</b> Oligonucleotide name and sequence (5'-3') used in Real-Time PCR.....	131
<b>Table 5.2.</b> Mechanical properties of vehicle and 7,8-DHF-treated calluses at 28-day post-fracture .....	135
<b>Table 5.3.</b> pQCT measurements of intact femora.....	138
<b>Table 5.4.</b> pQCT measurements of hBDNF <sup>Val66Met</sup> polymorphic mice.....	139

## List of Figures

	Page
<b>Figure 1.1.</b> Illustration of neurotrophin signalling.....	22
<b>Figure 1.2.</b> Illustration of the healing sequence in long bone fractures.....	36
<b>Figure 2.1.</b> The load-displacement graph.....	71
<b>Figure 3.1.</b> The effects of GA treatment on behavioural outcomes post-LFPI.....	88
<b>Figure 3.2.</b> The effects of GA treatment on brain water content in the ipsilateral and contralateral hemispheres following TBI at 72 h.....	89
<b>Figure 3.3.</b> The effects of GA treatment on TrkA expression and phosphorylated-Akt activation post-LFPI.....	90
<b>Figure 3.4.</b> The effects of GA treatment on expression of markers of neuroinflammation post-LFPI.....	91
<b>Figure 3.5.</b> Expression of apoptosis marker caspase-3 in mouse cortex (A) and hippocampus (B) 72 h after LFPI or SHAM-injury.....	92
<b>Figure 3.6.</b> The effects of GA treatment on expression of markers of neurite sprouting and synaptogenesis post-LFPI.....	93
<b>Figure 4.1.</b> The effects of GA treatment on callus structural parameters using $\mu$ CT.....	113
<b>Figure 4.2.</b> Representative histological sections of un-decalcified calluses stained with TRAP.....	115
<b>Figure 4.3.</b> TrkA expression and the effects of GA treatment in the mesenchymal stem cell line, Kusa O.....	117
<b>Figure 5.1.</b> Effects of 7,8-DHF treatment on 28-day callus structural parameters using $\mu$ CT.....	134
<b>Figure 5.2.</b> The effect of 7,8-DHF treatment in the osteoblastic mesenchymal cell line; Kusa4b10.....	136

## List of Abbreviations

$2^{-\Delta\Delta C_T}$	Livak method
7,8-DHF	7,8-dihydroxyflavone
$\alpha$ -MEM	$\alpha$ -Minimum Essential Medium
$\beta$	Beta
$^{\circ}\text{C}$	Degrees Celsius
=	Equals
>	Greater than
<	Less than
x	Multiply
%	Percentage
$\pi$	Pi
$\pm$	Plus minus
$\sigma$	Sigma
$A_{260}$	Absorbance at 260 nm
$A_{280}$	Absorbance at 280 nm
$A^{\circ 1}$	Primary antibody
$A^{\circ 2}$	Secondary antibody
ALP	Alkaline phosphatase
ANOVA	Analysis of variance
BBB	Blood brain barrier
BCA	Bicinchoninic acid
BDNF	Brain derived neurotrophic factor
BMD	Bone mineral density
BMP	Bone Morphogenetic Protein
BMU	Basic multi-cellular unit
BS	Bone surface
BSA	Bovine serum albumin
BV	New mineralized bone volume
BV/TV	Bone fractional volume
CCI	Controlled cortical impact
cDNA	Complementary deoxyribonucleic acid
CNS	Central nervous system
CSA	Cross-sectional area $\alpha$
DEPC	Diethylpyrocarbonate
DPX	Dibutylphthalate polystyrene xylene

DMP-1	Dentinmatrixacidicphosphoprotein1
DMSO	Dimethyl sulfoxide
E	Young's modulus
EDTA	Ethylenediaminetetraacetic acid
EPM	Elevated plus-maze
EPO	Erythropoietin
ETOH	Ethanol
F	Peak force
FBS	Foetal bovine serum
FPI	Fluid percussion injury
FGF-2	Fibroblast growth factor-2
g	Gram
GA	Gambogic amide
GFAP	Glial fibrillary acidic protein
h	Hour
Iba1	Ionized calcium binding adaptor molecule 1
ICP	Intracranial pressure
IL-1	Interleukin-1
IL-6	Interleukin-6
IC	Ipsilateral cortex
IH	Ipsilateral hippocampus
kDa	Kilodalton
kg	Kilogram
kV	Kilovolt
L	Length
LFPI	Lateral fluid percussion injury
LCN2	Lipcalin-2
LTU	La Trobe
m <sup>2</sup>	Metres squared
MAPK	Mitogen-activated protein kinase
M-CSF	Macrophage colony stimulating factor
mRNA	Messenger ribonucleic acid
Met	Methionine
μA	Microamplitude
μCT	Microcomputed tomography
μg	Microgram

μl	Microlitre
μm	Micrometre
mg	Milligram
min	Minutes
ml	Millilitre
mm	Millimetre
mm <sup>2</sup>	Millimetre squared
mmHg	Millimetres of mercury
ms	Millisecond
MVA	Motor vehicle accident
n	Number
N	Newtons
NB	New bone
ng	Nanogram
NGF	Nerve growth factor
N.m <sup>-1</sup>	Newtons per metre
N.m <sup>-2</sup>	Newtons per metre squared
NT	Neurotrophin
OPG	Osteoprotegerin
Osx	Osterix
p75NTR	p75 neurotrophin receptor
PBS	Phosphate buffer saline
PDGF	Platelet-derived growth factor
PCR	Polymerase chain reaction
PLC-γ1	Phospholipase C-γ1
pQCT	Peripheral quantitative computed tomography
PTHrP	Parathyroid hormone related protein
PVDF	Polyvinyl difluoride
RANK	Receptor activator of nuclear factor kappa-β
RANKL	Receptor activator of nuclear factor kappa-β ligand
Ras	Rat sarcoma
rhBMP-2	Recombinant human BMP-2
rhPTH	Recombinant human parathyroid hormone
RIPA	Radio immune precipitation assay buffer
RNA	Ribonucleic acid
ROI	Region of interest



rpm	Revolutions per minute
RT-PCR	Reverse transcription-polymerase chain reaction
Runx2	Runt-related transcription factor 2
s	Seconds
SEM	Standard error of the mean
SNP	Single nucleotide polymorphic
SOX9	Sex-Determining Region Y-box 9
$t_{1/2}$	Half-life
$T_a$ Opt	Optimal annealing temperature
TB	Total bone
TBI	Traumatic brain injury
TBST	Tris-buffered saline and 0.1% Tween 20
TA	Total callus area
TV	Total callus volume
TGF- $\beta$	Transforming growth factor-beta
$T_m$	Melting temperature
TNF- $\alpha$	Tumour necrosis factor-alpha
TRAP	Tartrate-resistant acid phosphatase
TrkA	Tropomyosin-related kinase A
TrkB	Tropomyosin-related kinase B
Val	Valine
V	Volts
VEGF	Vascular endothelial growth factor
VEH	Vehicle
YM	Young's modulus

## Thesis Summary

The neurotrophins, nerve growth factor (NGF) and brain derived neurotrophic factor (BDNF), appear to have positive roles in traumatic brain injury (TBI), skeletal metabolism and fracture healing. This thesis explored the roles of 1. the high affinity NGF receptor, tropomyosin receptor kinase A (TrkA), in TBI, skeletal metabolism and fracture healing and 2. the high affinity BDNF receptor, tropomyosin receptor B (TrkB), in skeletal metabolism and fracture healing. Firstly, systemic administration of the TrkA agonist, gambogic amide (GA), did not influence TBI-induced acute behavioural and motor deficits in mice. Furthermore, GA had no effect on neuroinflammatory, apoptotic, neurite sprouting and synaptogenesis markers, which indicated that GA treatment may not be suitable for attenuating TBI pathologies. Secondly, the influence of systemic GA was investigated on healing murine fibular fractures, with GA treatment resulting in smaller fracture calluses that were mechanically stronger per unit area than controls. Treatment with GA for 14 days decreased tissue volume and increased mechanical properties of calluses. Additionally, GA increased both mRNA expression of markers associated with osteoblastic differentiation as well as *in vitro* mineralisation in Kusa O progenitor cells, which suggested that GA, like NGF, may facilitate fracture healing through promoting both osteoprogenitor differentiation and mineralization. Finally, treatment with the TrkB agonist, 7,8-DHF, to mice with tibial fractures resulted in structurally smaller and mechanically weaker calluses than controls. It is proposed that 7,8-DHF acted centrally on TrkB receptors in the brain to negatively impact bone remodelling. Additionally, mice with BDNF polymorphisms were investigated for changes in bone mineral density and no changes were found in bone content of these mice. These findings suggest that BDNF has a role in bone remodelling, and that there may be two opposing outcomes on bone remodelling depending if TrkB signalling pathways are activated in either the central- or peripheral-nervous systems.

## **Chapter 1.**

### **Literature review**

#### **General introduction**

Neurotrophins are a group of biological growth factors responsible for development, differentiation and function of neurons in the central and peripheral nervous systems. Centrally and peripherally, neurotrophins are secreted by numerous cell types to assist in the regeneration of injured neurons. In addition to their important role in neural tissue maintenance, neurotrophins have a wide range of biological functions in non-neural tissues expressing their receptors. Emerging evidence suggests that neurotrophins, nerve growth factor (NGF), brain derived neurotrophic factor (BDNF) and neurotrophin 3 (NT3) and their receptors may play a role in repairing tissues following trauma. Exploring two components of neurotrophin signalling, this thesis will firstly investigate the role of the NGF tropomyosin receptor kinase A (TrkA) and the effects of the TrkA agonist, gambogic amide (GA), using animal models of moderate-severe traumatic brain injury and long bone fracture healing to determine its therapeutic potential in neural and non-neural tissues. Secondly, this thesis will investigate BDNF tropomyosin receptor kinase B (TrkB) and the effects of the TrkB agonist, 7,8-dihydroxyflavone, using animal models of long bone fracture healing to determine its therapeutic potential in skeletal metabolism and healing. Finally, this thesis will explore how common BDNF polymorphisms may impact on skeletal metabolism in mice.

#### **1.1. Neurotrophins**

Neurotrophins are growth factors that promote neuronal growth and survival and regulate synaptogenesis in central and peripheral nervous systems [1]. In adulthood following neuronal insult, neurotrophins promote survival and modulate neuronal pruning important for normal neural networking [2, 3]. A reduction in neurotrophin expression during development and adulthood results in poor memory acquisition, aggressiveness and loss of neurons in the periphery. Complete absence of neurotrophins results in death of rodent pups within weeks of birth, which emphasizes the importance of these growth factors in brain development and function [4]. In addition to being important trophic factors for development and maintenance of neurons, neurotrophins are also important for several non-neural cell types, which include endothelial cells (cells that line all blood vessels and the heart) and osseous cells (cells responsible for bone metabolism) [5, 6]. Likewise, reduced neurotrophin expression can impact non-neural cell types and cause pathologies such as cardiovascular defects [4].

The four proteins that form the mammalian neurotrophin family include NGF, BDNF, neurotrophin-3 (NT-3) and neurotrophin-4/5 (NT-4/5) [7]. There are two other non-mammalian

neurotrophins; neurotrophin-6 (NT-6) and neurotrophin-7 (NT-7), which have been discovered in aquatic species; the zebrafish (*Danio rerio*) [8] and the teleost fish (*Xiphophorus*) [9], however, since the last two have yet to be discovered in mammalian species, they will not be further mentioned in this thesis. The mammalian neurotrophins, NGF, BDNF, NT-3 and NT-4/5 are initially synthesised as pro-neurotrophins before the removal of the 'pro' sequence via post-translational processing [1], to form large dimer molecules (mature neurotrophins) that are two identical polypeptide chains joined together via disulphide bonds [1, 10]. Synthesis and release of neurotrophins occurs in both the central and peripheral nervous systems, and likewise their receptors can be located in a vast array of cells throughout the body. The next section of this review will explore roles of the two predominant neurotrophins, NGF and BDNF.

## 1.2. Nerve growth factor (NGF)

The first member of the neurotrophin family to be discovered was NGF in 1951 by Levi-Montalcini, who showed substantial increases in sensory ganglia supply to mouse osteosarcoma tissue that was transplanted into young chick embryos [11]. Three years later, Cohen and colleagues, discovered the submaxillary gland of the adult male mouse was a potent source of NGF [12], and to date, is the major source of NGF used in animal experimentation [1]. NGF is a complex molecule formed by three subunits ( $\alpha$ ,  $\beta$ , and  $\gamma$ ) [1];  $\alpha$ -subunit appears biologically inactive,  $\gamma$ -subunit is a protease that assists in the processing of pro-NGF into mature NGF, and  $\beta$ -subunit is fully responsible for the biological activity of NGF [1]. NGF is synthesised and secreted as pro-NGF in tissues, the  $\gamma$ -subunit with both serine protease plasmin and matrix metalloproteinase 7 (MMP7) cleaves the terminal domain of pro-NGF to form mature NGF via intracellular post-translational processing [13]. In mice, the post-translational processing occurs prior to secretion of NGF into saliva, resulting in no pro-NGF entering the submaxillary gland and peripheral circulation [13]. For all other tissues that produce NGF, it is secreted in a mixture of pro-NGF and NGF [13].

The location of NGF (**section 1.2.1**) and its receptors (**section 1.3**) are found throughout the body, including the central and peripheral nervous systems, and in turn has been associated with a variety of physiological processes and diseases, which include growth, differentiation, and survival of peripheral sensory and sympathetic neurons [11, 12, 14-18], synapse formation [1], chronic-inflammatory-allergic response [19, 20], wound healing [21-24], muscle healing [25], bone healing [20, 26-34], neurogenesis [35], inflammation [13, 36-38], apoptosis [39], angiogenesis [40] and arteriogenesis [41].

### **1.2.1. NGF expression**

NGF is widely expressed by several neural and non-neural tissues in the body. Neural expression of NGF has been localised in striatal and basal forebrain cholinergic neurons [42], astrocytes [43], oligodendrocytes [44], dorsal root ganglion [45], and sympathetic ganglia [45]. Peripherally, expression of NGF mRNA has also been localised in other tissues including the heart, liver, skeletal muscle, kidney, and spleen in humans [45]. Via immunohistochemistry, NGF has been localised in fractured and unfractured rat bone [28], and cartilage during fracture healing [46]. Additional cells shown to express NGF include inflammatory cells, immune cells, endothelial cells, epithelial cells, keratocytes, chondrocytes, osseous cells, Schwann cells, and fibroblasts [11, 13, 16, 46-50]. NGF expression in a variety of non-neural tissues suggests a possible diverse range of biological functions. NGF has been shown to be up-regulated in a variety of repairing tissues [13, 37, 51], and there is evidence that NGF may play an important role in tissue repair and regeneration due to its regulation of a variety of processes, which include inflammation [13, 36-38], apoptosis [39] and angiogenesis [40, 41].

### **1.3. NGF receptor function and distribution**

NGF exerts its effects by binding to two independent receptors; tropomyosin receptor kinase A (TrkA) and p75 neurotrophin receptor (p75NTR). NGF binds to TrkA with high affinity, and p75NTR with low affinity (See **Figure 1.1**) [52].

#### **1.3.1. TrkA**

TrkA was the first receptor identified for NGF and is a transmembrane glycoprotein that belongs to a family of tyrosine kinase receptors [13, 53]. TrkA receptors have been localised in many regions of the central nervous system (CNS), including dorsal root ganglion neurons [45], sympathetic ganglions [45], trigeminal ganglion [45], and spinal cord [45]. TrkA is widely distributed in non-neural human tissues and these include salivary glands, oesophagus, stomach, small intestine, colon, exocrine pancreas, thymus, adrenal glands, prostate, testes, ovaries, fallopian tubes, cervix, breast, kidney, bladder, skeletal muscle, bone, and skin [54]. In mouse and rat tissues, TrkA has been localised in osseous cells, immune cells, and endothelial cells [13, 39, 46]. Only mature NGF can activate the TrkA receptor, and not pro-NGF [55]. NGF binds with high affinity to TrkA, and upon binding, a dimer of NGF and TrkA is formed that causes transphosphorylation and activation of loop tyrosines [3]. NGF can then signal through TrkA by one of three signalling pathways, which include Ras/MAP kinase pathways, which stimulate neurite outgrowth, PI3 kinase/Akt pathways, which promote survival of neurons and non-neuronal cells and phospholipase C- $\gamma$ 1 (PLC- $\gamma$ 1)/protein C-regulated pathways, which enhance synaptic plasticity [1].

### **1.3.2. p75NTR**

Along with TrkA, NGF also binds to the low-affinity receptor, p75NTR, which is a member of the tumour necrosis factor cytokine family [56]. BDNF, NT-3 and NT4/5 also bind to p75NTR [56]. p75NTR is found throughout the developing brain, however, in the adult brain, physiological receptor expression is restricted to the cholinergic neurons of the septal-basal forebrain complex, oligodendrocytes, astrocytes and microglia [10]. Expression of p75NTR is upregulated in the brain after injury in cerebellar Purkinje neurons, hippocampal pyramidal neurons, retinal ganglion neurons, forebrain neurons, and the extended striatal complex [10]. Peripherally, p75NTR has been localised in neural cells such as dorsal root ganglion neurons, and sympathetic neurons [45], as well as on cells of non-neural tissues such as heart, liver, kidneys, lung, spleen, myocytes [57], dental pulp stem cells [58], lymphocytes, keratinocytes, fibroblasts, and macrophages [13, 45]. NGF responsiveness to p75NTR is multidimensional, with mature NGF displaying a low affinity to p75NTR when this receptor is expressed solely on cells [52]. Three signalling pathways can be activated upon neurotrophin binding to p75NTR; i) Jun kinase pathways, which promote apoptosis of neurons, ii) Rho pathways, which cause reduced growth cone motility in neurons, and iii) NF- $\kappa$ B pathways, which augment cell survival [1, 13]. The affinity of p75NTR changes in the presence of co-expressed receptors [52]. Co-expression of p75NTR and Trk receptors results in dimerization of the two receptors, which signify a much greater affinity for mature neurotrophins, and mediates pro-survival pathways [1]. Conversely, co-expression of p75NTR and sortilin; a pro-neurotrophin receptor, forms dimerised complexes that have high affinity for pro-NGF and pro-BDNF and mediates pro-apoptotic pathways [1].

In summary, NGF can be characterized as a pleiotropic factor because NGF and its receptors are expressed and utilized by a vast array of neural and non-neural cell types, and therefore have the potential to produce an array of biological functions, which are further discussed in **section 1.6.2** and **section 1.7.3**.

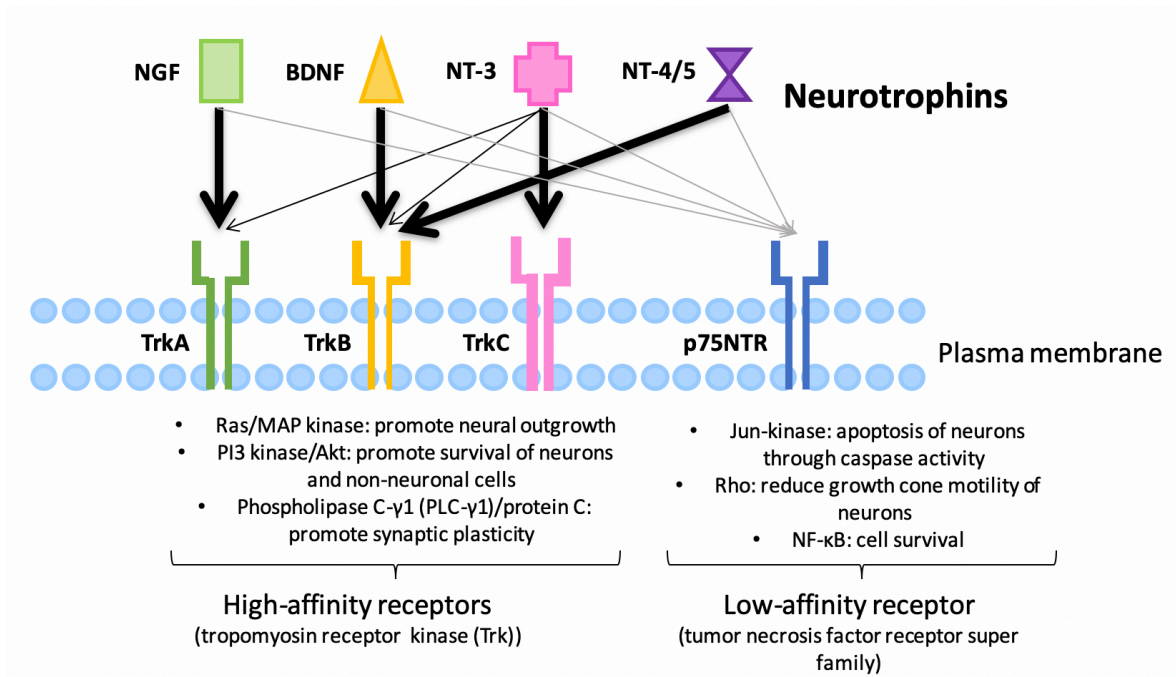


**Figure 2.1.** Illustration of neurotrophin signalling. Activation of each receptor can induce one of three pathways to cause responses in target cells. Thick black lines represent high-affinity binding to Trk receptors, thin black lines represent low-affinity binding to Trk receptors and thin grey lines represent low-affinity binding to p75NTR receptor. Adaptation of [1].

#### 1.4. Brain derived neurotropic factor (BDNF)

BDNF was the second member of the neurotrophin family to be discovered [59]. Since its discovery in 1982, BDNF has been established as an important modulator of synaptic plasticity, as well as enhancing both the survival and differentiation of neurons not responsive to NGF [1, 3]. BDNF is synthesised in the endoplasmic reticulum as pro-BDNF, stored in vesicles, and transported to the post-synaptic dendrites [60]. Similar to the production of NGF, pro-BDNF is cleaved to form the biologically active mature BDNF, however, this is achieved by a distinct protein convertase enzyme [60].

BDNF (**section 1.4.1**) and its receptors (**section 1.5**) are widely distributed throughout the central and peripheral nervous systems. BDNF has been associated with physiological processes that include brain development [35], angiogenesis [61], neurogenesis, blood pressure, lipid metabolism, a cardiovascular protective action [60], and conditions such as TBI [62], fracture healing [63], wound healing [37, 51], Alzheimer’s disease, Huntington’s disease, dementia, autism, schizophrenia, cardiovascular disease, allergic asthma and type-2 diabetes mellitus [60].

#### **1.4.1. BDNF expression**

BDNF is expressed by many cells, both neural and non-neural. During brain development, BDNF expression has been shown to be low in immature regions, with increased expression found as the brain reaches maturity [35]. In the adult brain, BDNF has been identified in cells of the olfactory bulb, cortex, hippocampus, basal forebrain, mesencephalon, hypothalamus, brainstem and spinal cord [60]. BDNF is neuroprotective to many structures in the brain, and reduced levels of BDNF are seen in neurodegenerative diseases such as Parkinson's disease, multiple sclerosis and Huntington's disease [60]. In addition to its expression and neuroprotective role in the brain, BDNF is expressed both physiologically and during times of injury and repair in non-neural cells of the heart, spleen and liver [45], and as well as endothelial cells [63], epithelial cells [64], osseous cells [46], fibroblasts [65] and immune cells [47]. Similarly to NGF, BDNF has been shown to be upregulated in repairing tissues [46, 66, 67], and has key roles in angiogenesis, apoptosis, and inflammation [5, 61, 63, 66-68].

#### **1.5. BDNF receptor function and distribution**

BDNF exerts its effects by binding to two independent receptors; tropomyosin receptor kinase B (TrkB) and the shared neurotrophin receptor, p75NTR. BDNF binds to TrkB with high affinity, and p75NTR with low affinity, **Figure 1.1** [52].

##### **1.5.1. TrkB**

BDNF binds to tropomyosin receptor TrkB, which is another transmembrane glycoprotein that belongs to a family of tyrosine kinase receptors [13, 53]. TrkB mRNA and protein have been localised in cells throughout the CNS in regions and cells that include the cerebral cortex, hippocampus, dentate gyrus, striatum, septal nuclei, substantia nigra, cerebellar Purkinje cells, brainstem, spinal motor neurons and hippocampus [69]. In non-neural tissues of humans, TrkB has been localised in salivary glands, small intestine, colon, endocrine pancreas, lymph nodes, and skin [54]. Expression of TrkB has been shown to upregulate in response to tissue injury [60]. Mature BDNF binds with high affinity to TrkB and activates similar signalling pathways to NGF such as PI3 kinase/Akt pathways, which promote survival of neurons and non-neuronal cells, and IRS1/2, which promotes synaptic plasticity [1, 60].

##### **1.5.2. p75NTR**

BDNF also binds to the low affinity receptor p75NTR, in the exact same manner as NGF, as mentioned in **section 1.3.2**. Likewise, BDNF binds to p75NTR to activate pro-apoptotic pathways, and to the p75NTR-TrkB dimer to activate pro-survival pathways [1].



In summary, neurotrophins and their Trk receptors not only play an important role in growth and regulation of nervous tissue, but their expression in a variety of non-neural tissues suggests a possible diverse range of biological functions. Neurotrophins have been shown to be upregulated in a variety of repairing tissues [13, 37, 51, 70], and there is evidence that they may play an important role in tissue repair and regeneration due to their regulation of a variety of processes, which include inflammation [13, 36-38, 67], apoptosis [39] and angiogenesis [40, 41, 61]. There is emerging evidence to suggest that neurotrophins may be particularly important in traumatic brain injury and bone fracture healing and targeting their receptors may hold promise for improving outcomes for patients with traumatic injuries. Accordingly, this review will discuss brain injuries and bone fracture healing, and the role neurotrophins have in these injuries.

### **1.6. Traumatic brain injury**

Traumatic brain injury (TBI) is the leading cause of death and disability worldwide for individuals under the age of 45 [71, 72]. Common causes of TBI include motor vehicle accidents (MVA), sporting injuries, violence and warzones [71]. From a global perspective, TBI is an increasing burden on society, which places large financial, emotional and medical stresses on families and the community. Over 10 million people are affected annually from TBI, and alone in the United States of America an estimated 5 million people are living with a TBI-related disability [71, 73]. Despite the high prevalence, there is currently no effective pharmaceutical treatment available to improve TBI outcomes [74, 75].

In the clinical setting, the level of patient consciousness following a TBI is assessed using the Glasgow coma scale (GCS). This assessment of eye, motor and verbal responses provides insight into the possible severity of the TBI, with the total score of these responses deeming patients as likely having either a mild (14-15), moderate (9-13) or severe (3-8) injury [76]. In additional assessment, TBI can be classified by the mechanism of injury; closed head versus penetrating head injury, diffuse versus focal injury, and the extent of axonal damage via neuroimaging [76]. Prognostic classification is another approach to determine expected patient outcome using models such as CRASH and IMPACT [76]. Clinical symptoms seen in moderate to severe TBI include vomiting, loss of consciousness, retrograde or post-traumatic amnesia, skull fractures, and neurological deficits [76]. Whilst acute TBI symptoms can be transient, more severe, permanent disabilities of TBI can include post-traumatic epilepsy, post-traumatic brain swelling, psychosocial changes, and chronic traumatic encephalopathy, which requires lifelong medical intervention [76, 77]. These functional deficits caused by TBI can be a result of the primary injury occurring at the moment of impact, or secondary injury mechanisms that can develop and persist for weeks to years following the initial injury.

### **1.6.1. Mechanisms of TBI**

Forces applied to the brain can produce focal and diffuse injury patterns [74, 78]. Focal injury patterns are typically seen in more severe TBI cases that involve significant force applied to the skull and/or brain, with common symptoms including contusions, haemorrhaging and lacerations of the brain parenchyma [74]. Diffuse injury patterns are typically seen when an object makes blunt force contact to the skull (i.e. without creating skull fracture), creating acceleration and/or deceleration forces that may cause stretching and shearing of axons and blood vessels across a range of brain structures [74, 78].

Brain damage in TBI is thought to result from a combination of primary and secondary injuries. Primary injury is the immediate and irreversible physical damage caused to the brain at the moment of impact [74, 76]. Both focal and diffuse injuries can induce mechanical deformation of the brain tissue, and in so doing, can induce a series of cellular and molecular events that activate several secondary injury pathways that may in turn lead to further brain damage [72, 74, 76, 78, 79]. Secondary injuries can develop within minutes of the primary injury and may progress and persist for years following the initial head impact. Common biological mechanisms that occur within the brain microenvironment during secondary injury include neuroinflammation, immune cell responses, excitotoxicity, increased neurotransmitter signalling, oxidative stress, calcium-mediated damage, mitochondrial dysfunction, proteopathies and free radical production [72, 74, 80]. Changes that occur within the brain microenvironment can lead to blood brain barrier (BBB) damage, oedema, increased intracranial pressure, ischemia and cell death; all features that can contribute to functional deficits [72, 74, 78]. Growing evidence suggests that brain damage resulting from activation of secondary injury mechanisms can result in long-term physical, emotional and cognitive abnormalities, and has also been associated with development of neurodegenerative diseases, which include Alzheimer's disease, depression and chronic traumatic encephalopathy [74, 81-83]. Current evidence suggests that neuroinflammation is one of the key secondary injury mechanisms that contribute to ongoing damage and cellular degeneration of the brain following TBI [79, 80, 84].

#### ***Neuroinflammation in TBI***

Neuroinflammation is a multi-factorial process that occurs following TBI. While the inflammatory response that follows brain injury can be neuroprotective and neuroreparative, evidence links chronic neuroinflammation to ongoing brain damage [79, 80]. During TBI, neuroinflammation can be characterized by the release of pro-inflammatory molecules and by the activation of microglia and astrocytes [80, 85].

In acute stages of inflammation, pro-inflammatory cytokines are secreted within minutes of tissue damage, which cause several types of leukocytes, including neutrophils, monocytes and macrophages to migrate to the site of damaged brain tissue [80]. Migration of blood-borne leukocytes typically peaks at 24-48 hours post-TBI and is initiated by disruption of the BBB at the time of trauma [79, 80, 86]. Leukocytes may cause additional tissue destruction and further increase BBB permeability through secretion of pro-inflammatory cytokines, adhesion molecules, neural toxic substances such as ROS, nitrogen species and metalloproteinases [79, 80]. Furthermore, resident glial cells; microglia and astrocytes can become activated and reactive during the inflammatory response following TBI [79, 85, 87]. Under normal conditions, astrocytes are responsible for maintenance of BBB integrity, pH buffering and transmitter homeostasis in the brain [88]. Together astrocytes and microglia are important in neural repair [85, 87, 89]. In response to TBI, activated microglia can become the primary source of pro-inflammatory cytokines in the brain, and typically precedes astrogliosis [85, 90]. Reactive microglia can be identified by the increase in expression of markers CD32, CD16 [91] and ionized calcium binding adaptor molecule 1 (Iba1) [92]. On the other hand, activated astrocytes (astrogliosis) surround the site of damaged tissue and secrete inhibitory extracellular matrix that contributes to the formation of glial scarring [79]. When astrocytes fail to maintain their function (i.e. normal neuronal support) and increase their production of cytotoxic factors, they are termed 'reactive astrocytes' [85]. Reactive astrocytes can be identified by the increase in expression of vimentin [93], glial fibrillary acidic protein (GFAP) [94] and lipocalin-2 (LCN2) [95]. As a result, a positive-feedback loop may be created by the interaction between leukocytes, reactive astrocytes and microglia, which leads to the amplification of the neuroinflammatory response and extent of neurodegeneration [87].

### ***Neuronal apoptosis in TBI***

Neuronal apoptosis is another secondary cellular response in TBI [96]. Death of neurons occurs in two patterns following TBI; 1. the primary injury immediately after impact results in neuronal necrosis; typically, via shearing of neurons or excitotoxicity, and 2. during secondary injury, where further insults (e.g. inflammation) can cause neurons to undergo apoptosis i.e. programmed cell death [97]. Both necrosis and apoptosis can be identified by the increase in calpain in neurons following TBI, however, neuronal apoptosis is distinguished from neuronal necrosis via the exclusive increase in expression of caspase-3 [98]. Apoptosis is a significant contributor to cell death following TBI [85, 90]. As neuronal apoptosis is a key secondary mechanism activated following TBI, therefore, preventing neuronal death and encouraging new neurons to sprout and form synaptic connections earlier, may be beneficial.

### ***Neurogenesis and synaptogenesis in TBI***

In early stages of TBI, the exact role for neural plasticity and repair remains poorly understood. Several theories suggest early neuronal repair and neurogenesis is neuroprotective by reducing the number of further neuronal death and damage following a TBI [99, 100]. Neuronal and synaptic changes have been shown to begin in the hippocampus and cortex within 72 hours of injury [99]. Neuronal sprouting and synaptogenesis (the formation of synapses) following TBI is thought to be associated with elevations in expression of GAP-43, synapsin, synaptophysin and agrin [99, 101-104]. GAP-43 is a marker of axonal cone formation during neurite sprouting [105], and synapsin, synaptophysin and agrin are markers of synaptogenesis [99, 101, 106]. In an experimental model of TBI, protein expression of GAP-43 and synaptophysin has been shown to elevate in the ipsilateral hippocampus at 24-, 48- and 72 hours post-TBI [99]. Additionally, agrin has been recently linked to having a role in the early sprouting phase of synaptogenesis in rats at 7 days post-TBI [101]. Neurite outgrowth and synaptogenesis are not currently a target for pharmaceutical agents, but by reducing neuroinflammation and apoptosis in the brain pharmacologically, may create an environment suitable for neurons to begin these connections earlier. Several experimental TBI studies in mice and rats have further shown that neuroinflammation and apoptosis can lead to worsened cognitive capacity, emotional disturbances and motor control dysfunction [72, 107-111], and that treatments targeting these mechanisms and promoting neurite sprouting and synapse formation have potential to improve TBI outcomes [79, 108, 112].

#### ***1.6.2. NGF and TBI***

There is abundant evidence that demonstrates the neuroprotective action of NGF following TBI. In the early 1980's, Nieto-Sampedro and colleagues (1982) were the first to show an increase in neurotrophic factors in wound fluid of young adult Sprague-Dawley rats with brain injury [113]. Shortly after, numerous studies explored NGF administration in rodent models of TBI, specifically investigating the effects of NGF on neuronal survival and TBI-associated behavioural changes. In four separate studies, NGF (34-40 µg) infused for 14 days into the right lateral ventricle of rats with lesions in the dorsal hippocampus, increased the survival of cholinergic neurons by 350%, reversed apparent cholinergic neuron loss and decreased the amount of NGF receptors lost due to acute brain injury [114-117]. Additional studies, using similar NGF infusion techniques, showed rats performed better in active avoidance tasks and radial maze performance (both tasks being cognitive measures) following fimbria and septal lesions [118, 119], which suggests that NGF treatment may contribute to functional recovery in rats with brain lesions. While these studies used older models of brain injury, more recent studies have been published using more modern models of TBI that reflect human-like symptoms associated with TBI. NGF treatment has been

shown to reduce TBI-induced cognitive latencies, tested using Morris water maze, one week after injury in rat and mouse models of TBI [120-123]. Furthermore, intranasal administration of NGF improved fine motor coordination and balance via a beam walking test at two weeks, in rat models of TBI [122].

Interestingly, NGF has so far been unable to mitigate gross motor deficits induced by TBI. Two studies have illustrated the inability of NGF to attenuate neurologic motor dysfunction caused by TBI via wire grid testing, and neurologic motor score in rodent models [120, 123, 124]. These findings indicate that the primary effects of NGF are seen in neurons associated with cognition and have limited effect of upper motor neurons following TBI.

Cerebral oedema is a pathological feature of secondary injury of TBI associated with unfavourable prognosis [125]. One study has demonstrated reduced cerebral oedema at 12-, 24- and 72-hours after TBI induced by weight drop model in Sprague-Dawley rats, when they were treated with 5 µg/day of NGF [126]. The same study suggested NGF reduced cerebral oedema by decreasing aquaporin 4, a membrane protein shown to regulate vasogenic and cytotoxic oedema in TBI models of rats [127], which suggests a role for NGF in reducing oedema in brain tissue, however, no other studies have documented this response. Neuroinflammation is another secondary mechanism that can determine the outcome of TBI. Lv and colleagues showed NGF (5 µg/day) decreased the neuroinflammatory markers, IL-1β and TNF-α, at one and three days post-TBI in rats undergoing a weight drop model-induced head injury [126, 128]. Taken together, these studies demonstrate a role for NGF agonists as potential therapies to mitigate behavioural deficits and reduce some of the secondary mechanisms associated with TBI such as cerebral oedema, apoptosis of neurons, and neuroinflammation.

### **1.6.3. Therapies for TBI**

The search for therapies to reduce cerebral oedema, neuroinflammation, cognitive and motor deficits seen in TBI has been constant, with several medical interventions including head elevation, seizure prophylaxis, hyperventilation, therapeutic cooling, intracranial pressure (ICP) monitoring and craniotomy, which are all designed to reduce oedema and secondary brain damage associated with raised ICP [129, 130]. There are limited pharmacological therapies currently used in medical practice that are efficacious at reducing cerebral oedema, and none that target neuroinflammation.

Mannitol is an osmotic diuretic that is widely used for the management of raised ICP in patients with TBI [131]. Mannitol increases erythrocyte deformability, which decreases blood viscosity [132]. Decreases in blood viscosity improves regional cerebral blood flow and compensatory vasoconstriction in regions of the brain where autoregulation is intact, which

maintains intravascular volume, and results in decreased ICP [131]. Additionally, mannitol produces an osmotic gradient between the cerebral extracellular space and plasma, drawing water from the brain into blood vessels, thus reducing cerebral oedema [131]. The major limitation of mannitol for the treatment of TBI, however, is an intact BBB is required for the osmotic gradient, and if the BBB is disrupted, mannitol administration may increase cerebral oedema and worsen TBI outcomes [131]. Additionally, a review by Wakai and colleagues on mannitol for acute traumatic brain injury conducted in 2007, suggested whilst effective in reversing acute raised ICP in patients with TBI, prolonged administration of mannitol may actually increase ICP [133]. Even though mannitol is routinely used to treat raised ICP in TBI patients presenting to hospitals, there is no evidence to guide physicians on dosage or duration of treatment.

Benzodiazepines and barbiturates used to put patients in a medically-induced comatose state is one of the final steps in management of TBI. In acute, severe TBI, precipitating factors such as pain and agitation increase patient blood pressure and ICP, which is associated with higher mortality rates [134]. A chemical infusion of benzodiazepines or barbiturates are thought to significantly reduce metabolic demand of the brain and ICP by protecting the brain from secondary damage, and in turn, accelerate healing [129]. Specifically, benzodiazepines have been shown to reduce the cerebral metabolic rate of oxygen and cerebral blood flow in TBI patients but have no effect on raised ICP [135]. Barbiturates act on ICP in TBI patients, but the exact mechanism remains debatable. Albanése et al. 1999, showed in a randomized crossover study that bolus administration of barbiturates alfentanil, sufentanil and fentanyl transiently increased ICP in patients with already raised ICP, but had no long-term effects on reducing ICP. Conversely, several other studies suggest that long term barbiturate treatment does result in a persistent reduction in ICP [136-138]. Regardless of the above findings, a systematic by Roberts and Sydenham in 2012 on medically-induced comatose states using barbiturates between 1982-2008 concluded “there is no evidence that barbiturates improve outcomes in people with acute brain injury” [139]. In addition to the lack of improvement of outcomes in patients with TBI, medically-induced comatose states can often cause more risk by altering blood pressure of patients [129, 139]. One in four patients treated with barbiturates were reported to have a significant reduction in blood pressure, offsetting any affect the drugs had on reducing ICP [139].

In addition to the limited therapies available, there are several emerging treatments for TBI that are either in the preclinical or clinical phase of development. The specific details for each of the emerging treatments, is beyond the scope of this thesis, however a brief description of the treatments currently in preclinical and clinical phases is discussed, along with references for appropriate reviews. Preclinical data has explored the anti-inflammatory and neuroprotective

effects of calcium channel blockers, amantadine (dopamine agonist), which show promise in reducing inflammatory responses, improving cognitive function, and reducing TBI-induced cellular death in animal models of TBI [129]. Erythropoietin (EPO), is another potential therapeutic for TBI that demonstrated neuroprotection and neurorestoration in preclinical animal models of TBI [140] and has since entered clinical trial phases for moderate to severe TBI [129, 130]. Other drugs that have entered clinical trials and show promise for the treatment of TBI fall under two broad categories; neuroprotective (protect neurons against damage and degeneration) and neurorestoration (regrowth and repair of neurons). The neuroprotective approaches include, calcium channel blockers, dexanabinol (excitatory amino acid (EAA) inhibitor), progesterone, and methylphenidate (monoaminergic agonist), whilst the neuroregenerative approaches include EPO, statins, nitric oxide, and bone marrow stromal cells [129, 130]. One of the biggest challenges faced by many of these TBI therapeutics mentioned above, occurs within the clinical trial phase, where drugs that were effective for animal models of TBI, may be safe but not efficacious for humans with TBI.

Idealistically, primary prevention of TBI would be the most effective way of eliminating cognitive and motor deficits associated with TBI, however, this is an unrealistic approach considering the numerous causes of TBI (sporting, war, MVA) as discussed in **section 1.6**. As such, there is a need for novel, more effective drugs to target as many of the pathological pathways of TBI, which include neuroinflammation, apoptosis, and cerebral oedema, as possible. Growth factors have been extensively analysed for their neuroprotective and neuroregenerative properties, particularly the NGF-TrkA pathway, which has been shown to target many of the secondary pathological mechanisms caused by TBI and is discussed in **section 1.6.2**. An NGF mimetic, gambogic amide (GA), has been shown to potently activate TrkA receptors in hippocampal neurons *in vitro* [141], and neurons in C57BL/6 mice when systemically delivered [142]. Furthermore, the same studies showed GA protected neurons from kainic-induced cellular apoptosis and reduced infarct volume in the brain in a transient model of ischemic stroke [141]. These studies verified TrkA agonism as a potential therapeutic pathway for treating TBI in humans (see **section 1.8.1** for additional information on GA). The next section will discuss the preclinical *in vivo* models of TBI currently used to explore potential pharmacological therapeutic strategies for TBI.

#### **1.6.4. Animal models of TBI**

Animal models of TBI are used to emulate the mechanics and injury patterns of TBI in a variety of species [72]. Whilst there is no one model of TBI that can replicate every aspect of injury seen in humans, there are numerous models that are used to mimic different pathological features

of TBI. Rodent models have evolved over time and rodents are one of the most commonly used species as they allow investigation of behavioural, psychosocial, and motor deficits similar to TBI patterns seen in humans [72, 143]. The most widely used TBI models in rodents are controlled cortical impact (CCI), weight drop (open- and closed-head models), and fluid percussion injuries.

The CCI is a highly reproducible, modified open-head weight drop model that requires a craniotomy [72]. The CCI device works by using a pneumatic or electromagnetic impact device to drive a solid impactor into the exposed dura mater covering the brain, which produces a mostly focal injury [72, 144]. The functional outcomes of brain injury seen in CCI models include cognitive and motor deficits, however, this model is unable to produce emotional changes seen in other models [72]. Pathological features of CCI rodent models that reflect human TBI include concussion, hemorrhage, axonal injury, and cortical contusions [72, 144]. Cortical contusions lead to the cavitation of white matter under the injury site and is commonly seen in the CCI model of TBI due to the focal nature of the injury [144]. These losses in brain tissue limit analyses of neuronal changes and oedema seen in TBI at the site of injury.

There are two broad types of weight drop models of TBI, closed-head models (no craniotomy) which include Shohami and Marmarou models, and open-head models (craniotomy) which include Feeney and Maryland models [72]. In brief, a free falling, guided weight strikes the skull or dura mater of the brain to cause brain injury [145]. Dependent on the model used, the type of injury is either mostly focal or mostly diffuse, and skull fractures are commonly seen in Shohami and Marmarou models that do not require craniotomy [72]. The functional outcomes and pathological features seen in weight drop models are similar to those described as above in the CCI model, however, for more comprehensive differences between the weight drop models, please refer to the review by Xiong et al. 2013. One major disadvantage of weight drop models is their poor reproducibility, and variability in injury severity in each model [72]. Additionally, the weight drop models produce either a mostly focal or mostly diffuse injury pattern which limits its usefulness when exploring full brain changes caused by TBI.

The fluid percussion injury (FPI) model is a highly reproducible, mixed focal cortical and diffuse subcortical injury pattern, making it the most used TBI model in rodents [72]. Following a midline or lateral parietal craniotomy, a pendulum striking the piston of a fluid reservoir produces a fluid pulse pressure, which impacts the brain causing displacement and deformation of brain tissue [72, 143]. The strength of fluid pressure pulse can be altered via the pendulum, which allows a range of severities from mild to severe [146]. FPI can replicate clinical TBI seen in humans without the skull fracture, and many of the pathophysiological and behavioural hallmarks of TBI [72]. Dependent on severity of fluid percussion injury, pathological changes that can be seen acutely are motor impairment, cognitive deficits, brain oedema, neuroinflammation, focal cortical



contusion, hippocampal neuronal injury, apoptosis, and neuroregeneration [72, 143, 147-150]. Taken together, the fluid percussion injury model is a combined focal and diffuse injury able to reproduce behavioural and pathological outcomes seen in human TBI.

### **1.7. Fracture healing**

Fracture healing is a complex process that involves interactions between various cell populations and activation of molecular pathways to return bone to its original morphology and strength [151]. Fractures are the most common type of injury that results in hospital admissions in Australia, and most fractures are caused by falls, transport accidents, sports injuries and machinery accidents [152]. Most fractures heal well, however, approximately 5-10% of all fractures do not heal properly and result in delayed- or non-union [153]. Delayed- and non-union of fractures occur when fractured ends of bone fail to unite within nine months following initial fracture [154]. Problematic non-union fractures create a burden on the health care system; costing the Australian government many millions of dollars per annum [155]. Similarly, non-union is particularly prevalent in elderly patients who present with co-morbidities such as diabetes and osteoporosis [156-159]. There are currently very limited options available for the treatment of fractures and an understanding of the biological processes that occur during fracture healing is crucial in endeavouring to identify potential pharmaceutical agents and therapeutic windows to improve fracture healing outcomes.

#### ***1.7.1. Osseous cell types in fracture healing***

Several cell types are involved in each stage of fracture healing, and they include osteoprogenitor cells, fibroblasts, myofibroblasts, chondrocytes, and specialised bone surface cell populations; osteoblasts, osteoclasts, and osteocytes [153]. Osteoprogenitor cells are mesenchymal stem cells with osteogenic potential [160] and bone marrow as well as the outer, fibrous membrane of bone i.e. periosteum, are the primary sources of osteoprogenitor cells, with secondary sources of osteoprogenitor cells found in soft tissues including skeletal muscle [161]. Osteoprogenitor cells can differentiate into either osteoblasts (bone forming cells) or chondrocytes (cartilage forming cells) and this is dependent largely on the degree of vascularization, mechanical environment, and transcription factors present in the bone matrix during fracture healing. Differentiation into the chondrocytic lineage is favoured in areas of poor vascularization (therefore low oxygen tension) [151, 162], and the expression of transcription factor, Sex-Determining Region Y-box 9 (SOX9) [163, 164]. The osteoblastic lineage is favoured in high oxygen tension regions i.e. in highly vascularized areas [151, 162] and induces the expression of transcription factors, Runt-related transcription factor 2 (Runx2) [165] and Osterix (Osx) [166].

Osteoblasts are one of the specialised bone surface cells, that lay down new, unmineralized bone collagen known as osteoid, and aid in mineralization of osteoid into mineralized lamellar bone during fracture healing [153, 167]. After mineralization, approximately 50-70% of osteoblasts that actively form bone, ultimately undergo apoptosis [168]. Remaining osteoblasts either become quiescent (lining cells) or embed themselves within bone matrix and differentiate into osteocytes [169]. Osteocytes embedded in matrix make up most of the bone cell population [169] and reside in fluid filled cavities termed lacunae [167]. In lacunae, osteocytes create a cellular network connecting to one another via long cytoplasmic processes through microchannels called canaliculi [167]. Due to their location within bone and their interconnecting canaliculi, osteocytes detect mechanical load and stresses placed on bone and translate load into biochemical signals that influence bone remodelling [170]. One protein recently discovered that is secreted by osteocytes and influences bone remodelling is sclerostin, which inhibits the formation of bone [171]. The gene which encodes sclerostin is SOST [170]. Sclerostin's main mechanism of action is to inhibit bone morphogenetic proteins (BMPs) [170], a group of proteins that are important in the formation of both bone and cartilage [172]. Due to osteocytes' prominent role in bone formation and maintaining bone density, current therapeutics in bone research are targeting osteocytes and associated signalling factors, including sclerostin, in order to treat and prevent bone disease and injury [170, 173-175].

The other specialised bone surface cells important in fracture healing are osteoclasts. Osteoclasts are large, multinucleated cells that are formed by fusion of monocytic precursors and are the principal resorptive cells in bone remodelling [176]. Osteoclasts are stimulated to resorb bone by factors such as macrophage colony stimulating factor (M-CSF) and receptor activator of nuclear factor kappa-B ligand (RANKL) [176]. When stimulated, osteoclasts attach to the surface of bone by plasma membrane specializations called "ruffled borders", which are projections of microvilli. On attachment, osteoclasts secrete tartrate-resistant acid phosphatase (TRAP) and hydrochloric acid into the region of the ruffled border. TRAP and hydrochloric acid cause the microenvironment pH to drop to approximately 4.5-5 [177], and causes degradation of the bone matrix [167, 176]. Degraded matrix is resorbed by osteoclasts via endocytosis and is then transported through the osteoclasts and released into the extracellular space [178].

### ***1.7.2. Mechanisms of fracture healing***

Fracture healing is a multistep process that results in the restoration of bone integrity minus scar tissue formation [151]. Healing in fractures can be categorized into two types; primary healing, where bone either side of the fracture directly unites by intramembranous ossification, or secondary healing, where there are several stages of healing that feature both

intramembranous and endochondral ossification to achieve a healed bone [153, 179]. Primary healing is uncommon and mainly limited to minor fractures (bone ends are not displaced), incomplete fractures, and in fractures that are rigidly fixed [153]. Secondary fracture healing is more common than primary healing [151, 153, 179] and can be divided into four overlapping stages; inflammation, soft callus formation, hard callus formation and remodelling [179]. Each stage in secondary fracture healing is important for restoring fractured bone to its original morphology. Each stage of the fracture healing is outlined below (also see **Figure 1.2**).

### ***Inflammatory phase***

The inflammatory phase is the first stage of fracture healing. The initial fracture site typically displays damage to vasculature and nerves within bone marrow, trabecular and cortical bone, and soft tissues surrounding bone [179, 180]. Bleeding is contained in the form of a blood clot called a haematoma [151], and non-specific wound healing pathways are activated [179]. The haematoma is very important for the progression of fracture healing, and it has been shown that its removal impairs the rate of fracture healing [181]. Inflammatory cells, which comprise macrophages, monocytes and neutrophils infiltrate the haematoma, releasing an array of growth factors that include vascular endothelial growth factor (VEGF), transforming growth factor- $\beta$  (TGF- $\beta$ ), fibroblast growth factor-2 (FGF-2), M-CSF and platelet-derived growth factor (PDGF), and also secrete cytokines such as interleukin-1 (IL-1), interleukin-6 (IL-6) and tumour necrosis factor- $\alpha$  (TNF- $\alpha$ ) [179]. The release of growth factors and cytokines within the haematoma assists in its conversion into granulation tissue and initiates neovascularisation and nerve sprouting within granulation tissue [179, 180]. Many of these above factors also act as mediators for osteoprogenitor cell migration from surrounding tissues and their proliferation at the fracture site [179, 180]. It is these mechanisms that are activated in the inflammatory phase that contribute to the initial callus response i.e. the formation of tissue that bridges the fractured bone ends.

### ***Soft callus phase***

Soft callus formation occurs within the first days up to approximately 2-3 weeks post-fracture [151]. During this stage, osteoprogenitor cells migrate from the surrounding soft tissue and differentiate into either osteoblasts or chondrocytes depending on blood supply and mechanical strain at the fracture site [153]. Osteoprogenitor cells close to the fractured ends favour osteoblastic differentiation over chondrocytic differentiation due to a rich blood supply, which is provided by blood vessels at the periphery of the callus [151, 162]. Therefore, at the edges of callus, bone is formed, and this process is known as intramembranous ossification. Typically, the need to stabilize the fracture and bridge fractured ends precedes the rate of intramembranous ossification and vascularization within the fibrinous clot, thereby creating a hypoxic (oxygen deficient) microenvironment [151, 182]. Due to the lack of oxygen within the fibrinous clot,

osteoprogenitor cells differentiate into chondrocytes. Chondrocytes, along with fibroblasts, undergo mass proliferation and form an avascular, semi-soft fibrocartilaginous callus [179]. Nerve sprouting is established within soft callus and osteoclasts begin to resorb the fibrocartilaginous soft callus [151, 179]. Growth factors and potent angiogenic factors including VEGF, BMP, FGF-1, TGF- $\beta$  and NGF are secreted within the soft fibrocartilaginous callus by osteogenic and inflammatory cells to promote capillary and nerve sprouting that aid in replacement of cartilage with bone to form bony callus [29, 40, 179].

#### ***Hard callus phase***

Hard callus formation is where most osteoblastic activity occurs during fracture healing [179]. Angiogenesis (neovascularisation) is crucial during this stage [151, 179] and as the fibrocartilaginous callus is resorbed by osteoclasts, osteoblasts synthesize immature woven bone in its place, a process known as endochondral ossification, and this process bridges the fractured ends with mineralized bone [151, 153]. Within months, the fractured ends are united by bone, and the entire callus is comprised of woven bone creating a mechanically stable fracture [151, 153].

#### ***Remodelling phase***

Immature woven bone is slowly remodelled into mature lamellar bone, thus restoring bone to its original cortical and trabecular structure [153, 179]. Osteoblasts initiate osteoclastogenesis (the fusion of monocytic precursors to form osteoclasts) by secreting M-CSF and RANKL, which activate osteoclasts to commence woven bone resorption in the areas lacking mechanical load in callus [151, 183]. To reduce resorption, osteoblasts secrete osteoprotegerin (OPG); a decoy receptor for RANKL, which prevents RANKL binding to receptor activator of nuclear factor kappa- $\beta$  (RANK) receptors on the plasma membranes of osteoclasts, to result in a reduction in osteoclastic activity [184]. Simultaneously, osteoblasts begin to secrete lamellar bone in areas of mechanical loading [151]. Remodelling of fractures occurs in accordance to Wolff's law, which basically states bone formation occurs in areas of increasing load and resorption occurs in areas that are not loaded [151]. Eventually, bone is recanalized, and returned to its original morphology, and absent of scar tissue.

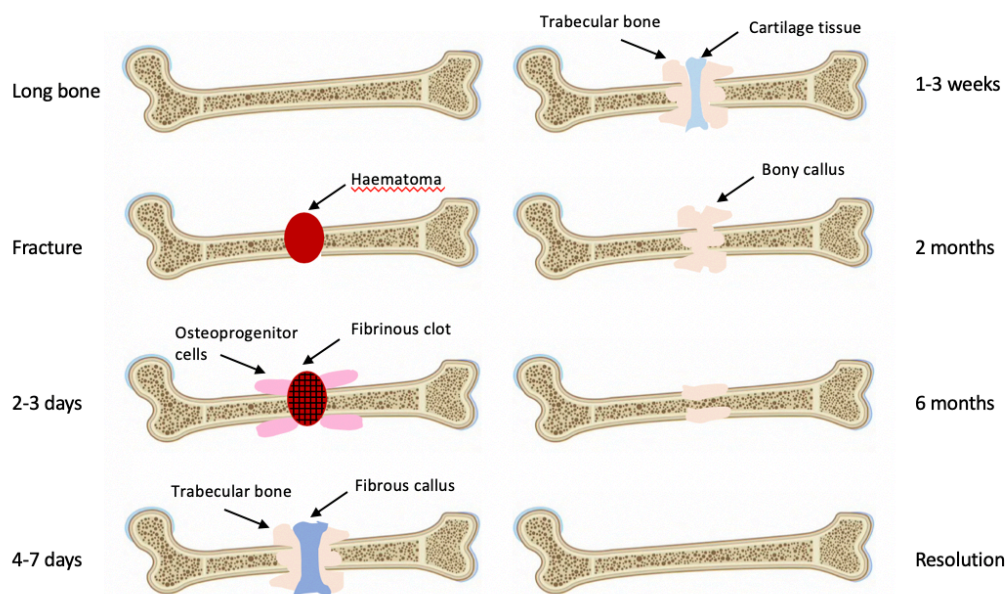


**Figure 1.2.** Illustration of the healing sequence in long bone fractures.

### **1.7.3. NGF and fracture healing**

#### **NGF function in bone healing and resorption**

Numerous studies have shown that NGF is able to modify fracture healing. The first group to demonstrate the potential roles of NGF in the healing of rat rib fractures occurred in 1997 [29]. Topical application of NGF to fractured rat ribs stimulated sympathetic nerve growth within fracture callus and as a result, accelerated the rate of healing [29]. Since this discovery, others have shown that in bone and callus remodelling, NGF may be important in maintaining resorption rates of bone, bone mineral density (BMD) and the conversion of woven bone to lamellar bone [27, 29, 31, 33, 186]. In a femoral mouse model, inhibition of NGF with anti-NGF antibody significantly increased the rate of bone resorption and caused a decreased BMD compared to wild-type mice [185], verifying that locally produced NGF has a regulatory role in normal bone metabolism. Furthermore, the administration of NGF accelerated remodelling processes, with delivery of 10 µg over 7 days of NGF to fractured rat rib calluses, increased the proportion of cartilage to fibrous tissue by 20%, in comparison to the control calluses at 21 days post-fracture [29].

#### **NGF function in bone healing and endochondral ossification**

Similarly, osseous tissue content was greater in NGF-treated calluses, suggesting that NGF promoted early endochondral ossification during fracture healing [27, 29, 33], which can again be supported by the vital role NGF has during endochondral ossification in developing bones [186]. Endochondral ossification rates were also enhanced with NGF treatment by increasing woven and lamellar bone content in callus gaps in animal models of distraction osteogenesis [27, 31, 32].

Distraction osteogenesis is also known as callus osteogenesis and is an osteotomy technique used in craniofacial and orthopaedic surgery to lengthen bones and as such generate a callus and induce bone formation via endochondral ossification, which is similar to that seen in fracture healing [187, 188]. NGF treatment in distraction osteogenesis also rapidly increased the rate of woven bone resorption and lamellar bone formation and mineralization [30, 33]. In one study, mineralization increased up to 19% in distraction osteogenesis calluses in response to NGF treatment [33], which indicates NGF ability to accelerate callus healing.

Lamellar and woven bone are mechanically stronger than fibrocartilaginous tissue [151, 153], and therefore, earlier transition of fibrocartilaginous tissue to woven and lamellar bone in healing calluses is associated with greater mechanical stability about the fracture site. By NGF treatment enhancing lamellar and woven bone content in the callus, it consequently increased the mechanical strength and load-bearing of calluses [27, 29, 31, 33]. Using a three-point bending apparatus, topical application of NGF to rat rib fracture calluses significantly increased breaking stress (the minimal load necessary to break bone [189]) by 260%, and Young's modulus (a measurement of bone rigidity [190]), by 350%, in comparison to controls [29]. The dramatic increase in mechanical strength was suggested to be a result of increased bone within callus, and a reduced callus cross-sectional area in response to accelerated remodelling [29], which is likely, as both measurements for breaking stress and Young's modulus incorporate cross-sectional area in their calculations [189, 190]. Other studies suggest the mechanically stronger calluses in NGF-treated calluses was a result of improved callus composition and enhanced mineralization, especially when calluses were equal in size in NGF-treated and control groups [27, 33]. Also, mechanical strength of fracture calluses was significantly increased as a result of advanced healing in the presence of NGF treatment.

As previously mentioned, apart from its role in the survival of sensory and sympathetic neurons in bone, a growing body of evidence suggests that NGF is produced and utilized by many osseous cells and other non-neural cells during fracture healing [28, 46, 66, 191]. NGF has been identified in osteoprogenitor cells, osteoblasts and certain chondrocytes during fracture healing [28, 46] and mandibular distraction osteogenesis [66]. Asaumi and co-workers reported that all chondrocytes within callus produce NGF during days 8-20 of endochondral ossification during fracture healing. However, other studies have reported only some chondrocytes stained for NGF during endochondral ossification within the same time-frame post-fracture [28, 46]. Additional studies indicate NGF stimulated and promoted differentiation and migration of osteoblasts to the fracture site [30, 46], which has been supported *in vitro*, by Yada and co-workers, who demonstrated that NGF treatment stimulated differentiation of cells of the osteoblastic lineage [191]. This same study showed that NGF treatment not only directly increased osteoblastic

production of alkaline phosphatase (ALP) and collagen type I [191], important bone forming proteins during osteoblast activity, but NGF also increased IL-6 production [191]. IL-6 is an important cytokine that is upregulated during the inflammatory phase of fracture healing [179], and therefore may have a role in the recruitment of inflammatory cells to the fracture site and the conversion of the haematoma into granulation tissue. Additionally, IL-6 has been shown to have a role in bone remodelling through stimulating osteoblasts to secrete pro-osteoclastic mediators, such as RANKL and parathyroid hormone related protein (PTHrP) to promote bone resorption, and more recently promote bone formation [192]. Furthermore, osteoblasts, osteocytes and chondrocytes all express the NGF high-affinity receptor, TrkA, suggesting NGF has a direct role in stimulating osseous cells during fracture healing via TrkA receptor signalling [46, 66, 193].

#### ***NGF function in bone healing and re-vascularization***

NGF may also be important in the re-vascularization of callus during endochondral ossification of fracture healing. During the first 21 days of healing in fractured rat ribs, endothelial cells within callus strongly expressed NGF, indicating that NGF has angiogenic properties [28]. Furthermore, NGF has been shown to directly activate endothelial cells by increasing endothelial cell proliferation [40], migration *in vitro* [194] and inducing capillary sprouting of human endothelial cells [40]. Similarly, during endochondral ossification of developing bones, progenitor cells secrete NGF within the cartilage matrix, which induced sensory innervation and capillary sprouting in the primary ossification sites and increased the number of active osteoblasts [186]. Therefore, it is highly possible NGF co-expressed with other angiogenic factors, promotes angiogenesis during fracture healing.

In summary, NGF is a pleiotropic factor that is locally produced and utilized by many cells participating in normal bone remodelling and fracture healing [28, 46, 191]. Key mechanisms to which NGF could influence fracture healing include re-establishment of nerves [29, 195], angiogenesis [29, 40, 41, 48, 186, 194] and stimulation of osseous cells to form bone [27, 29-31, 33, 46, 66, 186, 191]; all processes that can enhance fracture healing.

#### ***1.7.4. BDNF and fracture healing***

BDNF has also been associated with the process of fracture healing [46, 63]. BDNF is synthesized and released from several non-neural cells that are present in the fracture healing process and these cells include, leukocytes, fibroblasts, osteoblasts [46], and endothelial cells [61]. BDNF is expressed by these cells at various stages of fracture healing, therefore, it is suggested that BDNF may have numerous roles in this process [46, 63, 64]. In the inflammatory stages of fracture healing, BDNF and TrkB are expressed by haematopoietic cells, fibroblasts and endothelial cells [63]. These cells are important in the formation of a haematoma, and therefore, the

subsequent granulation tissue, which suggests that BDNF has a role during the early stages of fracture healing. Asami and colleagues, show BDNF mRNA expression is increased between days 2-8 in mice rib fracture callus tissue [46]. In the same study, immunohistochemistry detected BDNF in osteoblast-like cells in trabecular bone at the endochondral ossification front of healing mice rib fractures at 14-days [46]. Interestingly, TrkB receptors were not detected in any cells at any stage of fracture healing in mice rib calluses [46], which either suggests the BDNF expressed is acting on tissue other than bone in the fracture site, or it could be non-specificity of immunohistochemistry probing. In another study however, TrkB was reported in a several cells in human fracture calluses [63]. Furthermore, in human calluses BDNF and TrkB were reportedly regulated in osteoblasts at the ossification front during the osteoid phase and woven bone formation and was detected in human osteoblasts *in vitro* [63], which suggests that BDNF is important during the endochondral ossification process, but may also be involved in intramembranous ossification. The results in this human fracture study were supported in a rodent model of distraction osteogenesis, where BDNF expression was seen in osteoblasts and TrkB was expressed by both osteoblasts and hypertrophic chondrocytes during intramembranous ossification and endochondral ossification [66]. BDNF gene expression remained elevated 28-35 days post-osteotomy in callus, which is the transition period of when cartilage is replaced by woven bone and woven bone is remodelled of into lamellar bone [66].

One of the important processes that drives the transition of cartilage to woven bone as well as the remodelling process is the re-establishment of blood vessels within callus. BDNF has been shown *in vitro* and *in vivo* to directly stimulate endothelial cell migration, proliferation and the formation of new blood vessels [5, 61, 63, 196] as well as to increase the potent angiogenic factor VEGF [68]. Another mechanism through which BDNF may also promote fracture healing is via the direct upregulation of bone forming proteins ALP and BMP-2 in osteoblasts. BDNF treatment increased gene expression of ALP and BMP-2 in cementoblasts, cells that form mineral on the outer layer of tooth roots and function similarly to osteoblasts, therefore it is possible that BDNF may cause a similar effect on osteoblasts [197]. In summary, BDNF may participate in fracture healing through mediating angiogenesis and promoting the formation of bone, however, further studies are needed to determine the precise roles of this neurotrophin during bone healing.

#### **1.7.5. Therapies for fracture healing**

Surgical fixation of fractures is by far the most common treatment for fracture healing. The two main types of fixation for long bones are internal and external fixation. Internal fixation provides flexible fixation of fractures, consisting of locked nailing, bridge plating, and internal



fixator-like devices, which aim to align the fractured fragments of bone, providing long-term treatment and minimising surgical trauma to the surrounding tissue [198]. On the other hand, external fixation, the Ilizarov apparatus, is a temporary fixation device reserved for more severe fractures, that consists of either aluminium or titanium pins, or wires that insert into long bones and are connected to an external frame [198].

Two non-surgical approaches that are being developed to clinically enhance fracture healing are biophysical enhancement; electromagnetic field stimulation, and low-intensity pulsed ultrasonography [199-202], and biological enhancement; therapeutic use of recombinant human BMP-2 (rhBMP-2) and teriparatide [199, 203]. rhBMP-2 is currently the only drug the US Food and Drug Administration (FDA) has granted premarket approval for the treatment of open tibial fractures [199]. rhBMP-2 was approved in 2004, following a clinical trial of 450 people with open tibial fractures, which showed that rhBMP-2 impregnated collagen sponges inserted into tibial fractures reduced time to union, improved wound healing, and reduced the rate of infections compared to usual care patients [204]. Since then, two additional studies have concluded rhBMP-2 does not accelerate fracture healing. A double-blinded, randomised, controlled phase II-III trial of 180 patients showed rhBMP-2 did not shorten fracture union compared to usual care patients [199, 205]. A similar study additionally showed no change in fracture union of open tibial fractures treated with rhBMP-2 impregnated sponge [206].

Teriparatide is a synthetic polypeptide hormone that contains the 1-34 amino acid fragment of recombinant human parathyroid hormone (rhPTH) [207]. Teriparatide is not approved by the FDA, yet there are several clinical trials investigating its effectiveness in enhancing fracture healing. In an initial observational study, teriparatide seemed to improve fracture healing by reducing time to union in intertrochanteric fractures of patient with osteoporosis [208]. Furthermore, in a randomised trial of 65 women with pelvic fractures, teriparatide accelerated fracture healing by also reducing time to union [208]. These two studies showed promising data for the use of teriparatide in fracture healing, however, data is inconsistent when compared to randomised clinical trials. A randomised double-blind study of 102 post-menopausal women, showed that teriparatide did not improve fracture healing in distal radial fractures [210]. Similarly, teriparatide showed no radiographic enhancement of healing in the fractures of the proximal humerus, in a randomised control study of 40 post-menopausal women [211].

The limited availability and effectiveness of pharmacological therapies accessible for fracture healing warrants investigations into novel molecules that would improve or accelerate bone healing as an adjunct to surgical treatment.

### **1.7.6. Animal models of fracture healing**

In an attempt to understand the processes of bone healing and their possible treatments, a variety of fracture healing animal models have been used over the years [212-216]. As orthopaedic surgery advanced, and new techniques were developed for the treatment of fractures, animal models also progressed to better replicate fractures in a clinical setting. The most effective species used in animal models of fracture healing are rodents due to low cost, multiple housing, and the many parameters that can be measured including mechanical testing, histological evaluation and molecular biological studies, that are translatable to human fracture healing [213]. Subsequently, there are several of types of animal models, including fixed and non-fixed long bone fractures, which are used in mice to analyse endochondral healing [213, 217, 218].

#### ***Fixed long bone fracture models***

Fixed, long bone fractures involve the insertion of an intramedullary rod into the medullary cavity to stabilise the fracture site and is commonly used in femoral and tibial fracture healing [212, 213, 218, 219]. Femora are straight bones with relatively equal diameter down the diaphysis of bone, which allows for consistently reproducible fractures [217, 218]. For a standard intramedullary, pinned, closed-femoral fracture, an incision is made medial to the patella, and an intramedullary rod (0.25 mm stainless steel wire) is inserted into the medullary cavity at the intercondylar notch and sealed via a small wedge [218]. After insertion of the rod, a transverse mid-diaphyseal fracture of the femur is made using a three-point bending device [218]. Common parameters used to measure endochondral fracture healing following fixed femoral fractures include mechanical assessment, microcomputed tomography ( $\mu$ CT) analysis, histomorphometry and molecular analysis [213, 220, 221]. One recurring problem with the closed femoral fracture is the large muscle mass surrounding the femur, which makes it is difficult to perform closed surgeries using this type of model [213, 216, 218]. Additionally, the femoral model can be prone to unstable intramedullary rod fixation when only an intramedullary rod is inserted, as seen in numerous mouse models [221-223]. Lack of stability leads to a decrease in axial and rotational stability and increased risk of dislocation, which affects the biomechanical environment of bone and impairs the rate of healing [217, 218]. To counteract the lack of stability, invasive open-fracture surgeries are performed with addition of implants that include intramedullary pins, intramedullary locking nails, intramedullary compression screws, external fixators, pin-clips and locking plates, to stabilise the intramedullary rod and prevent rotation during fracture healing [217, 218, 224]. Using multiple implants during surgery, however, requires very precise animal surgical expertise, and if required, secondary surgery for implant removal [217].

Tibial fracture is the most established fracture model and was the first fracture model to be standardized by Hiltunen and colleagues in 1993 [225]. In a standard, closed tibial fracture, an

incision is made and the proximal, antero-medial surface of the leg, and an intramedullary rod (0.2 mm stainless steel rod) is inserted down the medullary cavity of the tibia [225]. Traditionally, an impact device was used to create a transverse or a slightly oblique tibial fracture in the mid-diaphysis, however, recent studies show an equivalent fracture can be made using a pair of modified skin staple removers [225-229]. Rate of endochondral fracture healing using the mouse tibial fracture is commonly measured by mechanical assessment,  $\mu$ CT and histological analyses [226, 227]. Open tibial fracture models are produced by increasing incision size and scraping away the periosteal surface of the tibia [226]. An important decision when using either the closed- or open-tibial fracture is the site of fracture along the diaphysis. The tibia is fused distally with the fibula and can be itself prone to fracturing during the tibial fracture surgery [218, 225]. Combined tibial and fibular fractures can result in a fused tibial and fibular callus, or two separate calluses forming each bone [218, 225]. A mid-high diaphyseal tibial fracture or tibial fracture below the fusion of the tibia and fibula are shown to have lower incidence of dual bone fractures and are therefore recommended as the fracture of choice [218, 226].

#### ***Non-fixed long bone fracture models***

Non-fixed, long bone fracture models are used in mice and rats on bones with low weight-bearing capability. During rib fractures the superficial muscles of the back are laterally retracted and an osteotomy is made on the posterior-lateral aspect of the eighth rib using scissors [28, 29, 230-233]. Rib fracture models are useful when examining molecular changes during fracture healing [213], however, treatment route of administration that requires gross movement of fractures, such as scruffing mice for intraperitoneal injections and osmotic pump insertion are unfeasible due to the position of dorsal rib fractures and can disrupt the biomechanical environment and impair fracture healing.

Fibular fractures in mice is another non-fixed, long bone fracture. This is a low invasive surgery, where a 5 mm incision is made over the fibula, and using osteotomy scissors the fibula is fractured [234, 235]. Studies have shown the fibular fracture model is suitable for mechanical assessment, histological analysis and  $\mu$ CT analysis in various stages of endochondral fracture healing [233, 235]. An advantage of the fibular fracture model is fracture fixation is not required, this is because the tibia and fibula are fused distally in mice, and the fibula bears less than 5% body weight. Additionally, the fibular fracture model can be performed bilaterally in mice, which allows a wider range of post-mortem analysis and a reduction in the number of animals used compared to the unilateral, fixed tibial and femoral fracture models [234].

## **1.8. Trk receptor ligands as possible therapeutic agents for TBI and fracture healing**

New approaches have been explored in the pharmaceutical industry for the development of non-peptide molecules that selectively bind and activate Trk receptors [236]. Trk signalling can be modified with neurotrophin ligands through direct modification of the receptor action. Using either agonists or antagonists, pharmacological therapies can increase or decrease Trk signalling, block the action of antagonists, or increase local synthesis of neurotrophins [236]. Several Trk receptor ligands have been developed, and their efficacy in *in vitro* and *in vivo* models have been investigated. For TrkA, four agonists have been developed and all stimulate Trk phosphorylation; D3 [236], amitriptyline [238], MT-2 [239], and gambogic amide (GA) [141], however, only GA shows selective, potent TrkA activity [141]. D3 is only a partial agonist [237], amitriptyline is non-specific; binding to both TrkA and TrkB [238], and MT-2 is less potent than the other agonists, and only stimulates low TrkA phosphorylation [239].

Additionally, there are several partial agonists that have shown TrkB activation [240], and full agonists including, non-specific amitriptyline as mentioned before, non-specific BNN-20 (binds to TrkA, TrkB and p75NTR) [241], and selectively potent 7,8-dihydroxyflavone (7,8-DHF) [242]. By far, 7,8-DHF has shown most promise to use as a pharmacological agent of TrkB agonism, which is described in **section 1.8.2** [242]. For more comprehensive information on all the above-mentioned ligands, please refer to these articles. In summary, the two most promising non-peptide molecules that have been discovered to show robust neurotrophic activity are the selective TrkA agonist, gambogic amide (GA) and the selective TrkB agonist, 7,8-dihydroxyflavone (7,8-DHF) [141, 242], which will be described in the next sections.

### **1.8.1. GA as a therapeutic drug**

GA is a derivative of gambogic acid, a substance sourced from the *Garcinia hanburryi* tree, which is located in South East Asia [141]. GA is a potent molecule that selectively binds to and stimulates TrkA receptors, similarly to that of NGF [141]. When applied to the murine PC12 cell line and primary hippocampal neurons *in vitro*, GA induced TrkA receptor phosphorylation [141], and stimulated neurite outgrowth [243, 244], thus displaying its effectiveness at TrkA receptor activation. GA is also BBB penetrable, this was seen when systemic administration of 2 mg/kg/day via intraperitoneal injection of GA for 3 weeks in C57BL/6 mice resulted in TrkA phosphorylation in the brain [142], and 0.5-4 mg/kg/day of GA upregulated TrkA hippocampal protein and mRNA levels in C57BL/6 mice after 5 days of treatment [244]. Additionally, GA protects neurons from apoptosis; this is evident via *in vitro* and *in vivo* studies. *In vitro*, GA protected hippocampal neurons from glutamate triggered apoptosis and PC12 cells from oxygen-glucose deprivation [141]. In addition, *in vivo* studies showed that 2 mg/kg/day of GA systemically administered in

mice protected neurons from kainic-induced cellular apoptosis and reduced infarct volume in the brain in a transient model of ischemic stroke [141]. Furthermore, GA is a more attractive pharmaceutical agent than NGF, with a 10-fold greater half-life than NGF [245]. To date, there have been no investigations or reports of the therapeutic potential of GA in TBI or in bone metabolism and fracture healing. Hence, it would be beneficial to observe the effects of GA treatment in TBI, bone metabolism and the process of fracture healing.

### **1.8.2. 7,8-DHF as a therapeutic drug**

Flavonoids are sourced from a variety of plants and many fruits and vegetables [246]. Research into flavonoids has increased due to their antioxidant effects, some of which include anti-inflammatory effects [246], protection against infectious agents [247], cancers and cardiovascular diseases [248] and their neuroprotective actions [249]. 7,8-dihydroxyflavone (7,8-DHF) is a flavonoid derivative that is isolated from *Tridax procumbens* and the leaves of *Primula* trees [250]. Preliminary data of 7,8-DHF showed it to be a selective TrkB agonist with potent neurotrophic activity, including activation of TrkB receptors in the brain of BDNF knockout mice, reducing kainic acid-induced apoptosis in mouse hippocampal neurons at 5 mg/kg/day and reducing infarct volume of the brain in a transient mouse model of ischemic injury [242]. *In vitro*, 7,8-DHF protected hippocampal neurons and T48 murine cells from oxygen-glucose deprivation-induced apoptosis [242] and upregulated TrkB signalling in retinal ganglion cell line [251]. In the case of *in vivo* animal experiments, treatment of 7,8-DHF at doses of 5 mg/kg/day has shown to protect neurons from death induced by TBI [252, 253], as well as improve neurological functions in rodent models of TBI [254, 255], depression [256], Alzheimer's disease [257, 258], aging [259] and stress [260]. 7,8-DHF is well tolerated in rodent models with no detrimental effects reported in mice and there has not been any data describing the effects of 7,8-DHF on the skeletal system [242]. Thus, it would be beneficial to look at the effects of 7,8-DHF on bone as well as the process of bone fracture healing.

## **1.9. BDNF polymorphisms**

### **1.9.1. BDNF polymorphism and BMD**

BDNF polymorphism is a single nucleotide polymorphic (SNP) genetic variation in the non-coding region of BDNF on chromosome 11 [261]. The location where the SNP occurs is codon 6, also known as Val66Met or rs6265, and is located in the pro-BDNF (immature form of BDNF) region [262, 263]. The SNP results in the substitution of C to T, which transforms the amino acid valine (Val) into methionine (Met) [263]. The three genotypes that arise from this SNP are Val/Val, Val/Met, and Met/Met. Epidemiological studies have shown genotype frequency varies based on ethnicity, and most notably amongst Caucasian and Asian populations [264-268]. The genotype

frequency in Caucasian populations is Val/Val (64%), Val/Met (33%) and Met/Met (3%) and is the same in both sexes [264]. Asian population genotype frequency of Val/Met and Met/Met is increased [264, 267], and varies between the sexes; with male Val/Val (28%), female Val/Val (34%); male Val/Met (53%), female Val/Met (38%); male Met/Met (19%), and female Met/Met (28%) [264]. Additionally, genotype variation in combination with ethnicity determines increased susceptibility for specific conditions, and not all diseases associated with polymorphism variation are seen across ethnicities [267].

The effect of BDNF polymorphism is heavily researched in the fields of neurology and psychiatry and is based on the strong correlation between Met substitution, subsequent reduction in BDNF levels, and the predisposition of neuropsychiatric disorders that include schizophrenia, Alzheimer's disease, depression and bipolar affective disorder [261, 269-272]. More recently, a publication was released that implicated BDNF polymorphism and bone [273]. BMD of Caucasian and Asian BDNF polymorphic populations was measured and found that BMD in the Caucasian population was affected more than the Asian population. In the Caucasian population, the Met/Met genotype had significantly reduced BMD compared to Val/Val and Val/Met genotypes [273], and there was no difference between BMD and BDNF polymorphism in Asian populations [273], which can be supported by the theory that genotype and ethnicity together determine susceptibility to disease. In the same study, mechanisms on how BDNF polymorphism influenced bone integrity was explored via *in vitro* methods. Primary osteoblasts transfected with BDNF<sup>MET</sup>, had overall decreased BDNF phosphorylation and reduced expression of osteoblastic markers; BMP-1, ALP and osteopontin [273], which suggests that Met substitution is detrimental to bone formation to result in reduced BMD.

Mouse models of BDNF polymorphism; Val/Val, Val/Met, Met/Met, were developed to study common behavioural changes associated with neuropsychiatric disorders such as schizophrenia and Alzheimer's disease [263, 272]. The behavioural changes, including anxiety-like behaviour and cognitive impairments seen in certain neuropsychiatric disorders as a result of BDNF polymorphism, are comparable between mice and humans, which supports the continual use of mouse models to study BDNF polymorphism [263]. There are currently no data that show whether the altered BMD phenotype seen in humans as a result of BDNF polymorphism, is translated into the mouse model, and thus this is an area to be further investigated.

### 1.10. Research aims and hypotheses

The general aim of this thesis was to investigate the roles of TrkA and TrkB in two murine models of injury; TBI and long bone fracture healing by using TrkA agonist, GA, and TrkB agonist, 7,8-DHF, and BDNF polymorphism variants in a BDNF<sup>Val66Met</sup> mouse line. Specifically;

**Chapter 2** summaries all general methodology used for animal studies and cell culture experiments.

**Chapter 3** examines the effects of TrkA agonist, GA, on acute pathophysiological processes and behavioural outcomes of TBI.

*Hypothesis* – Treating acute moderate-severe TBI with 2 mg/kg/day of TrkA agonist, GA, will have a positive effect on processes of neuroinflammation, cellular apoptosis, neurite outgrowth, synaptogenesis and behavioural outcomes in mice.

*Aims* – The aims of this study were to investigate GA treatment in a murine moderate-severe LFPI model as a pharmacotherapy for TBI, focussing on the outcomes of several behavioural paradigms including sensorimotor, anxiety-like behaviour and spatial memory, cerebral oedema, neuroinflammation, cellular apoptosis and synaptogenesis.

**Chapter 4** examines the effects of TrkA agonist, GA, on fracture healing and osteogenic cells *in vitro*.

*Hypothesis* – TrkA agonist, GA, will have positive effects on fracture healing.

*Aims* – The aims of this study were to explore the influence of 1 mg/kg/day GA treatment in a bilateral fibular fracture model as a potential therapy for fracture healing, and investigated the outcome of TrkA activation on mechanical properties, bone formation and osteoclastogenesis in endochondral fracture healing.

**Chapter 5** investigates the effects of TrkB agonist, 7,8-DHF, on fracture healing and osteogenic cells *in vitro*, and BMD changes in BDNF polymorphism variants in BDNF<sup>Val66Met</sup> mice.

*Hypotheses* – i) TrkB agonist, 7,8-DHF, will have positive effects on fracture healing. ii) BMD will differ between BDNF polymorphism variant mice, Met/Met mice will have lower BMD, than Val/Val and Val/Met.

*Aims* – i) The effects of selective TrkB agonist, 7,8-DHF treatment on biomechanical properties, bone formation and osteoclastogenesis, in a closed tibial fracture model of fracture healing in mice was investigated. ii) Femora of mice with BDNF polymorphisms were assessed via peripheral quantitative computed tomography (pQCT) to observe if there were any changes in BMD among variants.

### 1.11. References

1. Reichardt, L.F., *Neurotrophin-regulated signalling pathways*. Philos Trans R Soc Lond B Biol Sci, 2006. **361**(1473): p. 1545-64.
2. Thoenen, H., *Neurotrophins and neuronal plasticity*. Science, 1995. **270**(5236): p. 593-8.
3. Huang, E.J. and L.F. Reichardt, *Neurotrophins: roles in neuronal development and function*. Annu Rev Neurosci, 2001. **24**: p. 677-736.
4. Chao, M.V., *Neurotrophins and their receptors: a convergence point for many signalling pathways*. Nat Rev Neurosci, 2003. **4**(4): p. 299-309.
5. Kermani, P., D. Rafii, D.K. Jin, P. Whitlock, W. Schaffer, A. Chiang, L. Vincent, M. Friedrich, K. Shido, N.R. Hackett, R.G. Crystal, S. Rafii, and B.L. Hempstead, *Neurotrophins promote revascularization by local recruitment of TrkB+ endothelial cells and systemic mobilization of hematopoietic progenitors*. J Clin Invest, 2005. **115**(3): p. 653-63.
6. Su, Y.W., X.F. Zhou, B.K. Foster, B.L. Grills, J. Xu, and C.J. Xian, *Roles of neurotrophins in skeletal tissue formation and healing*. J Cell Physiol, 2018. **233**(3): p. 2133-2145.
7. Lewin, G.R. and Y.A. Barde, *Physiology of the neurotrophins*. Annu Rev Neurosci, 1996. **19**: p. 289-317.
8. Nilsson, A.S., M. Fainzilber, P. Falck, and C.F. Ibanez, *Neurotrophin-7: a novel member of the neurotrophin family from the zebrafish*. FEBS Lett, 1998. **424**(3): p. 285-90.
9. Gotz, R., R. Koster, C. Winkler, F. Raulf, F. Lottspeich, M. Scharf, and H. Thoenen, *Neurotrophin-6 is a new member of the nerve growth factor family*. Nature, 1994. **372**(6503): p. 266-9.
10. Sofroniew, M.V., C.L. Howe, and W.C. Mobley, *Nerve growth factor signaling, neuroprotection, and neural repair*. Annu Rev Neurosci, 2001. **24**: p. 1217-81.
11. Levi-Montalcini, R. and V. Hamburger, *Selective growth stimulating effects of mouse sarcoma on the sensory and sympathetic nervous system of the chick embryo*. J Exp Zool, 1951. **116**(2): p. 321-61.
12. Cohen, S., R. Levi-Montalcini, and V. Hamburger, *A Nerve Growth-Stimulating Factor Isolated from Sarcoma 37 and 180*. Proc Natl Acad Sci U S A, 1954. **40**(10): p. 1014-8.
13. Micera, A., A. Lambiase, B. Stampacchia, S. Bonini, and F. Levi-Schaffer, *Nerve growth factor and tissue repair remodeling: trkA(NGFR) and p75(NTR), two receptors one fate*. Cytokine Growth Factor Rev, 2007. **18**(3-4): p. 245-56.
14. Levi-Montalcini, R., *The nerve growth factor 35 years later*. Science, 1987. **237**(4819): p. 1154-62.
15. Levi-Montalcini, R. and P.U. Angeletti, *Nerve growth factor*. Physiol Rev, 1968. **48**(3): p. 534-69.



16. Levi-Montalcini, R., F. Caramia, S.A. Luse, and P.U. Angeletti, *In vitro effects of the nerve growth factor on the fine structure of the sensory nerve cells*. Brain Res, 1968. **8**(2): p. 347-62.
17. Levi-Montalcini, R. and S. Cohen, *In Vitro and in Vivo Effects of a Nerve Growth-Stimulating Agent Isolated from Snake Venom*. Proc Natl Acad Sci U S A, 1956. **42**(9): p. 695-9.
18. Levi-Montalcini, R., H. Meyer, and V. Hamburger, *In vitro experiments on the effects of mouse sarcomas 180 and 37 on the spinal and sympathetic ganglia of the chick embryo*. Cancer Res, 1954. **14**(1): p. 49-57.
19. Bonini, S., A. Lambiase, S. Bonini, F. Angelucci, L. Magrini, L. Manni, and L. Aloe, *Circulating nerve growth factor levels are increased in humans with allergic diseases and asthma*. Proc Natl Acad Sci U S A, 1996. **93**(20): p. 10955-60.
20. Matsuda, H., Y. Kannan, H. Ushio, Y. Kiso, T. Kanemoto, H. Suzuki, and Y. Kitamura, *Nerve growth factor induces development of connective tissue-type mast cells in vitro from murine bone marrow cells*. J Exp Med, 1991. **174**(1): p. 7-14.
21. Lawman, M.J., M.D. Boyle, A.P. Gee, and M. Young, *Nerve growth factor accelerates the early cellular events associated with wound healing*. Exp Mol Pathol, 1985. **43**(2): p. 274-81.
22. Tuveri, M., S. Generini, M. Matucci-Cerinic, and L. Aloe, *NGF, a useful tool in the treatment of chronic vasculitic ulcers in rheumatoid arthritis*. Lancet, 2000. **356**(9243): p. 1739-40.
23. Lambiase, A., P. Rama, S. Bonini, G. Caprioglio, and L. Aloe, *Topical treatment with nerve growth factor for corneal neurotrophic ulcers*. N Engl J Med, 1998. **338**(17): p. 1174-80.
24. Bernabei, R., F. Landi, S. Bonini, G. Onder, A. Lambiase, R. Pola, and L. Aloe, *Effect of topical application of nerve-growth factor on pressure ulcers*. Lancet, 1999. **354**(9175): p. 307.
25. Kasemkijwattana, C., Menetrey, J., Bosch, P., Somogyi, G., Moreland, M. S., Fu, F. H., Buranapanitkit, B., Watkins, S. S., Huard, J., ***Use of growth factors to improve muscle healing after strain injury***. Clin Orthop Relat Res, 2000. **370**: p. 272-285.
26. Bao, Y.N., F. Huang, X.F. Tang, Y. Wen, Z.C. Shan, and J.Y. Zeng, *[Effect of nerve growth factor on the early phase of osseointegration around oral implants]*. Zhonghua Kou Qiang Yi Xue Za Zhi, 2010. **45**(11): p. 687-90.
27. Cao, J., L. Wang, D.L. Lei, Y.P. Liu, Z.J. Du, and F.Z. Cui, *Local injection of nerve growth factor via a hydrogel enhances bone formation during mandibular distraction osteogenesis*. Oral Surg Oral Med Oral Pathol Oral Radiol, 2012. **113**(1): p. 48-53.
28. Grills, B.L. and J.A. Schuijers, *Immunohistochemical localization of nerve growth factor in fractured and unfractured rat bone*. Acta Orthop Scand, 1998. **69**(4): p. 415-9.
29. Grills, B.L., J.A. Schuijers, and A.R. Ward, *Topical application of nerve growth factor improves fracture healing in rats*. J Orthop Res, 1997. **15**(2): p. 235-42.

30. Letic-Gavrilovic, A., A. Piattelli, and K. Abe, *Nerve growth factor beta(NGF beta) delivery via a collagen/hydroxyapatite (Col/HAp) composite and its effects on new bone ingrowth.* J Mater Sci Mater Med, 2003. **14**(2): p. 95-102.
31. Wang, L., J. Cao, D.L. Lei, X.B. Cheng, H.Z. Zhou, R. Hou, Y.H. Zhao, and F.Z. Cui, *Application of nerve growth factor by gel increases formation of bone in mandibular distraction osteogenesis in rabbits.* Br J Oral Maxillofac Surg, 2010. **48**(7): p. 515-9.
32. Wang, L., Y. Zhao, X. Cheng, Y. Yang, G. Liu, Q. Ma, H. Shang, L. Tian, and D. Lei, *Effects of locally applied nerve growth factor to the inferior alveolar nerve histology in a rabbit model of mandibular distraction osteogenesis.* Int J Oral Maxillofac Surg, 2009. **38**(1): p. 64-9.
33. Wang, L., S. Zhou, B. Liu, D. Lei, Y. Zhao, C. Lu, and A. Tan, *Locally applied nerve growth factor enhances bone consolidation in a rabbit model of mandibular distraction osteogenesis.* J Orthop Res, 2006. **24**(12): p. 2238-45.
34. Yasui, M., Y. Shiraishi, N. Ozaki, K. Hayashi, K. Hori, M. Ichianagi, and Y. Sugiura, *Nerve growth factor and associated nerve sprouting contribute to local mechanical hyperalgesia in a rat model of bone injury.* Eur J Pain, 2012. **16**(7): p. 953-65.
35. Maisonpierre, P.C., L. Belluscio, B. Friedman, R.F. Alderson, S.J. Wiegand, M.E. Furth, R.M. Lindsay, and G.D. Yancopoulos, *NT-3, BDNF, and NGF in the developing rat nervous system: parallel as well as reciprocal patterns of expression.* Neuron, 1990. **5**(4): p. 501-9.
36. Kawamoto, K. and H. Matsuda, *Nerve growth factor and wound healing.* Prog Brain Res, 2004. **146**: p. 369-84.
37. Werner, S. and R. Grose, *Regulation of wound healing by growth factors and cytokines.* Physiol Rev, 2003. **83**(3): p. 835-70.
38. Scuri, M., L. Samsell, and G. Piedimonte, *The role of neurotrophins in inflammation and allergy.* Inflamm Allergy Drug Targets, 2010. **9**(3): p. 173-80.
39. Graiani, G., C. Emanuelli, E. Desortes, S. Van Linthout, A. Pinna, C.D. Figueroa, L. Manni, and P. Madeddu, *Nerve growth factor promotes reparative angiogenesis and inhibits endothelial apoptosis in cutaneous wounds of Type 1 diabetic mice.* Diabetologia, 2004. **47**(6): p. 1047-54.
40. Raychaudhuri, S.K., S.P. Raychaudhuri, H. Weltman, and E.M. Farber, *Effect of nerve growth factor on endothelial cell biology: proliferation and adherence molecule expression on human dermal microvascular endothelial cells.* Arch Dermatol Res, 2001. **293**(6): p. 291-5.
41. Emanuelli, C., M.B. Salis, A. Pinna, G. Graiani, L. Manni, and P. Madeddu, *Nerve growth factor promotes angiogenesis and arteriogenesis in ischemic hindlimbs.* Circulation, 2002. **106**(17): p. 2257-62.

42. Niewiadomska, G., A. Mietelska-Porowska, and M. Mazurkiewicz, *The cholinergic system, nerve growth factor and the cytoskeleton*. Behav Brain Res, 2011. **221**(2): p. 515-26.
43. Goss, J.R., M.E. O'Malley, L. Zou, S.D. Styren, P.M. Kochanek, and S.T. DeKosky, *Astrocytes are the major source of nerve growth factor upregulation following traumatic brain injury in the rat*. Exp Neurol, 1998. **149**(2): p. 301-9.
44. Zhang, Y.W., J. Denham, and R.S. Thies, *Oligodendrocyte progenitor cells derived from human embryonic stem cells express neurotrophic factors*. Stem Cells Dev, 2006. **15**(6): p. 943-52.
45. Yamamoto, M., G. Sobue, K. Yamamoto, S. Terao, and T. Mitsuma, *Expression of mRNAs for neurotrophic factors (NGF, BDNF, NT-3, and GDNF) and their receptors (p75NGFR, trkA, trkB, and trkC) in the adult human peripheral nervous system and nonneural tissues*. Neurochem Res, 1996. **21**(8): p. 929-38.
46. Asaumi, K., T. Nakanishi, H. Asahara, H. Inoue, and M. Takigawa, *Expression of neurotrophins and their receptors (TRK) during fracture healing*. Bone, 2000. **26**(6): p. 625-33.
47. Vega, J.A., O. Garcia-Suarez, J. Hannestad, M. Perez-Perez, and A. Germana, *Neurotrophins and the immune system*. J Anat, 2003. **203**(1): p. 1-19.
48. Cantarella, G., L. Lempereur, M. Presta, D. Ribatti, G. Lombardo, P. Lazarovici, G. Zappala, C. Pafumi, and R. Bernardini, *Nerve growth factor-endothelial cell interaction leads to angiogenesis in vitro and in vivo*. FASEB J, 2002. **16**(10): p. 1307-9.
49. Fox, A.J., H.J. Patel, P.J. Barnes, and M.G. Belvisi, *Release of nerve growth factor by human pulmonary epithelial cells: role in airway inflammatory diseases*. Eur J Pharmacol, 2001. **424**(2): p. 159-62.
50. Johnson, E.M., Jr., M. Taniuchi, and P.S. DiStefano, *Expression and possible function of nerve growth factor receptors on Schwann cells*. Trends Neurosci, 1988. **11**(7): p. 299-304.
51. Cheret, J., N. Lebonvallet, J.L. Carre, L. Misery, and C. Le Gall-Ianotto, *Role of neuropeptides, neurotrophins, and neurohormones in skin wound healing*. Wound Repair Regen, 2013. **21**(6): p. 772-88.
52. Friedman, W.J. and L.A. Greene, *Neurotrophin signaling via Trks and p75*. Exp Cell Res, 1999. **253**(1): p. 131-42.
53. Barbacid, M., *The Trk family of neurotrophin receptors*. J Neurobiol, 1994. **25**(11): p. 1386-403.
54. Shibayama, E. and H. Koizumi, *Cellular localization of the Trk neurotrophin receptor family in human non-neuronal tissues*. Am J Pathol, 1996. **148**(6): p. 1807-18.
55. Lee, R., P. Kermani, K.K. Teng, and B.L. Hempstead, *Regulation of cell survival by secreted proneurotrophins*. Science, 2001. **294**(5548): p. 1945-8.

56. Chao, M.V. and B.L. Hempstead, *p75 and Trk: a two-receptor system*. Trends Neurosci, 1995. **18**(7): p. 321-6.
57. Wheeler, E.F., H. Gong, R. Grimes, D. Benoit, and L. Vazquez, *p75NTR and Trk receptors are expressed in reciprocal patterns in a wide variety of non-neural tissues during rat embryonic development, indicating independent receptor functions*. J Comp Neurol, 1998. **391**(4): p. 407-28.
58. Pan, W., K.L. Kremer, X. Kaidonis, V.E. Ludlow, M.L. Rogers, J. Xie, C.G. Proud, and S.A. Koblar, *Characterization of p75 neurotrophin receptor expression in human dental pulp stem cells*. Int J Dev Neurosci, 2016. **53**: p. 90-8.
59. Barde, Y.A., D. Edgar, and H. Thoenen, *Purification of a new neurotrophic factor from mammalian brain*. EMBO J, 1982. **1**(5): p. 549-53.
60. Bathina, S. and U.N. Das, *Brain-derived neurotrophic factor and its clinical implications*. Arch Med Sci, 2015. **11**(6): p. 1164-78.
61. Kermani, P. and B. Hempstead, *Brain-derived neurotrophic factor: a newly described mediator of angiogenesis*. Trends Cardiovasc Med, 2007. **17**(4): p. 140-3.
62. Oyesiku, N.M., C.O. Evans, S. Houston, R.S. Darrell, J.S. Smith, Z.L. Fulop, C.E. Dixon, and D.G. Stein, *Regional changes in the expression of neurotrophic factors and their receptors following acute traumatic brain injury in the adult rat brain*. Brain Res, 1999. **833**(2): p. 161-72.
63. Kilian, O., S. Hartmann, N. Dongowski, S. Karnati, E. Baumgart-Vogt, F.V. Hartel, T. Noll, R. Schnettler, and K.S. Lips, *BDNF and its TrkB receptor in human fracture healing*. Ann Anat, 2014. **196**(5): p. 286-95.
64. Botchkarev, V.A., M. Metz, N.V. Botchkareva, P. Welker, M. Lommatzsch, H. Renz, and R. Paus, *Brain-derived neurotrophic factor, neurotrophin-3, and neurotrophin-4 act as "epitheliotrophins" in murine skin*. Lab Invest, 1999. **79**(5): p. 557-72.
65. Cartwright, M., A.M. Mikheev, and G. Heinrich, *Expression of neurotrophin genes in human fibroblasts: differential regulation of the brain-derived neurotrophic factor gene*. Int J Dev Neurosci, 1994. **12**(8): p. 685-93.
66. Aiga, A., K. Asami, Y.J. Lee, H. Kadota, S. Mitani, T. Ozaki, and M. Takigawa, *Expression of neurotrophins and their receptors tropomyosin-related kinases (Trk) under tension-stress during distraction osteogenesis*. Acta Med Okayama, 2006. **60**(5): p. 267-77.
67. Calabrese, F., A.C. Rossetti, G. Racagni, P. Gass, M.A. Riva, and R. Molteni, *Brain-derived neurotrophic factor: a bridge between inflammation and neuroplasticity*. Front Cell Neurosci, 2014. **8**: p. 430.
68. Lin, C.Y., S.Y. Hung, H.T. Chen, H.K. Tsou, Y.C. Fong, S.W. Wang, and C.H. Tang, *Brain-derived neurotrophic factor increases vascular endothelial growth factor expression and*

- enhances angiogenesis in human chondrosarcoma cells*. *Biochem Pharmacol*, 2014. **91**(4): p. 522-33.
69. Swanwick, C.C., M.B. Harrison, and J. Kapur, *Synaptic and extrasynaptic localization of brain-derived neurotrophic factor and the tyrosine kinase B receptor in cultured hippocampal neurons*. *J Comp Neurol*, 2004. **478**(4): p. 405-17.
  70. Shen, L., W. Zeng, Y.X. Wu, C.L. Hou, W. Chen, M.C. Yang, L. Li, Y.F. Zhang, and C.H. Zhu, *Neurotrophin-3 accelerates wound healing in diabetic mice by promoting a paracrine response in mesenchymal stem cells*. *Cell Transplant*, 2013. **22**(6): p. 1011-21.
  71. Hyder, A.A., C.A. Wunderlich, P. Puvanachandra, G. Gururaj, and O.C. Kobusingye, *The impact of traumatic brain injuries: a global perspective*. *NeuroRehabilitation*, 2007. **22**(5): p. 341-53.
  72. Xiong, Y., A. Mahmood, and M. Chopp, *Animal models of traumatic brain injury*. *Nat Rev Neurosci*, 2013. **14**(2): p. 128-42.
  73. Roozenbeek, B., A.I. Maas, and D.K. Menon, *Changing patterns in the epidemiology of traumatic brain injury*. *Nat Rev Neurol*, 2013. **9**(4): p. 231-6.
  74. Blennow, K., J. Hardy, and H. Zetterberg, *The neuropathology and neurobiology of traumatic brain injury*. *Neuron*, 2012. **76**(5): p. 886-99.
  75. Maas, A.I., B. Roozenbeek, and G.T. Manley, *Clinical trials in traumatic brain injury: past experience and current developments*. *Neurotherapeutics*, 2010. **7**(1): p. 115-26.
  76. Maas, A.I., N. Stocchetti, and R. Bullock, *Moderate and severe traumatic brain injury in adults*. *Lancet Neurol*, 2008. **7**(8): p. 728-41.
  77. Tator, C.H., *Concussions and their consequences: current diagnosis, management and prevention*. *CMAJ*, 2013. **185**(11): p. 975-979.
  78. Johnson, V.E., W. Stewart, and D.H. Smith, *Axonal pathology in traumatic brain injury*. *Exp Neurol*, 2013. **246**: p. 35-43.
  79. Kumar, A. and D.J. Loane, *Neuroinflammation after traumatic brain injury: opportunities for therapeutic intervention*. *Brain Behav Immun*, 2012. **26**(8): p. 1191-201.
  80. Finnie, J.W., *Neuroinflammation: beneficial and detrimental effects after traumatic brain injury*. *Inflammopharmacology*, 2013. **21**(4): p. 309-20.
  81. Faden, A.I. and D.J. Loane, *Chronic neurodegeneration after traumatic brain injury: Alzheimer disease, chronic traumatic encephalopathy, or persistent neuroinflammation?* *Neurotherapeutics*, 2015. **12**(1): p. 143-50.
  82. Ragnarsson, K.T., *Results of the NIH consensus conference on "rehabilitation of persons with traumatic brain injury"*. *Restor Neurol Neurosci*, 2002. **20**(3-4): p. 103-8.

83. Rapoport, M.J., S. McCullagh, P. Shammi, and A. Feinstein, *Cognitive impairment associated with major depression following mild and moderate traumatic brain injury*. J Neuropsychiatry Clin Neurosci, 2005. **17**(1): p. 61-5.
84. Loane, D.J., A. Kumar, B.A. Stoica, R. Cabatbat, and A.I. Faden, *Progressive neurodegeneration after experimental brain trauma: association with chronic microglial activation*. J Neuropathol Exp Neurol, 2014. **73**(1): p. 14-29.
85. Carson, M.J., J.C. Thrash, and B. Walter, *The cellular response in neuroinflammation: The role of leukocytes, microglia and astrocytes in neuronal death and survival*. Clin Neurosci Res, 2006. **6**(5): p. 237-245.
86. Finnie, J.W., *Pathology of traumatic brain injury*. Vet Res Commun, 2014. **38**(4): p. 297-305.
87. Myer, D.J., G.G. Gurkoff, S.M. Lee, D.A. Hovda, and M.V. Sofroniew, *Essential protective roles of reactive astrocytes in traumatic brain injury*. Brain, 2006. **129**(Pt 10): p. 2761-72.
88. Sofroniew, M.V. and H.V. Vinters, *Astrocytes: biology and pathology*. Acta Neuropathol, 2010. **119**(1): p. 7-35.
89. Loane, D.J. and K.R. Byrnes, *Role of microglia in neurotrauma*. Neurotherapeutics, 2010. **7**(4): p. 366-77.
90. Streit, W.J., R.E. Mrak, and W.S. Griffin, *Microglia and neuroinflammation: a pathological perspective*. J Neuroinflammation, 2004. **1**(1): p. 14.
91. Walker, D.G. and L.F. Lue, *Immune phenotypes of microglia in human neurodegenerative disease: challenges to detecting microglial polarization in human brains*. Alzheimers Res Ther, 2015. **7**(1): p. 56.
92. Ito, D., Y. Imai, K. Ohsawa, K. Nakajima, Y. Fukuuchi, and S. Kohsaka, *Microglia-specific localisation of a novel calcium binding protein, Iba1*. Brain Res Mol Brain Res, 1998. **57**(1): p. 1-9.
93. Hill, S.J., E. Barbarese, and T.K. McIntosh, *Regional heterogeneity in the response of astrocytes following traumatic brain injury in the adult rat*. J Neuropathol Exp Neurol, 1996. **55**(12): p. 1221-9.
94. Eng, L.F. and R.S. Ghirnikar, *GFAP and astrogliosis*. Brain Pathol, 1994. **4**(3): p. 229-37.
95. Bi, F., C. Huang, J. Tong, G. Qiu, B. Huang, Q. Wu, F. Li, Z. Xu, R. Bowser, X.G. Xia, and H. Zhou, *Reactive astrocytes secrete Icn2 to promote neuron death*. Proc Natl Acad Sci U S A, 2013. **110**(10): p. 4069-74.
96. Raghupathi, R., D.I. Graham, and T.K. McIntosh, *Apoptosis after traumatic brain injury*. J Neurotrauma, 2000. **17**(10): p. 927-38.

97. Zhang, X., Y. Chen, L.W. Jenkins, P.M. Kochanek, and R.S. Clark, *Bench-to-bedside review: Apoptosis/programmed cell death triggered by traumatic brain injury*. Crit Care, 2005. **9**(1): p. 66-75.
98. Wang, K.K., *Calpain and caspase: can you tell the difference?* Trends Neurosci, 2000. **23**(1): p. 20-6.
99. Thompson, S.N., T.R. Gibson, B.M. Thompson, Y. Deng, and E.D. Hall, *Relationship of calpain-mediated proteolysis to the expression of axonal and synaptic plasticity markers following traumatic brain injury in mice*. Exp Neurol, 2006. **201**(1): p. 253-65.
100. Whitney, N.P., T.M. Eidem, H. Peng, Y. Huang, and J.C. Zheng, *Inflammation mediates varying effects in neurogenesis: relevance to the pathogenesis of brain injury and neurodegenerative disorders*. J Neurochem, 2009. **108**(6): p. 1343-59.
101. Faló, M.C., T.M. Reeves, and L.L. Phillips, *Agrin expression during synaptogenesis induced by traumatic brain injury*. J Neurotrauma, 2008. **25**(7): p. 769-83.
102. Hulsebosch, C.E., D.S. DeWitt, L.W. Jenkins, and D.S. Prough, *Traumatic brain injury in rats results in increased expression of Gap-43 that correlates with behavioral recovery*. Neurosci Lett, 1998. **255**(2): p. 83-6.
103. Ding, J.Y., C.W. Kreipke, P. Schafer, S. Schafer, S.L. Speirs, and J.A. Rafols, *Synapse loss regulated by matrix metalloproteinases in traumatic brain injury is associated with hypoxia inducible factor-1alpha expression*. Brain Res, 2009. **1268**: p. 125-34.
104. Hall, K.D. and J. Lifshitz, *Diffuse traumatic brain injury initially attenuates and later expands activation of the rat somatosensory whisker circuit concomitant with neuroplastic responses*. Brain Res, 2010. **1323**: p. 161-73.
105. Benowitz, L.I. and A. Routtenberg, *GAP-43: an intrinsic determinant of neuronal development and plasticity*. Trends Neurosci, 1997. **20**(2): p. 84-91.
106. Chin, L.S., L. Li, A. Ferreira, K.S. Kosik, and P. Greengard, *Impairment of axonal development and of synaptogenesis in hippocampal neurons of synapsin I-deficient mice*. Proc Natl Acad Sci U S A, 1995. **92**(20): p. 9230-4.
107. Fox, G.B., L. Fan, R.A. Levasseur, and A.I. Faden, *Sustained sensory/motor and cognitive deficits with neuronal apoptosis following controlled cortical impact brain injury in the mouse*. J Neurotrauma, 1998. **15**(8): p. 599-614.
108. Hicks, R.R., D.H. Smith, D.H. Lowenstein, R. Saint Marie, and T.K. McIntosh, *Mild experimental brain injury in the rat induces cognitive deficits associated with regional neuronal loss in the hippocampus*. J Neurotrauma, 1993. **10**(4): p. 405-14.
109. Nimmo, A.J., I. Cernak, D.L. Heath, X. Hu, C.J. Bennett, and R. Vink, *Neurogenic inflammation is associated with development of edema and functional deficits following traumatic brain injury in rats*. Neuropeptides, 2004. **38**(1): p. 40-7.

110. Sinson, G., B.R. Perri, J.Q. Trojanowski, E.S. Flamm, and T.K. McIntosh, *Improvement of cognitive deficits and decreased cholinergic neuronal cell loss and apoptotic cell death following neurotrophin infusion after experimental traumatic brain injury*. J Neurosurg, 1997. **86**(3): p. 511-8.
111. Wright, D.K., J. Trezise, A. Kamnaksh, R. Bekdash, L.A. Johnston, R. Ordidge, B.D. Semple, A.J. Gardner, P. Stanwell, T.J. O'Brien, D.V. Agoston, and S.R. Shultz, *Behavioral, blood, and magnetic resonance imaging biomarkers of experimental mild traumatic brain injury*. Sci Rep, 2016. **6**: p. 28713.
112. Loane, D.J. and A.I. Faden, *Neuroprotection for traumatic brain injury: translational challenges and emerging therapeutic strategies*. Trends Pharmacol Sci, 2010. **31**(12): p. 596-604.
113. Nieto-Sampedro, M., E.R. Lewis, C.W. Cotman, M. Manthorpe, S.D. Skaper, G. Barbin, F.M. Longo, and S. Varon, *Brain injury causes a time-dependent increase in neuronotrophic activity at the lesion site*. Science, 1982. **217**(4562): p. 860-1.
114. Kromer, L.F., *Nerve growth factor treatment after brain injury prevents neuronal death*. Science, 1987. **235**(4785): p. 214-6.
115. Hagg, T., B. Fass-Holmes, H.L. Vahlsing, M. Manthorpe, J.M. Conner, and S. Varon, *Nerve growth factor (NGF) reverses axotomy-induced decreases in choline acetyltransferase, NGF receptor and size of medial septum cholinergic neurons*. Brain Res, 1989. **505**(1): p. 29-38.
116. Hagg, T., F. Hagg, H.L. Vahlsing, M. Manthorpe, and S. Varon, *Nerve growth factor effects on cholinergic neurons of neostriatum and nucleus accumbens in the adult rat*. Neuroscience, 1989. **30**(1): p. 95-103.
117. Hagg, T., M. Manthorpe, H.L. Vahlsing, and S. Varon, *Delayed treatment with nerve growth factor reverses the apparent loss of cholinergic neurons after acute brain damage*. Exp Neurol, 1988. **101**(2): p. 303-12.
118. Will, B. and F. Hefti, *Behavioural and neurochemical effects of chronic intraventricular injections of nerve growth factor in adult rats with fimbria lesions*. Behav Brain Res, 1985. **17**(1): p. 17-24.
119. Eclancher, F., J.J. Ramirez, and D.G. Stein, *Neonatal brain damage and recovery: intraventricular injection of NGF at time of injury alters performance of active avoidance*. Brain Res, 1985. **351**(2): p. 227-35.
120. Longhi, L., D.J. Watson, K.E. Saatman, H.J. Thompson, C. Zhang, S. Fujimoto, N. Royo, D. Castelbuono, R. Raghupathi, J.Q. Trojanowski, V.M. Lee, J.H. Wolfe, N. Stocchetti, and T.K. McIntosh, *Ex vivo gene therapy using targeted engraftment of NGF-expressing human*



- NT2N neurons attenuates cognitive deficits following traumatic brain injury in mice.* J Neurotrauma, 2004. **21**(12): p. 1723-36.
121. Dixon, C.E., P. Flinn, J. Bao, R. Venya, and R.L. Hayes, *Nerve growth factor attenuates cholinergic deficits following traumatic brain injury in rats.* Exp Neurol, 1997. **146**(2): p. 479-90.
122. Tian, L., R. Guo, X. Yue, Q. Lv, X. Ye, Z. Wang, Z. Chen, B. Wu, G. Xu, and X. Liu, *Intranasal administration of nerve growth factor ameliorate beta-amyloid deposition after traumatic brain injury in rats.* Brain Res, 2012. **1440**: p. 47-55.
123. Sinson, G., M. Voddi, and T.K. McIntosh, *Nerve growth factor administration attenuates cognitive but not neurobehavioral motor dysfunction or hippocampal cell loss following fluid-percussion brain injury in rats.* J Neurochem, 1995. **65**(5): p. 2209-16.
124. Young, J., T. Pionk, I. Hiatt, K. Geeck, and J.S. Smith, *Environmental enrichment aides in functional recovery following unilateral controlled cortical impact of the forelimb sensorimotor area however intranasal administration of nerve growth factor does not.* Brain Res Bull, 2015. **115**: p. 17-22.
125. Jha, R.M., P.M. Kochanek, and J.M. Simard, *Pathophysiology and treatment of cerebral edema in traumatic brain injury.* Neuropharmacology, 2019. **145**(Pt B): p. 230-246.
126. Lv, Q., X. Fan, G. Xu, Q. Liu, L. Tian, X. Cai, W. Sun, X. Wang, Q. Cai, Y. Bao, L. Zhou, Y. Zhang, L. Ge, R. Guo, and X. Liu, *Intranasal delivery of nerve growth factor attenuates aquaporins-4-induced edema following traumatic brain injury in rats.* Brain Res, 2013. **1493**: p. 80-9.
127. Zhang, C., J. Chen, and H. Lu, *Expression of aquaporin-4 and pathological characteristics of brain injury in a rat model of traumatic brain injury.* Mol Med Rep, 2015. **12**(5): p. 7351-7.
128. Lv, Q., W. Lan, W. Sun, R. Ye, X. Fan, M. Ma, Q. Yin, Y. Jiang, G. Xu, J. Dai, R. Guo, and X. Liu, *Intranasal nerve growth factor attenuates tau phosphorylation in brain after traumatic brain injury in rats.* J Neurol Sci, 2014. **345**(1-2): p. 48-55.
129. Galgano, M., G. Toshkezi, X. Qiu, T. Russell, L. Chin, and L.R. Zhao, *Traumatic Brain Injury: Current Treatment Strategies and Future Endeavors.* Cell Transplant, 2017. **26**(7): p. 1118-1130.
130. Xiong, Y., A. Mahmood, and M. Chopp, *Emerging treatments for traumatic brain injury.* Expert Opin Emerg Drugs, 2009. **14**(1): p. 67-84.
131. Shawkat, H., Mortimer, A., Westwood, M., *Mannitol: a review of its clinical uses.* Continuing Education in Anaesthesia Critical Care & Pain, 2012. **12**(2): p. 82-85.
132. Burke, A.M., D.O. Quest, S. Chien, and C. Cerri, *The effects of mannitol on blood viscosity.* J Neurosurg, 1981. **55**(4): p. 550-3.

133. Wakai, A., I. Roberts, and G. Schierhout, *Mannitol for acute traumatic brain injury*. Cochrane Database Syst Rev, 2007(1): p. CD001049.
134. Rangel-Castilla, L., S. Gopinath, and C.S. Robertson, *Management of intracranial hypertension*. Neurol Clin, 2008. **26**(2): p. 521-41, x.
135. Albanese, J., X. Viviani, F. Potie, M. Rey, B. Alliez, and C. Martin, *Sufentanil, fentanyl, and alfentanil in head trauma patients: a study on cerebral hemodynamics*. Crit Care Med, 1999. **27**(2): p. 407-11.
136. Shapiro, H.M., S.R. Wyte, and J. Loeser, *Barbiturate-augmented hypothermia for reduction of persistent intracranial hypertension*. J Neurosurg, 1974. **40**(1): p. 90-100.
137. Eisenberg, H.M., R.F. Frankowski, C.F. Contant, L.F. Marshall, and M.D. Walker, *High-dose barbiturate control of elevated intracranial pressure in patients with severe head injury*. J Neurosurg, 1988. **69**(1): p. 15-23.
138. Rockoff, M.A., L.F. Marshall, and H.M. Shapiro, *High-dose barbiturate therapy in humans: a clinical review of 60 patients*. Ann Neurol, 1979. **6**(3): p. 194-9.
139. Roberts, I. and E. Sydenham, *Barbiturates for acute traumatic brain injury*. Cochrane Database Syst Rev, 2012. **12**: p. CD000033.
140. Peng, W., Z. Xing, J. Yang, Y. Wang, W. Wang, and W. Huang, *The efficacy of erythropoietin in treating experimental traumatic brain injury: a systematic review of controlled trials in animal models*. J Neurosurg, 2014. **121**(3): p. 653-64.
141. Jang, S.W., M. Okada, I. Sayeed, G. Xiao, D. Stein, P. Jin, and K. Ye, *Gambogic amide, a selective agonist for TrkA receptor that possesses robust neurotrophic activity, prevents neuronal cell death*. Proc Natl Acad Sci U S A, 2007. **104**(41): p. 16329-34.
142. Chan, C.B., X. Liu, S.W. Jang, S.I. Hsu, I. Williams, S. Kang, J. Chen, and K. Ye, *NGF inhibits human leukemia proliferation by downregulating cyclin A1 expression through promoting acinus/CtBP2 association*. Oncogene, 2009. **28**(43): p. 3825-36.
143. Prins, M.L. and D.A. Hovda, *Developing experimental models to address traumatic brain injury in children*. J Neurotrauma, 2003. **20**(2): p. 123-37.
144. Dixon, C.E., G.L. Clifton, J.W. Lighthall, A.A. Yaghmai, and R.L. Hayes, *A controlled cortical impact model of traumatic brain injury in the rat*. J Neurosci Methods, 1991. **39**(3): p. 253-62.
145. Morales, D.M., N. Marklund, D. Lebold, H.J. Thompson, A. Pitkanen, W.L. Maxwell, L. Longhi, H. Laurer, M. Maegele, E. Neugebauer, D.I. Graham, N. Stocchetti, and T.K. McIntosh, *Experimental models of traumatic brain injury: do we really need to build a better mousetrap?* Neuroscience, 2005. **136**(4): p. 971-89.

146. McIntosh, T.K., R. Vink, L. Noble, I. Yamakami, S. Fernyak, H. Soares, and A.L. Faden, *Traumatic brain injury in the rat: characterization of a lateral fluid-percussion model*. Neuroscience, 1989. **28**(1): p. 233-44.
147. Alder, J., W. Fujioka, J. Lifshitz, D.P. Crockett, and S. Thakker-Varia, *Lateral fluid percussion: model of traumatic brain injury in mice*. J Vis Exp, 2011(54).
148. Conti, A.C., R. Raghupathi, J.Q. Trojanowski, and T.K. McIntosh, *Experimental brain injury induces regionally distinct apoptosis during the acute and delayed post-traumatic period*. J Neurosci, 1998. **18**(15): p. 5663-72.
149. Dietrich, W.D., J. Truettner, W. Zhao, O.F. Alonso, R. Busto, and M.D. Ginsberg, *Sequential changes in glial fibrillary acidic protein and gene expression following parasagittal fluid-percussion brain injury in rats*. J Neurotrauma, 1999. **16**(7): p. 567-81.
150. Hamm, R.J., B.R. Pike, D.M. O'Dell, B.G. Lyeth, and L.W. Jenkins, *The rotarod test: an evaluation of its effectiveness in assessing motor deficits following traumatic brain injury*. J Neurotrauma, 1994. **11**(2): p. 187-96.
151. McKibbin, B., *The biology of fracture healing in long bones*. J Bone Joint Surg Br, 1978. **60-B**(2): p. 150-62.
152. Bradley C, H.J., *Descriptive epidemiology of traumatic fractures in Australia*. Injury Research and Statistics, 2004. **Series Number 17**.
153. Einhorn, T.A., *The cell and molecular biology of fracture healing*. Clin Orthop Relat Res, 1998(355 Suppl): p. S7-21.
154. Buza, J.A., 3rd and T. Einhorn, *Bone healing in 2016*. Clin Cases Miner Bone Metab, 2016. **13**(2): p. 101-105.
155. Ekergren, C.L., B.J. Gabbe, E.R. Edwards, R. de Steiger, and R. Page, *791 Incidence, costs and outcomes of non-union, delayed union and mal union following long bone fracture*. Injury Prevention, 2016. **22**: p. A283.
156. Rajbhandari, S.M., R.C. Jenkins, C. Davies, and S. Tesfaye, *Charcot neuroarthropathy in diabetes mellitus*. Diabetologia, 2002. **45**(8): p. 1085-96.
157. Bibbo, C., S.S. Lin, H.A. Beam, and F.F. Behrens, *Complications of ankle fractures in diabetic patients*. Orthop Clin North Am, 2001. **32**(1): p. 113-33.
158. Tsujio, T., H. Nakamura, H. Terai, M. Hoshino, T. Namikawa, A. Matsumura, M. Kato, A. Suzuki, K. Takayama, W. Fukushima, K. Kondo, Y. Hirota, and K. Takaoka, *Characteristic radiographic or magnetic resonance images of fresh osteoporotic vertebral fractures predicting potential risk for nonunion: a prospective multicenter study*. Spine (Phila Pa 1976), 2011. **36**(15): p. 1229-35.
159. Volgas, D.A., J.P. Stannard, and J.E. Alonso, *Nonunions of the humerus*. Clin Orthop Relat Res, 2004(419): p. 46-50.

160. Urist, M.R., R.J. DeLange, and G.A. Finerman, *Bone cell differentiation and growth factors*. Science, 1983. **220**(4598): p. 680-6.
161. Bosch, P., D.S. Musgrave, J.Y. Lee, J. Cummins, T. Shuler, T.C. Ghivizzani, T. Evans, T.D. Robbins, and Huard, *Osteoprogenitor cells within skeletal muscle*. J Orthop Res, 2000. **18**(6): p. 933-44.
162. Ortega, N., D.J. Behonick, and Z. Werb, *Matrix remodeling during endochondral ossification*. Trends Cell Biol, 2004. **14**(2): p. 86-93.
163. Lefebvre, V., W. Huang, V.R. Harley, P.N. Goodfellow, and B. de Crombrughe, *SOX9 is a potent activator of the chondrocyte-specific enhancer of the pro alpha1(II) collagen gene*. Mol Cell Biol, 1997. **17**(4): p. 2336-46.
164. Akiyama, H., M.C. Chaboissier, J.F. Martin, A. Schedl, and B. de Crombrughe, *The transcription factor Sox9 has essential roles in successive steps of the chondrocyte differentiation pathway and is required for expression of Sox5 and Sox6*. Genes Dev, 2002. **16**(21): p. 2813-28.
165. Lian, J.B., A. Javed, S.K. Zaidi, C. Lengner, M. Montecino, A.J. van Wijnen, J.L. Stein, and G.S. Stein, *Regulatory controls for osteoblast growth and differentiation: role of Runx/Cbfa/AML factors*. Crit Rev Eukaryot Gene Expr, 2004. **14**(1-2): p. 1-41.
166. Nakashima, K., X. Zhou, G. Kunkel, Z. Zhang, J.M. Deng, R.R. Behringer, and B. de Crombrughe, *The novel zinc finger-containing transcription factor osterix is required for osteoblast differentiation and bone formation*. Cell, 2002. **108**(1): p. 17-29.
167. Parfitt, A.M., *The actions of parathyroid hormone on bone: relation to bone remodeling and turnover, calcium homeostasis, and metabolic bone disease. Part I of IV parts: mechanisms of calcium transfer between blood and bone and their cellular basis: morphological and kinetic approaches to bone turnover*. Metabolism, 1976. **25**(7): p. 809-44.
168. Jilka, R.L., R.S. Weinstein, T. Bellido, A.M. Parfitt, and S.C. Manolagas, *Osteoblast programmed cell death (apoptosis): modulation by growth factors and cytokines*. J Bone Miner Res, 1998. **13**(5): p. 793-802.
169. Bonewald, L.F., *The Amazing Osteocyte*. J Bone Miner Res, 2011. **26**(2): p. 229-38.
170. Bonewald, L.F. and M.L. Johnson, *Osteocytes, mechanosensing and Wnt signaling*. Bone, 2008. **42**(4): p. 606-15.
171. Poole, K.E., R.L. van Bezooijen, N. Loveridge, H. Hamersma, S.E. Papapoulos, C.W. Lowik, and J. Reeve, *Sclerostin is a delayed secreted product of osteocytes that inhibits bone formation*. FASEB J, 2005. **19**(13): p. 1842-4.
172. Chen, D., M. Zhao, and G.R. Mundy, *Bone morphogenetic proteins*. Growth Factors, 2004. **22**(4): p. 233-41.

173. Rochefort, G.Y., *The osteocyte as a therapeutic target in the treatment of osteoporosis*. Ther Adv Musculoskelet Dis, 2014. **6**(3): p. 79-91.
174. Plotkin, L.I. and T. Bellido, *Osteocytic signalling pathways as therapeutic targets for bone fragility*. Nat Rev Endocrinol, 2016. **12**(10): p. 593-605.
175. Lewiecki, E.M., *Role of sclerostin in bone and cartilage and its potential as a therapeutic target in bone diseases*. Ther Adv Musculoskelet Dis, 2014. **6**(2): p. 48-57.
176. Teitelbaum, S.L., *Bone resorption by osteoclasts*. Science, 2000. **289**(5484): p. 1504-8.
177. Silver, I.A., R.J. Murrills, and D.J. Etherington, *Microelectrode studies on the acid microenvironment beneath adherent macrophages and osteoclasts*. Exp Cell Res, 1988. **175**(2): p. 266-76.
178. Nesbitt, S.A. and M.A. Horton, *Trafficking of matrix collagens through bone-resorbing osteoclasts*. Science, 1997. **276**(5310): p. 266-9.
179. Schindeler, A., M.M. McDonald, P. Bokko, and D.G. Little, *Bone remodeling during fracture repair: The cellular picture*. Semin Cell Dev Biol, 2008. **19**(5): p. 459-66.
180. Hukkanen, M., Y.T. Konttinen, S. Santavirta, P. Paavolainen, X.H. Gu, G. Terenghi, and J.M. Polak, *Rapid proliferation of calcitonin gene-related peptide-immunoreactive nerves during healing of rat tibial fracture suggests neural involvement in bone growth and remodelling*. Neuroscience, 1993. **54**(4): p. 969-79.
181. Grundnes, O. and O. Reikeras, *The importance of the hematoma for fracture healing in rats*. Acta Orthop Scand, 1993. **64**(3): p. 340-2.
182. Hollinger, J. and M.E. Wong, *The integrated processes of hard tissue regeneration with special emphasis on fracture healing*. Oral Surg Oral Med Oral Pathol Oral Radiol Endod, 1996. **82**(6): p. 594-606.
183. Udagawa, N., N. Takahashi, E. Jimi, K. Matsuzaki, T. Tsurukai, K. Itoh, N. Nakagawa, H. Yasuda, M. Goto, E. Tsuda, K. Higashio, M.T. Gillespie, T.J. Martin, and T. Suda, *Osteoblasts/stromal cells stimulate osteoclast activation through expression of osteoclast differentiation factor/RANKL but not macrophage colony-stimulating factor: receptor activator of NF-kappa B ligand*. Bone, 1999. **25**(5): p. 517-23.
184. Simonet, W.S., D.L. Lacey, C.R. Dunstan, M. Kelley, M.S. Chang, R. Luthy, H.Q. Nguyen, S. Wooden, L. Bennett, T. Boone, G. Shimamoto, M. DeRose, R. Elliott, A. Colombero, H.L. Tan, G. Trail, J. Sullivan, E. Davy, N. Bucay, L. Renshaw-Gegg, T.M. Hughes, D. Hill, W. Pattison, P. Campbell, S. Sander, G. Van, J. Tarpley, P. Derby, R. Lee, and W.J. Boyle, *Osteoprotegerin: a novel secreted protein involved in the regulation of bone density*. Cell, 1997. **89**(2): p. 309-19.
185. Sevcik, M.A., J.R. Ghilardi, C.M. Peters, T.H. Lindsay, K.G. Halvorson, B.M. Jonas, K. Kubota, M.A. Kuskowski, L. Boustany, D.L. Shelton, and P.W. Mantyh, *Anti-NGF therapy profoundly*

- reduces bone cancer pain and the accompanying increase in markers of peripheral and central sensitization.* Pain, 2005. **115**(1-2): p. 128-41.
186. Tomlinson, R.E., Z. Li, Q. Zhang, B.C. Goh, Z. Li, D.L. Thorek, L. Rajbhandari, T.M. Brushart, L. Minichiello, F. Zhou, A. Venkatesan, and T.L. Clemens, *NGF-TrkA Signaling by Sensory Nerves Coordinates the Vascularization and Ossification of Developing Endochondral Bone.* Cell Rep, 2016. **16**(10): p. 2723-35.
187. McCarthy, J.G., E.J. Stelnicki, B.J. Mehrara, and M.T. Longaker, *Distraction osteogenesis of the craniofacial skeleton.* Plast Reconstr Surg, 2001. **107**(7): p. 1812-27.
188. Kuryszko, J., P. Kurozka, and I. Jedrzejowska, *Distraction osteogenesis and fracture healing. Differences and similarities.* Acta of Bioengineering and Biomechanics, 2000. **2**(2): p. 83-88.
189. Ascenzi, A. and E. Bonucci, *The Ultimate Tensile Strength of Single Osteons.* Acta Anat (Basel), 1964. **58**: p. 160-83.
190. Bonfield, W. and P.K. Datta, *Young's modulus of compact bone.* Journal of Biomechanics, 1974. **7**(2): p. 147-149.
191. Yada, M., K. Yamaguchi, and T. Tsuji, *NGF stimulates differentiation of osteoblastic MC3T3-E1 cells.* Biochem Biophys Res Commun, 1994. **205**(2): p. 1187-93.
192. McGregor, N.E., M. Murat, J. Elango, I.J. Poulton, E.C. Walker, B. Crimeen-Irwin, P.W.M. Ho, J.H. Gooi, T.J. Martin, and N.A. Sims, *IL-6 exhibits both cis- and trans-signaling in osteocytes and osteoblasts, but only trans-signaling promotes bone formation and osteoclastogenesis.* J Biol Chem, 2019. **294**(19): p. 7850-7863.
193. Pinski, J., A. Weeraratna, A.R. Uzgare, J.T. Arnold, S.R. Denmeade, and J.T. Isaacs, *Trk receptor inhibition induces apoptosis of proliferating but not quiescent human osteoblasts.* Cancer Res, 2002. **62**(4): p. 986-9.
194. Dolle, J.P., A. Rezvan, F.D. Allen, P. Lazarovici, and P.I. Leikes, *Nerve growth factor-induced migration of endothelial cells.* J Pharmacol Exp Ther, 2005. **315**(3): p. 1220-7.
195. Castaneda-Corral, G., J.M. Jimenez-Andrade, A.P. Bloom, R.N. Taylor, W.G. Mantyh, M.J. Kaczmarek, J.R. Ghilardi, and P.W. Mantyh, *The majority of myelinated and unmyelinated sensory nerve fibers that innervate bone express the tropomyosin receptor kinase A.* Neuroscience, 2011. **178**: p. 196-207.
196. Matsuda, S., T. Fujita, M. Kajiyama, K. Takeda, H. Shiba, H. Kawaguchi, and H. Kurihara, *Brain-derived neurotrophic factor induces migration of endothelial cells through a TrkB-ERK-integrin alphaVbeta3-FAK cascade.* J Cell Physiol, 2012. **227**(5): p. 2123-9.
197. Kajiyama, M., H. Shiba, T. Fujita, K. Ouhara, K. Takeda, N. Mizuno, H. Kawaguchi, M. Kitagawa, T. Takata, K. Tsuji, and H. Kurihara, *Brain-derived neurotrophic factor stimulates*

- bone/cementum-related protein gene expression in cementoblasts*. J Biol Chem, 2008. **283**(23): p. 16259-67.
198. Perren, S.M., *Evolution of the internal fixation of long bone fractures. The scientific basis of biological internal fixation: choosing a new balance between stability and biology*. J Bone Joint Surg Br, 2002. **84**(8): p. 1093-110.
  199. Einhorn, T.A. and L.C. Gerstenfeld, *Fracture healing: mechanisms and interventions*. Nat Rev Rheumatol, 2015. **11**(1): p. 45-54.
  200. Warden, S.J., K.L. Bennell, J.M. McMeeken, and J.D. Wark, *Acceleration of fresh fracture repair using the sonic accelerated fracture healing system (SAFHS): a review*. Calcif Tissue Int, 2000. **66**(2): p. 157-63.
  201. Pounder, N.M. and A.J. Harrison, *Low intensity pulsed ultrasound for fracture healing: a review of the clinical evidence and the associated biological mechanism of action*. Ultrasonics, 2008. **48**(4): p. 330-8.
  202. Leighton, R., J.T. Watson, P. Giannoudis, C. Papakostidis, A. Harrison, and R.G. Steen, *Healing of fracture nonunions treated with low-intensity pulsed ultrasound (LIPUS): A systematic review and meta-analysis*. Injury, 2017. **48**(7): p. 1339-1347.
  203. Ghiasi, M.S., J. Chen, A. Vaziri, E.K. Rodriguez, and A. Nazarian, *Bone fracture healing in mechanobiological modeling: A review of principles and methods*. Bone Rep, 2017. **6**: p. 87-100.
  204. Govender, S., C. Csimma, H.K. Genant, A. Valentin-Opran, Y. Amit, R. Arbel, H. Aro, D. Atar, M. Bishay, M.G. Borner, P. Chiron, P. Choong, J. Cinats, B. Courtenay, R. Feibel, B. Geulette, C. Gravel, N. Haas, M. Raschke, E. Hammacher, D. van der Velde, P. Hardy, M. Holt, C. Josten, R.L. Ketterl, B. Lindeque, G. Lob, H. Mathevon, G. McCoy, D. Marsh, R. Miller, E. Munting, S. Oevre, L. Nordsletten, A. Patel, A. Pohl, W. Rennie, P. Reynders, P.M. Rommens, J. Rondia, W.C. Rossouw, P.J. Daneel, S. Ruff, A. Ruter, S. Santavirta, T.A. Schildhauer, C. Gekle, R. Schnettler, D. Segal, H. Seiler, R.B. Snowdowne, J. Stapert, G. Taglang, R. Verdonk, L. Vogels, A. Weckbach, A. Wentzensen, T. Wisniewski, and B.M.P.E.i.S.f.T.T.S. Group, *Recombinant human bone morphogenetic protein-2 for treatment of open tibial fractures: a prospective, controlled, randomized study of four hundred and fifty patients*. J Bone Joint Surg Am, 2002. **84-A**(12): p. 2123-34.
  205. Aro, H.T., S. Govender, A.D. Patel, P. Hernigou, A. Perera de Gregorio, G.I. Popescu, J.D. Golden, J. Christensen, and A. Valentin, *Recombinant human bone morphogenetic protein-2: a randomized trial in open tibial fractures treated with reamed nail fixation*. J Bone Joint Surg Am, 2011. **93**(9): p. 801-8.
  206. Simmonds, M.C., J.V. Brown, M.K. Heirs, J.P. Higgins, R.J. Mannion, M.A. Rodgers, and L.A. Stewart, *Safety and effectiveness of recombinant human bone morphogenetic protein-2*

- for spinal fusion: a meta-analysis of individual-participant data.* Ann Intern Med, 2013. **158**(12): p. 877-89.
207. Giannotti, S., V. Bottai, G. Dell'osso, E. Pini, G. De Paola, G. Bugelli, and G. Guido, *Current medical treatment strategies concerning fracture healing.* Clin Cases Miner Bone Metab, 2013. **10**(2): p. 116-20.
208. Huang, T.W., P.Y. Chuang, S.J. Lin, C.Y. Lee, K.C. Huang, H.N. Shih, M.S. Lee, R.W. Hsu, and W.J. Shen, *Teriparatide Improves Fracture Healing and Early Functional Recovery in Treatment of Osteoporotic Intertrochanteric Fractures.* Medicine (Baltimore), 2016. **95**(19): p. e3626.
209. Peichl, P., L.A. Holzer, R. Maier, and G. Holzer, *Parathyroid hormone 1-84 accelerates fracture-healing in pubic bones of elderly osteoporotic women.* J Bone Joint Surg Am, 2011. **93**(17): p. 1583-7.
210. Aspenberg, P., H.K. Genant, T. Johansson, A.J. Nino, K. See, K. Krohn, P.A. Garcia-Hernandez, C.P. Recknor, T.A. Einhorn, G.P. Dalsky, B.H. Mitlak, A. Fierlinger, and M.C. Lakshmanan, *Teriparatide for acceleration of fracture repair in humans: a prospective, randomized, double-blind study of 102 postmenopausal women with distal radial fractures.* J Bone Miner Res, 2010. **25**(2): p. 404-14.
211. Johansson, T., *PTH 1-34 (teriparatide) may not improve healing in proximal humerus fractures. A randomized, controlled study of 40 patients.* Acta Orthop, 2016. **87**(1): p. 79-82.
212. Auer, J.A., A. Goodship, S. Arnoczky, S. Pearce, J. Price, L. Claes, B. von Rechenberg, M. Hofmann-Antenbrinck, E. Schneider, R. Muller-Terpitz, F. Thiele, K.P. Rippe, and D.W. Grainger, *Refining animal models in fracture research: seeking consensus in optimising both animal welfare and scientific validity for appropriate biomedical use.* BMC Musculoskelet Disord, 2007. **8**: p. 72.
213. Nunamaker, D.M., *Experimental models of fracture repair.* Clin Orthop Relat Res, 1998(355 Suppl): p. S56-65.
214. Schotte, M., *The influence of therapeutic substances on bone repair.* Deutsche Medizinische Wochenschrift, 1931. **57**: p. 849-851.
215. Mourgue, M., *Biochemical studies of the action of the parathyroid hormone and vitamin D on the repair of fractures.* Journal de Physiologie et de Pathologie generale, 1939. **37**: p. 1269-1276.
216. Compere, E.H., B; Dewar, M, *The influence of vitamin D upon bone repair; the healing of fractures of rachitic bones.* Surgery, Gynecology and Obstetrics. **68**: p. 878-891.
217. Histing, T., P. Garcia, J.H. Holstein, M. Klein, R. Matthys, R. Nuetzi, R. Steck, M.W. Laschke, T. Wehner, R. Bindl, S. Recknagel, E.K. Stuermer, B. Vollmar, B. Wildemann, J. Lienau, B.



- Willie, A. Peters, A. Ignatius, T. Pohlemann, L. Claes, and M.D. Menger, *Small animal bone healing models: standards, tips, and pitfalls results of a consensus meeting*. *Bone*, 2011. **49**(4): p. 591-9.
218. Holstein, J.H., P. Garcia, T. Histing, A. Kristen, C. Scheuer, M.D. Menger, and T. Pohlemann, *Advances in the establishment of defined mouse models for the study of fracture healing and bone regeneration*. *J Orthop Trauma*, 2009. **23**(5 Suppl): p. S31-8.
219. Lybrand, K., B. Bragdon, and L. Gerstenfeld, *Mouse models of bone healing: fracture, marrow ablation, and distraction osteogenesis*. *Curr Protoc Mouse Biol*, 2015. **5**(1): p. 35-49.
220. Holstein, J.H., R. Matthys, T. Histing, S.C. Becker, M. Fiedler, P. Garcia, C. Meier, T. Pohlemann, and M.D. Menger, *Development of a stable closed femoral fracture model in mice*. *J Surg Res*, 2009. **153**(1): p. 71-5.
221. Manigrasso, M.B. and J.P. O'Connor, *Characterization of a closed femur fracture model in mice*. *J Orthop Trauma*, 2004. **18**(10): p. 687-95.
222. Bhandari, M. and E.H. Schemitsch, *Bone formation following intramedullary femoral reaming is decreased by indomethacin and antibodies to insulin-like growth factors*. *J Orthop Trauma*, 2002. **16**(10): p. 717-22.
223. Street, J., M. Bao, L. deGuzman, S. Bunting, F.V. Peale, Jr., N. Ferrara, H. Steinmetz, J. Hoeffel, J.L. Cleland, A. Daugherty, N. van Bruggen, H.P. Redmond, R.A. Carano, and E.H. Filvaroff, *Vascular endothelial growth factor stimulates bone repair by promoting angiogenesis and bone turnover*. *Proc Natl Acad Sci U S A*, 2002. **99**(15): p. 9656-61.
224. Qi, B., Yu, J., Zhao, Y., Zhu, D., Yu, T., *Mouse fracture models: a primer*. *Int J Clin Exp Med*, 2016. **9**(7): p. 12418-12429.
225. Hiltunen, A., E. Vuorio, and H.T. Aro, *A standardized experimental fracture in the mouse tibia*. *J Orthop Res*, 1993. **11**(2): p. 305-12.
226. Schindeler, A., A. Morse, L. Harry, C. Godfrey, K. Mikulec, M. McDonald, J.A. Gasser, and D.G. Little, *Models of tibial fracture healing in normal and Nf1-deficient mice*. *J Orthop Res*, 2008. **26**(8): p. 1053-60.
227. Brady, R.D., B.L. Grills, J.E. Church, N.C. Walsh, A.C. McDonald, D.V. Agoston, M. Sun, T.J. O'Brien, S.R. Shultz, and S.J. McDonald, *Closed head experimental traumatic brain injury increases size and bone volume of callus in mice with concomitant tibial fracture*. *Sci Rep*, 2016. **6**: p. 34491.
228. Shultz, S.R., M. Sun, D.K. Wright, R.D. Brady, S. Liu, S. Beynon, S.F. Schmidt, A.H. Kaye, J.A. Hamilton, T.J. O'Brien, B.L. Grills, and S.J. McDonald, *Tibial fracture exacerbates traumatic brain injury outcomes and neuroinflammation in a novel mouse model of multitrauma*. *J Cereb Blood Flow Metab*, 2015. **35**(8): p. 1339-47.

229. Sun, M., R.D. Brady, D.K. Wright, H.A. Kim, S.R. Zhang, C.G. Sobey, M.R. Johnstone, T.J. O'Brien, B.D. Semple, S.J. McDonald, and S.R. Shultz, *Treatment with an interleukin-1 receptor antagonist mitigates neuroinflammation and brain damage after polytrauma*. *Brain Behav Immun*, 2017. **66**: p. 359-371.
230. Uchida, R., K. Nakata, F. Kawano, Y. Yonetani, I. Ogasawara, N. Nakai, T. Mae, T. Matsuo, Y. Tachibana, H. Yokoi, and H. Yoshikawa, *Vibration acceleration promotes bone formation in rodent models*. *PLoS One*, 2017. **12**(3): p. e0172614.
231. Nakase, T., S. Nomura, H. Yoshikawa, J. Hashimoto, S. Hirota, Y. Kitamura, S. Oikawa, K. Ono, and K. Takaoka, *Transient and localized expression of bone morphogenetic protein 4 messenger RNA during fracture healing*. *J Bone Miner Res*, 1994. **9**(5): p. 651-9.
232. Hashimoto, J., H. Yoshikawa, K. Takaoka, N. Shimizu, K. Masuhara, T. Tsuda, S. Miyamoto, and K. Ono, *Inhibitory effects of tumor necrosis factor alpha on fracture healing in rats*. *Bone*, 1989. **10**(6): p. 453-7.
233. Shimomura, Y., T. Yoneda, and F. Suzuki, *Osteogenesis by chondrocytes from growth cartilage of rat rib*. *Calcif Tissue Res*, 1975. **19**(3): p. 179-87.
234. Brady, R.D., B.L. Grills, J.A. Schuijers, A.R. Ward, B.A. Tonkin, N.C. Walsh, and S.J. McDonald, *Thymosin beta4 administration enhances fracture healing in mice*. *J Orthop Res*, 2014. **32**(10): p. 1277-82.
235. Kellum, E., H. Starr, P. Arounleut, D. Immel, S. Fulzele, K. Wenger, and M.W. Hamrick, *Myostatin (GDF-8) deficiency increases fracture callus size, Sox-5 expression, and callus bone volume*. *Bone*, 2009. **44**(1): p. 17-23.
236. Saragovi, H.U. and K. Gehring, *Development of pharmacological agents for targeting neurotrophins and their receptors*. *Trends Pharmacol Sci*, 2000. **21**(3): p. 93-8.
237. Brahimi, F., J. Liu, A. Malakhov, S. Chowdhury, E.O. Purisima, L. Ivanisevic, A. Caron, K. Burgess, and H.U. Saragovi, *A monovalent agonist of TrkA tyrosine kinase receptors can be converted into a bivalent antagonist*. *Biochim Biophys Acta*, 2010. **1800**(9): p. 1018-26.
238. Jang, S.W., X. Liu, C.B. Chan, D. Weinschenker, R.A. Hall, G. Xiao, and K. Ye, *Amitriptyline is a TrkA and TrkB receptor agonist that promotes TrkA/TrkB heterodimerization and has potent neurotrophic activity*. *Chem Biol*, 2009. **16**(6): p. 644-56.
239. Scarpi, D., D. Cirelli, C. Matrone, G. Castronovo, P. Rosini, E.G. Occhiato, F. Romano, L. Bartali, A.M. Clemente, G. Bottegoni, A. Cavalli, G. De Chiara, P. Bonini, P. Calissano, A.T. Palamara, E. Garaci, M.G. Torcia, A. Guarna, and F. Cozzolino, *Low molecular weight, non-peptidic agonists of TrkA receptor with NGF-mimetic activity*. *Cell Death Dis*, 2012. **3**: p. e389.
240. Tsai, S.J., *TrkB partial agonists: potential treatment strategy for major depression*. *Med Hypotheses*, 2007. **68**(3): p. 674-6.

241. Botsakis, K., T. Mourtzi, V. Panagiotakopoulou, M. Vreka, G.T. Stathopoulos, I. Pediaditakis, I. Charalampopoulos, A. Gravanis, F. Delis, K. Antoniou, D. Zisimopoulos, C.D. Georgiou, N.T. Panagopoulos, N. Matsokis, and F. Angelatou, *BNN-20, a synthetic microneurotrophin, strongly protects dopaminergic neurons in the "weaver" mouse, a genetic model of dopamine-denervation, acting through the TrkB neurotrophin receptor*. *Neuropharmacology*, 2017. **121**: p. 140-157.
242. Jang, S.W., X. Liu, M. Yepes, K.R. Shepherd, G.W. Miller, Y. Liu, W.D. Wilson, G. Xiao, B. Bianchi, Y.E. Sun, and K. Ye, *A selective TrkB agonist with potent neurotrophic activities by 7,8-dihydroxyflavone*. *Proc Natl Acad Sci U S A*, 2010. **107**(6): p. 2687-92.
243. Shah, A.G., M.J. Friedman, S. Huang, M. Roberts, X.J. Li, and S. Li, *Transcriptional dysregulation of TrkA associates with neurodegeneration in spinocerebellar ataxia type 17*. *Hum Mol Genet*, 2009. **18**(21): p. 4141-52.
244. Shen, J. and Q. Yu, *Gambogic amide selectively upregulates TrkA expression and triggers its activation*. *Pharmacol Rep*, 2015. **67**(2): p. 217-23.
245. Ding, L., D. Huang, J. Wang, and S. Li, *Determination of gambogic acid in human plasma by liquid chromatography-atmospheric pressure chemical ionization-mass spectrometry*. *J Chromatogr B Analyt Technol Biomed Life Sci*, 2007. **846**(1-2): p. 112-8.
246. Kumar, S. and A.K. Pandey, *Chemistry and biological activities of flavonoids: an overview*. *ScientificWorldJournal*, 2013. **2013**: p. 162750.
247. Cushnie, T.P. and A.J. Lamb, *Antimicrobial activity of flavonoids*. *Int J Antimicrob Agents*, 2005. **26**(5): p. 343-56.
248. Garcia-Lafuente, A., E. Guillaumon, A. Villares, M.A. Rostagno, and J.A. Martinez, *Flavonoids as anti-inflammatory agents: implications in cancer and cardiovascular disease*. *Inflamm Res*, 2009. **58**(9): p. 537-52.
249. Dajas, F., A.C. Andres, A. Florencia, E. Carolina, and R.M. Felicia, *Neuroprotective actions of flavones and flavonols: mechanisms and relationship to flavonoid structural features*. *Cent Nerv Syst Agents Med Chem*, 2013. **13**(1): p. 30-5.
250. Colombo, P.S., G. Flamini, M.S. Christodoulou, G. Rodondi, S. Vitalini, D. Passarella, and G. Fico, *Farinose alpine Primula species: phytochemical and morphological investigations*. *Phytochemistry*, 2014. **98**: p. 151-9.
251. Gupta, V.K., Y. You, J.C. Li, A. Klistorner, and S.L. Graham, *Protective effects of 7,8-dihydroxyflavone on retinal ganglion and RGC-5 cells against excitotoxic and oxidative stress*. *J Mol Neurosci*, 2013. **49**(1): p. 96-104.
252. Zhao, S., A. Yu, X. Wang, X. Gao, and J. Chen, *Post-Injury Treatment of 7,8-Dihydroxyflavone Promotes Neurogenesis in the Hippocampus of the Adult Mouse*. *J Neurotrauma*, 2016. **33**(22): p. 2055-2064.

253. Chen, L., X. Gao, S. Zhao, W. Hu, and J. Chen, *The Small-Molecule TrkB Agonist 7, 8-Dihydroxyflavone Decreases Hippocampal Newborn Neuron Death After Traumatic Brain Injury*. *J Neuropathol Exp Neurol*, 2015. **74**(6): p. 557-67.
254. Agrawal, R., E. Noble, E. Tyagi, Y. Zhuang, Z. Ying, and F. Gomez-Pinilla, *Flavonoid derivative 7,8-DHF attenuates TBI pathology via TrkB activation*. *Biochim Biophys Acta*, 2015. **1852**(5): p. 862-72.
255. Zhao, S., X. Gao, W. Dong, and J. Chen, *The Role of 7,8-Dihydroxyflavone in Preventing Dendrite Degeneration in Cortex After Moderate Traumatic Brain Injury*. *Mol Neurobiol*, 2016. **53**(3): p. 1884-95.
256. Liu, X., C.B. Chan, S.W. Jang, S. Pradoldej, J. Huang, K. He, L.H. Phun, S. France, G. Xiao, Y. Jia, H.R. Luo, and K. Ye, *A synthetic 7,8-dihydroxyflavone derivative promotes neurogenesis and exhibits potent antidepressant effect*. *J Med Chem*, 2010. **53**(23): p. 8274-86.
257. Devi, L. and M. Ohno, *7,8-dihydroxyflavone, a small-molecule TrkB agonist, reverses memory deficits and BACE1 elevation in a mouse model of Alzheimer's disease*. *Neuropsychopharmacology*, 2012. **37**(2): p. 434-44.
258. Castello, N.A., M.H. Nguyen, J.D. Tran, D. Cheng, K.N. Green, and F.M. LaFerla, *7,8-Dihydroxyflavone, a small molecule TrkB agonist, improves spatial memory and increases thin spine density in a mouse model of Alzheimer disease-like neuronal loss*. *PLoS One*, 2014. **9**(3): p. e91453.
259. Zeng, Y., Y. Liu, M. Wu, J. Liu, and Q. Hu, *Activation of TrkB by 7,8-dihydroxyflavone prevents fear memory defects and facilitates amygdalar synaptic plasticity in aging*. *J Alzheimers Dis*, 2012. **31**(4): p. 765-78.
260. Andero, R., N. Daviu, R.M. Escorihuela, R. Nadal, and A. Armario, *7,8-dihydroxyflavone, a TrkB receptor agonist, blocks long-term spatial memory impairment caused by immobilization stress in rats*. *Hippocampus*, 2012. **22**(3): p. 399-408.
261. Riemenschneider, M., S. Schwarz, S. Wagenpfeil, J. Diehl, U. Muller, H. Forstl, and A. Kurz, *A polymorphism of the brain-derived neurotrophic factor (BDNF) is associated with Alzheimer's disease in patients lacking the Apolipoprotein E epsilon4 allele*. *Mol Psychiatry*, 2002. **7**(7): p. 782-5.
262. Morales-Marin, M.E., A.D. Genis-Mendoza, C.A. Tovilla-Zarate, N. Lanzagorta, M. Escamilla, and H. Nicolini, *Association between obesity and the brain-derived neurotrophic factor gene polymorphism Val66Met in individuals with bipolar disorder in Mexican population*. *Neuropsychiatr Dis Treat*, 2016. **12**: p. 1843-8.
263. Soliman, F., C.E. Glatt, K.G. Bath, L. Levita, R.M. Jones, S.S. Pattwell, D. Jing, N. Tottenham, D. Amso, L.H. Somerville, H.U. Voss, G. Glover, D.J. Ballon, C. Liston, T. Teslovich, T. Van

- Kempen, F.S. Lee, and B.J. Casey, *A genetic variant BDNF polymorphism alters extinction learning in both mouse and human*. *Science*, 2010. **327**(5967): p. 863-6.
264. Pivac, N., B. Kim, G. Nedic, Y.H. Joo, D. Kozaric-Kovacic, J.P. Hong, and D. Muck-Seler, *Ethnic differences in brain-derived neurotrophic factor Val66Met polymorphism in Croatian and Korean healthy participants*. *Croat Med J*, 2009. **50**(1): p. 43-8.
265. Verhagen, M., A. van der Meij, P.A. van Deurzen, J.G. Janzing, A. Arias-Vasquez, J.K. Buitelaar, and B. Franke, *Meta-analysis of the BDNF Val66Met polymorphism in major depressive disorder: effects of gender and ethnicity*. *Mol Psychiatry*, 2010. **15**(3): p. 260-71.
266. Shimizu, E., K. Hashimoto, and M. Iyo, *Ethnic difference of the BDNF 196G/A (val66met) polymorphism frequencies: the possibility to explain ethnic mental traits*. *Am J Med Genet B Neuropsychiatr Genet*, 2004. **126B**(1): p. 122-3.
267. Hong, C.J., S.J. Huo, F.C. Yen, C.L. Tung, G.M. Pan, and S.J. Tsai, *Association study of a brain-derived neurotrophic-factor genetic polymorphism and mood disorders, age of onset and suicidal behavior*. *Neuropsychobiology*, 2003. **48**(4): p. 186-9.
268. Ribeiro, L., J.V. Busnello, R.M. Cantor, F. Whelan, P. Whittaker, P. Deloukas, M.L. Wong, and J. Licinio, *The brain-derived neurotrophic factor rs6265 (Val66Met) polymorphism and depression in Mexican-Americans*. *Neuroreport*, 2007. **18**(12): p. 1291-3.
269. Numata, S., S. Ueno, J. Iga, K. Yamauchi, S. Hongwei, K. Ohta, S. Kinouchi, S. Shibuya-Tayoshi, S. Tayoshi, M. Aono, N. Kameoka, S. Sumitani, M. Tomotake, Y. Kaneda, T. Taniguchi, Y. Ishimoto, and T. Ohmori, *Brain-derived neurotrophic factor (BDNF) Val66Met polymorphism in schizophrenia is associated with age at onset and symptoms*. *Neurosci Lett*, 2006. **401**(1-2): p. 1-5.
270. Hwang, J.P., S.J. Tsai, C.J. Hong, C.H. Yang, J.F. Lirng, and Y.M. Yang, *The Val66Met polymorphism of the brain-derived neurotrophic-factor gene is associated with geriatric depression*. *Neurobiol Aging*, 2006. **27**(12): p. 1834-7.
271. Lang, U.E., R. Hellweg, P. Kalus, M. Bajbouj, K.P. Lenzen, T. Sander, D. Kunz, and J. Gallinat, *Association of a functional BDNF polymorphism and anxiety-related personality traits*. *Psychopharmacology (Berl)*, 2005. **180**(1): p. 95-9.
272. Notaras, M., R. Hill, and M. van den Buuse, *A role for the BDNF gene Val66Met polymorphism in schizophrenia? A comprehensive review*. *Neurosci Biobehav Rev*, 2015. **51**: p. 15-30.
273. Deng, F.Y., L.J. Tan, H. Shen, Y.J. Liu, Y.Z. Liu, J. Li, X.Z. Zhu, X.D. Chen, Q. Tian, M. Zhao, and H.W. Deng, *SNP rs6265 regulates protein phosphorylation and osteoblast differentiation and influences BMD in humans*. *J Bone Miner Res*, 2013. **28**(12): p. 2498-507.

## Chapter 2.

### General Methods

#### 2.1. Animals

##### 2.1.1. Ethics

All experimental procedures were carried out within the guidelines of the Code of Practice for the Care and Use of Animals for Scientific Purposes by the Australian National Health and Medical Research Council, and in compliance with the ARRIVE guidelines for how to report animal experiments. All experiments were approved by the La Trobe (LTU) Animal Ethics Committee, and/or The Florey Institute of Neuroscience and Mental Health (FINMH) Animal Ethics Committee. The C57BL/6 strain of mouse was used and, unless otherwise stated, all experimental mice were male. Mice were aged 12 weeks of age at the beginning of experimentation for **Chapters 3 and 5**, and 16 weeks of age at the beginning of experimentation for **Chapter 4**. In **Chapter 3**, at the end of the behavioural experiments, mice were anaesthetized with isoflurane and decapitated to preserve and harvest brains for further analysis. At the end of **Chapters 4 and 5**, mice were euthanised via carbon dioxide asphyxiation, and mouse (skeletal) tissue was harvested for further analysis.

##### 2.1.2. Housing

Throughout all experiments, mice were housed at either LTU Central Animal House or at the FINMH Animal Facility. All mice were housed in standard mouse boxes (48 x 15 x 13 cm) with appropriate sawdust bedding materials. TBI apparatus and behavioural equipment was not accessible at LTU at the time of experimentation; so, mice allocated to the TBI study (**Chapter 3**) were housed at the FINMH. Mice at FINMH were housed in groups of five per box prior to surgery, then individually housed due to concerns that group housing may affect the injury site. Mice allocated to long bone fracture studies (**Chapters 4 and 5**) were housed in groups up to five per mouse box at LTU Central Animal House. Prior to any experimentation, mice were acclimatised to holding rooms at all facility sites for a minimum of 1 week. Housing rooms were maintained under a 12 h light/dark cycle at a temperature of 22°C, and mice had *ad libitum* access to standard mouse chow and water. A Petri dish containing DietGel<sup>®</sup> was added to the cage of mice unable to feed in the acute stages post-surgery.

#### 2.2. Drugs and reagents

The TrkA agonist, gambogic amide (GA) (used in **Chapters 3 and 4**), was supplied by Sapphire Bioscience Pty Ltd (Waterloo, Australia). The TrkB agonist, 7,8-dihydroxyflavone (7,8-DHF) (used in **Chapter 5**) was supplied by Abcam<sup>®</sup> (ab120996; Abcam plc. Cambridge, UK). For details regarding vehicle (VEH) choice and drug administration, please view individual chapters.

Additional drugs that were used and their appropriate chapters are: Kolliphor® HS 15 – **Chapters 3 and 5** (Sigma-Aldrich), isoflurane – **Chapters 3, 4 and 5** (Sigma-Aldrich), Carprofen - **Chapters 4 and 5** (RIMADYL®; Zoetis, USA), buprenorphine – **Chapter 5** (Jurox, Australia), dimethyl sulfoxide (DMSO) – **Chapter 4** (Sigma-Aldrich). Please refer to individual chapters for all other reagents used throughout experimentation.

### **2.3. Microcomputed tomography ( $\mu$ CT)**

$\mu$ CT was used to measure structural architecture of fracture calluses in mice, specifically size of callus and amount of mineralized tissue present (**Chapters 4 and 6**).  $\mu$ CT analysis was performed similarly to Brady *et al* (2014, 2016). Calluses were dissected at the time of euthanasia and immersed in fixative solution (4% paraformaldehyde in 0.1 M sodium cacodylate buffer) for 48 h, then washed and stored in bone storage solution (10% sucrose in 0.1 M sodium cacodylate buffer) at 4°C until time of scanning. Scanning took place at St Vincent’s Institute of Medical Research (Fitzroy), using SKYSCAN 1076 *in vivo* X-ray microcomputed tomography (Bruker- $\mu$ CT). Samples were transferred to 70% ethanol on day of scanning and transported on ice. The following acquisition parameters were used based on previous publications; 9  $\mu$ m voxel resolution, 0.5 mm aluminium filter, 48 kV voltage, 100  $\mu$ A current, 2,400 ms exposure, rotation 0.5° across 180°, frame averaging of 1 [1, 2]. Data was loaded onto a hardware device and images were reconstructed at La Trobe University using NRecon (V1.6.3.1) with the following parameters: smoothing factor, 1; ring artefacts, 6; beam-hardening correction; 35%; pixel defect mask, 5%; C.S rotation, 0; and misalignment compensation, <3. Images were realigned and orientated using Dataviewer (V1.4.4) to obtain transaxial datasets for calluses. Analysis of the transaxial datasets was performed using CTAn (V1.11.8.0) and the region of interest (ROI) was obtained and the border of each callus was manually traced. Thresholds used for parameter quantification were determined using the automatic “otsu” algorithm within CTAn and visual examination of unreconstructed x-ray images. A grayscale adaptive threshold was calculated for each experimental data set and used for structural analysis of calluses. Please see individual chapters for additional details of parameters and thresholds used.

### **2.4. Biomechanics**

Three-point bending tests were used to assess the structure and mechanical properties of fracture calluses in mice (**Chapters 4 and 5**) [1, 3]. Dissected at time of euthanasia, calluses were stripped of muscle and stored in silicon oil at -20°C until the day of assessment. On the day of mechanical testing, samples were removed from the freezer and allowed to equilibrate to room temperature (RT) for 1 h. Each callus was mounted onto the three-point bending apparatus with the callus lying centrally under the fulcrum; this ensured peak stress was applied directly onto the

centre of the callus. A force transducer descended at a constant rate of 1.67 mm/sec and loaded each callus. Force (g) and deflection (mm) values were recorded using LabChart (ADInstruments Pty Ltd., AU) and plotted an x-y (load-displacement) graph. Fractured ends of calluses were collected and re-stored in silicon oil. Please refer to individual chapters for specific details of bone position and size of force transducer.

#### **2.4.1. Cross-sectional area of calluses**

The cross-sectional area for each fractured end of callus was measured in order to calculate bending stress and Young's modulus. Any callus that fractured in an oblique plain was cut into a transverse plain in order to measure true cross-sectional area. Fractured ends were imprinted onto dental wax and individually viewed using Leica DFC420 light microscope (Leica Microsystems Ltd., Heerbrugg, Switzerland). Imprints were viewed and photographed under magnification using Leica IM50 imaging software (Leica). Cross-sectional areas were obtained for each callus by averaging the total area values traced with software Leica Qwin V3 Standard (Leica).

#### **2.4.2. Mechanical properties analysis**

Differences in elastic and plastic properties were analysed using a load-displacement graph (**Figure 2.1**) from which peak force, bending stress, stiffness and Young's modulus could be calculated.

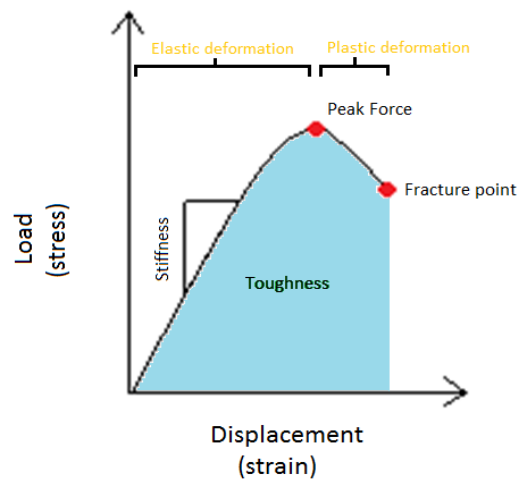


**Figure 2.1.** The load-displacement graph showing the biomechanical strain placed on a bone, including elastic deformation and plastic deformation, until the bone fractures (courtesy of Dr Brian Grills and Dr Stuart McDonald).

All calculations for callus biomechanics were set for solid objects and not hollow objects, and all calluses displayed minimal or no signs of recanalization at the time-points of mechanical testing.



Firstly, value corrections were made to cross-sectional area and peak force in order to calculate other mechanical properties. Cross-sectional area values were corrected from mm<sup>2</sup> to m<sup>2</sup>, by multiplying the values with 10<sup>-6</sup>. Peak force values (x) were corrected from volts to newtons (N) using,  $N = x \times 2.5545 + 0.2615$ . Bending stress ( $\sigma$ , Nm<sup>-2</sup>) is the minimal load necessary to break a structure, and in bone is defined as the relationship between the peak force (N) and cross-sectional area (m<sup>2</sup>) of bone [4]. Bending stress was calculated using the following equation;  $\sigma = F \times L / (\pi A^{3/2})$ . Where,  $\sigma$  is bending stress (Nm<sup>-2</sup>), F is the peak force (N), L is the distance between the two platforms (m),  $\pi$  is 3.14 and A is the cross-sectional area (m<sup>2</sup>) of the calluses at the site of re-fracture. Stiffness (N.m<sup>-1</sup>) was calculated directly from the gradient of the linear portion (i.e. elastic phase) of the load-displacement trace produced during the three-point bending (**Figure 2.1**). Young's modulus (E, N.m<sup>-2</sup>) is the total rigidity of the bone; it is the direct relationship between stress and strain applied to the bone, and their influence on bone structure [5]. Young's modulus was calculated using the following equation;  $E = (F/Y) \times (\pi L^3/12A^2)$ . Where, E is Young's modulus (N.m<sup>-2</sup>), F/Y is stiffness (N.m<sup>-1</sup>),  $\pi$  is 3.14, L is the distance between the two platforms (m) and A is the cross-sectional area (m<sup>2</sup>) of calluses as the site of re-fracture.

## **2.5. Histology**

Murine fracture calluses that were previously scanned via  $\mu$ CT, were histologically processed to assess tissue composition at various stages of fracture healing (**Chapter 4 and 5**). Embedding and sectioning protocols were identical to that already published by Brady *et al* (2014).

### **2.5.1. Tissue preparation and embedding**

Each callus was stripped of skeletal muscle in preparation of processing in LR White Resin Hard Grade Acrylic (London Resin Company, Reading, UK). Samples were consecutively washed for 1 h in 70%, 90% and 100% ethanol (ETOH) under agitation to remove any bone storage buffer residue and were then left overnight in 100% ethanol. Chloroform and 100% ETOH were used cyclically to wash samples 1 h each time, for a total of 4 h. Samples were transferred into glass vials in a 50/50 100% ETOH/LR White Resin solution for 3 h, then, in order for the resin penetration into tissue, the solution was replaced 100% LR White Resin and vacuum sealed overnight. 100% LR White Resin was replaced for each sample and left to agitate under vacuum all day. Callus samples were then positioned centrally in the bottom of the glass vials and LR White Resin was topped up 1 cm above the sample. To polymerise LR White resin, vials were placed in an oven for 24 h at 60°C. Once the resin had polymerised and cooled, the glass vials were wrapped in a tea towel a gently struck with a hammer to shatter the glass off the solid resin blocks.

### **2.5.2. Sectioning tissue**

Resin blocks containing callus samples were mounted onto a Leica RM 2155 Rotary Microtome (Leica). Sections of non-decalcified callus were cut longitudinally with a Tungsten blade knife (approximately 5  $\mu\text{m}$  thick) at the mid-point of each callus. Sliced sections were floated in 70°C water then placed four per slide onto Menzel-Gläser Superfrost® Plus glass slides (Lomb Scientific Pty Ltd, Tarenpoint, Australia), and baked on a hotplate for 1 h at 70°C.

### **2.5.3. Tissue section staining**

All stains for histological assessment were supplied by Sigma-Aldrich (Sigma Aldrich) (see **Appendix A** for stain composition). Alcian blue (cartilage stain) and alcoholic eosin (bone stain) are two commonly used stains to assess cartilage vs. bone formation in healing calluses [6, 7]. Using a staining rack, two slides containing eight callus sections were stained for 30 min in 1% Alcian blue, rinsed in 1% acetic acid for 10 s, dH<sub>2</sub>O for 30 s, then stained in Eosin for 1 min 30 s. Sections were then rinsed in dH<sub>2</sub>O, allowed to air-dry and then cover slipped with dibutylphthalate polystyrene xylene (DPX) mountant (Sigma-Aldrich). Sections were viewed and photographed at x25 magnification using a light microscope. Fibrous tissue, cartilage, new bone area and callus area were manually traced and quantified using Leica Qwin V3 Standard (Leica).

Tartrate-resistant acid phosphatase (TRAP) stain is well developed stain used to assess bone resorption in healing calluses [1, 8, 9]. The stain seeks out TRAP; an enzyme secreted by active osteoclasts and pigments the enzyme pink [10]. Sections were incubated with 0.2M acetate buffer for 20 min in a humidified chamber at RT. Acetate buffer was removed, and TRAP-reagent was added to each section and incubated in a 37°C humid chamber for 4 h. Sections were rinsed in distilled water, air-dried and cover slipped in DPX mountant. Sections were viewed and photographed at x200 magnification with a light microscope. TRAP stain area was quantified using Leica Qwin V3 Standard (Leica).

## **2.6. Cell Culture**

Two multi-potential bone marrow stromal cell lines were used in **Chapters 4** and **5**. Kusa O cells (used in **Chapter 4**) had been previously gifted to our lab from Dr Julian Quinn (The Garvin Institute, Sydney) therefore, these were the first cell line used. Kusa O cells are multi-potential bone marrow stromal cells [11], and that have been characterised as cells with an osteogenic phenotype, suitable for investigations on osteoblastic differentiation [12]. Apart from their osteogenic potential, they can, with slight altercations in culture medium, also display an adipocytic phenotype [12], which typically results in a mixed osteoblastic/adipocytic cell population. A genetic subclone, Kusa4b10, was gifted to our lab from Dr Natalie Sims (St. Vincent's

Institute of Medical Research) just prior to the start of **Chapter 5**. Kusa4b10 cells have demonstrated a more osteoblastic phenotype than the Kusa Os, thus they are more suitable for investigations on osteoblastic differentiation [12, 13]. Unless otherwise stated, both cell lines were stored, maintained and cultured under that same conditions.

### **2.6.1. Cell storage and maintenance**

Cells were stored in 1 ml vials at temperatures below  $-195^{\circ}\text{C}$  in liquid nitrogen filled cryogenic protective dewars until use. Vials were thawed at RT, then transferred into a 75 cm<sup>2</sup> canted neck flask and maintained in alpha-Minimum Essential Medium ( $\alpha$ -MEM, Gibco® Life Technologies™, Auckland, NZ) plus 10% Australian Premium foetal bovine serum (FBS, Australian Ethical Biologicals Pty. Ltd., Coburg, AU). Cells actively used for experiments were stored in 5% CO<sub>2</sub>/H<sub>2</sub>O jacketed incubator (HEPA Class 100 Forma Series II, Thermoline) at 37°C and culture medium was replaced every three days. Cells were used between passages 10-22, as beyond passage 25, cells have been reported to be unstable and lose their mineralization characteristics [12].

### **2.6.2. Cell subculture and freezing process**

To maintain stock of several passages for future studies, a series of cells were sub-cultured and/or 1 ml vials were frozen and returned to the dewars. For subculture, cells were lifted from flasks via aspiration of media, followed by 3 x 15 s wash of 10 ml phosphate buffered saline (PBS) and then the addition of 1.5 ml of TrypLE™ Express (Gibco®, Denmark), and incubated for 5-7 min.  $\alpha$ -Minimum Essential Medium ( $\alpha$ -MEM) (8.5 ml) was added to cell/TrypLE™ Express mix to maintain cell stability and cells were gently transferred from the flask into a Corning® CentriStar™ tube (Corning Incorporated, USA). Cells were then subdivided in up to five new flasks or culture plates. For the cells to be frozen down, cell/ TrypLE™ Express mix was centrifuged and the pellet was re-suspended in  $\alpha$ -MEM plus 10% DMSO and stored in 1 ml aliquots in cryovials at  $-80^{\circ}\text{C}$  overnight. Cryovials were transferred to the dewar.

### **2.6.3. Western blotting**

#### **Protein sample preparation**

Western blotting assays were used to determine TrkA and TrkB receptors on Kusa O and Kusa4b10. The Western blotting protocol used throughout these experiments was the '*General Western blot protocol*' available as a PDF through Abcam online (Abcam). Cells were sub-cultured at a density of 3000 cells/ml in  $\alpha$ -MEM plus 10% FBS for 3 days. Cells were either maintained in  $\alpha$ -MEM plus 10% FBS, or osteoblastic differentiating medium ( $\alpha$ -MEM plus 10% FBS supplemented

with 50 µg/ml ascorbate and 10mM β-glycerophosphate) [12, 13]. Medium was replenished three days a week. Lysate was isolated from the undifferentiated and differentiated cell populations. Briefly, cells were washed three times in PBS and then lysed in RIPA-EDTA buffer (150mM NaCl, 1% Triton X, 0.5% sodium deoxycholate, 0.1% SDS, 50mM Tris, 0.5mM EDTA) with added protease and phosphatase cocktail inhibitors.

Protein sample concentration was determined using Pierce™ BCA™ Protein Assay Kit (Pierce Biotechnology, Rockford, USA). Nine diluted bovine albumin (BSA) standards were prepared in sterile tubes in accordance to the kit instructions. 25 µl triplicates of each standard and unknown sample was loaded onto a 96-well plate followed by 200 µl of working reagent. The plate was incubated at 37°C for 30 min and then absorbance was read at 550 nm using a Microplate Spectrophotometer (DYNEX Technologies Ltd, UK) to determine protein concentration and supernatant protein concentration was mixed [1:1 (v/v) ratio] with Laemmli x2 loading buffer. Left over volumes of standards and samples were stored in -20°C for future use.

### ***Gel electrophoresis***

For gel electrophoresis, samples were boiled for 5 min to denature proteins and allow for protein migration. Using a Precast Mini-PROTEAN® TGX™ gel (Bio-Rad Laboratories Inc., Hercules, USA), 10 µg pf protein from each sample was loaded, alongside 5 µl of molecular weight marker, Precision Plus Protein™ WesternC™ Standard (Bio-Rad). The gel electrophoresis was run for 45 min at 30 constant Amps and 200 V. Once electrophoresis was complete, the apparatus was disassembled, and the gel was suspended in transfer buffer.

### ***Transfer of protein to polyvinyl difluoride (PVDF) membrane***

Protein bands were transferred onto PVDF membranes (pre-soaked in methanol) using the Mini Trans-Blot® Electrophoretic Transfer Cell (Bio-Rad). A 'sandwich' was assembled by layering of sponges, filter papers, gel and membrane, and clamped into the transfer cell, which was filled with transfer buffer. The membrane side of the sandwich was faced towards the positive electrode and the gel side towards the negative electrode. The transfer was run for 1 h at 4°C at 100 V.

### ***Chemiluminescent protein detection***

For protein detection, PVDF membranes were blocked in 5% skim milk blocking buffer at RT for 2 h under agitation. Skim milk blocking buffer prevented the non-specific binding of proteins during the primary and secondary antibody probing stages [14]. Antibodies used for Western blotting were supplied by Abcam® (Sapphire Bioscience) and were diluted in 1x Tris-Buffered Saline and 0.1% Tween 20 (TBST) each time they were used. For a list of antibodies and dilutions used, please refer to individual chapter sections 'Materials and Methods' and 'Western blotting'.

At 4°C, membranes were probed with primary antibodies overnight. The next morning, membranes were thoroughly washed in TBST, and then incubated with secondary antibodies for 2 h at RT. Signal detection was developed with chemiluminescence (Immuno-Star™ HRP kit, Bio-Rad). Immunoreactive bands were digitally imaged using Molecular Imager® Chemidoc™ XRS+ (Bio-Rad) and results were quantified using Image Lab™ Software (Bio-Rad). Values were normalised using the loading control,  $\alpha$ -tubulin.

#### **2.6.4. Proliferation Assays**

Cells were sub-cultured in a 96-well plate at a density of 3000 cells/ml in  $\alpha$ -MEM plus 10% FBS. After 3 h, medium was aspirated and replaced with  $\alpha$ -MEM plus 2% FBS. Cells were treated with either GA (**Chapter 4**) or 7,8-DHF (**Chapter 5**) for 72 h. The negative controls were  $\alpha$ -MEM only and positive controls were  $\alpha$ -MEM+10% FBS,  $\alpha$ -MEM + 100 ng/ml IGF (Life Technologies™, Scoresby, AU). Cell proliferation was measured using CellTiter 96® AQueous One Solution Cell Proliferation Assay kit (Promega Corporation, Madison, USA) as per manufacturer's instructions, with absorbance read at 490 nm using Multiskan GO (Thermo Fisher Scientific Oy, Finland). Data was normalized to controls.

#### **2.6.5. Gene expression analysis by reverse transcription-polymerase chain reaction (RT-PCR)**

Cells were sub-cultured at a density of 3000 cells/ml in  $\alpha$ -MEM plus 10% FBS. After 24 h, medium was aspirated and replaced with osteoblastic differentiation medium of  $\alpha$ -MEM plus 10% FBS with added 50  $\mu$ g/ml ascorbate [12, 13]. Cells were maintained in this medium and treated daily with GA (**Chapter 4**) and 7,8-DHF (**Chapter 5**) and media was replenished three times a week. Total RNA was prepared from cells lysed in PureZol™ (Bio-Rad) and stored at -80°C for further RNA extraction. Chloroform (1/5 of lysate volume) was added to the cell lysate and centrifuged to separate homogenate into three phases; pink phenol-chloroform phase, interphase and clear aqueous phase (where the RNA is located). The aqueous phase was collected, and an equal volume of isopropanol was added. The RNA mixture was stored at -20°C overnight to precipitate the RNA. The mixture was centrifuged at 13,000 rpm for 15 min to result in a pellet of pure RNA. The pellet was isolated and washed in 75% ETOH in diethylpyrocarbonate (DEPC) treated H<sub>2</sub>O at 8,000 rpm for 8 min. The ethanol was removed, and the pellet was allowed to dry before being dissolved in 10  $\mu$ l of nuclease-free H<sub>2</sub>O. The eluted RNA was analysed for purity and quantity using the Nanodrop 2000 (Thermo Fisher Scientific, USA), which assessed the amount of nucleic acid (ng/ml) and absorbance  $A_{260/280}$ . 1  $\mu$ g of total RNA underwent reverse transcription using iScript™ cDNA Synthesis Kit (Bio-Rad). The mixture was thoroughly mixed, placed in the Bio-Rad CFX96™ Real-Time System (Bio-Rad) and underwent a series of incubation settings; 5 min at 25°C, increasing to 42°C for 30 min, then it was further incubated for 5 min for 85°C. The resulting cDNA produced was

stored at -80°C until it was used in RT-PCR analysis. PCR was performed in quadruplicate using SsoFast™ EvaGreen® Supermix (Bio-Rad) on an iQ 96-well PCR system (Bio-Rad). Each amplification reaction contained 1 µl of cDNA and 300 nM of primer. Thermal cycling conditions included initial denaturation at 95°C for 30 s, followed by 40 cycles of 95°C for 5 s and 55°C for 5 s. Melt-curve analysis was performed post-cycling to confirm specificity of the amplified products. Relative quantification of genes of interest mRNA expression normalised to the house-keeping gene and was determined using the  $2^{-\Delta\Delta Ct}$  method.

Please refer to each chapter under 'Material and Methods' and 'RT-PCR' for specific primers that were used. Primers were designed using Beacon designer 3.00 (PREMIER Biosoft International., USA). Primers for RT-PCR were synthesized and supplied by GeneWorks Pty Ltd (GeneWorks Pty Ltd, Thebarton, AU).

#### **2.6.6. Mineralization assays**

Cells were sub-cultured at a density of 3000 cells/ml in  $\alpha$ -MEM plus 10% FBS for 24 h, then changed to osteoblastic differentiating medium of  $\alpha$ -MEM plus 10% FBS with 50 µg/ml ascorbate and 10 nM beta-glycerophosphate [12, 13]. Cells were maintained in this medium for 21 days and medium was replaced three times per week. Kusa O cells were treated daily with GA (**Chapter 4**) and Kusa4b10 cells were treated daily with 7,8-DHF (**Chapter 5**). After 21 days, cells were washed three times in cold PBS and fixed in ice cold 70% ETOH for 30 min. Cells were then washed in cold PBS and stained for 30 min with 0.5% Alizarin Red stain solution (pH 4.2). Alizarin Red stain was removed with five PBS washes and cells were imaged with a flatbed colour scanner. Mineralized areas were quantified using ImageJ software (National Institutes of Health, Bethesda, USA).

#### **2.7. Statistical analysis**

All outcomes were analysed using GraphPad Prism software versions 6-7 (GraphPad Software, Inc., La Jolla, USA). All data was subject to Shapiro-Wilk normality tests. Data was presented as the mean  $\pm$  SEM and statistical significance was defined as  $p \leq 0.05$ . The number of asterisks defined the p value; \* $p < 0.05$ , \*\* $p < 0.01$ , \*\*\* $p < 0.001$ . Please refer to each chapter 'Material and methods' and 'Statistical analysis' for specific statistical analyses used.

## 2.8. References

1. Brady, R.D., B.L. Grills, J.A. Schuijers, A.R. Ward, B.A. Tonkin, N.C. Walsh, and S.J. McDonald, *Thymosin beta4 administration enhances fracture healing in mice*. J Orthop Res, 2014. **32**(10): p. 1277-82.
2. Brady, R.D., B.L. Grills, J.E. Church, N.C. Walsh, A.C. McDonald, D.V. Agoston, M. Sun, T.J. O'Brien, S.R. Shultz, and S.J. McDonald, *Closed head experimental traumatic brain injury increases size and bone volume of callus in mice with concomitant tibial fracture*. Sci Rep, 2016. **6**: p. 34491.
3. Grills, B.L., J.A. Schuijers, and A.R. Ward, *Topical application of nerve growth factor improves fracture healing in rats*. J Orthop Res, 1997. **15**(2): p. 235-42.
4. Ascenzi, A. and E. Bonucci, *The Ultimate Tensile Strength of Single Osteons*. Acta Anat (Basel), 1964. **58**: p. 160-83.
5. Bonfield, W. and P.K. Datta, *Young's modulus of compact bone*. Journal of Biomechanics, 1974. **7**(2): p. 147-149.
6. Ishikawa, M., H. Ito, T. Kitaori, K. Murata, H. Shibuya, M. Furu, H. Yoshitomi, T. Fujii, K. Yamamoto, and S. Matsuda, *MCP/CCR2 signaling is essential for recruitment of mesenchymal progenitor cells during the early phase of fracture healing*. PLoS One, 2014. **9**(8): p. e104954.
7. Gooch, H.L., J.E. Hale, H. Fujioka, G. Balian, and S.R. Hurwitz, *Alterations of cartilage and collagen expression during fracture healing in experimental diabetes*. Connect Tissue Res, 2000. **41**(2): p. 81-91.
8. Cherruau, M., P. Facchinetti, B. Baroukh, and J.L. Saffar, *Chemical sympathectomy impairs bone resorption in rats: a role for the sympathetic system on bone metabolism*. Bone, 1999. **25**(5): p. 545-51.
9. Yin, G., T.J. Sheu, P. Menon, J. Pang, H.C. Ho, S. Shi, C. Xie, E. Smolock, C. Yan, M.J. Zuscik, and B.C. Berk, *Impaired angiogenesis during fracture healing in GPCR kinase 2 interacting protein-1 (GIT1) knock out mice*. PLoS One, 2014. **9**(2): p. e89127.
10. Blumer, M.J., B. Hausott, C. Schwarzer, A.R. Hayman, J. Stempel, and H. Fritsch, *Role of tartrate-resistant acid phosphatase (TRAP) in long bone development*. Mech Dev, 2012. **129**(5-8): p. 162-76.
11. Kawashima, N., K. Shindo, K. Sakamoto, H. Kondo, A. Umezawa, S. Kasugai, B. Perbal, H. Suda, M. Takagi, and K. Katsube, *Molecular and cell biological properties of mouse osteogenic mesenchymal progenitor cells, Kusa*. J Bone Miner Metab, 2005. **23**(2): p. 123-33.

12. Allan, E.H., P.W. Ho, A. Umezawa, J. Hata, F. Makishima, M.T. Gillespie, and T.J. Martin, *Differentiation potential of a mouse bone marrow stromal cell line*. J Cell Biochem, 2003. **90**(1): p. 158-69.
13. Allan, E.H., K.D. Hausler, T. Wei, J.H. Gooi, J.M. Quinn, B. Crimeen-Irwin, S. Pompolo, N.A. Sims, M.T. Gillespie, J.E. Onyia, and T.J. Martin, *EphrinB2 regulation by PTH and PTHrP revealed by molecular profiling in differentiating osteoblasts*. J Bone Miner Res, 2008. **23**(8): p. 1170-81.
14. Mahmood, T. and P.C. Yang, *Western blot: technique, theory, and trouble shooting*. N Am J Med Sci, 2012. **4**(9): p. 429-34.



## Chapter 3.

### The effects of the selective TrkA agonist, gambogic amide, on the outcomes of traumatic brain injury in mice

Note: A version of this chapter has been published prior to the completion of this thesis. The extent of contributions for this chapter as well as permissions and a copy of the publication can be found in **Appendix B**.

**Johnstone M. R.**, Sun M., Taylor C. J., Brady R. D., Grills B. L., Church J. E., Shultz S. R., and McDonald S. J., Gambogic amide, selective TrkA agonist, does not improve outcomes from traumatic brain injury in mice. *Brain Injury*. 2018 32(2) 257-268.

#### 3.1. Introduction

Traumatic brain injury (TBI) is a form of acquired brain injury and is a leading cause of death and disability worldwide [1]. Whilst some TBI patients recover within months of injury [2], TBI can result in chronic physical, cognitive and emotional abnormalities, and has been associated with the development of neurodegenerative diseases [3-7]. The brain damage in TBI results from both the irreversible primary mechanical insult and the activation of secondary injury mechanisms, such as neuroinflammation and apoptosis that evolve over the hours to months after the initial impact [3, 5, 8]. Neuroinflammation in TBI is characterized by the activation of microglia and astrocytes and release of pro-inflammatory cytokines, whereas apoptosis is a significant contributor to cell death following TBI [9, 10]. Several experimental TBI studies have shown that activation of neuroinflammation and apoptosis can lead to worsened cognitive capacity, emotional disturbances and motor control dysfunction [11-16], and that treatments targeting these mechanisms have potential to improve TBI outcomes [17-19].

Nerve growth factor (NGF) is a neurotrophin responsible for the growth and maintenance of target neurons in the CNS [20, 21]. Several studies have demonstrated that NGF exerts pro-survival responses in neurons by binding to its high affinity receptor TrkA [22, 23]. Although there is currently no reported data on the therapeutic use of NGF in clinical trials for TBI, there have been promising animal studies that support the potential benefit of TrkA activation post-TBI. In experimental rodent TBI models, NGF administration has been shown to alleviate several of the deficits associated with the secondary mechanisms of TBI, including promoting neuron survival, reducing expression of inflammatory markers, and reducing cerebral edema [15, 24-29]. Furthermore, NGF treatment following TBI was found to improve spatial memory of rodents during Morris water maze testing [15, 28-31].

A potential issue with using NGF in the treatment of CNS injuries is the poor pharmacokinetic properties of the peptide. NGF has low blood brain barrier (BBB) penetrability and has a short elimination half-life (~2 h) following systemic administration [32-34]. As such, the use of small non-peptide neurotrophic mimetics may have superior therapeutic potential. One such substance is gambogic amide (GA), a recently discovered, BBB permeable, selective high affinity TrkA agonist [35-37]. GA was found to selectively bind to TrkA and activate downstream Akt and mitogen-activated protein kinase (MAPK) signaling in neurons *in vitro*, resulting in the promotion of neurite outgrowth and increased resistance to glutamate-induced cell death [35]. *In vivo*, systemic administration of 2 mg/kg/day of GA in mice protected neurons from kainic acid-induced apoptosis, and reduced infarct volume in a transient model of ischemic brain injury [35]. No studies, however, have investigated the therapeutic potential of GA in TBI. Accordingly, the aim of the present study was to investigate the effects of GA treatment on neuroinflammation, apoptosis, neurite outgrowth and behavioural outcomes following lateral fluid percussion injury (LFPI) in mice.

## **3.2. Materials and methods**

### **3.2.1. Subjects**

Thirty, C57BL/6 male mice were obtained from the Australian Animal Resource Centre (ARC, Western Australia). Mice were 12 weeks of age at time of injury and were housed individually throughout the experiment under a 12 h light/dark cycle with access to food and water *ad libitum*. All experimental procedures were approved by The Florey Institute of Neuroscience and Mental Health Animal Ethics Committee (#14-006 UM), were within the guidelines of the Australian code of practice for the care and use of animals for scientific purposes by the Australian National Health and Medical Research Council, and in compliance with the ARRIVE guidelines for how to report animal experiments.

### **3.2.2. Experimental groups**

Mice were randomly assigned to receive either a LFPI (n = 16) or a sham-injury (n = 14). One mouse died immediately post-LFPI and another mouse given LFPI was euthanized after failing to recover basic motor function after injury. To assess the effects of GA on acute TBI outcomes, mice were then randomly assigned to one of four experimental groups: sham injury + vehicle (i.e. 30% w/v of Kolliphor<sup>®</sup> HS 15 in saline; SHAM+VEH; n = 7), sham injury + GA in vehicle (SHAM+GA; n = 7), TBI + vehicle (TBI+VEH; n = 7), and TBI + GA (TBI+GA; n = 7). As GA had poor water solubility at the concentration suitable for subcutaneous injection, a vehicle consisting of 30% w/v of Kolliphor<sup>®</sup> HS 15 and saline was used to form a microemulsion of GA. Kolliphor<sup>®</sup> HS 15 (Solutol<sup>®</sup> HS 15) is a non-ionic emulsifier, a white, odorless paste that is well tolerated and commonly used as

a vehicle in human and veterinary injection formulations [38-41] Subcutaneous injections of GA (2 mg/kg/day) or vehicle were made at 1-, 24- and 48-h post-injury. GA and this dosing regimen were chosen due to the previously demonstrated potent and selective neurotrophic actions of GA *in vitro*, and promising neuroprotective properties at 2 mg/kg/day following ischemic brain injury [35, 36]. All mice were euthanized at 72 h post-injury, a time-point chosen as it would allow for acute behavioral assessments, as well as capturing several pathological/physiological events (e.g. edema, apoptosis, microglia activation, astrocyte activation, neurite outgrowth, synaptogenesis) at a single acute post-injury time-point [5, 7, 42, 43].

### **3.2.3. Lateral fluid percussion injury**

The LFPI is a commonly used and well-validated model of TBI. LFPI and sham injury procedures were conducted using previously described standard protocols [44]. Briefly, mice were anaesthetized with isoflurane and underwent a 3 mm craniotomy over the lateral parietal cortex to expose the intact dura mater of the brain. A hollow injury cap was placed over the craniotomy and was secured by dental acrylic, the mouse was removed from anesthesia and attached to the fluid percussion device via the injury cap. At first response of hind-limb withdrawal, the fluid percussion device delivered a fluid pulse of 1-1.5 atm to the brain. Upon resumption of spontaneous breathing, the injury cap was removed and the wound sutured. Sham-injury mice underwent the identical procedures as the LFPI mice except for the delivery of the fluid pulse.

### **3.2.4. Acute injury severity**

Apnoea, hind-limb withdrawal and self-righting reflex times were monitored and recorded in all mice after injury as an indicator of acute injury severity [13, 43]. Apnoea was defined as the time from injury to spontaneous breathing, loss of consciousness was the time from injury to a hind-limb withdrawal response to a toe pinch, and self-righting reflex was the time from injury to the return of an upright position.

### **3.2.5. Behavioural testing**

Mice underwent a series of behavioural tests in rotarod, open-field, elevated plus-maze (EPM) and Y-maze over a period of three days beginning at 1-day post-injury.

#### **Rotarod**

The accelerated rotarod was used at 1-, 2- and 3-days post-injury to assess sensorimotor ability [44, 45]. The testing apparatus consisted of rotating barrels (diameter = 3 cm) in four consecutive lanes (diameter = 5 cm) separated by walls (diameter = 10 cm; Harvard Apparatus, Holliston, TX, USA). Mice completed training one day before injury followed by three days of

consecutive trials starting day 1 post-injury. Each trial consisted of the mouse being placed on the rotating barrel, the speed was increased from 4 to 40 rpm over a period of 5 min, and the average duration of time the mouse was able to stay on the rotating barrel was recorded for each trial period (maximum time of 5 min).

### ***Open-field***

One day post-injury mice underwent open-field testing to assess locomotion and anxiety-like behaviour as previously described [43, 44]. Briefly, the testing area consisted of a 100 cm diameter circular field surrounded by a 20 cm high plastic wall, with mice were individually placed in the centre of field and allowed to explore the arena for a 5 min test period. Using EthoVision® tracking software (Noldus, Leesburg, VA, USA) behaviour was recorded and quantified with the following parameters; time spent in inner field (66 cm diameter) and total distance travelled. Time spent in the inner field was a measure of anxiety-like behaviour in mice and total distance travelled in the field was as a measure of locomotion.

### ***Elevated plus-maze***

At two days post-injury mice completed EPM testing to assess anxiety-like behaviour [44, 46]. The testing apparatus consisted of four arms (length = 30 cm, width = 6 cm) shaped in a plus. Two opposing arms (closed-arms) had 15 cm high walls bounding them and the other two opposing arms (open-arms) had no walls. Mice were placed in the centre of the EPM facing the open-arm and allowed to explore the arena for 5 min. Behaviour was recorded using an overhead camera and was quantified using EthoVision® tracking software (Noldus). Decreased amount of time spent in the open-arm equated to increased anxiety-related behaviour in mice [44]. Total distance travelled was used as a measure of locomotion.

### ***Y-maze***

Y-maze was completed at three days post-injury to assess spatial memory [44]. The Y-maze testing apparatus consisted of three arms (length = 38 cm, width = 8 cm) enclosed by 13 cm high walls shaped in a Y-shape (San Diego Instruments, San Diego, CA, USA). Unique visual cues were placed at the distal end of each arm. Mice completed a 15 min training period prior to testing. During the training period, two of the arms remained open (start arm and old arm) and one of the three arms (novel arm) was blocked by a barrier. The mouse was given a 15 min interval period between training and testing. Commencing the 5 min testing period, the novel arm of the Y-maze was unblocked, and the mouse was again placed in the start arm and allowed to freely explore all three arms. Behaviour was recorded using an overhead camera and analysed using EthoVision® tracking software (Noldus). Time spent exploring the novel and total distance travelled was used as a measure of spatial memory.

### **3.2.6. Oedema**

Brain water content was used to measure oedema. At 72 h post-injury mice were killed and the brain was harvested. A piece of injured and uninjured cerebral cortex was dissected and individually weighed (wet weight). The tissue was dried at 100°C for 24 h and then weighed again (dry weight). To calculate brain water content the following formula was used: water content (%) = (wet weight – dry weight)/wet weight.

### **3.2.7. Brain tissue preparation**

Anesthetized mice (4% isoflurane for 1 min) were decapitated at 72 h post-injury. Brains were removed and dissected, and the tissue was rapidly frozen in liquid nitrogen and stored at –80°C. One piece of brain tissue (~10 mg) from the ipsilateral cortex (IC) and ipsilateral hippocampus (IH) was collected for RT-PCR, with an adjacent region of IC (~5 mg) collected for Western blot analysis.

### **3.2.8. RNA extraction and RT-PCR**

Samples were homogenized in 600 µl of PureZOL™ RNA isolation reagent using Precelly's 24 Bead Mill Homogenizer (Bertin Technologies, Villeurbanne, France) at 4°C, before being centrifuged at 12,000 rpm for 20 min at 4°C. Lysate from each sample was collected ready for RNA extraction. RNA was extracted using the spin protocol in Aurum™ Total RNA Fatty and Fibrous Tissue Kit (Bio-Rad Laboratories Inc., USA) according to the manufacturer's instructions. Reverse transcription was performed from 600 ng of total RNA using iScript™ cDNA Synthesis Kit (Bio-Rad) according to manufacturer's instructions. PCR was performed to quantify expression of genes associated with neuroinflammation (vimentin, GFAP, LCN2, Iba1, CD31, CD16), apoptosis (caspase-3), neurite outgrowth (GAP-43) and synaptogenesis (synaptophysin, synapsin, agrin) (view **Table 3.1** for oligonucleotide primer sequences). Glyceraldehyde 3-phosphate dehydrogenase (GAPDH) was used as an internal control gene. RT-PCR was performed using SsoFast EvaGreen Supermix (Bio-Rad) on an iQ 96-well PCR system (Bio-Rad). Each amplification reaction contained 1 µl of cDNA (30 ng input RNA) and 300 nM of primer and was performed in triplicate. Thermal cycling conditions included initial denaturation at 95°C for 30 s, followed by 40 cycles of 95°C for 5 s and 55°C for 5 s. Melt curve analysis was performed post-cycling to confirm specificity of the amplified products. Relative quantification of genes of interest mRNA expression was determined using the  $2^{-\Delta\Delta C_t}$  method.

**Table 3.1.** RT-PCR oligonucleotide name and sequence (5'-3').

Oligonucleotide name	Sequence (5'-3')
<b>mGAPDH</b>	Sense: ATGACATCAAGAAGGTGGTG
	Anti-sense: CATAACCAGGAAATGAGCTTG
<b>mVimentin</b>	Sense: GGCTGCCAACCGGAACAA
	Anti-sense: CGCTCCAGGGACTCGTTA
<b>mGFAP</b>	Sense: TCCTGGAACAGCAAACAAG
	Anti-sense: CAGCCTCAGGTTGGTTTCAT
<b>mLCN2</b>	Sense: CCCCATCTCTGCTCACTGTC
	Anti-sense: TTTTCTGGACCGCATTG
<b>mlba1</b>	Sense: GGATTTGCAGGGAGGAAAA
	Anti-sense: TGGGATCATCGAGGAATTG
<b>mCD32</b>	Sense: AATCCTGCCGTTCCCTACTGATC
	Anti-sense: GTGTACCGTGTCTTCCTTGAG
<b>mCD16</b>	Sense: TTTGGACACCCAGATGTTTCAG
	Anti-sense: GTCTTCCTTGAGCACCTGGATC
<b>mCaspase-3</b>	Sense: TGTCATCTCGTCTGGTACG
	Anti-sense: AAATGACCCCTTCATCACCA
<b>mGAP-43</b>	Sense: AGCCTAAACAAGCCGATGTG
	Anti-sense: GCAGGAGAGACAGGGTTCAG
<b>mSynaptophysin</b>	Sense: TGCCAACAAGACGGAG
	Anti-sense: GCGGATGAGCTAACT
<b>mSynapsin</b>	Sense: CAGCACAACATACCCTGTGG
	Anti-sense: GGTCTTCCAGTTACCCGACA
<b>mAgrin</b>	Sense: CTTTGATGGGCGGACCTACA
	Anti-sense: GTGATAGCTGAGTTGCAGGT

### **3.2.9. Western blot analysis**

Western blotting was used to detect expression of TrkA receptors, and phosphorylated-Akt, a downstream indicator of TrkA receptor activation. IC tissue was homogenized with RIPA-EDTA buffer with added protease and phosphatase cocktail inhibitors [43]. To determine sample protein concentration, Pierce™ BCA™ Protein Assay Kit (Pierce Biotechnology, USA) was used and, supernatant protein concentration was mixed [3:1 (v/v) ratio] with 4 × SDS loading buffer (Bio-Rad). Samples were heated at 95°C for 5 min, centrifuged, and then stored at -20°C for Western blot analysis. Protein (10 µg) was loaded into each well and protein was separated using Precast Mini-PROTEAN® TGX™ gel (Bio-Rad). Protein bands were transferred onto polyvinyl difluoride (PVDF) membranes. Primary antibodies used included: anti-TrkA (1:1000, Abcam, USA), anti-Akt (1:1000, Cell Signaling Technology, USA) and anti-phosphorylated-Akt (S438, 1:1000, Cell Signaling Technology). Signal detection was developed with chemiluminescent substrate kit (Clarity™ ECL Western Blotting Substrate, Bio-Rad). Immunoreactive bands were digitally imaged using Molecular Imager® Chemidoc™ XRS+ (Bio-Rad) and results were quantified using Image Lab™ Software (Bio-Rad). Values were normalized for protein loading using β-actin as a loading control.

### **3.2.10. Statistical analysis**

Rotarod data were analysed with a mixed design analysis of variance (**ANOVA**) using SPSS Statistics 22.0 software (IBM, New York, USA). All other outcomes were analysed with a **two-way ANOVA**, with **Bonferroni post-hoc comparisons** carried out when appropriate. Statistical analyses were performed using GraphPad Prism 6, with significance defined as  $p < 0.05$ .

### 3.3. Results

#### 3.3.1. Acute injury severity measures

Apnoea was observed in LFPI mice only ( $p < 0.001$ ), and increased durations of unconsciousness ( $p < 0.001$ ) and self-righting ( $p < 0.001$ ) were observed in LFPI mice compared to sham injured mice (**Table 3.2.**). There were no significant differences in injury severity measures between vehicle- and GA-treated mice. Additionally, no difference in oedema was seen between the injury or treatment groups.

**Table 3.2.** Acute injury severity outcomes in mice given SHAM or TBI and assigned to a VEH or GA treatment group.

	Apnoea (s)	Hind-limb (s)	Self-righting (s)
SHAM-VEH	0	0	75.1 ± 7.0
SHAM-GA	0	0	83.0 ± 7.3
TBI-VEH	49.9 ± 3.3 <sup>a</sup>	253.6 ± 11.4 <sup>a</sup>	439.9 ± 13.2 <sup>a</sup>
TBI-GA	56.0 ± 3.8 <sup>a</sup>	256.1 ± 9.9 <sup>a</sup>	440.9 ± 16.9 <sup>a</sup>

<sup>a</sup>TBI significantly greater than sham injured groups,  $p < 0.001$ , VEH, vehicle; GA, gambogic amide; TBI, traumatic brain injury.

#### 3.3.2. Behavioural outcomes

Rotarod analysis revealed that TBI mice spent significantly less time on the rotarod (**Figure. 3.1A**,  $p < 0.01$ ), a measure of motor function, compared to sham-injured mice. There was also a significant effect for test day, with mice spending significantly more time on the rotarod during the third day of rotarod testing (**Figure. 3.1A**,  $p < 0.001$ ). There was no effect of GA treatment on rotarod performance.

In the EPM, TBI mice had significantly reduced distance travelled (**Figure. 3.1C**,  $p < 0.01$ ), a measure of locomotion, compared to sham-injured mice. Mice given a TBI also displayed a trend for spending increased time in the open arm of the EPM (**Figure. 3.1C**,  $p = 0.0622$ ) compared to sham-injured mice. There was no GA-treatment effect on EPM measures.

Although no injury effect was seen in the Y-maze (**Figure. 3.1B**), GA-treated mice had significantly reduced distance travelled (**Figure. 3.1B**,  $p < 0.05$ ) and spent significantly less time (**Figure. 3.1B**,  $p < 0.01$ ) in the novel arm compared to vehicle-treated mice. No statistically significant differences were found in the open-field (**Figure. 3.1D**).



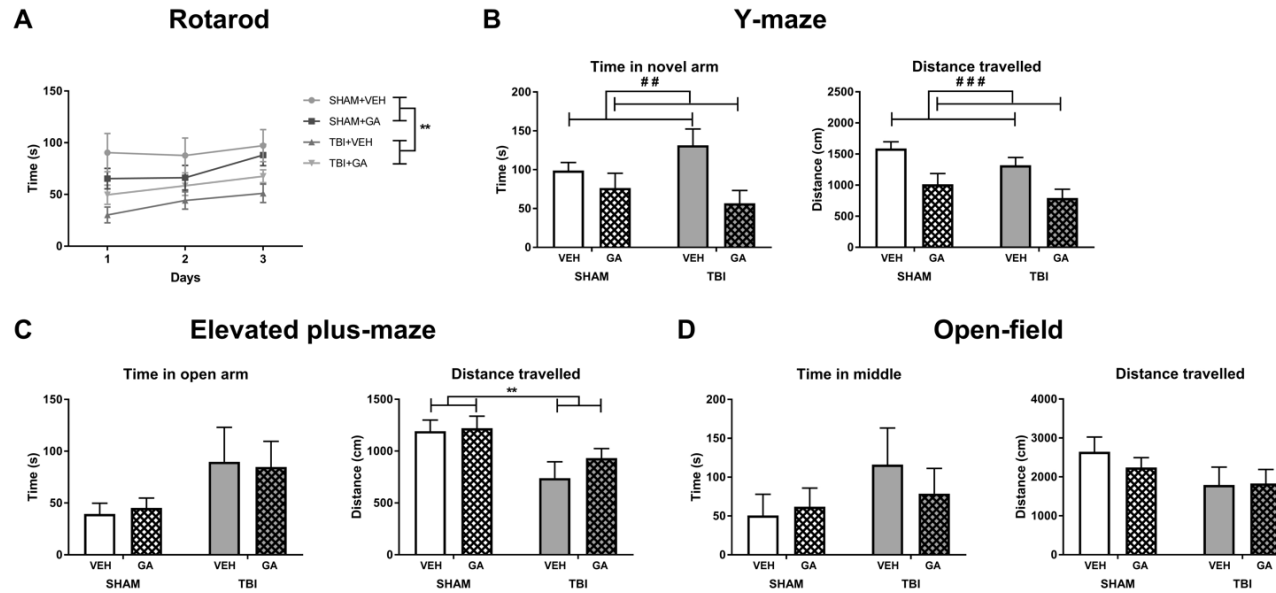


**Figure 3.1. The effects of GA treatment on behavioural outcomes post-LFPI. (A)** Rotarod testing found that LFPI groups had motor deficits compared to SHAM groups ( $p = 0.005$ ) as indicated by significantly less time spent on the rotarod during testing. GA treatment did not affect rotarod performance. **(B)** No injury effect was seen in the Y-Maze, however mice treated with GA spent less time in the novel arm compared to vehicle-treated mice ( $p = 0.0095$ ). **(C)** There was a non-significant trend for LFPI mice spending more time in the open arm of the elevated-plus maze (EPM) compared to SHAM mice ( $p = 0.0622$ ). LFPI mice had a significant reduction in the distance travelled in the EPM ( $p = 0.0064$ ). There were no treatment effects on EPM measures. **(D)** No differences were found between groups in open-field. Data expressed as mean  $\pm$  SEM,  $n = 7$ /group. Double asterix injury effect,  $p < 0.01$ , number sign treatment effect, ##  $p < 0.01$ ; ###  $p < 0.001$ .

### 3.3.3. Brain water content

Brain water content was analysed as a measure of BBB breakdown. Brain water content was not altered in the IC or contralateral cortex (CC) between SHAM or injury groups at 72 h. GA did not affect brain water content compared to vehicle-treated mice (**Figure 3.2.**).

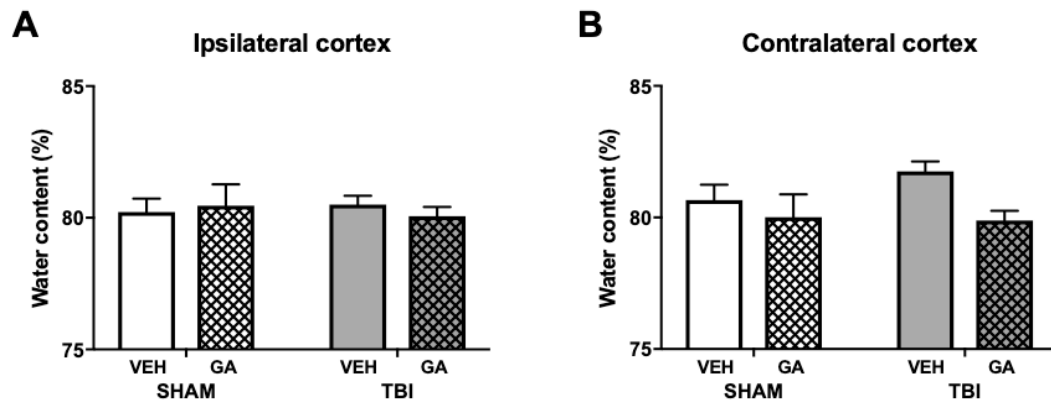


**Figure 3.2.** The effects of GA treatment on brain water content in the ipsilateral (A) and contralateral (B) hemispheres following TBI at 72 h. Brain water content did not significantly increase in the ipsilateral or contralateral hemispheres following LFPI at 72 h. No differences were found after treatment with GA. Data expressed as mean  $\pm$  SEM,  $n = 6$ /group.

### 3.3.4. TrkA expression and phosphorylation

Western blot analysis of mouse IC was performed to analyse the expression of TrkA receptors and activation of pro-survival pathways phosphorylated-Akt (p-Akt). At 72 h post-TBI, TrkA receptors were down regulated in TBI groups compared to sham groups (**Figure. 3.3A**,  $p < 0.001$ ). GA did not alter the expression of TrkA receptors. There was no significant GA treatment effect on p-Akt, yet there was a trend that TBI increased p-Akt (**Figure. 3.3B**,  $p = 0.07$ ).

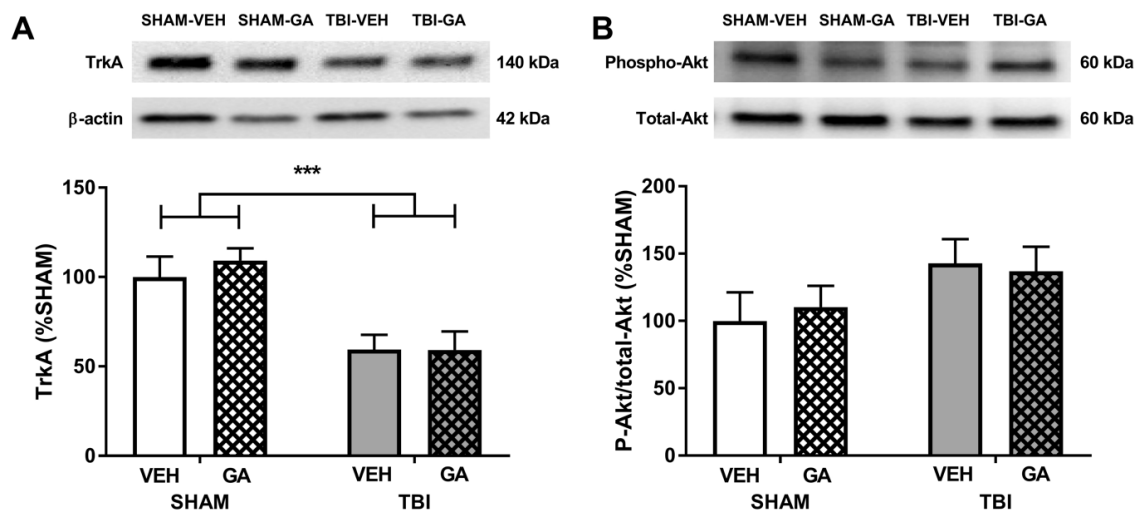
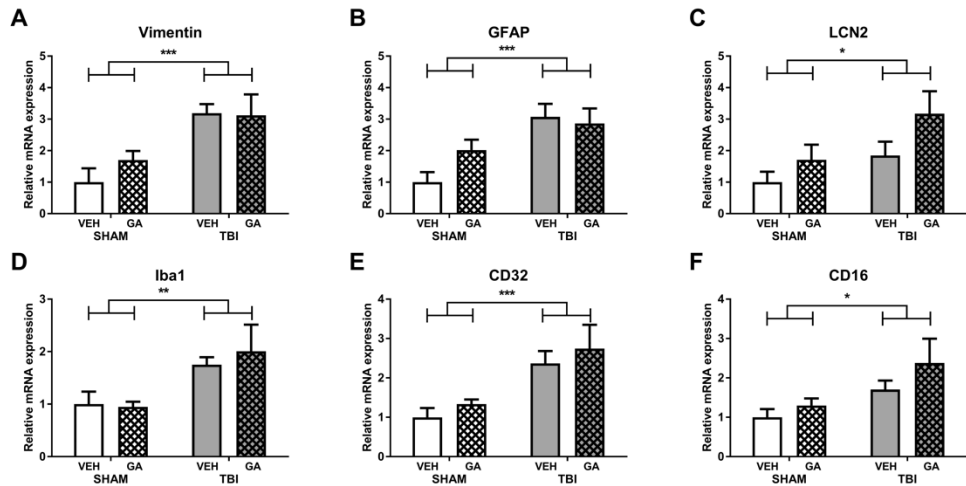


**Figure 3.3. The effects of GA treatment on TrkA expression and phosphorylated-Akt activation post-LFPI. (A)** Western blotting found LFPI caused a significant decrease in TrkA receptor expression compared to SHAM groups ( $p = 0.0001$ ). GA treatment did not affect TrkA expression. **(B)** There was a trend for LFPI to increase the pAkt/total Akt ratio compared with SHAM groups ( $p = 0.0735$ ). No differences were found following GA treatment. Data expressed as mean  $\pm$  SEM,  $n = 6$ /group. *Triple asterix* injury effect,  $p < 0.001$ .

### 3.3.5. Neuroinflammation

PCR analysis of mouse IC and ipsilateral hippocampus (IH) was performed to analyse the relative fold-change in genes commonly associated with neuroinflammation: vimentin, GFAP, LCN2, Iba1, CD32 and CD16. As seen in **Figure 3.4.**, mice with TBI had significantly increased mRNA expression in both the IC and IH in all the markers of neuroinflammation (vimentin, IC,  $p < 0.001$ , **Figure. 3.4A**, IH  $p < 0.05$ , **Figure. 3.4G**; GFAP, IC,  $p < 0.01$ , **Figure. 3.4B**, IH  $p < 0.05$ , **Figure. 3.4H**; LCN2, IC,  $p < 0.05$ , **Figure. 3.4C**, IH,  $p < 0.05$ ; Iba1, **Figure. 3.4I**, IC,  $p < 0.01$ , **Figure. 3.4D**, IH,  $p < 0.01$ , **Figure. 3.4J**; CD32, IC,  $p < 0.001$ , **Figure. 3.4E**, IH,  $p < 0.05$ , **Figure. 3.4K**; and CD16, IC,  $p < 0.05$ , **Figure. 3.4F**, IH,  $p < 0.01$ , **Figure. 3.4L**) at 72 h post-injury compared with sham-injured groups. There was no significant GA treatment effect on neuroinflammatory markers. GA-treated mice had significantly increased LCN2 expression in the IH (**Figure. 3.4I**,  $p < 0.05$ ) but not in the IC compared to vehicle-treated mice.

## Cortex



## Hippocampus

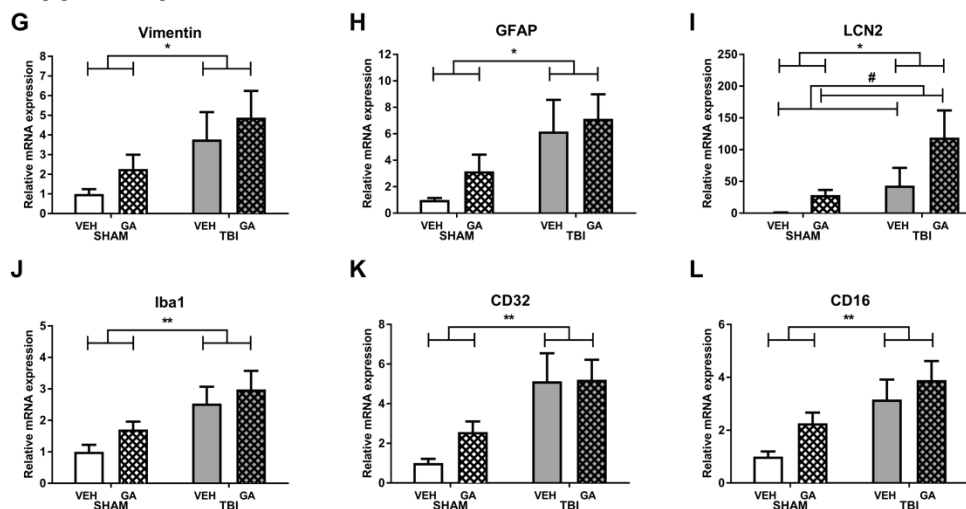


**Figure 3.4.** The effects of GA treatment on expression of markers of neuroinflammation post-LFPI. Cortex and hippocampus from mice with LFPI had significantly increased vimentin (**A, G**), GFAP (**B, H**), LCN2 (**C, I**), Iba1 (**D, J**), CD32 (**E, K**) and CD16 (**F, L**) at 72 h post-injury compared to sham-injured mice, however treatment with GA did not alter the expression of these markers. LCN2 (**C, I**) expression was significantly increased in response to LFPI in the cortex and in the hippocampus. GA-treated groups had significantly increased LCN2 expression in the hippocampus (#  $p < 0.05$ ) but not in the cortex compared to vehicle-treated groups. Data expressed as mean  $\pm$  SEM,  $n = 7/\text{group}$ . Asterix injury effect, \*  $p < 0.05$ ; \*\*  $p < 0.01$ ; \*\*\*  $p < 0.001$ .

### 3.3.6. Apoptosis

PCR analysis of apoptotic marker; caspase-3, was assessed in mouse IC and IH. At 72 h post-injury there was an overall significant increase in caspase-3 expression in the IC (**Figure 3.5A**,  $p < 0.05$ ) and IH (**Figure 3.5B**,  $p < 0.01$ ) in mice with TBI compared to sham-injury. GA did not alter expression of caspase-3.

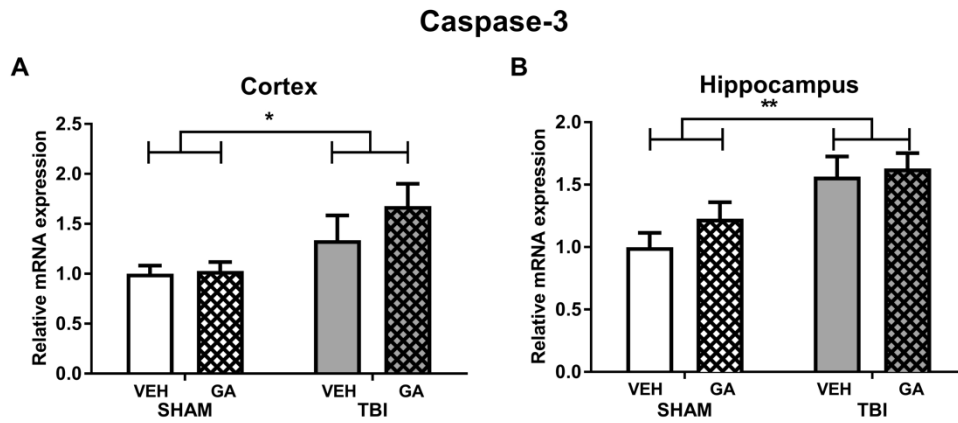
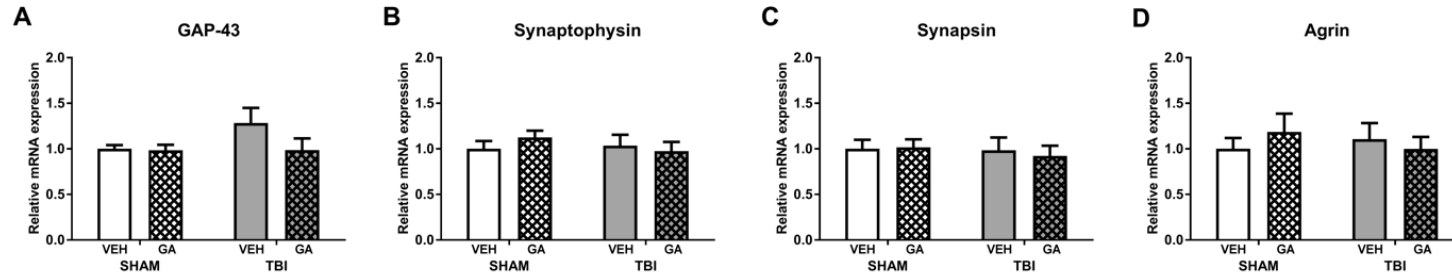


**Figure 3.5. Expression of apoptosis marker caspase-3 in mouse cortex (A) and hippocampus (B) 72 h after LFPI or SHAM-injury.** Caspase-3 mRNA expression increased in mice with LFPI in the cortex ( $p < 0.05$ ) and hippocampus ( $p < 0.01$ ). GA treatment did not alter caspase-3 expression. Data expressed as mean  $\pm$  SEM,  $n = 7$ /group. Asterix injury effect, \*  $p < 0.05$ ; \*\*  $p < 0.01$ .

### 3.3.7. Neurite sprouting and synaptogenesis

Expression of markers associated with neurite outgrowth (GAP-43) and synaptogenesis (synaptophysin, synapsin and agrin) within the IC and IH was analysed. At 72 h post-injury, expression of GAP-43, synaptophysin and synapsin did not alter in response to TBI nor GA-treatment in the IC and IH (**Figure. 3.6A-C, E-G**). Agrin mRNA expression was significantly increased in the IH (**Figure. 3.6H**,  $p < 0.05$ ) of LFPI mice, however GA-treatment had no effect on agrin expression (**Figure. 3.6D, H**).

## Cortex



## Hippocampus

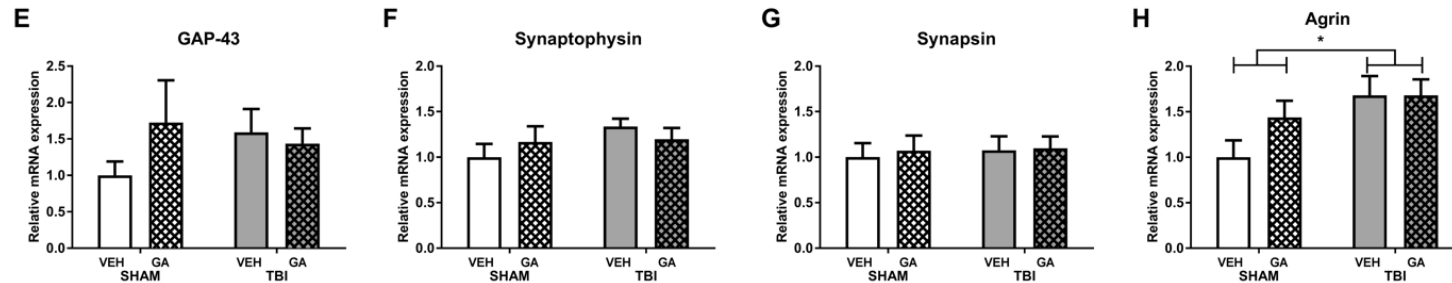


**Figure 3.6.** The effects of GA treatment on expression of markers of neurite sprouting and synaptogenesis post-LFPI. LFPI did not alter the mRNA expression of markers of neurite sprouting (GAP-43) and synaptogenesis (synaptophysin, synapsin) in mouse cortex (**A-C**) and hippocampus (**E-G**) at 72 h post-injury compared with sham-injured mice. Likewise, treatment with GA had no effect on the expression of neurite sprouting and synaptogenic markers compared to vehicle groups. The LFPI-injured mice had significantly increased agrin expression in the hippocampus (**H**), but not in the cortex (**D**), compared to sham-injured mice at 72 h post-injury ( $*p < 0.05$ ). GA treatment did not alter the expression of agrin compared to vehicle groups. Data expressed as mean  $\pm$  SEM,  $n = 7$ /group.

### 3.4. Discussion

Previous studies have found that treatment with NGF reduced neuronal apoptosis [15, 26], suppressed neuroinflammation [24, 25], and improved cognitive outcomes in rodents with TBI [28, 29, 31]. The pro-survival effects of NGF are thought to be mediated via TrkA activation [22], and TrkA activation has been shown to promote neurite outgrowth [35, 47]. High affinity selective TrkA agonist, GA, has previously been shown to stimulate neurite outgrowth [36, 48], prevent apoptosis of primary neurons *in vitro* [35], and through systemic delivery, protect neurons from kainic acid-induced apoptosis and reduce infarct volume following ischemic injury [35]. Despite these findings, no studies have investigated the specific effects of GA treatment following TBI. Accordingly, in this study a LFPI model of TBI was used in mice to examine the effects of GA treatment on behavioural outcomes, neuroinflammation, apoptosis, neurite growth and synaptogenesis in the acute stages of TBI. Overall, the present findings suggest that treatment with GA did not affect the TBI-induced changes in motor function, neuroinflammation or apoptosis at 72 h post-injury.

The present findings of TBI-induced motor deficits, as indicated by decreased time on the rotarod and decreased distance traveled in the EPM, are similar to findings of other experimental TBI studies [13, 14, 49]. Treatment with GA did not attenuate motor deficits; a finding which is comparable to studies that have reported that NGF treatment did not improve post-TBI performance in an open wire grid [30], foot-fault test [50] and beam balance test [29, 31].

It was found that TBI did not affect novel arm preference in the Y-maze at 3 days post-injury. This lack of spatial memory deficit post-TBI may reflect the acute nature of the behavioural testing, with previous studies showing that neurodegeneration and hippocampal atrophy following a single LFPI in rodents takes weeks to months to fully manifest [51, 52]. The finding that GA-treated mice spent significantly less time in the novel arm compared to vehicle-treated mice may be contributed to by the fact that the GA-treated mice had travelled significantly less distance compared to vehicle-treated mice during Y-maze testing. However, no effects of GA treatment were observed on distance travelled and sensorimotor performance in the rotarod and open-field, which indicates that GA did not likely induce gross changes in sickness behaviour, motor ability or locomotion. As such, the possible influence of GA on spatial memory and locomotion warrants further investigation. While this is the first study to report the effects of GA on spatial memory outcomes in mice following acute TBI, several studies have investigated the effects of NGF on spatial cognition following experimental TBI [28-31]. Behavioural testing during and at cessation of NGF treatment following TBI reduced cognitive latencies and improved spatial memory in rodents at weeks 1 and 2 post-injury using the Morris water maze [28, 29, 31], but not at 1-, 2-

and 3-days post-injury [28]. Accordingly, future investigations may consider assessments on the influence of GA and NGF on spatial memory at later time-points post-injury.

Brain water content is a commonly used measurement of BBB breakdown following TBI [44]. In the current study TBI did not induce cerebral oedema at 72 h post-injury in the ipsilateral or contralateral hemispheres. One previous study using a moderate LFPI in mice has shown that cerebral oedema is measurably increased at 3 h and 1-day post-injury [53] and that measuring at 72 h post-injury the window cerebral oedema is affected may have been missed. Additionally, size of tissue used to measure cerebral oedema may have impacted the results, as a small piece of brain tissue (> 10 mg) was used to analyse oedema in the ipsilateral and contralateral hemispheres, as other pieces of ipsilateral cortex for molecular analysis was used. Ferreira and colleagues had a subset of animals and used whole ipsilateral hemispheres to measure brain water content [53].

Neuroinflammation is an important secondary injury mechanism that occurs after TBI [18]. At 72 h post-TBI, there was an apparent increase in the neuroinflammatory response, with the increased expression of markers associated with astrocytic activation (vimentin, GFAP and LCN2) and reactive microglia (CD32, CD16 and Iba1) in the IC and IH of the TBI groups. These findings are similar to previous studies involving acute-phase analysis of brain tissue following LFPI [52, 54-56], and provide evidence of a substantial neuroinflammatory response following LFPI in mice. Previous rodent TBI studies have shown NGF treatment to be beneficial in attenuating the cortical neuroinflammatory response by reducing protein expression of pro-inflammatory cytokines TNF- $\alpha$  and IL-1 $\beta$  during the first 72 h post-injury [24, 25]. It was found that GA-treatment had no effect on the mRNA expression of the majority of neuroinflammatory markers compared to vehicle-treated groups [35]. These findings may suggest that TrkA activation does not suppress neuroinflammation post-TBI, and that the previously reported anti-inflammatory effects of NGF post-TBI may not be mediated through TrkA signaling. Interestingly, however GA treatment did not increase LCN2 expression. Though increased LCN2 expression is associated with astrogliosis [57], this protein is expressed by a variety of cells, and increased expression has been previously associated with non-inflammatory processes such as angiogenesis [58], cell migration, iron transport and tissue regeneration [59, 60]. Furthermore, a recent study has shown that NGF treatment also increased expression of LCN2 [61], therefore together with the present finding, this may suggest that TrkA activation promotes expression of LCN2; however, further studies are required to establish this association and understand the possible impact of LCN2 up-regulation in both the uninjured and injured brain. Finally, as the neuroinflammatory response induced by TBI can persist well beyond the acute stages post-TBI, future studies may consider assessment of any effects of GA treatment at later time-points post-injury [42].



Neuronal apoptosis is another acute cellular response to TBI [62-64]. Similar to other experimental TBI studies, in the current study it was found that LFPI in mice increased the expression of the apoptotic marker caspase-3 at 72 h post-injury [65-67]. GA treatment did not reduce expression of caspase-3 in TBI. This result was unexpected, as this treatment regime (2 mg GA/kg/day) has previously been shown to significantly reduce kainic acid-induced apoptosis in the hippocampus of mice and reduce infarct volume 24 h following ischemic injury [35]. Furthermore, NGF treatment also strongly reduced caspase-3 expression following weight-drop TBI [24]. The current findings suggest that GA did not prevent TBI-induced apoptosis; however further analysis featuring multiple time-points and other measurements of apoptosis such as TUNEL-staining may provide further insight.

Neuronal and synaptic changes can begin in the hippocampus and cortex within 72 h of TBI [68]. Neuronal sprouting is associated with elevations in mRNA and protein expression of GAP-43, synapsin, synaptophysin and agrin [68-72]. GAP-43 is a marker of axonal cone formation during neurite sprouting [73], whereas synapsin, synaptophysin and agrin are markers of synaptogenesis [68, 70, 74]. In the current study, GAP-43, synapsin and synaptophysin mRNA expression were not significantly altered in response to LFPI in the IC or IH at 72 h post-injury. This finding may be attributed to the early time-point analysed, with a previous study finding increased hippocampal synaptophysin and GAP-43 mRNA expression at 28- but not 7-days post-FPI [71]. There was, however, find an effect of TBI on the expression of agrin, a protein associated with synaptogenesis that has similarly been shown to be upregulated at 7 days post-FPI. Taken together, these findings suggest agrin may be a suitable marker of the early sprouting phase of synaptogenesis post-TBI [70]. Finally, though several studies have shown NGF induces synaptogenesis and neurite outgrowth [35, 75-77], in the present experiments, no effect of GA-treatment was observed on markers of these processes at 72 h post-injury. These preliminary findings, together with the behavioural findings of the current experiments, suggest GA may not increase neurite outgrowth and synaptogenesis in the acute stages post-TBI, however further analysis featuring multiple time-points and protein markers are required, particularly considering development and reestablishment of functioning circuits can take multiple weeks post-injury [78, 79]. Therefore, analysis of GA-treatment on TBI long-term may reveal positive effects on neurogenesis and behavioural outcomes.

The lack of efficacy the GA observed in the current study may be attributed to the significant decrease in cortical TrkA expression observed in mice with TBI. Similarly, downregulation of TrkB expression post-TBI has been found in several studies and hypothesized as possibly contributing to the lack of neuroprotection induced by exogenous BDNF treatment [80]. Relatively few studies have investigated TrkA expression post-TBI, with the findings of these

studies largely mixed [81-83], therefore further profiling of the temporal and regional expression patterns of TrkA expression post-TBI will provide greater insights into the potential suitability and timing of therapies targeting this signaling pathway.

Although no beneficial effects of GA treatment were found, this study does provide some novel characteristics of the lateral fluid percussion injury in mice. LFPI injury is most commonly used in rats [7], however, a small number of studies have recently demonstrated successful adaptation of this model to mice [44, 84]. One such study found that the same injury parameters used in this study produced substantial behavioural deficits, brain atrophy, and astrogliosis at 3 months post-injury [44]. The mortality rates (10-20%) and self-righting reflex (7-8 minutes) were very similar to the findings of the current study, and considered together, indicate that this TBI model is of moderate severity [44, 84]. It is however important to note that acute effects of this particular TBI model in mice have not been well characterized; therefore, the current findings do provide some novel insights, particularly regarding the cortical and hippocampal neuroinflammatory response.

It is important to note that this study does contain limitations. Firstly, although significant TBI-induced motor deficits and increased expression of several neuroinflammatory and apoptotic markers was observed, a limitation of the single time-point approach is that the peak activation of some processes may have been missed and thus any beneficial effects of GA treatment. Although a dosing regimen of GA that was previously shown to improve outcomes following ischemic injury [35] was used, it is possible that GA administered at higher doses or for a prolonged duration may have provided neuroprotection following TBI was found. In addition, though no effects of GA treatment on behaviour and neuropathology during the first 72 h post-TBI, it is possible that GA has beneficial effects that may only be detectable at later time-points; however, it is noteworthy that several studies have shown beneficial effects of NGF during the early stages post-TBI [15, 24, 25, 29, 31, 85]. Furthermore, this study did not analyse brain concentrations of GA, and tissue collection at 24 h following the final GA treatment limited inferences that could be made on TrkA signaling, however the work of Jang and colleagues provided strong evidence that GA does selectively activate TrkA signaling and can exert central neurotrophic effects [35]. Nonetheless, additional work is needed to advance understanding of pharmacological profile and functionality of GA. Finally, due to the poor water solubility of GA, an emulsifying agent, Kolliphor<sup>®</sup> HS 15 (Solutol<sup>®</sup> HS 15) mixed with saline was used as a vehicle to deliver GA. Solutol<sup>®</sup> HS 15 is widely used as a vehicle in veterinary and pre-clinical research, however a recent study found preliminary evidence that Solutol<sup>®</sup> HS 15 may have neuroprotective properties, with mice treated with this vehicle found to have significantly reduced neuronal loss and infarct volume following ischemic injury [86]. As such, the neuroprotective potential of GA may have been limited by the

choice of vehicle, however, it is worth noting that in vehicle-treated mice, significant motor and pathophysiological changes induced by TBI was observed, and that previous TBI studies using this vehicle, found significant effects of treatment delivered in Solutol® HS 15 compared to vehicle alone [40, 41].

### **3.5. Conclusions**

GA is a small, potent TrkA agonist that has previously been shown to penetrate the BBB, protect neurons from apoptosis, and promote neurogenesis in the rodent brain. This study found that treatment with GA at a dose previously shown to reduce the effects ischemic injury did not attenuate TBI-induced motor deficits, neuroinflammation, or apoptosis. Future studies may consider analysis of the effects of GA at different doses or at later time-points post-injury.

### 3.6. References

1. Hyder, A.A., C.A. Wunderlich, P. Puvanachandra, G. Gururaj, and O.C. Kobusingye, *The impact of traumatic brain injuries: a global perspective*. NeuroRehabilitation, 2007. **22**(5): p. 341-53.
2. Carroll, L.J., J.D. Cassidy, P.M. Peloso, J. Borg, H. von Holst, L. Holm, C. Paniak, M. Pepin, and W.H.O.C.C.T.F.o.M.T.B. Injury, *Prognosis for mild traumatic brain injury: results of the WHO Collaborating Centre Task Force on Mild Traumatic Brain Injury*. J Rehabil Med, 2004(43 Suppl): p. 84-105.
3. Faden, A.I. and D.J. Loane, *Chronic neurodegeneration after traumatic brain injury: Alzheimer disease, chronic traumatic encephalopathy, or persistent neuroinflammation?* Neurotherapeutics, 2015. **12**(1): p. 143-50.
4. Rapoport, M.J., S. McCullagh, P. Shammi, and A. Feinstein, *Cognitive impairment associated with major depression following mild and moderate traumatic brain injury*. J Neuropsychiatry Clin Neurosci, 2005. **17**(1): p. 61-5.
5. Blennow, K., J. Hardy, and H. Zetterberg, *The neuropathology and neurobiology of traumatic brain injury*. Neuron, 2012. **76**(5): p. 886-99.
6. Ragnarsson, K.T., *Results of the NIH consensus conference on "rehabilitation of persons with traumatic brain injury"*. Restor Neurol Neurosci, 2002. **20**(3-4): p. 103-8.
7. Shultz, S.R., S.J. McDonald, C. Vonder Haar, A. Meconi, R. Vink, P. van Donkelaar, C. Taneja, G.L. Iverson, and B.R. Christie, *The potential for animal models to provide insight into mild traumatic brain injury: Translational challenges and strategies*. Neurosci Biobehav Rev, 2017. **76**(Pt B): p. 396-414.
8. Shojo, H., Y. Kaneko, T. Mabuchi, K. Kibayashi, N. Adachi, and C.V. Borlongan, *Genetic and histologic evidence implicates role of inflammation in traumatic brain injury-induced apoptosis in the rat cerebral cortex following moderate fluid percussion injury*. Neuroscience, 2010. **171**(4): p. 1273-82.
9. Streit, W.J., R.E. Mrak, and W.S. Griffin, *Microglia and neuroinflammation: a pathological perspective*. J Neuroinflammation, 2004. **1**(1): p. 14.
10. Carson, M.J., J.C. Thrash, and B. Walter, *The cellular response in neuroinflammation: The role of leukocytes, microglia and astrocytes in neuronal death and survival*. Clin Neurosci Res, 2006. **6**(5): p. 237-245.
11. Hicks, R.R., D.H. Smith, D.H. Lowenstein, R. Saint Marie, and T.K. McIntosh, *Mild experimental brain injury in the rat induces cognitive deficits associated with regional neuronal loss in the hippocampus*. J Neurotrauma, 1993. **10**(4): p. 405-14.

12. Nimmo, A.J., I. Cernak, D.L. Heath, X. Hu, C.J. Bennett, and R. Vink, *Neurogenic inflammation is associated with development of edema and functional deficits following traumatic brain injury in rats*. *Neuropeptides*, 2004. **38**(1): p. 40-7.
13. Wright, D.K., J. Trezise, A. Kamnaksh, R. Bekdash, L.A. Johnston, R. Ordidge, B.D. Semple, A.J. Gardner, P. Stanwell, T.J. O'Brien, D.V. Agoston, and S.R. Shultz, *Behavioral, blood, and magnetic resonance imaging biomarkers of experimental mild traumatic brain injury*. *Sci Rep*, 2016. **6**: p. 28713.
14. Xiong, Y., A. Mahmood, and M. Chopp, *Animal models of traumatic brain injury*. *Nat Rev Neurosci*, 2013. **14**(2): p. 128-42.
15. Sinson, G., B.R. Perri, J.Q. Trojanowski, E.S. Flamm, and T.K. McIntosh, *Improvement of cognitive deficits and decreased cholinergic neuronal cell loss and apoptotic cell death following neurotrophin infusion after experimental traumatic brain injury*. *J Neurosurg*, 1997. **86**(3): p. 511-8.
16. Fox, G.B., L. Fan, R.A. Levasseur, and A.I. Faden, *Sustained sensory/motor and cognitive deficits with neuronal apoptosis following controlled cortical impact brain injury in the mouse*. *J Neurotrauma*, 1998. **15**(8): p. 599-614.
17. Loane, D.J. and A.I. Faden, *Neuroprotection for traumatic brain injury: translational challenges and emerging therapeutic strategies*. *Trends Pharmacol Sci*, 2010. **31**(12): p. 596-604.
18. Kumar, A. and D.J. Loane, *Neuroinflammation after traumatic brain injury: opportunities for therapeutic intervention*. *Brain Behav Immun*, 2012. **26**(8): p. 1191-201.
19. Hellewell, S., B.D. Semple, and M.C. Morganti-Kossmann, *Therapies negating neuroinflammation after brain trauma*. *Brain Res*, 2016. **1640**(Pt A): p. 36-56.
20. Levi-Montalcini, R. and P.U. Angeletti, *Nerve growth factor*. *Physiol Rev*, 1968. **48**(3): p. 534-69.
21. Levi-Montalcini, R. and S. Cohen, *In Vitro and in Vivo Effects of a Nerve Growth-Stimulating Agent Isolated from Snake Venom*. *Proc Natl Acad Sci U S A*, 1956. **42**(9): p. 695-9.
22. Yoon, S.O., P. Casaccia-Bonnel, B. Carter, and M.V. Chao, *Competitive signaling between TrkA and p75 nerve growth factor receptors determines cell survival*. *J Neurosci*, 1998. **18**(9): p. 3273-81.
23. Reichardt, L.F., *Neurotrophin-regulated signalling pathways*. *Philos Trans R Soc Lond B Biol Sci*, 2006. **361**(1473): p. 1545-64.
24. Lv, Q., X. Fan, G. Xu, Q. Liu, L. Tian, X. Cai, W. Sun, X. Wang, Q. Cai, Y. Bao, L. Zhou, Y. Zhang, L. Ge, R. Guo, and X. Liu, *Intranasal delivery of nerve growth factor attenuates aquaporin-4-induced edema following traumatic brain injury in rats*. *Brain Res*, 2013. **1493**: p. 80-9.

25. Lv, Q., W. Lan, W. Sun, R. Ye, X. Fan, M. Ma, Q. Yin, Y. Jiang, G. Xu, J. Dai, R. Guo, and X. Liu, *Intranasal nerve growth factor attenuates tau phosphorylation in brain after traumatic brain injury in rats*. Journal of the Neurological Sciences, 2014. **345**(1–2): p. 48-55.
26. Kromer, L.F., *Nerve growth factor treatment after brain injury prevents neuronal death*. Science, 1987. **235**(4785): p. 214-6.
27. Sinson, G., M. Voddi, and T.K. McIntosh, *Nerve Growth Factor Administration Attenuates Cognitive but Not Neurobehavioral Motor Dysfunction or Hippocampal Cell Loss Following Fluid-Percussion Brain Injury in Rats*. Journal of Neurochemistry, 1995. **65**(5): p. 2209-2216.
28. Tian, L., R. Guo, X. Yue, Q. Lv, X. Ye, Z. Wang, Z. Chen, B. Wu, G. Xu, and X. Liu, *Intranasal administration of nerve growth factor ameliorate  $\beta$ -amyloid deposition after traumatic brain injury in rats*. Brain Research, 2012. **1440**: p. 47-55.
29. Dixon, C.E., P. Flinn, J. Bao, R. Venya, and R.L. Hayes, *Nerve growth factor attenuates cholinergic deficits following traumatic brain injury in rats*. Exp Neurol, 1997. **146**(2): p. 479-90.
30. Longhi, L., D.J. Watson, K.E. Saatman, H.J. Thompson, C. Zhang, S. Fujimoto, N. Royo, D. Castelbuono, R. Raghupathi, J.Q. Trojanowski, V.M. Lee, J.H. Wolfe, N. Stocchetti, and T.K. McIntosh, *Ex vivo gene therapy using targeted engraftment of NGF-expressing human NT2N neurons attenuates cognitive deficits following traumatic brain injury in mice*. J Neurotrauma, 2004. **21**(12): p. 1723-36.
31. Sinson, G., M. Voddi, and T.K. McIntosh, *Nerve growth factor administration attenuates cognitive but not neurobehavioral motor dysfunction or hippocampal cell loss following fluid-percussion brain injury in rats*. J Neurochem, 1995. **65**(5): p. 2209-16.
32. Tria, M.A., M. Fusco, G. Vantini, and R. Mariot, *Pharmacokinetics of nerve growth factor (NGF) following different routes of administration to adult rats*. Exp Neurol, 1994. **127**(2): p. 178-83.
33. Friden, P.M., L.R. Walus, P. Watson, S.R. Doctrow, J.W. Kozarich, C. Backman, H. Bergman, B. Hoffer, F. Bloom, and A.C. Granholm, *Blood-brain barrier penetration and in vivo activity of an NGF conjugate*. Science, 1993. **259**(5093): p. 373-7.
34. Angeletti, R.H., P.U. Aneletti, and R. Levi-Montalcini, *Selective accumulation of ( <sup>125</sup> I) labelled nerve growth factor in sympathetic ganglia*. Brain Res, 1972. **46**: p. 421-5.
35. Jang, S.W., M. Okada, I. Sayeed, G. Xiao, D. Stein, P. Jin, and K. Ye, *Gambogic amide, a selective agonist for TrkA receptor that possesses robust neurotrophic activity, prevents neuronal cell death*. Proc Natl Acad Sci U S A, 2007. **104**(41): p. 16329-34.

36. Shen, J. and Q. Yu, *Gambogic amide selectively upregulates TrkA expression and triggers its activation*. Pharmacol Rep, 2015. **67**(2): p. 217-23.
37. Chan, C.B., X. Liu, S.W. Jang, S.I. Hsu, I. Williams, S. Kang, J. Chen, and K. Ye, *NGF inhibits human leukemia proliferation by downregulating cyclin A1 expression through promoting acinus/CtBP2 association*. Oncogene, 2009. **28**(43): p. 3825-36.
38. Scheller, K.J., S.J. Williams, A.J. Lawrence, B. Jarrott, and E. Djouma, *An improved method to prepare an injectable microemulsion of the galanin-receptor 3 selective antagonist, SNAP 37889, using Kolliphor((R)) HS 15*. MethodsX, 2014. **1**: p. 212-6.
39. Scheller, K.J., S.J. Williams, A.J. Lawrence, and E. Djouma, *The galanin-3 receptor antagonist, SNAP 37889, suppresses alcohol drinking and morphine self-administration in mice*. Neuropharmacology, 2017. **118**: p. 1-12.
40. Yang, Y., V.M. Salayandia, J.F. Thompson, L.Y. Yang, E.Y. Estrada, and Y. Yang, *Attenuation of acute stroke injury in rat brain by minocycline promotes blood-brain barrier remodeling and alternative microglia/macrophage activation during recovery*. J Neuroinflammation, 2015. **12**: p. 26.
41. Singleton, R.H., H.Q. Yan, W. Fellows-Mayle, and C.E. Dixon, *Resveratrol attenuates behavioral impairments and reduces cortical and hippocampal loss in a rat controlled cortical impact model of traumatic brain injury*. J Neurotrauma, 2010. **27**(6): p. 1091-9.
42. Simon, D.W., M.J. McGeachy, H. Bayir, R.S. Clark, D.J. Loane, and P.M. Kochanek, *The far-reaching scope of neuroinflammation after traumatic brain injury*. Nat Rev Neurol, 2017. **13**(3): p. 171-191.
43. Shultz, S.R., M. Sun, D.K. Wright, R.D. Brady, S. Liu, S. Beynon, S.F. Schmidt, A.H. Kaye, J.A. Hamilton, T.J. O'Brien, B.L. Grills, and S.J. McDonald, *Tibial fracture exacerbates traumatic brain injury outcomes and neuroinflammation in a novel mouse model of multitrauma*. J Cereb Blood Flow Metab, 2015. **35**(8): p. 1339-47.
44. Shultz, S.R., X.L. Tan, D.K. Wright, S.J. Liu, B.D. Semple, L. Johnston, N.C. Jones, A.D. Cook, J.A. Hamilton, and T.J. O'Brien, *Granulocyte-macrophage colony-stimulating factor is neuroprotective in experimental traumatic brain injury*. J Neurotrauma, 2014. **31**(10): p. 976-83.
45. Hamm, R.J., B.R. Pike, D.M. O'Dell, B.G. Lyeth, and L.W. Jenkins, *The rotarod test: an evaluation of its effectiveness in assessing motor deficits following traumatic brain injury*. J Neurotrauma, 1994. **11**(2): p. 187-96.
46. Johnstone, V.P., D.K. Wright, K. Wong, T.J. O'Brien, R. Rajan, and S.R. Shultz, *Experimental Traumatic Brain Injury Results in Long-Term Recovery of Functional Responsiveness in Sensory Cortex but Persisting Structural Changes and Sensorimotor, Cognitive, and Emotional Deficits*. J Neurotrauma, 2015. **32**(17): p. 1333-46.

47. Sofroniew, M.V., C.L. Howe, and W.C. Mobley, *Nerve growth factor signaling, neuroprotection, and neural repair*. *Annu Rev Neurosci*, 2001. **24**: p. 1217-81.
48. Shah, A.G., M.J. Friedman, S. Huang, M. Roberts, X.J. Li, and S. Li, *Transcriptional dysregulation of TrkA associates with neurodegeneration in spinocerebellar ataxia type 17*. *Hum Mol Genet*, 2009. **18**(21): p. 4141-52.
49. Li, S., T. Kuroiwa, S. Ishibashi, L. Sun, S. Endo, and K. Ohno, *Transient cognitive deficits are associated with the reversible accumulation of amyloid precursor protein after mild traumatic brain injury*. *Neurosci Lett*, 2006. **409**(3): p. 182-6.
50. Young, J., T. Pionk, I. Hiatt, K. Geeck, and J.S. Smith, *Environmental enrichment aides in functional recovery following unilateral controlled cortical impact of the forelimb sensorimotor area however intranasal administration of nerve growth factor does not*. *Brain Res Bull*, 2015. **115**: p. 17-22.
51. Shultz, S.R., D.K. Wright, P. Zheng, R. Stuchbery, S.J. Liu, M. Sashindranath, R.L. Medcalf, L.A. Johnston, C.M. Hovens, N.C. Jones, and T.J. O'Brien, *Sodium selenate reduces hyperphosphorylated tau and improves outcomes after traumatic brain injury*. *Brain*, 2015. **138**(Pt 5): p. 1297-313.
52. Bao, F., S.R. Shultz, J.D. Hepburn, V. Omana, L.C. Weaver, D.P. Cain, and A. Brown, *A CD11d monoclonal antibody treatment reduces tissue injury and improves neurological outcome after fluid percussion brain injury in rats*. *J Neurotrauma*, 2012. **29**(14): p. 2375-92.
53. Ferreira, A.P., F.S. Rodrigues, I.D. Della-Pace, B.C. Mota, S.M. Oliveira, C. Velho Gewehr Cde, F. Bobinski, C.V. de Oliveira, J.S. Brum, M.S. Oliveira, A.F. Furian, C.S. de Barros, J. Ferreira, A.R. Santos, M.R. Figuera, and L.F. Royes, *The effect of NADPH-oxidase inhibitor apocynin on cognitive impairment induced by moderate lateral fluid percussion injury: role of inflammatory and oxidative brain damage*. *Neurochem Int*, 2013. **63**(6): p. 583-93.
54. Shultz, S.R., D.F. MacFabe, K.A. Foley, R. Taylor, and D.P. Cain, *Sub-concussive brain injury in the Long-Evans rat induces acute neuroinflammation in the absence of behavioral impairments*. *Behav Brain Res*, 2012. **229**(1): p. 145-52.
55. Dietrich, W.D., J. Truettner, W. Zhao, O.F. Alonso, R. Busto, and M.D. Ginsberg, *Sequential changes in glial fibrillary acidic protein and gene expression following parasagittal fluid-percussion brain injury in rats*. *J Neurotrauma*, 1999. **16**(7): p. 567-81.
56. Rall, J.M., D.A. Matzilevich, and P.K. Dash, *Comparative analysis of mRNA levels in the frontal cortex and the hippocampus in the basal state and in response to experimental brain injury*. *Neuropathol Appl Neurobiol*, 2003. **29**(2): p. 118-31.
57. Bi, F., C. Huang, J. Tong, G. Qiu, B. Huang, Q. Wu, F. Li, Z. Xu, R. Bowser, X.G. Xia, and H. Zhou, *Reactive astrocytes secrete lcn2 to promote neuron death*. *Proc Natl Acad Sci U S A*, 2013. **110**(10): p. 4069-74.



58. Wu, L., Y. Du, J. Lok, E.H. Lo, and C. Xing, *Lipocalin-2 enhances angiogenesis in rat brain endothelial cells via reactive oxygen species and iron-dependent mechanisms*. J Neurochem, 2015. **132**(6): p. 622-8.
59. Lee, S., M.K. Jha, and K. Suk, *Lipocalin-2 in the Inflammatory Activation of Brain Astrocytes*. Crit Rev Immunol, 2015. **35**(1): p. 77-84.
60. Suk, K., *Lipocalin-2 as a therapeutic target for brain injury: An astrocentric perspective*. Prog Neurobiol, 2016. **144**: p. 158-72.
61. Kao, T.H., Y.J. Peng, D.M. Salter, and H.S. Lee, *Nerve growth factor increases MMP9 activity in annulus fibrosus cells by upregulating lipocalin 2 expression*. Eur Spine J, 2015. **24**(9): p. 1959-68.
62. Rink, A., K.M. Fung, J.Q. Trojanowski, V.M. Lee, E. Neugebauer, and T.K. McIntosh, *Evidence of apoptotic cell death after experimental traumatic brain injury in the rat*. Am J Pathol, 1995. **147**(6): p. 1575-83.
63. Raghupathi, R., D.I. Graham, and T.K. McIntosh, *Apoptosis after traumatic brain injury*. J Neurotrauma, 2000. **17**(10): p. 927-38.
64. Conti, A.C., R. Raghupathi, J.Q. Trojanowski, and T.K. McIntosh, *Experimental brain injury induces regionally distinct apoptosis during the acute and delayed post-traumatic period*. J Neurosci, 1998. **18**(15): p. 5663-72.
65. Yakovlev, A.G., S.M. Knoblach, L. Fan, G.B. Fox, R. Goodnight, and A.I. Faden, *Activation of CPP32-like caspases contributes to neuronal apoptosis and neurological dysfunction after traumatic brain injury*. J Neurosci, 1997. **17**(19): p. 7415-24.
66. Yakovlev, A.G., K. Ota, G. Wang, V. Movsesyan, W.L. Bao, K. Yoshihara, and A.I. Faden, *Differential expression of apoptotic protease-activating factor-1 and caspase-3 genes and susceptibility to apoptosis during brain development and after traumatic brain injury*. J Neurosci, 2001. **21**(19): p. 7439-46.
67. Beer, R., G. Franz, A. Srinivasan, R.L. Hayes, B.R. Pike, J.K. Newcomb, X. Zhao, E. Schmutzhard, W. Poewe, and A. Kampfl, *Temporal profile and cell subtype distribution of activated caspase-3 following experimental traumatic brain injury*. J Neurochem, 2000. **75**(3): p. 1264-73.
68. Thompson, S.N., T.R. Gibson, B.M. Thompson, Y. Deng, and E.D. Hall, *Relationship of calpain-mediated proteolysis to the expression of axonal and synaptic plasticity markers following traumatic brain injury in mice*. Exp Neurol, 2006. **201**(1): p. 253-65.
69. Hulsebosch, C.E., D.S. DeWitt, L.W. Jenkins, and D.S. Prough, *Traumatic brain injury in rats results in increased expression of Gap-43 that correlates with behavioral recovery*. Neurosci Lett, 1998. **255**(2): p. 83-6.

70. Faló, M.C., T.M. Reeves, and L.L. Phillips, *Agrin expression during synaptogenesis induced by traumatic brain injury*. J Neurotrauma, 2008. **25**(7): p. 769-83.
71. Hall, K.D. and J. Lifshitz, *Diffuse traumatic brain injury initially attenuates and later expands activation of the rat somatosensory whisker circuit concomitant with neuroplastic responses*. Brain Res, 2010. **1323**: p. 161-73.
72. Ding, J.Y., C.W. Kreipke, P. Schafer, S. Schafer, S.L. Speirs, and J.A. Rafols, *Synapse loss regulated by matrix metalloproteinases in traumatic brain injury is associated with hypoxia inducible factor-1alpha expression*. Brain Res, 2009. **1268**: p. 125-34.
73. Benowitz, L.I. and A. Routtenberg, *GAP-43: an intrinsic determinant of neuronal development and plasticity*. Trends Neurosci, 1997. **20**(2): p. 84-91.
74. Chin, L.S., L. Li, A. Ferreira, K.S. Kosik, and P. Greengard, *Impairment of axonal development and of synaptogenesis in hippocampal neurons of synapsin I-deficient mice*. Proc Natl Acad Sci U S A, 1995. **92**(20): p. 9230-4.
75. Garofalo, L., A. Ribeiro-da-Silva, and A.C. Cuello, *Nerve growth factor-induced synaptogenesis and hypertrophy of cortical cholinergic terminals*. Proc Natl Acad Sci U S A, 1992. **89**(7): p. 2639-43.
76. Burgos, I., A.C. Cuello, P. Liberini, E. Pioro, and E. Masliah, *NGF-mediated synaptic sprouting in the cerebral cortex of lesioned primate brain*. Brain Res, 1995. **692**(1-2): p. 154-60.
77. Tuszynski, M.H., H. Sang, K. Yoshida, and F.H. Gage, *Recombinant human nerve growth factor infusions prevent cholinergic neuronal degeneration in the adult primate brain*. Ann Neurol, 1991. **30**(5): p. 625-36.
78. Wieloch, T. and K. Nikolich, *Mechanisms of neural plasticity following brain injury*. Curr Opin Neurobiol, 2006. **16**(3): p. 258-64.
79. Nudo, R.J., *Adaptive plasticity in motor cortex: implications for rehabilitation after brain injury*. J Rehabil Med, 2003(41 Suppl): p. 7-10.
80. Conte, V., R. Raghupathi, D.J. Watson, S. Fujimoto, N.C. Royo, N. Marklund, N. Stocchetti, and T.K. McIntosh, *TrkB gene transfer does not alter hippocampal neuronal loss and cognitive deficits following traumatic brain injury in mice*. Restor Neurol Neurosci, 2008. **26**(1): p. 45-56.
81. Oyesiku, N.M., C.O. Evans, S. Houston, R.S. Darrell, J.S. Smith, Z.L. Fulop, C.E. Dixon, and D.G. Stein, *Regional changes in the expression of neurotrophic factors and their receptors following acute traumatic brain injury in the adult rat brain*. Brain Res, 1999. **833**(2): p. 161-72.

82. O'Dell, D.M., R. Raghupathi, P.B. Crino, J.H. Eberwine, and T.K. McIntosh, *Traumatic brain injury alters the molecular fingerprint of TUNEL-positive cortical neurons In vivo: A single-cell analysis*. J Neurosci, 2000. **20**(13): p. 4821-8.
83. Cekic, M., S.J. Johnson, V.H. Bhatt, and D.G. Stein, *Progesterone treatment alters neurotrophin/proneurotrophin balance and receptor expression in rats with traumatic brain injury*. Restor Neurol Neurosci, 2012. **30**(2): p. 115-26.
84. Alder, J., W. Fujioka, J. Lifshitz, D.P. Crockett, and S. Thakker-Varia, *Lateral fluid percussion: model of traumatic brain injury in mice*. J Vis Exp, 2011(54).
85. Tian, L., R. Guo, X. Yue, Q. Lv, X. Ye, Z. Wang, Z. Chen, B. Wu, G. Xu, and X. Liu, *Intranasal administration of nerve growth factor ameliorate beta-amyloid deposition after traumatic brain injury in rats*. Brain Res, 2012. **1440**: p. 47-55.
86. Lin, H.W., I. Saul, V.L. Gresia, J.T. Neumann, K.R. Dave, and M.A. Perez-Pinzon, *Fatty acid methyl esters and Solutol HS 15 confer neuroprotection after focal and global cerebral ischemia*. Transl Stroke Res, 2014. **5**(1): p. 109-17.

## Chapter 4.

### The effects of the selective TrkA agonist, gambogic amide, on fracture healing in mice and osteoblasts *in vitro*

Note: A version of this chapter has been published prior to the completion of this thesis. The extent of contributions for this chapter as well as permissions and a copy of the publication can be found in **Appendix C**.

**Johnstone M. R.**, Brady R. D., Schuijers J. A., Church J. E., Orr D., Quinn J. M. W., McDonald S. J., Grills B. L., The selective TrkA agonist, gambogic amide, promotes osteoblastic differentiation and improves fracture healing in mice. *Journal of Musculoskeletal and Neuronal Interactions*. 2019 19(1) 94-103.

#### 4.1. Introduction

Poor bone fracture healing is a common clinical problem that severely affects the quality of life to patients, particularly in the case of non-union (i.e., failure to join the broken bone surfaces) which frequently necessitates surgery [1-3]. Most fractures heal successfully within 2 months, but delayed and non-union fractures affect approximately 5-10% of all patients worldwide [3, 4]. However, there are few non-surgical options available to improve patient outcomes and avoid non-union. One approach for identifying novel therapeutic agents that improve healing is by study of the biological mechanisms that underlie proper fracture union; such mechanisms include re-establishment of adequate blood supply and innervation of the fracture site [1, 2, 5, 6]. In particular, it is notable that both sensory and sympathetic innervation during fracture healing improves both mineral callus composition and mechanical strength [6-8]. Nerve sprouting rapidly increases in the periosteum and callus in the early stages of fracture healing, and several studies have shown that reduced fracture site innervation result in significantly larger calluses that have low bone mineral content and are consequently mechanically weaker than calluses in appropriately innervated fractures [6-11]. Accordingly, non-surgical treatments for fracture healing that increase both bone formation and innervation may improve bone repair and reduce the chance of delayed union (or non-union) of the fractured bone.

Nerve growth factor (NGF) is a neurotrophin responsible for the growth and maintenance of sympathetic and sensory neurons in the peripheral nervous system [12] and exerts its effects via two receptors: the high-affinity/pro-growth and survival receptor TrkA, or the low-affinity/pro-apoptotic receptor, p75NTR [13, 14]. Several studies in rodents have identified a beneficial role for NGF treatment in fracture healing and distraction osteogenesis, showing that topical administration of NGF increased sympathetic neurite outgrowth, accelerated the transition of immature woven bone to mature lamellar bone, increased mineralized bone within healing callus and improved the mechanical properties of fractures [15-19]. Additionally, during fracture healing,

both NGF and TrkA have been detected in skeletal cells that include bone-forming osteoblasts and osteoprogenitor cells (precursor cells of osteoblasts) as well as cartilage-forming chondrocytes [20-22]. Osteoblastic MC3T3-E1 cells in an *in vitro* study also respond to NGF treatment with increased migration and greater osteoblastic differentiation indicated by expression of ALP and type 1 collagen [23]. Taken together, these findings suggest that in addition to promoting re-innervation of the fracture site, NGF may directly promote bone formation and this may enhance fracture healing.

While NGF has shown promise in pre-clinical studies, it shows poor pharmacokinetic properties which severely limit its potential as a therapeutic agent. NGF is susceptible to proteolytic degradation and has a short elimination half-life (~2 h) following systemic administration [24-26]. Therefore, use of small non-peptide neurotrophic mimetics may be a superior approach. Gambogic amide (GA) is a non-peptide molecule that has already been shown to have selective high affinity for TrkA receptors and is tolerated *in vivo* [27-29]. Systemic administration of 2 mg/kg/day of GA in mice selectively induces TrkA activation in hippocampal neurons, reduced infarct size in a model of ischemic stroke and increased neurite outgrowth in PC12 cells [27-30]. However, to date, no studies have investigated the potential of GA treatment on fracture healing. Accordingly, the effects of GA on the structural and mechanical features of healing fractures in mice, and on osteoprogenitor cell differentiation and mineralization *in vitro* were investigated in the current experiments.

## **4.2. Materials and methods**

### **4.2.1. Solubility and delivery of GA**

GA arrived from manufacturers as yellow-orange powdered substance. According to manufacturer instructions and several articles published by research groups using GA in animal studies, GA readily suspends into solution in either DMSO (20 mg/ml) or ETOH (20 mg/ml) and can be diluted with PBS to a desired concentration of 1-2 mg/ml [27-29]. Unfortunately, after a series of attempts to suspend GA using either vehicle, it became clear GA would not remain in solution. GA precipitated as soon as PBS was added at room temperature. The GA amide solution was heated, cooled, vortexed, and changed to new diluting agents like water in an attempt to keep GA in solution; yet the solution remained opaque, filled with precipitants.

GA only remained suspended in solution in a vehicle of 50% DMSO in PBS, which was a much greater concentration of DMSO than previously published [27-29], and was the maximum DMSO range allowed to use in the ALZET® mini osmotic pump (DURECT Corporation, CA, USA) the mode of drug delivery for these experiments (see manufacturers information guide).

ALZET® Model 1002 were used to subcutaneously deliver GA or vehicle to mice. Model 1002 is an osmotic pump that delivers a fixed volume of solution at a constant rate. The maximum reservoir volume of Model 1002 is 100 µl, and the pump delivers at a constant rate of 0.25 µl/h for a maximum of 14 days. Mice were given a 1 mg/kg/day of GA. Therefore, a mouse weighing 30 mg (average mouse at 16 weeks) will require  $1 \times 30 \div 1000 = 0.03$  mg/day. This equates to  $0.03 \div 24 = 0.00125$  mg/hr = 1.25 µg/h/mouse. For the 1002 pump, the concentration of GA needed to be loaded into 100 µl pump is:  $1.25 \mu\text{g/h} \div 0.25 \mu\text{l/h}$  (flow rate of pump) = 5 µg/µl. This equates to 500 µg in 100 µl or 0.5 mg in 100 µl.

#### **4.2.2. Experimental groups**

Eighty mice received bilateral fibular fractures and were randomly allocated to one of six experimental groups. The two main groups were GA or vehicle treated, then three subgroups for each treatment were based on time of euthanasia, 14-, 21- or 42 days post fracture. Therefore, the six experimental groups were GA-14, GA-21, GA-42, VEH-14, VEH-21, and VEH-42. Each chosen timepoint reflects variations in callus composition during the stages of fracture healing, which can be reviewed in **Chapter 1**, section **1.2.4**. ‘*Mechanisms of endochondral fracture repair*’.

#### **4.2.3. Bilateral fibular osteotomy and pump insertion**

Bilateral fibular osteotomies were conducted using previously described standard protocols [31, 32]. In brief, under isoflurane anaesthesia, a 5 mm skin incision was made over the fibula. Using microtenotomy scissors, mice received a bilateral transverse fibular osteotomy at the midpoint of the fibula, approximately 12 mm proximal to the calcaneal tuberosity. Skin incisions were closed using skin glue (3M™ Vetbond™ Tissue Adhesive, St. Paul, MN, USA). Immediately post-fracture, a 10 mm incision was made on the dorsal surface of mice in between the scapulae. Mini-osmotic pumps (ALZET® Model 1002) were then subcutaneously inserted and incisions were closed using Reflex wound clips. Post-surgery, all mice were injected subcutaneously with 5 mg/kg of analgesic, Carprofen, in the hind region and allowed to recover on a heated veterinary pad.

#### **4.2.4. Region of interest and grayscale thresholds used in µCT callus reconstruction**

For µCT, fibular calluses were dissected out and scanned (see **section 2.3** for protocol), the region of interest (ROI) was identified as a 2 mm longitudinal region of callus (i.e. 1 mm proximal and distal to the fracture line of the callus); the border of the callus was manually traced. Thresholds used for parameter quantification were determined using the automatic “otsu” algorithm within CTAn and visual examination of unreconstructed X-ray images. A grayscale adaptive threshold of 42-255 was used for structural analysis of calluses 14-, 21- and 42-day post-fracture. 2D and 3D data, and 3D models were generated, and the following parameters were

used for structural analysis of callus: total callus volume (TV); new mineralized tissue bone volume (BV), bone fractional volume (BV/TV) and bone surface (BS).

#### **4.2.5. Callus position during biomechanical testing**

Biomechanical testing was used to assess the effects of GA on the mechanical properties of 42-day calluses. During biomechanical testing (**section 2.4**), each fibula was mounted onto a 4 mm stabilizing platform in an anterior-posterior direction. The callus was oriented in this position to reduce the rotation of the fibula when the fulcrum ascended and applied force to the centre of the callus. A 10 N force transducer descended at a constant rate of 1.67 mm/sec and loaded each callus, force (g) and deflection (mm) values was recorded and plotted an x-y (load-displacement) graph.

#### **4.2.6. Histological assessment**

Fibular calluses from GA-14, GA-21, VEH-14, and VEH-21 underwent tissue processing, and were embedded in LR White Resin for histology purposes as outlined in **section 2.5 'Histology'**. To identify whether GA treatment influenced bone resorption during fracture healing, the percentage of TRAP was measured as the total area of callus stained positive for TRAP activity divided by total callus area using Leica Qwin software (Leica), as described in **section 2.5.3 'Tissue section staining'**.

#### **4.2.7. Cell culture**

In this section are additional reagents and dosages used for each for all analyses. For detailed cell culture protocols, please refer to **Chapter 2**, section 2.6 '*Cell Culture*'.

#### **Western blotting**

Western blot analysis was performed to assess expression of high-affinity receptor, TrkA, in undifferentiated Kusa O cells and 14 day differentiated Kusa O cells. Membranes were incubated in rabbit polyclonal Anti-TrkA primary antibodies:

- Abcam (ab8871), dilution 1:1000. Reactivity to rat tissue.

For further details please refer to **Chapter 2**, section 2.6.3.

#### **Proliferation Assay**

Kusa O cells were treated with various concentrations of GA (0.05nM, 0.1nM, 0.5nM, 1nM, 5nM, 10nM, 50nM, 100nM, 500nM, 1 $\mu$ M, 5 $\mu$ M, 10 $\mu$ M) for 72 h, negative control was  $\alpha$ -MEM only, and positive controls were  $\alpha$ -MEM+10% FBS,  $\alpha$ -MEM + 100 ng/ml IGF. The proliferation assay was completed to an n = 4 using cells of different passages (10-22) and data was normalized to relative cell proliferation changes in relation to the control.

### **RT-PCR**

Kusa O cells were cultured daily in osteoblastic differentiation media and treated with 0.5nM of GA or vehicle for 3-, 7-, and 14-days. Total RNA was prepared using PureZOL™ (Bio-Rad). RT-PCR was performed as described previously in **section 2.6.5**.  $\beta$ -actin was used as an internal control gene. PCR was performed in triplicate using SsoFast™ EvaGreen® Supermix (Bio-Rad) and specific oligonucleotide primers (**Table 4.1**) on an iQ 96-well PCR system (Bio-Rad).

### **Mineralization**

For investigating the effects GA treatment has on osteoblast cell mineralization, Kusa O cells were treated with 0.5nM of GA for 21 days. After 21 days, cells were stained with Alizarin red and inspected for mineralization nodules within the Kusa O colonies.

**Table 4.1.** Oligonucleotide name and sequence (5'-3') used in Real-Time PCR.

<b>Oligonucleotide name</b>	<b>Sequence (5'-3')</b>
<b>Beta actin</b>	Sense - GCTGTGCTATGTTGCTCTAG
	Anti-sense - CGCTGCTTGCCAATAGTG
<b>mOsterix</b>	Sense - TATGCTCCGACCTCCTCAAC
	Anti-sense - AATAAGATTGGGAAGCAGAAAG
<b>mRunx2</b>	Sense - AGCAACAGCAACAACAGCAG
	Anti-sense - GTAATCTGACTCTGCCTTG
<b>mAlkaline phosphatase</b>	Sense - AAACCCAGACACAAGCATTCC
	Anti-sense - TCCACCAGCAAGAAGAAGCC
<b>mOsteocalcin</b>	Sense - TCTCTCTGACCTCACAGATCCC
	Anti-sense - TACCTTATTGCCCTCCTGCTTG
<b>mDentin matrix acidic phosphoprotein 1 (DMP-1)</b>	Sense - CGCCGATAAGGAGGATGATG
	Anti-sense - GTGTGGTGTCTGTGGAGTC
<b>mRANKL</b>	Sense - ATCAGAAGACAGCACTCACT
	Anti-sense - ATCTAGGACATCCATGCTAATGT
<b>mOsteoprotegerin</b>	Sense - TGACCACTCTTATACGGACAG
	Anti-sense - GCCCTTCCTCACACTCAC



#### **4.2.8. Statistical analysis**

Shapiro-Wilk normality tests were used through the entirety on this chapter. Mann-Whitney U tests were used for  $\mu$ CT, biomechanical analysis, histology, and *in vitro* mineralization assays. One-way ANOVA was used to analyse *in vitro* proliferation assays, and two-way ANOVA with Bonferroni *post-hoc* comparisons were used for RT-PCR.

### **4.3. Results**

There were no apparent behavioural changes, side effects, or changes in the weight gain pattern of GA treatment in mice.

#### **4.3.1. Calluses are structurally smaller when treated with GA**

Representative  $\mu$ CT reconstructions of longitudinal mid-point hemi calluses are shown in **Figure 4.1(a-f)**. Bony union was reached in all calluses by 21 days in both the GA-treated and control groups. For all  $\mu$ CT parameters, no effects of GA were seen at either 14- or 42- days post fracture. In contrast, analyses revealed that calluses from 21-day GA-treated mice (**Figure 4.1g-j**) had significantly reduced tissue volume (**Figure 4.1g**;  $p < 0.05$ ) which suggested a smaller callus. The measured bone surface in calluses (**Figure 4.1j**;  $p < 0.05$ ) was also lower compared to 21-day vehicle-treated mice, which suggested more consolidated bone was present in these calluses. Consistent with these observations, at 21 days post-fracture, calluses from GA-treated mice also showed increased BV/TV, i.e. bone volume fraction corrected for tissue volume (**Figure 4.1i**;  $p < 0.05$ ) compared to vehicle-treated mice.

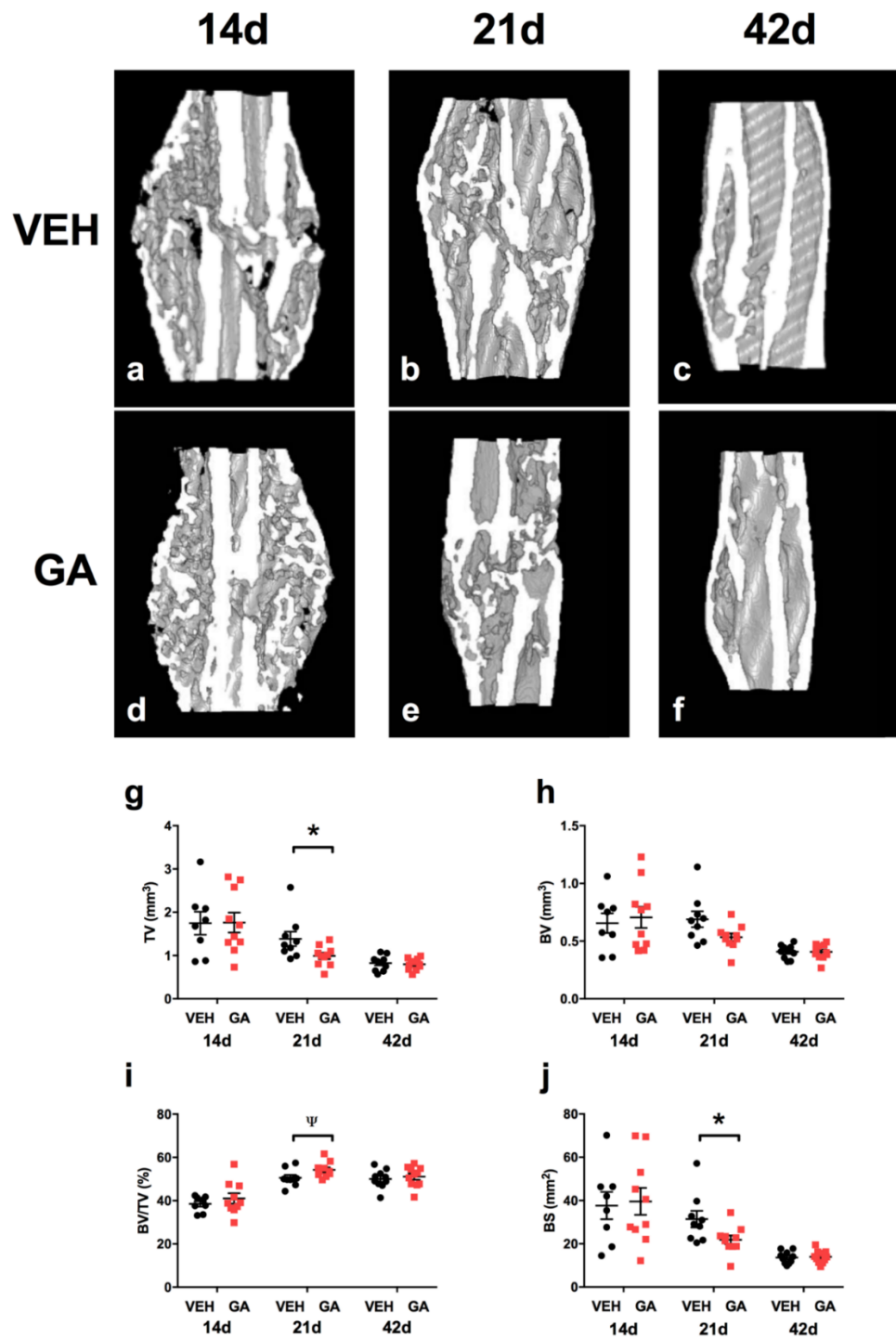


**Figure 4.1.** The effects of GA treatment on callus structural parameters using  $\mu$ CT. Longitudinal mid-point images representative of  $\mu$ CT reconstructions of hemi-calluses (a-f).  $\mu$ CT analysis found that GA-treated decreased callus tissue volume (g; TV) and bone surface area (j; BS) at 21 days post-fracture ( $*p < 0.05$ ) compared to vehicle-treated mice. There was a trend that GA increased bone fractional volume of calluses (i;  $\psi p = 0.05$ ) compared to vehicle-treated mice. No differences were seen at 14-, and 42-days post-fracture between GA-treated and vehicle-treated mice. Bars are mean  $\pm$  SEM,  $n = 8-11$ /group.

### 4.3.2. Biomechanical analyses

A three-point bending test was used to assess the biomechanical properties of 42-day fibular calluses. The average cross-sectional area of fracture callus at its breaking point was significantly smaller in samples from GA-treated mice (36%, **Table 4.2.**,  $p < 0.001$ ) compared to vehicle-treated mice. Calluses from GA-treated mice showed an increased load per unit area (52%) and stiffness per unit area (53%) (**Table 4.2.**,  $p < 0.01$ ) compared to vehicle-treated mice. However, the peak force to failure and stiffness of calluses were not significantly different between vehicle-treated and GA-treated mice.

**Table 4.2.** Mechanical properties of vehicle and GA-treated calluses at 42 days post-fracture.

Treatment	Peak Force (N)	Stiffness ( $\times 10^4 \text{ Nm}^2$ )	CSA ( $\times 10^{-7} \text{ m}^2$ )	Bending stress ( $\times 10^7 \text{ Nm}^{-2}$ )	YM ( $\times 10^9 \text{ Nm}^{-2}$ )
Vehicle (n = 20) Mean $\pm$ SEM	3.92 $\pm$ 0.20	5.41 $\pm$ 0.30	5.22 $\pm$ 0.30	1.45 $\pm$ 0.13	4.15 $\pm$ 0.63
GA (n = 17) Mean $\pm$ SEM	3.76 $\pm$ 0.28	5.09 $\pm$ 0.38	3.59 $\pm$ 0.28	2.72 $\pm$ 0.43	8.63 $\pm$ 1.53
<i>p</i> -value	0.39	0.38	< 0.001	< 0.01	< 0.01

CSA, cross-sectional area; YM, Young's modulus. Values are means  $\pm$  SEM.

### 4.3.3. Histological Assessment

A TRAP histochemical stain was used to assess osteoclastic density on the bone surface at 14, and 21 days post fracture. Representative TRAP stained histological sections, shown in **Figure 4.2a-d**. Quantitative assessment revealed less dense TRAP histochemical staining; this was calculated as the proportion of TRAP staining/total callus surface area, in 21-day calluses compared to 14-day calluses (**Figure 4.2e**;  $p < 0.01$ ). No differences in the percentage of TRAP staining in calluses were found between GA-treated and vehicle-treated mice, both at 14- and 21-days post-fracture.

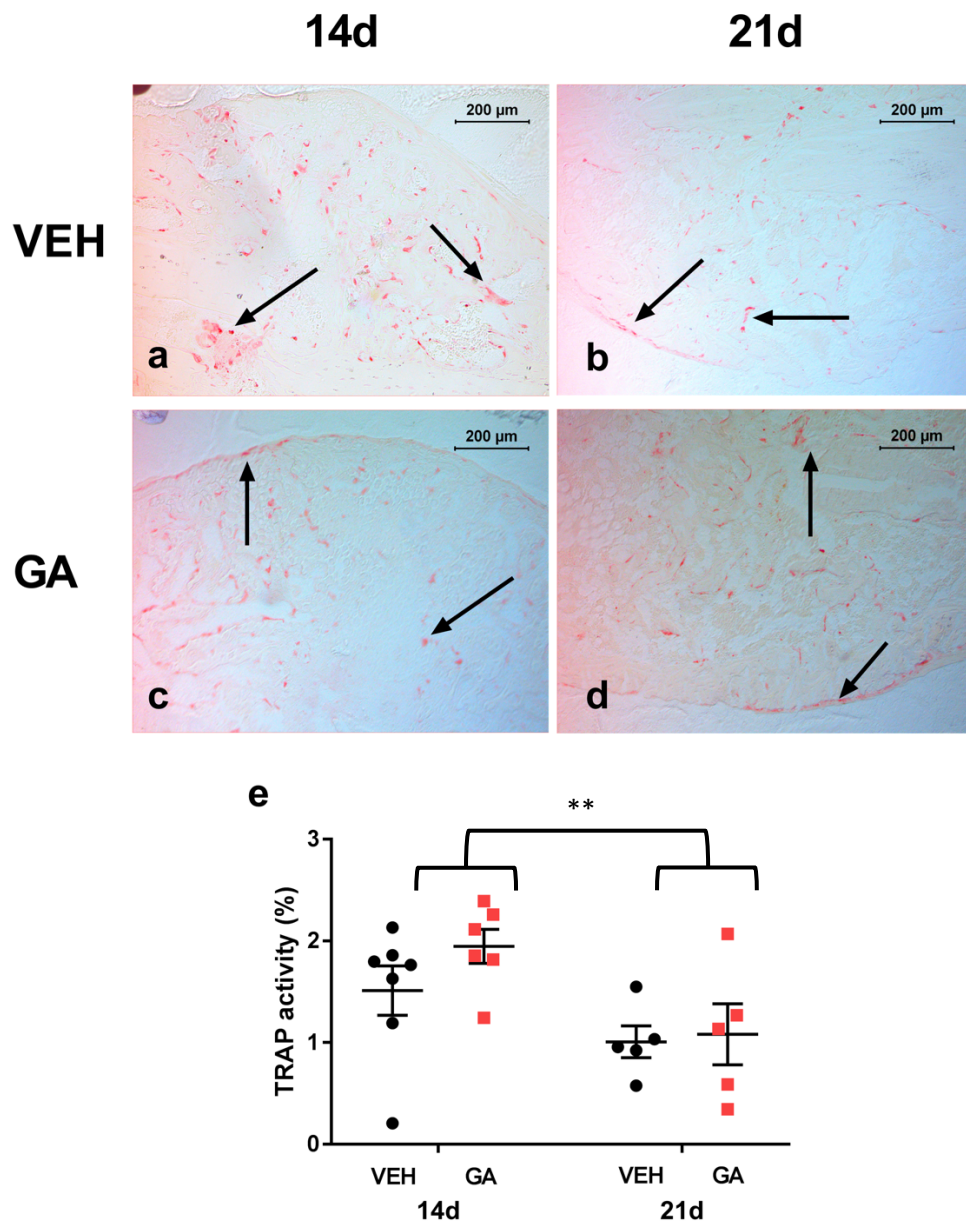


**Figure 4.2.** Representative histological sections of undecalcified calluses stained with TRAP at 14- and 21-day post-fracture from GA and vehicle treated mice (a-d; magnification 200x). TRAP staining was present in 14- and 21-day post-fracture, there was reduced TRAP activity in both GA and vehicle treated mice at 21 days post-fracture compared to 14 days post-fracture (a, c, e;  $**p < 0.01$ ). There was no GA treatment effect at 14- or 21-days post-fracture (e). GA, gambogic amide; TRAP, tartrate-resistant acid phosphatase. Bars are mean  $\pm$  SEM, n = 5-7/group.

#### **4.3.4. Cell Culture**

##### ***TrkA receptors are present on mature osteoblast-like cells***

Western blot analysis of high-affinity receptor, TrkA, was assessed in undifferentiated Kusa O cells and 14 days differentiated Kusa O cells. TrkA receptor protein expression was absent in undifferentiated Kusa O cells, however, TrkA expression was detected in 14 day differentiated Kusa O cells (**Figure 4.3a**). Proliferation assays were used to assess GA influence on Kusa O cell proliferation. At 72 h following treatment, Kusa O cell proliferation was not affected in response to daily GA-treatment ranging from 0 to 100nM. However, daily GA-treatment ranging from 500nM to 10 $\mu$ M significantly reduced Kusa O cell proliferation (**Figure 4.3b**;  $p < 0.001$ ) suggesting toxic effects at these doses.

##### ***GA increases markers of mature osteoblasts and osteocytes***

A pilot study on the effect of GA treatments on Kusa O differentiation *in vitro* revealed that a daily GA dose of 0.5nM appeared to increase expression of osteoblast-associated genes to a greater extent than for GA doses ranging from 1-10nM (data not shown). As such, a dose of 0.5nM of GA was chosen for all further *in vitro* studies.

Kusa O cells differentiated and treated daily with 0.5nM of GA for 3-, 7-, and 14-days were analysed for expression of genes associated with early osteoblasts (Osx and Runx2; data not shown), mature osteoblasts (ALP and osteocalcin; **Figures 4.3c,d**), osteocytes (DMP-1; **Figure 4.3e**) and osteoclastogenesis (OPG and RANKL; **Figures 4.3f,g**). Significant main effects of time and treatment, as well as an interaction were present for Kusa O expression of ALP, osteocalcin, and DMP. Post-hoc analysis revealed that daily GA treatment increased the expression of ALP (**Figure 4.3c**;  $p < 0.01$ ), osteocalcin (**Figure 4.3d**;  $p < 0.001$ ) and DMP-1 (**Figure 4.3e**;  $p < 0.001$ ) in 14-day, but not 3- and 7-day differentiated Kusa O cells. Daily GA treatment did not influence expression of either Osx or Runx2 (data not shown). Gene expression of markers associated with osteoclastogenesis, OPG and RANKL, in Kusa O cells did not alter at 3-, 7-, and 14-days of differentiating or in response to daily GA treatment (**Figures 4.3f,g**).

##### ***GA promotes mineral nodule formation***

Kusa O cells formed mineralized matrix during 21 days of incubation with ascorbate and  $\beta$ -glycerophosphate. Daily treatment of 0.5nM of GA increased mineralization area in Kusa O cells compared to control cultures (**Figure 4.3i**;  $p < 0.05$ ). There was no mineralization evident in negative control cultures that employed undifferentiated Kusa O cells.

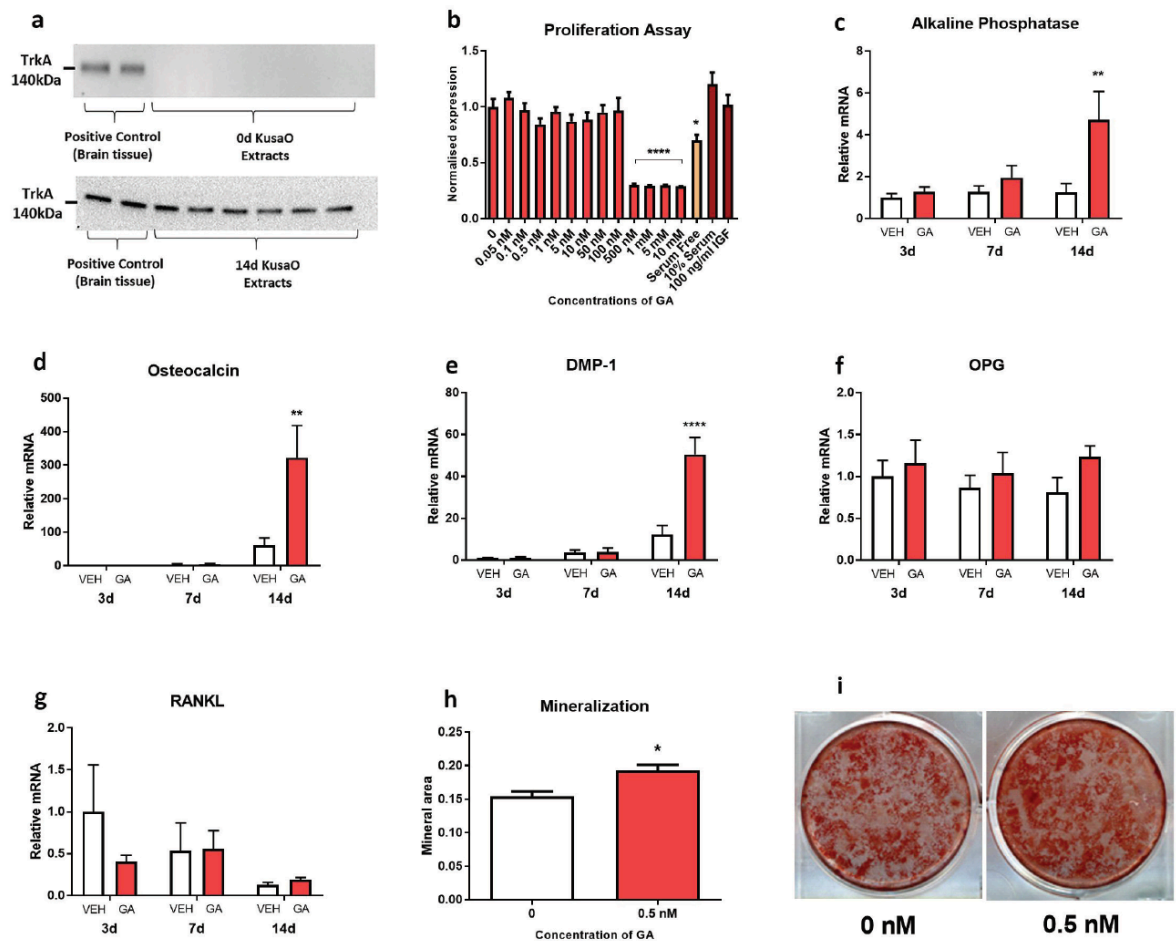


**Figure 4.3.** TrkA expression and the effects of GA treatment in the mesenchymal stem cell line, Kusa O. Western blotting (a) revealed that differentiated but not undifferentiated Kusa O cells expressed TrkA. GA did not increase proliferation after 72 h of treatment; however, GA was cytotoxic at concentrations  $\geq 500$  nM (b; \*\*\*\* $p < 0.0001$ ). Gene expression markers of mature osteoblasts (c,d), early osteocytes (e), and osteoclastic formation (f,g), were analysed at 3-, 7-, and 14-days of differentiation. GA treatment increased alkaline phosphatase (c; \*\* $p < 0.01$ ), osteocalcin (d; \*\* $p < 0.01$ ), and DMP-1 (e; \*\*\*\* $p < 0.0001$ ) gene expression of Kusa O's at 14 days compared to vehicle. Time or GA had no effect on OPG or RANKL expression (f,g). Kusa O cells formed mineral after 21 days of incubation. GA increased mineralization of Kusa O cells compared to vehicle (h,i; \* $p < 0.05$ ). GA, gambogicamide; DMP-1, dentin matrix acidic phosphoprotein 1; OPG, osteoprotegerin; RANKL, receptor activator of nuclear factor kappa-B ligand. Bars are mean  $\pm$  SEM,  $n = 6-8$ /group.

#### 4.4. Discussion

In this study, the influence of GA, a small molecule TrkA receptor agonist was investigated on healing murine fibular fractures and found strong evidence that suggests GA acts in a similar manner to the reported actions of NGF on fracture healing. GA treatment resulted in fracture calluses that were smaller in size and mechanically stronger per unit area. It was shown that treatment with 1 mg/kg/day GA systemically delivered for 14 days to mice with fibular fractures decreased tissue volume of the callus at 21 days post-fracture and increased the mechanical properties; bending stress and Young's modulus of the fractures at 42 days. Additionally, GA increased the mRNA expression of markers associated with osteoblastic and osteocytic differentiation. Consistent with a direct action of GA on osteoblasts, it was found that osteoblastic differentiation and *in vitro* mineralization was increased in Kusa O osteoprogenitor cells. The present data therefore suggests that GA, like NGF, may promote fracture healing through promoting both osteoprogenitor differentiation and mineralization.

$\mu$ CT analysis was used to determine the influence of GA on the bone content of the calluses at various stages during fracture healing. Of the three time-points analysed; 14-, 21-, and 42-days after fracture, significant differences in callus architecture was only seen in the 21-day group. At 21 days post-fracture, while there was no change in the amount of bone volume, calluses of GA-treated mice had overall reduced tissue volume and elevated bone fractional volume in comparison to mice treated with vehicle, which suggests that GA treatment influenced bone remodelling of healing fractures. This finding is similar to that previously reported, with NGF treatment in rats with rib fractures; where after for 14 days of NGF treatment, fractured bone had smaller calluses at 21 days post-fracture [15], with enhanced bony content within calluses compared to vehicle-treated fractures. It is unclear whether this smaller callus trait is this previous experiment reflected a change in cartilage formation, however, it would be consistent with a more rapid maturation of the fracture site [15]. Several other studies involving distraction osteogenesis have also reported that NGF treatment enhanced both bone formation and callus development during the consolidation phase (28 days) of healing, compared to vehicle-treated calluses [16, 18, 19]. One possible mechanism by which GA, like NGF, resulted in smaller calluses is likely through the stimulation of nerve growth in and around the fracture site. The periosteum of bone is densely lined with TrkA positive nerve fibres [33]. NGF treatment increased nerve growth and activity in healing rat rib calluses by upregulating catecholamine synthesis [15] which has been directly linked to stimulate both blood vessel and sensory nerve sprouting through TrkA signalling in developing endochondral bone [34]. Innervation of bone is important for angiogenesis and bone formation, which are two factors that mediate both ossification [34] and fracture healing rate [35]. It has been documented that both sensory and sympathetic nerves within callus contribute

positively in regard to fracture callus remodelling [9], with numerous studies reporting that removal of sensory and sympathetic neural input results in the formation of larger, disorganised fracture calluses [6-8]. GA, similarly to NGF, may have indirectly facilitated fracture healing by stimulating sensory and sympathetic nerve growth within the callus via TrkA, which in turn assisted in co-ordinating vascularisation and ossification of fractured bone to produce smaller calluses by 21 days.

Whilst the present  $\mu$ CT data shows no difference in tissue or bone volume of calluses by 42 days post-fracture, fracture sites from mice treated with GA had increased stiffness per unit area and load per unit area compared to vehicle-treated mice. These outcomes are identical to a previous study in our lab where NGF treatment to healing rat rib fractures improved the mechanical properties of calluses at 42 days post-fracture [15]. Nonetheless, it is important to note GA treatment in the current study, as well as NGF treatment in the previous study [15], did not alter the mechanical properties of peak force to failure and stiffness. Mechanical strength of healing fractures is highly dependent on callus structure and degree of mineralization [36], and whilst there may not be an overall difference in the amount of bone present, there may be a difference in the quality of bone present in the callus. The present findings may indicate that there could have been a higher portion of mature, mechanically stronger lamellar bone than immature woven bone in the calluses of the GA-treated mice compared to vehicle-treated mice at 42 days, however, it was impossible to distinguish the two types of bone via  $\mu$ CT analysis. It is postulated that this may explain why there was no difference in the amount of bone in calluses between treatments at 42 days via  $\mu$ CT analysis, even though biomechanically, the calluses of the GA-treated group were stronger per unit area compared to controls. Furthermore,  $\mu$ CT findings indicated that when compared to 21 days post-fracture, calluses at 42 days were at a substantially more advanced stage of healing in both vehicle- and GA-treated groups; as such, it is possible that mechanical testing at an earlier time point of healing (i.e. when healing was less advanced and the structural effects of GA treatment were apparent) may have yielded difference findings.

Given the aforementioned findings of reduced callus size and enhanced mechanical properties, it was apparent that GA treatment caused changes to callus remodelling. TRAP staining was used to assess whether GA treatment influenced osteoclastic cell density during fracture healing, but no differences in this parameter were observed. This suggests that GA may not have influenced remodelling through bone resorption and is consistent with the current *in vitro* data, which showed that GA did not affect gene expression of osteoblastic OPG or RANKL, factors which together regulate osteoclastic formation and activity. The current results are supported by a recent study that reported both TRAP staining density and osteoclastic number was not affected during endochondral ossification of TrkA-variant mouse pups, whereas bone formation was



severely impacted, which was presumably due to the lack of NGF-TrkA signalling [34]. Additionally, other studies using immunofluorescence analysis did not find TrkA on osteoclasts, nor was this receptor found on osteoclastic precursors in callus tissue during fracture healing [20, 21]. Therefore, it appears that GA may not influence remodelling of calluses via osteoclastic activity and is more likely to affect bone mass in callus through promoting osteoblastic differentiation and bone mineralization.

To determine whether GA exerted an effect on osteoblasts and mineralization, Kusa O cells, a murine, multi-potential bone marrow stromal cell line was utilised [37]. Undifferentiated Kusa O cells (day 0) do not contain mature osteoblasts and display a phenotype that is osteoprogenitor-like [38, 39]. However, by 14 days of differentiation, Kusa O cells contain many mature osteoblasts [38, 39]. In the current experiments, Western blotting analysis showed that the osteoblast-like Kusa O cells expressed TrkA receptors, but the undifferentiated Kusa O cells did not, which suggests that TrkA activation is more likely to occur in osteoblasts rather than osteoprogenitors in bone. This data is supported by previous reports using *in vivo* rodent models, which localised TrkA receptors in mature osteoblasts and not pre-osteoblasts during fracture healing [20-22] and suggests that TrkA signalling may be conducted via mature osteoblastic populations in bone. NGF does not influence proliferation of the murine osteoblastic precursor cell line, MC3T3-E1 [23], which is consistent with the present Kusa O data. Additionally, in the current experiments, GA did not influence gene expression of markers associated with early osteoblasts maturation, i.e., *Osx* and *Runx2* in Kusa O cells, however, GA did increase the gene expression of markers of mature osteoblasts namely ALP, osteocalcin, as well as osteocytic marker, DMP-1, as well as matrix mineralization [40, 41]. Again, this is consistent with earlier studies of NGF treatment in MC3T3-E1 cells that increased ALP *in vitro* [23]. Furthermore, both NGF and TrkA receptor have been localised in osteoblasts during bone healing [20-22] and NGF has been shown to be important during bone formation by directly stimulating osteoblasts to synthesize bone [17, 23, 34].

The current findings provide evidence that GA treatment stimulated osteoblastic differentiation and mineralization *in vitro* and improved fracture callus strength *in vivo*. The improvement in callus strength may have been, in part, due to the direct action of GA on osteoblasts, however, the possible direct action of GA on stimulating local nerves around the callus, cannot be dismissed, and this may have also contributed to improving fracture healing.

The present study had some limitations. Firstly, although the findings indicate that GA had mild, positive effects on fracture healing. Due to solubility issues with osmotic pump delivery, the current study was limited to use of a dosing regimen of 1 mg/kg/day. It is possible that higher doses of GA may have a more profound effect on fracture healing. Previous studies utilized doses

up to 4 mg/kg/day of GA using intraperitoneal injection [28], however osmotic pump delivery was chosen to ensure constant systemic delivery of GA. In addition, the current *in vitro* findings indicate that GA may increase osteoblastic differentiation and mineralization, however quantifications of other osteoblast-associated markers and additionally time-points of mineralization analysis in future studies are likely to provide further insights.

#### **4.5. Conclusions**

The present study showed that systemic administration of GA at 1 mg/kg/day for 14 days via mini-osmotic pumps in mice that were given fibular fractures had mild positive effects on fracture healing. GA treatment resulted in smaller fracture calluses with some enhancement of mechanical properties, without any detrimental side effects to the animals. Additionally, *in vitro* analysis implied that GA may act directly on osteoblasts to stimulate mineralization. These results complement previous research and the concept that neurotrophin signalling can influence skeletal maintenance and healing.

#### 4.6. References

1. Hak, D.J., D. Fitzpatrick, J.A. Bishop, J.L. Marsh, S. Tilp, R. Schnettler, H. Simpson, and V. Alt, *Delayed union and nonunions: epidemiology, clinical issues, and financial aspects*. Injury, 2014. **45 Suppl 2**: p. S3-7.
2. Gomez-Barrena, E., P. Rosset, D. Lozano, J. Stanovici, C. Ermthaller, and F. Gerbhard, *Bone fracture healing: cell therapy in delayed unions and nonunions*. Bone, 2015. **70**: p. 93-101.
3. Mills, L.A. and A.H. Simpson, *The relative incidence of fracture non-union in the Scottish population (5.17 million): a 5-year epidemiological study*. BMJ Open, 2013. **3**(2).
4. Zura, R., Z. Xiong, T. Einhorn, J.T. Watson, R.F. Ostrum, M.J. Prayson, G.J. Della Rocca, S. Mehta, T. McKinley, Z. Wang, and R.G. Steen, *Epidemiology of Fracture Nonunion in 18 Human Bones*. JAMA Surg, 2016. **151**(11): p. e162775.
5. Brinker, M.R. and D.P. O'Connor, *The Biological Basis for Nonunions*. JBJS Rev, 2016. **4**(6).
6. Madsen, J.E., M. Hukkanen, A.K. Aune, I. Basran, J.F. Moller, J.M. Polak, and L. Nordsletten, *Fracture healing and callus innervation after peripheral nerve resection in rats*. Clin Orthop Relat Res, 1998(351): p. 230-40.
7. Hukkanen, M., Y.T. Konttinen, S. Santavirta, L. Nordsletten, J.E. Madsen, R. Almaas, A.B. Oestreicher, T. Rootwelt, and J.M. Polak, *Effect of sciatic nerve section on neural ingrowth into the rat tibial fracture callus*. Clin Orthop Relat Res, 1995(311): p. 247-57.
8. Nordsletten, L., J.E. Madsen, R. Almaas, T. Rootwelt, J. Halse, Y.T. Konttinen, M. Hukkanen, and S. Santavirta, *The neuronal regulation of fracture healing. Effects of sciatic nerve resection in rat tibia*. Acta Orthop Scand, 1994. **65**(3): p. 299-304.
9. Hukkanen, M., Y.T. Konttinen, S. Santavirta, P. Paavolainen, X.H. Gu, G. Terenghi, and J.M. Polak, *Rapid proliferation of calcitonin gene-related peptide-immunoreactive nerves during healing of rat tibial fracture suggests neural involvement in bone growth and remodelling*. Neuroscience, 1993. **54**(4): p. 969-79.
10. Li, J., T. Ahmad, M. Spetea, M. Ahmed, and A. Kreicbergs, *Bone reinnervation after fracture: a study in the rat*. J Bone Miner Res, 2001. **16**(8): p. 1505-10.
11. Li, J., A. Kreicbergs, J. Bergstrom, A. Stark, and M. Ahmed, *Site-specific CGRP innervation coincides with bone formation during fracture healing and modeling: A study in rat angulated tibia*. J Orthop Res, 2007. **25**(9): p. 1204-12.
12. Levi-Montalcini, R. and P.U. Angeletti, *Nerve growth factor*. Physiol Rev, 1968. **48**(3): p. 534-69.
13. Micera, A., A. Lambiase, B. Stampachiachchiere, S. Bonini, and F. Levi-Schaffer, *Nerve growth factor and tissue repair remodeling: trkA(NGFR) and p75(NTR), two receptors one fate*. Cytokine Growth Factor Rev, 2007. **18**(3-4): p. 245-56.

14. Reichardt, L.F., *Neurotrophin-regulated signalling pathways*. Philos Trans R Soc Lond B Biol Sci, 2006. **361**(1473): p. 1545-64.
15. Grills, B.L., J.A. Schuijers, and A.R. Ward, *Topical application of nerve growth factor improves fracture healing in rats*. J Orthop Res, 1997. **15**(2): p. 235-42.
16. Cao, J., L. Wang, D.L. Lei, Y.P. Liu, Z.J. Du, and F.Z. Cui, *Local injection of nerve growth factor via a hydrogel enhances bone formation during mandibular distraction osteogenesis*. Oral Surg Oral Med Oral Pathol Oral Radiol, 2012. **113**(1): p. 48-53.
17. Wang, L., J. Cao, D.L. Lei, X.B. Cheng, H.Z. Zhou, R. Hou, Y.H. Zhao, and F.Z. Cui, *Application of nerve growth factor by gel increases formation of bone in mandibular distraction osteogenesis in rabbits*. Br J Oral Maxillofac Surg, 2010. **48**(7): p. 515-9.
18. Wang, L., S. Zhou, B. Liu, D. Lei, Y. Zhao, C. Lu, and A. Tan, *Locally applied nerve growth factor enhances bone consolidation in a rabbit model of mandibular distraction osteogenesis*. J Orthop Res, 2006. **24**(12): p. 2238-45.
19. Letic-Gavrilovic, A., A. Piattelli, and K. Abe, *Nerve growth factor beta(NGF beta) delivery via a collagen/hydroxyapatite (Col/HAp) composite and its effects on new bone ingrowth*. J Mater Sci Mater Med, 2003. **14**(2): p. 95-102.
20. Asaumi, K., T. Nakanishi, H. Asahara, H. Inoue, and M. Takigawa, *Expression of neurotrophins and their receptors (TRK) during fracture healing*. Bone, 2000. **26**(6): p. 625-33.
21. Grills, B.L. and J.A. Schuijers, *Immunohistochemical localization of nerve growth factor in fractured and unfractured rat bone*. Acta Orthop Scand, 1998. **69**(4): p. 415-9.
22. Aiga, A., K. Asaumi, Y.J. Lee, H. Kadota, S. Mitani, T. Ozaki, and M. Takigawa, *Expression of neurotrophins and their receptors tropomyosin-related kinases (Trk) under tension-stress during distraction osteogenesis*. Acta Med Okayama, 2006. **60**(5): p. 267-77.
23. Yada, M., K. Yamaguchi, and T. Tsuji, *NGF stimulates differentiation of osteoblastic MC3T3-E1 cells*. Biochem Biophys Res Commun, 1994. **205**(2): p. 1187-93.
24. Friden, P.M., L.R. Walus, P. Watson, S.R. Doctrow, J.W. Kozarich, C. Backman, H. Bergman, B. Hoffer, F. Bloom, and A.C. Granholm, *Blood-brain barrier penetration and in vivo activity of an NGF conjugate*. Science, 1993. **259**(5093): p. 373-7.
25. Tria, M.A., M. Fusco, G. Vantini, and R. Mariot, *Pharmacokinetics of nerve growth factor (NGF) following different routes of administration to adult rats*. Exp Neurol, 1994. **127**(2): p. 178-83.
26. Angeletti, R.H., P.U. Aneletti, and R. Levi-Montalcini, *Selective accumulation of ( 125 I) labelled nerve growth factor in sympathetic ganglia*. Brain Res, 1972. **46**: p. 421-5.

27. Jang, S.W., M. Okada, I. Sayeed, G. Xiao, D. Stein, P. Jin, and K. Ye, *Gambogic amide, a selective agonist for TrkA receptor that possesses robust neurotrophic activity, prevents neuronal cell death*. Proc Natl Acad Sci U S A, 2007. **104**(41): p. 16329-34.
28. Shen, J. and Q. Yu, *Gambogic amide selectively upregulates TrkA expression and triggers its activation*. Pharmacol Rep, 2015. **67**(2): p. 217-23.
29. Chan, C.B., X. Liu, S.W. Jang, S.I. Hsu, I. Williams, S. Kang, J. Chen, and K. Ye, *NGF inhibits human leukemia proliferation by downregulating cyclin A1 expression through promoting acinus/CtBP2 association*. Oncogene, 2009. **28**(43): p. 3825-36.
30. Shah, A.G., M.J. Friedman, S. Huang, M. Roberts, X.J. Li, and S. Li, *Transcriptional dysregulation of TrkA associates with neurodegeneration in spinocerebellar ataxia type 17*. Hum Mol Genet, 2009. **18**(21): p. 4141-52.
31. Kellum, E., H. Starr, P. Arounleut, D. Immel, S. Fulzele, K. Wenger, and M.W. Hamrick, *Myostatin (GDF-8) deficiency increases fracture callus size, Sox-5 expression, and callus bone volume*. Bone, 2009. **44**(1): p. 17-23.
32. Brady, R.D., B.L. Grills, J.A. Schuijers, A.R. Ward, B.A. Tonkin, N.C. Walsh, and S.J. McDonald, *Thymosin beta4 administration enhances fracture healing in mice*. J Orthop Res, 2014. **32**(10): p. 1277-82.
33. Castaneda-Corral, G., J.M. Jimenez-Andrade, A.P. Bloom, R.N. Taylor, W.G. Mantyh, M.J. Kaczmarska, J.R. Ghilardi, and P.W. Mantyh, *The majority of myelinated and unmyelinated sensory nerve fibers that innervate bone express the tropomyosin receptor kinase A*. Neuroscience, 2011. **178**: p. 196-207.
34. Tomlinson, R.E., Z. Li, Q. Zhang, B.C. Goh, Z. Li, D.L. Thorek, L. Rajbhandari, T.M. Brushart, L. Minichiello, F. Zhou, A. Venkatesan, and T.L. Clemens, *NGF-TrkA Signaling by Sensory Nerves Coordinates the Vascularization and Ossification of Developing Endochondral Bone*. Cell Rep, 2016. **16**(10): p. 2723-35.
35. Beamer, B., C. Hettrich, and J. Lane, *Vascular endothelial growth factor: an essential component of angiogenesis and fracture healing*. HSS J, 2010. **6**(1): p. 85-94.
36. Morgan, E.F., Z.D. Mason, K.B. Chien, A.J. Pfeiffer, G.L. Barnes, T.A. Einhorn, and L.C. Gerstenfeld, *Micro-computed tomography assessment of fracture healing: relationships among callus structure, composition, and mechanical function*. Bone, 2009. **44**(2): p. 335-44.
37. Umezawa, A., T. Maruyama, K. Segawa, R.K. Shaddock, A. Waheed, and J. Hata, *Multipotent marrow stromal cell line is able to induce hematopoiesis in vivo*. J Cell Physiol, 1992. **151**(1): p. 197-205.

38. Allan, E.H., P.W. Ho, A. Umezawa, J. Hata, F. Makishima, M.T. Gillespie, and T.J. Martin, *Differentiation potential of a mouse bone marrow stromal cell line*. J Cell Biochem, 2003. **90**(1): p. 158-69.
39. Nakamura, A., C. Ly, M. Cipetic, N.A. Sims, J. Vieuxseux, V. Kartsogiannis, S. Bouralexis, H. Saleh, H. Zhou, J.T. Price, T.J. Martin, K.W. Ng, M.T. Gillespie, and J.M. Quinn, *Osteoclast inhibitory lectin (OCIL) inhibits osteoblast differentiation and function in vitro*. Bone, 2007. **40**(2): p. 305-15.
40. Zhou, H., P. Choong, R. McCarthy, S.T. Chou, T.J. Martin, and K.W. Ng, *In situ hybridization to show sequential expression of osteoblast gene markers during bone formation in vivo*. J Bone Miner Res, 1994. **9**(9): p. 1489-99.
41. Day, T.F., X. Guo, L. Garrett-Beal, and Y. Yang, *Wnt/beta-catenin signaling in mesenchymal progenitors controls osteoblast and chondrocyte differentiation during vertebrate skeletogenesis*. Dev Cell, 2005. **8**(5): p. 739-50.

## Chapter 5.

### The effects of BDNF signalling and polymorphisms on bone.

#### A. The effects of the TrkB agonist, 7,8-dihydroxyflavone on tibial fracture healing in mice.

#### B. BDNF polymorphism in mice and their influence on bone.

Note: A large proportion of part A of this chapter has been accepted for publication. The extent of contributions for this chapter can be found in **Appendix D**.

**Johnstone M. R.**, Brady R. D., Church J. E., Orr D., McDonald S. J., Grills B. L. The TrkB agonist, 7,8-dihydroxyflavone, impairs fracture healing in mice. *J Musculoskelet Neuronal Interact*. Accepted for publication 9 November 2020.

### 5.1. Introduction

Fractures are an extremely common injury of the skeletal system, with the residual lifetime risk of a minimal trauma fracture approximately 44% for women and 25% for men over the age of 60 in Australia [1]. To date, there are very few effective non-surgical treatments to aid in the healing of fractures, and to prevent malunion and non-union of fractures, a complication that affects approximately 5-10% of patients worldwide [2, 3]. Two non-surgical approaches that are being developed to clinically enhance fracture healing are biophysical enhancement e.g. electromagnetic field stimulation, and low-intensity pulsed ultrasonography [4-7], and biological enhancement e.g. therapeutic use of vascular and osteogenic growth factors, stem-cells, and morphogenic molecules to aid bone regeneration [4, 8]. Identifying novel molecules that promote some of the key biological events of fracture healing, including angiogenesis and innervation, required for proper fracture healing, appear to have the greatest potential to improve bony repair.

Circulating neurotrophic factors are a branch of osteogenic stimulating peptides that have such potential. Neurotrophins are upregulated in a variety of repairing tissues with evidence to suggest that they have important roles during angiogenesis [9-12] and inflammation [13-16], which are two key processes in fracture healing [17]. Specifically, the neurotrophin, nerve growth factor (NGF) and signalling via its high affinity receptor, TrkA, have been shown to stimulate osteoblastic mineralization and improve mechanical properties of healing bone fractures [18-26]. Another neurotrophic factor that has recently been shown to have a role in fracture healing is brain derived neurotrophic factor (BDNF). Since its discovery in 1982, BDNF has been established as an important modulator of synaptic plasticity and pruning in the CNS via either the high affinity TrkB (pro-survival) receptor or the low affinity p75NTR (pro-apoptotic) receptor [27-30] pathways. Several studies in rodents and humans have identified high levels of BDNF and TrkB, in and around the site of fracture healing [31-33]. BDNF has shown to be synthesized and released from several non-neural cells, including leukocytes, fibroblasts, osteoblasts [33] and endothelial cells [9, 10] at

various stages of fracture healing. Through immunochemistry, both BDNF and TrkB have been detected in hematopoietic cells and platelets (both which are initially present in the hematoma at fracture sites), as well as in fibroblasts and endothelial cells, which are present during granulation tissue formation [31]. In addition to its role in the inflammatory phase of fracture healing, there is evidence to suggest that BDNF and TrkB are expressed in the early stages of soft fracture callus formation, and during endochondral ossification in fracture healing and long bone growth. Gene and protein expression of BDNF and TrkB were markedly elevated in chondrocytes and active osteoblasts in proliferating and mature zones of the endochondral ossification front in 7-week old rats [34]. Furthermore, immunostaining located BDNF in high levels in osteoblast-like cells close to the ossification front in healing mice rib calluses at 14 days post-fracture [33]. One study investigating BDNF gene expression levels during various stages of distraction osteogenesis healing in mice suggested that BDNF may continually increase during consolidation phases (similar callus composition to 28 days post-fracture) of this process [35]. BDNF gene expression was elevated in callus tissue 28 days post-osteotomy in rats, which is the transition period of cartilaginous callus being replaced by woven bone, as well as remodelling of woven bone to lamellar bone [35, 36]. Location of BDNF and TrkB in the inflammatory phase of fracture healing and soft callus stages where endochondral ossification begins, may indicate that BDNF has an important, early role in bone healing via endochondral ossification and intramembranous ossification.

One of the important processes that drives the transition of cartilage to woven bone, and remodelling of callus is re-establishment of blood vessels. BDNF has been shown both *in vitro* and *in vivo* to stimulate endothelial cell migration, proliferation and formation of new blood vessels [9, 10, 31, 37] largely by increasing the production of vascular endothelial growth factor (VEGF) [38]. Another mechanism through which BDNF may also promote fracture healing is via the up-regulation of ossification proteins ALP and BMP-2 in osteoblasts, with BDNF treatment found to upregulate both ALP and BMP-2 in cementoblasts, a tooth root enamel mineralizing cell type similar to osteoblasts [39]. *In vitro*, BDNF has been identified in osteoblastic MC3T3-E1 cells [40] however, an osteoblastic response to BDNF treatment has yet to be described in the literature. Taken together, these findings suggest that BDNF may have an active role in fracture healing, possibly by mediating angiogenesis and promoting bone formation, however, there are no studies investigating topical or systemic administration of BDNF, or activation of its receptor TrkB during fracture healing. Since BDNF can stimulate both pro-survival and pro-apoptotic pathways, it is not an appropriate choice of molecule to investigate the sole signaling pathway of BDNF and TrkB. Small novel molecules such as 7,8-dihydroxyflavone (7,8-DHF) have been identified to target and potentially activate only TrkB [41].



7,8-DHF is a flavonoid derivative that displays both antioxidant and anti-inflammatory effects [41-45] and has been shown to potently activate the TrkB receptor [41, 42, 46]. Doses of 5 mg/kg/day of 7,8-DHF strongly activated TrkB receptors in BDNF knockout mice [41]. Additionally, 7,8-DHF reduced neuronal apoptosis and inflammation in rodent models subjected to traumatic brain injury (TBI) at a dose of 5 mg/kg/day [41, 44, 46, 47]. 7,8-DHF is well tolerated in rodent models of TBI [42, 44], depression [43], Alzheimer's disease [48, 49], aging [50] and stress [51], with no detrimental effects reported in mice, however, to my knowledge, there has been no data describing the effects of 7,8-DHF on the skeletal system. Therefore, on assessing all the previous literature, it is hypothesized that 7,8-DHF treatment should have a positive effect on fracture healing. In the current experiments, effects of 7,8-DHF on the structural and biomechanical features of healing fractures in mice, murine bone growth, and osteoblastic differentiation and mineralization *in vitro* were investigated.

In addition to BDNF and its role in fracture healing, there is emerging evidence that common polymorphisms of the BDNF gene may impact bone structure. BDNF polymorphism is a single nucleotide polymorphism (SNP) in which a Valine (Val) to Methionine (Met) substitution occurs at codon 66 (Val66Met) on chromosome 11, resulting in three potential genotypes Val/Val, Val/Met, and Met/Met [52]. In Caucasian populations, it has been reported that Met/Met genotype have significantly reduced bone mineral density (BMD) compared to Val/Val and Val/Met genotypes [53]. Mechanisms on how BDNF polymorphism influences bone integrity was explored in the same study via *in vitro* experiments and showed that primary osteoblasts that were transfected with BDNF<sup>MetMet</sup>, had an overall decrease in BDNF phosphorylation and a reduced expression of osteoblastic markers; BMP-1, ALP and osteopontin [53]. These results suggest that Met substitution is detrimental to bone formation, resulting in reduced BMD. Mouse models of BDNF polymorphism; Val/Val, Val/Met, Met/Met, have been developed to study primarily neuropsychiatric disorders [54, 55], yet there is no literature to show whether bone changes reported in humans with BDNF polymorphisms can be translated into a mouse model. Thus, the second aim of this chapter was to investigate if BDNF polymorphism affect bone structure in Val66Met mouse models.

## **5.2. Materials and methods**

All experimental procedure were approved by the La Trobe Animal Ethics Committee (AEC 17-05), were within the guidelines the Australian code of practice for the care and use of animals for scientific purposes by the Australian National Health and Medical Research Council, and in compliance with the ARRIVE guidelines for how to report animal experiments.

### **5.2.1. Solubility and delivery of 7,8-DHF**

7,8-DHF was supplied by Abcam® (Abcam) and, as per manufactures instructions, was stored at 4°C until use. DMSO (100nM) or ETOH (25nM) were the recommended choice of vehicles from the manufacturer, and the vehicles used in all published studies using 7,8-DHF up to date [41-51]. However, like the other NT mimetic, GA, used in this thesis (**section 3.2.1** and **4.2.1**), 7,8-DHF would not remain in solution, and precipitated as soon as an aqueous solution was added. To overcome 7,8-DHF insolubility, Kolliphor® HS 15 was used to form a microemulsion of 7,8-DHF, which was suitable for animal treatment (please see **section 3.2.1**). 10 mg of 7,8-DHF was diluted in 10 ml of 30% Kolliphor® HS 15 in 0.1M sodium phosphate buffer [56]. Stock vials of 500 µl were stored at -20°C and thawed at RT for 1 h prior to use in mice, for the protocol please refer to **Appendix E**.

Based on previous research, a regimen of intraperitoneal injections of 5 mg/kg/day of 7,8-DHF was chosen. This regimen has been previously shown to be effective at activating TrkB receptors centrally and peripherally [42, 45, 47-49].

### **5.2.2. Experimental groups**

Eighty-four 12-week-old mice received unilateral tibial fractures and were randomly allocated to one of four experimental groups. The two main groups were 7,8-DHF-treated and vehicle-treated, and subgroups for each treatment were based on time of euthanasia, 14-, or 28-days post-fracture. Timepoints were chosen based on differences in callus composition, which can be reviewed in **section 1.2.4** '*Mechanisms of endochondral fracture repair*'.

### **5.2.3. Closed tibial fracture model**

The tibial fracture model is the most used orthopaedic fracture model in laboratory animals and has been used and published by our laboratory for several years [57-61]. This fracture featured a closed, internally fixated fracture of the right tibial mid-shaft. Buprenorphine (0.1 mg/kg) was delivered via subcutaneous injection to mice half an hour prior to surgery. Mice were anaesthetized with gaseous isoflurane, and had their right anteromedial hind limb shaved. A 5 mm incision was made in the skin superficial to the anteromedial surface of the tibia, distal to the knee joint. The periosteum was scrapped away using a size 15 surgical blade, an entry point was made using a 26-gauge hypodermic needle, and an intramedullary rod ('000' stainless steel entomology pin) was inserted down into the medullary cavity of the tibia. Using a pair of modified surgical staple removers (improvised three-point bending scissors) a non-invasive fracture was created in the middle of the tibial shaft. An X-ray of the tibia was performed to confirm fracture using DEXCOWIN® portable X-ray device (DEXCOWIN Co., Ltd. Pasadena, CA, USA). The intramedullary

rod was removed and replaced with a larger stabilizing rod ('00' stainless steel entomology pin). Another X-ray of the tibia was performed to confirm the position of the stabilizing rod and the wound was closed using 5-0 synthetic surgical suture. Mice were given a subcutaneous injection of 5 mg/kg Carprofen (RIMADYL®; Zoetis, Parsippany, NJ, USA) and placed on a veterinary heat pad for recovery.

#### **5.2.4. Regions of interest and grayscale thresholds $\mu$ CT callus reconstruction**

$\mu$ CT was performed on fractured tibial calluses as outlined in **section 2.3**. The region of interest (ROI) was identified as a 3 mm longitudinal region of callus (i.e. 1.5 mm proximal and distal to the fracture line of the callus); the border of the callus was manually traced. Thresholds used for parameter quantification were determined using the automatic "otsu" algorithm within CTAn and visual examination of unreconstructed X-ray images. A grayscale adaptive threshold of 41-255 was used for structural analysis of calluses 14-, and 28-days post-fracture. 2D and 3D data, and 3D models were generated and the following parameters were used for structural analysis of callus: total callus volume (TV); new mineralized bone tissue volume (BV), bone fractional volume (BV/TV), mean polar moment of inertia (MMI), bone surface (BS) and mean cross sectional area (T.Ar).

#### **5.2.5. Callus position during biomechanical testing**

Biomechanical testing was performed on 28-day post-fracture calluses to assess the potential effects of 7,8-DHF treatment on the biomechanical properties of bone. For biomechanical testing, outlined in **section 2.4**, each tibia was mounted onto an 8 mm stabilizing platform in a mediolateral position. A 200 N force transducer descended at a constant rate of 1.67 mm/sec and loaded each tibia. A load-displacement (x-y) graph was plotted and force (g) and deflection (mm) values were recorded.

#### **5.2.6. Histological assessment**

Please refer to **section 2.5** 'Histology' for the detailed protocols regarding bone embedding, and staining and histomorphometric analysis.

Tibial calluses were processed and embedded in LR White Resin to assess potential histological changes in callus composition between 7,8-DHF and vehicle-treated groups at 14-days post-fracture. Sections of callus were stained with either Alcian blue/alcoholic eosin to determine changes in formation of both cartilage and bone from 7,8-DHF treatment, or TRAP to predict the influence of 7,8-DHF on osteoclastic density, and therefore, bone resorption.

### 5.2.7. Cell culture

Cell culture was used to investigate the effects of 7,8-DHF on osteoblastic cell line, Kusa4b10. For these experiments, in order to gain an insight into the role BDNF has on fracture healing, the influence of 7,8-DHF on osteoblastic marker expression, as well as mineralization was investigated. Dosages of 7,8-DHF and specific primers for RT-PCR can be found below. Please refer to **section 2.6** titled 'Cell culture' for all other detailed cell culture protocols.

#### RT-PCR

Kusa4b10 cells were cultured daily in osteoblastic differentiation medium and treated with 50nM of 7,8-DHF (based on pilot research) or vehicle. The medium was replaced three times per week. Cells were isolated at three different timepoints; 3-, 7-, and 14-days. These three timepoints were chosen because they reflect three stages of Kusa4b10 cell differentiation, are similar timepoints used in the current studies investigating Kusa4b10 and were professional advised to use by colleagues at the Garvin Institute of Medical Research [62-65]. Total RNA was prepared using PureZOL™ (Bio-Rad). RT-PCR was performed as described previously in **section 2.6.5**. Glyceraldehyde 3-phosphate dehydrogenase (GAPDH) was used as an internal control gene. Specific oligonucleotide primers (**Table 5.1**) were Runx2; a marker of early osteoblasts [66], and ALP; a marker of mature osteoblasts [62].

**Table 5.1.** Oligonucleotide name and sequence (5'-3') used in Real-Time PCR.

Oligonucleotide name	Sequence (5'3')
mGAPDH	Sense - AATCTCCACTTTGCCACTG
	Anti-sense - CCTCGTCCCGTAGACAAAA
mRunx2	Sense – AGCAACAGCAACAACAGCAG
	Anti-sense – GTAATCTGACTCTGTCCTTG
mALP	Sense – AAACCCAGACACAAGCATTCC
	Anti-sense - TCCACCAGCAAGAAGCC

PCR, polymerase chain reaction; GAPDH, glyceraldehyde 3-phosphate dehydrogenase; ALP, alkaline phosphatase

#### Mineralization Analysis

For investigating the effects 7,8-DHF treatment has on osteoblastic cell mineralization, Kusa4b10 cells were treated with 0-, 10-, 50-, and 100nM of 7,8-DHF for 21 days. After 21 days, cells were stained with Alizarin red and inspected for mineralization nodules within the Kusa4b10 colonies.

### **5.2.8. Peripheral quantitative computed tomography (pQCT)**

To determine whether 7,8-DHF treatment influenced trabecular and cortical bone parameters of mice femora, bone measurements were made using pQCT (Stratec XCT-Research SA +. Stratec Research Pty. Ltd., Pforzheim, Germany) with accompanying software. Additionally, bone structural changes of murine femora between BDNF polymorphisms (Val66Met) were also investigated. pQCT calculates bone content, volumetric density and geometric measurements to distinguish between trabecular and cortical bone [67]. Additionally, cross-sectional moment of inertia (stress strain index) can be calculated using pQCT to determine bone mechanical strength [68, 69].

pQCT was performed as described by Anevskaja *et al* (2015, 2017, 2019a, 2019b) [70-73]. At autopsy, femora were stripped of muscle, fixed and then stored in bone storage buffer at 4°C until use. The left femur was chosen for pQCT analysis. On scanning, each femur was placed into a small cylindrical plastic tube (7.5 cm x 1.2 cm) and positioned into the specimen holder of the pQCT machine. Specimen alignment was made, and a low-resolution scout scan was performed. A reference line was determined as the upper border of the distal condyle of the femur. Three slices of 1 mm thickness with a voxel size of 0.1000 mm<sup>3</sup>, peel mode 20, contour mode 1, were taken at distances from the line of reference at 5%, 15% and 50% of the total femoral length. An automatic density thresholding (400 mg/cm<sup>3</sup>) was used to exclude any remaining soft tissue. Trabecular bone was identified as tissue density equal to or less than 280 mg/cm<sup>3</sup>, and cortical bone was identified as tissue density equal to or greater than 710 mg/cm<sup>3</sup>.

### **5.2.9. BDNF polymorphic (hBDNFVal66Met) mice**

Collaboration with Professor Maarten van den Buuse, and his neuroscience research team at La Trobe University allowed access to hBDNF<sup>Val66Met</sup> polymorphic mice for the current experiments. The hBDNF<sup>Val66Met</sup> mice have knock-in alleles that express human BDNF genes, replacing in part the mouse BDNF gene, but is controlled by endogenous mouse BDNF regulatory proteins [74, 75]. Professor van den Buuse's laboratory had a large colony of Val/Val, Val/Met, and Met/Met mice aged between 132-144 weeks of age, which were being used for behavioural testing, and brain tissue analysis. Permission was granted to join Professor van den Buuse's autopsy sessions and collect femora from the BDNF polymorphic mice, for pQCT analysis. Mice from which the femora were collected, were housed in groups of up to five and fed standard mouse chow. These BDNF polymorphic mice were a part of a treatment study in Professor van den Buuse's lab, so femora were only collected from vehicle-treated mice, where the vehicle was saline (injected intraperitoneally). For each mouse that was collected, pQCT was performed on left femora using the same parameters mentioned above (**section 5.2.8**).

#### **5.2.10. Statistical analysis**

All outcomes were analysed using GraphPad Prism 6 software (GraphPad Software, Inc., USA). All data was subject to Shapiro-Wilk normality tests. Biomechanical,  $\mu$ CT, histological analysis and *in vitro* mineralization assays were analysed via **Mann-Whitney U tests**. pQCT of intact femora and *in vitro* gene expression were analysed via **two-way ANOVA**. BDNF polymorphism data were analysed via **one-way ANOVA**.

### **5.3. Results**

For the duration of this work there were no overt behavioural changes or side effects, nor changes in the weight gain pattern of 7,8-DHF-treated mice (data not shown).

#### **5.3.1. 7,8-DHF reduces callus size**

Representative  $\mu$ CT reconstruction of longitudinal mid-point, hemi-calluses are shown in **Figure 5.1a-b**. Bony union was reached in all calluses by 28 days post-fracture in both the 7,8-DHF-treated and control groups. Analysis revealed the 7,8-DHF-treated group had a significant reduction in total tissue volume (**Figure 5.1c**;  $p < 0.05$ ), mean polar moment of inertia (**Figure 5.1e**;  $p < 0.01$ ) and mean cross-sectional area (**Figure 5.1f**;  $p < 0.05$ ) of callus compared to controls, which suggested a reduced callus size at 28 days post-fracture. On the contrary, there was no difference in the ratio of mineralized tissue to total tissue volume between 7,8-DHF and controls (**Figure 5.1d**), which indicated although the callus size was smaller in the 7,8-DHF group, there was equal amounts of mineralized tissue in both groups. No effects of 7,8-DHF treatment was seen at 14 days (data not shown).

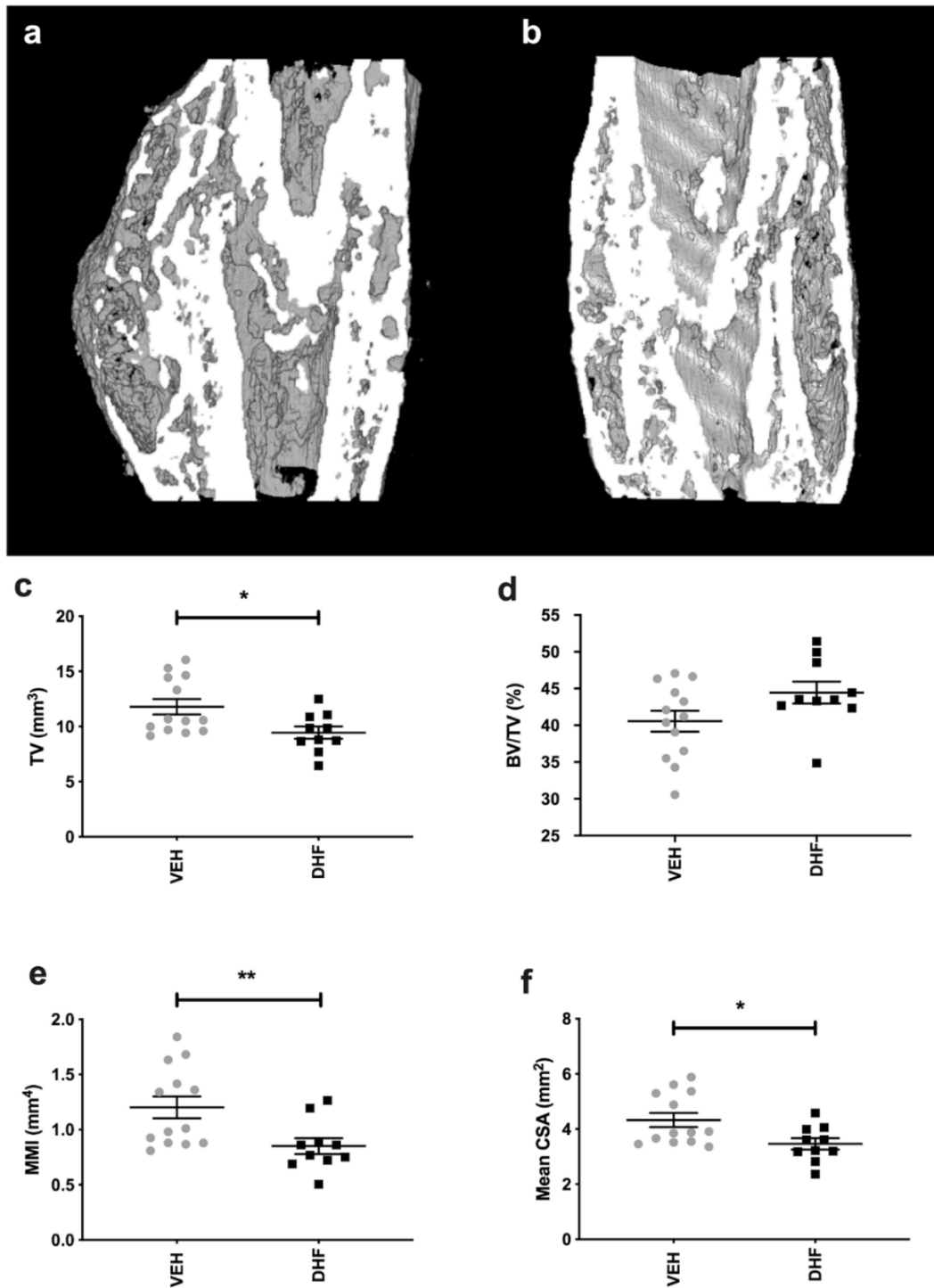


**Figure 5.1.** Effects of 7,8-DHF treatment on 28-day callus structural parameters using  $\mu$ CT. Longitudinal mid-point images representative of 300 slice reconstructed hemi-callus (a-b). 7,8-DHF treatment decreased total callus volume (TV, c;  $*p = 0.042$ ), mean polar moment of inertia (MMI, e;  $**p = 0.004$ ) and mean cross-sectional area (CSA, f;  $*p = 0.047$ ) at 28 days post-fracture compared to vehicle treatment. 7,8-DHF; 7,8-dihydroxyflavone. Bars are mean  $\pm$  SEM,  $n = 15/\text{group}$ .

### 5.3.2. 7,8-DHF reduces peak force to failure in fracture calluses

A three-point bending test was used to assess the biomechanical properties of 28-day tibial calluses. As seen in **Table 5.2.**, calluses of mice treated with 7,8-DHF following fracture had a significantly decreased peak force to failure ( $p < 0.05$ ) and increased stiffness ( $p < 0.05$ ) compared to controls. There was no significant difference in bending stress, cross-sectional area or Young's modulus between groups (**Table 5.2**).

**Table 5.2.** Mechanical properties of vehicle and 7,8-DHF-treated calluses at 28-day post-fracture.

Treatment	Peak force (N)	Stiffness ( $\times 10^4 \text{ Nm}^2$ )	CSA ( $\times 10^{-6} \text{ m}^2$ )	Bending stress ( $\times 10^6 \text{ Nm}^{-2}$ )	YM ( $\times 10^8 \text{ Nm}^{-2}$ )
Vehicle (n=12) Mean $\pm$ SEM	13.48 $\pm$ 0.84	9.38 $\pm$ 0.50	4.56 $\pm$ 0.30	3.84 $\pm$ 0.39	7.21 $\pm$ 1.18
7,8-DHF (n=10) Mean $\pm$ SEM	10.64 $\pm$ 0.51	13.01 $\pm$ 1.04	3.94 $\pm$ 0.29	3.75 $\pm$ 0.46	13.79 $\pm$ 2.96
p-value	* 0.011	*0.012	0.13	0.65	0.06

7,8-DHF; 7,8-dihydroxyflavone; CSA, cross-sectional area; YM, Young's modulus. Values are means  $\pm$  SEM. \*symbol indicates statistical significance ( $p < 0.05$ ) determined by a Mann-Whitney U tests.

### 5.3.3. 7,8-DHF treatment has no discernible effects on either callus histomorphometry or osteoclastic density in callus

Quantitative histological analysis of calluses 14-days post-fracture showed no difference in the amount of tissue area, cartilage, and fibrous tissue between 7,8-DHF and control groups.

TRAP staining of osteoclasts in calluses at 14-days post-fracture showed no difference in the percentage of staining in calluses between 7,8-DHF-treated animals and controls (data not shown).

### 5.3.4. Cell culture

#### 7,8-DHF does not alter expression of osteoblastic markers in Kusa4b10 cells

Messenger RNA levels of osteoblastic markers Runx2 and alkaline phosphatase (**Figure 5.2**) were detected by quantitative RT-PCR in Kusa4b10 cells at 3-, 7-, and 14-days of differentiation. There was no significant change in expression of Runx2 between time-points (**Figure 5.2a**). Alkaline phosphatase expression increased from 3 to 7 days and plateaued between



7- and 14-days (**Figure 5.2b**). 7,8-DHF did not influence expression of either Runx2 or alkaline phosphatase at any time-point (**Figure 5.2a-b**).

**7,8-DHF does not influence mineralization in Kusa4b10 cells**

Mineralization nodules were detected at 21 days in Kusa4b10 cells at all concentrations (0, 10, 50, 100 nm) of 7,8-DHF treatment (**Figures 5.2c-d**). There were no apparent changes in the number of nodules or mineralization between the treatment groups or controls, and there was no mineralization evident in the negative control cultures of undifferentiated Kusa4b10s.

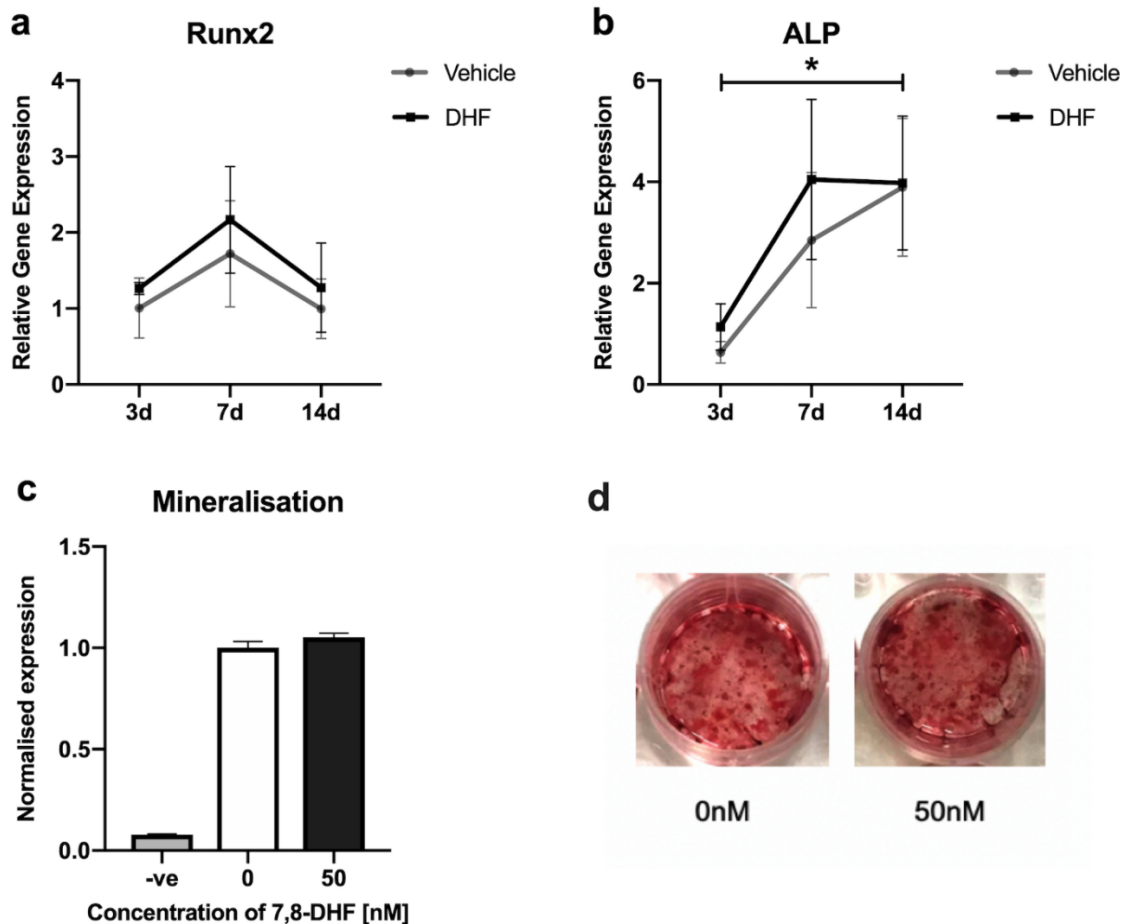


**Figure 5.2.** The effect of 7,8-DHF treatment in the osteoblastic mesenchymal cell line; Kusa4b10. Gene expression of osteoblastic markers Runx2 (**a**) and alkaline phosphatase (ALP) (**b**) were analysed at 3-, 7-, and 14-days of differentiation. There was no effect of time or 7,8-DHF on expression of Runx2 (**a**), and there was a time effect of increased alkaline phosphatase expression at 7-, and 14-days compared to 3-days, but no 7,8-DHF treatment effect (**b**;  $p < 0.04$ ). Kusa4b10 cells formed mineral at 21 days of incubation and 7,8-DHF did not increase mineralization at any dose (**c-d**). Bars are mean  $\pm$  SEM,  $n = 6$ /group.

### **5.3.5. 7,8-DHF treatment did not affect intact bone**

Femoral lengths of mice increased as they aged from 14- to 16-weeks of age (**Table 5.3**), which suggested mice were still reaching skeletal maturity at time of experimentation. There was, however, no effect of 7,8-DHF treatment on the lengths of femora when compared to controls (**Table 5.3**). Age also influenced cortical content and mineral density, periosteal and endosteal circumference, with all these parameters increasing in 16-week-old mice compared to 14-week-old mice ( $p = 0.001$ ,  $p = 0.036$ ,  $p = 0.002$ , and  $p = 0.02$ , respectively, **Table 5.3**). Age, however, did not have an impact on trabecular content or mineral density (**Table 5.3**). Treatment with 7,8-DHF did not influence any of the measured parameters measured at any timepoint (**Table 5.3**).

**Table 5.3.** pQCT measurements of intact femora of mice aged 14- and 16-weeks following 14 days of treatment with either 7,8-DHF or vehicle after a unilateral tibial fracture at 12 weeks of age.

	Controls		7,8-DHF		Two-Way ANOVA ( <i>p</i> -value)		
	14 weeks	16 weeks	14 weeks	16 weeks	Time	Treatment	Interaction
Femoral length (mm)	15.20 ± 0.12	15.75 ± 0.09	15.50 ± 0.11	15.75 ± 0.09	0.0004***	0.1566 NS	0.1547 NS
Trabecular content (mg/mm)	0.57 ± 0.03	0.65 ± 0.03	0.66 ± 0.04	0.58 ± 0.02	0.9801 NS	0.7625 NS	0/0129*
Trabecular density (mg/cm <sup>3</sup> )	310.12 ± 11.12	316.98 ± 9.01	334.02 ± 10.22	296.56 ± 6.93	0.1170 NS	0.8596 NS	0.0255*
Cortical content (mg/mm)	1.06 ± 0.02	1.15 ± 0.03	1.04 ± 0.03	1.18 ± 0.03	0.0011**	0.9384 NS	0.4903 NS
Cortical density (mg/cm <sup>3</sup> )	1099.37 ± 8.20	1109.00 ± 7.09	1096.58 ± 8.58	1119.32 ± 5.30	0.0360*	0.6186 NS	0.3870 NS
Periosteal circumference (mm)	5.16 ± 0.04	5.30 ± 0.05	5.16 ± 0.06	5.39 ± 0.06	0.0021**	0.4587 NS	0.4567 NS
Endosteal circumference (mm)	3.80 ± 0.03	3.89 ± 0.04	3.83 ± 0.06	3.98 ± 0.05	0.0196*	0.2051 NS	0.5001 NS

Data are means ± SEM; n = 11-19/group. pQCT measurements. *p* values indicate statistical significance (\**p* < 0.05, \*\* *p* < 0.01, \*\*\**p* < 0.001) determined by a two-way ANOVA for differences between time (14- and 16-weeks) and treatment (7,8-DHF or vehicle). NS, Not Significant. pQCT, peripheral quantitative computed tomography; 7,8-DHF, 7,8-dihydroxyflavone.

### 5.3.6. hBDNF<sup>Val66Met</sup> polymorphism does not influence bone

Femora from hBDNF<sup>Val66Met</sup> polymorphic male mice were scanned by pQCT, for possible differences femoral length, trabecular and cortical bone measurements (**Table 5.4**). There were no significant differences in any measured bone parameter; femoral length, trabecular content, trabecular density, cortical content, cortical density, periosteal circumference, and endosteal circumference between hBDNF<sup>MetMet</sup>, hBDNF<sup>ValMet</sup>, hBDNF<sup>ValVal</sup> polymorphic mice (**Table 5.4**).

**Table 5.4.** pQCT measurements of hBDNF<sup>Val66Met</sup> polymorphic mice.

	hBDNF <sup>MetMet</sup>	hBDNF <sup>ValMet</sup>	hBDNF <sup>ValVal</sup>	One-way ANOVA
Femoral length (mm)	15.90 ± 0.16	15.40 ± 0.08	15.30 ± 0.12	0.5451 NS
Trabecular content (mg/mm)	3.027 ± 0.14	2.93 ± 0.23	2.72 ± 0.18	0.5873 NS
Trabecular density (mg/cm <sup>3</sup> )	474.60 ± 21.13	439.00 ± 27.50	400.90 ± 27.48	0.7024 NS
Cortical content (mg/mm)	1.38 ± 0.08	1.25 ± 0.05	1.29 ± 1.52	0.7379 NS
Cortical density (mg/cm <sup>3</sup> )	1171.00 ± 12.68	1143.00 ± 9.47	1139.00 ± 14.58	0.1786 NS
Periosteal circumference (mm)	5.43 ± 0.11	5.43 ± 0.08	5.47 ± 0.13	0.9429 NS
Endosteal circumference (mm)	3.84 ± 0.07	3.97 ± 0.07	3.98 ± 0.08	0.3951 NS

Data are means ± SEM; n = 7-9/group. pQCT measurements. p values indicate statistical significance (p < 0.05) determined by a one-way ANOVA for differences between BDNF polymorphism variants. NS, Not Significant.

#### 5.4. Discussion

Although BDNF and its TrkB receptor have been localized in healing fractures of mice, rats, and humans, the role of TrkB signaling in fracture healing is not well understood. The first aim was to determine if TrkB agonism using the flavonoid, 7,8-DHF, would have positive effects on fracture healing, measured by structural and biomechanical analysis. In the current experiments, systemic administration of 5 mg/kg/day of 7,8-DHF for 14 days in mice with healing tibial fracture, resulted in mechanically weaker calluses with reduced bone and tissue volume at 28 days of healing. Furthermore, the effects of 7,8-DHF *in vitro*, on an osteogenic cell line, Kusa4b10, were also investigated and it was shown that 7,8-DHF had no effect on either osteoblastic differentiation or mineralization. Together, these data show that fracture healing was impaired by 7,8-DHF however, it is unclear how 7,8-DHF impaired fracture healing.

$\mu$ CT was used to investigate the influence of 7,8-DHF on the bone and callus content at architecturally different stages of fracture healing. At the two timepoints analysed, 14- and 28-days, all significant differences between vehicle- and 7,8-DHF-treated animals were found at 28-days post-fracture. Calluses in 7,8-DHF-treated animals had overall reduced tissue volume, mean cross-sectional area, and decreased mean polar moment of inertia; a measurement of inherent rotational stiffness of bone [76] compared to controls. Furthermore, the same 28-day calluses underwent biomechanical assessment via three-point bending test, to which peak-force to failure was significantly reduced in the 7,8-DHF-treated mice compared to controls. Considered together, these findings indicate that 7,8-DHF negatively impacted upon the remodelling of healing fractures. Interestingly, the present findings are dissimilar to a study that investigated BDNF-functionalized cement treatment during femoral fracture healing in mice, which found BDNF treatment was beneficial in fracture healing [77].

Histomorphometric analysis of femoral fractures in their study found that BDNF, significantly increased newly formed bone at the implant interface between cement and fracture, compared to controls at 35 days post fracture [77]. Although, histomorphometric analysis at 28 days post-fracture was not undertaken, the 28-day calluses in the 7,8-DHF-treated group were mechanically weaker, which suggests a reduction in newly formed bone content compared to controls [78]. A difference between the studies that may explain why there were opposing outcomes of TrkB activation during fracture healing, is that in the current study, 7,8-DHF was used and this compound has been shown to readily cross the blood brain barrier (BBB) upon systemic administration [42, 48-51], whereas Kauschke and colleagues (2018), used exogenous BDNF, which is unable to cross the blood brain barrier (BBB) when administered peripherally [79]. Thus, it is proposed that 7,8-DHF's action on central TrkB receptors in the brain, overrode possible positive peripheral effects on bone to negatively impact on fracture healing. Due to these

contradictory results, it is proposed that BDNF, has opposite central and peripheral effects on bone, which are like those described for the hormone leptin [80, 81]. Supporting this proposal that 7,8-DHF may have acted centrally to negatively impact on bone, is a definitive study that investigated the selective deletion of BDNF in brains of mice and its effect on bone phenotype [82]. In centrally-deleted BDNF mice, there was an increase in femoral lengths, and an overall increase in bone mineral density (BMD) compared to wild-type mice [82]. Therefore, it is proposed that in the current experiments, central activation of TrkB, via 7,8-DHF, negatively impacted on bone metabolism, which resulted in smaller fracture calluses and weaker fracture sites.

Additionally, in the present study, an *in vitro* model using Kusa4b10 osteoprogenitor cells was used to determine the effects of 7,8-DHF on osteoblasts and bone mineralization. Kusa4b10 cells are a more osteogenic sub-clone of murine multipotential bone marrow stromal cell line, Kusa O [62]. Like Kusa O cells at day 0, Kusa4b10 resemble an osteoprogenitor phenotype and by day 14 resemble a mature osteoblastic phenotype [62]. Our laboratory has previously localized TrkB receptors on parent line Kusa O, at day 14 of differentiation via Western blot (unpublished data). Likewise, TrkB receptors have also been localised in a murine osteoblastic precursor cell line, MC3T3-E1 [40], which suggests a possible role for TrkB agonists on bone metabolism. This data is additionally supported in *in vivo* rodent models and human fracture healing, which have localised TrkB receptors on chondrocytes and osteoblasts during bone growth and fracture healing [31, 34]. In the current study, it was found that 3-, 7-, or 14-days of 7,8-DHF treatment to Kusa4b10 cells did not alter gene expression of Runx2 and ALP, which are two markers osteoblastic differentiation. The current findings are similar to a study that showed that BDNF administration did not alter ALP gene expression in MC3T3-E1 after 5 days of treatment [36]. However, in the same study, MC3TC-E1 had increased mineralization following BDNF treatment [36], whereas in the current study 7,8-DHF did not increase mineralization of Kusa4b10 cells at 21 days differentiation. Lack of difference in mineralization between the current experiments and those of the MC3T3-E1 study may be a result of either the use of different osteoprogenitor cell lines or the timepoints that were analysed for mineralization. At 21 days, there was dense mineralization seen in both controls and treated Kusa4b10. Had mineralization been analysed at an earlier timepoint, such as when the cells were just starting to form mineral, then there may have been a difference between the two groups.

pQCT analysis was used to determine the effects 2 weeks of 7,8-DHF treatment had on bone remodelling in intact femora of the same mice that received tibial fractures. Femoral lengths of mice aged 16 weeks were significantly longer than mice aged 14 weeks, which indicated that mice were still growing. Increased femoral lengths of mice 16-week-old mice compared to 14-week-old mice was an anticipated result, as C57BL/6 male mice can take up to 42 weeks to reach

skeletal maturity [83]. Similarly, other measured bone parameters, such as cortical content, mineral density, endosteal circumference, and periosteal circumference were all increased in 16-week-old mice compared to 14-week-old mice, which also indicated that mice were still growing. Compared to previous research that analysed 16-week-old male C57BL/6 mice by pQCT, the mice in the current study had smaller mean femoral measurements [84], which could potentially be due to reduced weight-bearing on fractured hind-limbs. Two-week treatment with 7,8-DHF did not show any differences in bone measurements at either time-point, i.e. 14- and 16-weeks of age, when compared to controls. The lack of differences in bone measurements seen in femora between control and 7,8-DHF-treated mice could be due to a combination of factors, which include, an insufficient length of time of treatment and/or sex differences of mice. Although there is no current research that demonstrates the effects of 7,8-DHF on bone metabolism, there has been a study published that showed that BDNF is sex-dependent in terms of its effects on the skeleton, with female mice being more affected than male mice when central BDNF is depleted [82]. Complete central deletion of BDNF minimally increased BMD in male mice, compared to vastly increased BMD in female mice [82]. Therefore, in the present study, it was reasonable to see no effects to BMD when treating wild-type male mice for two weeks with a suspected centrally acting BDNF agonist.

In part B of the present study, the role of BDNF polymorphism,  $BDNF^{Val66Met}$ , on bone metabolism in a mouse knock-in model  $hBDNF^{Val66Met}$  was investigated, with no changes in the amount of cortical or trabecular content between polymorphic variants found. There is a small body of literature highlighting differences in BMD in humans with BDNF Val66Met polymorphisms; Val/Val, Val/Met, and Met/Met [53]. Deng and colleagues (2013), showed that Caucasian populations with Met/Met polymorphism had significantly reduced BMD compared to Val/Val and Val/Met variations. However, in the current experiments, femora of mice with the same BDNF polymorphic variations,  $hBDNF^{Val66Met}$ , had no differences in amount or thickness of trabecular and cortical bone. The same researchers that published BMD variations in Caucasians, also investigated Asian populations with BDNF polymorphisms and found no difference in BMD across the three polymorphic variations [53]. Deng and colleagues' paper was not the first publication describing discrepancies of BDNF Val66Met polymorphisms among different ethnic groups. It has recently been reported that non-genetic factors including age, sex, and environment all contribute to phenotypic and neuropsychiatric variances [74]. Together, these findings suggest this  $hBDNF^{Val66Met}$  animal model, may not reflect the variable BMD phenotype seen in  $BDNF^{Val66Met}$  mutations in differing ethnic groups. Alternatively, there is the possibility that the studies were underpowered to detect differences between genotypes in the present studies.

In summary, 5 mg/kg/day of 7,8-DHF treatment to mice with tibial fractures resulted in structurally smaller calluses and mechanically weaker fracture sites. It is proposed that 7,8-DHF acted centrally on TrkB receptors in the brain to negatively impact bone remodelling. Additionally, mice with BDNF polymorphisms were investigated for changes in bone mineral density. No changes were found in trabecular or cortical bone content of these mice with BDNF polymorphisms. The present findings suggest that BDNF has a role in bone remodelling, and it is proposed that there may be two opposing outcomes on bone remodelling depending if TrkB signalling pathways are activated in the central or peripheral nervous systems.



## 5.5. References

1. Nguyen, N.D., H.G. Ahlborg, J.R. Center, J.A. Eisman, and T.V. Nguyen, *Residual lifetime risk of fractures in women and men*. J Bone Miner Res, 2007. **22**(6): p. 781-8.
2. Mills, L.A. and A.H. Simpson, *The relative incidence of fracture non-union in the Scottish population (5.17 million): a 5-year epidemiological study*. BMJ Open, 2013. **3**(2).
3. Zura, R., Z. Xiong, T. Einhorn, J.T. Watson, R.F. Ostrum, M.J. Prayson, G.J. Della Rocca, S. Mehta, T. McKinley, Z. Wang, and R.G. Steen, *Epidemiology of Fracture Nonunion in 18 Human Bones*. JAMA Surg, 2016. **151**(11): p. e162775.
4. Einhorn, T.A. and L.C. Gerstenfeld, *Fracture healing: mechanisms and interventions*. Nat Rev Rheumatol, 2015. **11**(1): p. 45-54.
5. Warden, S.J., K.L. Bennell, J.M. McMeeken, and J.D. Wark, *Acceleration of fresh fracture repair using the sonic accelerated fracture healing system (SAFHS): a review*. Calcif Tissue Int, 2000. **66**(2): p. 157-63.
6. Pounder, N.M. and A.J. Harrison, *Low intensity pulsed ultrasound for fracture healing: a review of the clinical evidence and the associated biological mechanism of action*. Ultrasonics, 2008. **48**(4): p. 330-8.
7. Leighton, R., J.T. Watson, P. Giannoudis, C. Papakostidis, A. Harrison, and R.G. Steen, *Healing of fracture nonunions treated with low-intensity pulsed ultrasound (LIPUS): A systematic review and meta-analysis*. Injury, 2017. **48**(7): p. 1339-1347.
8. Ghiasi, M.S., J. Chen, A. Vaziri, E.K. Rodriguez, and A. Nazarian, *Bone fracture healing in mechanobiological modeling: A review of principles and methods*. Bone Rep, 2017. **6**: p. 87-100.
9. Kermani, P. and B. Hempstead, *Brain-derived neurotrophic factor: a newly described mediator of angiogenesis*. Trends Cardiovasc Med, 2007. **17**(4): p. 140-3.
10. Kermani, P., D. Rafii, D.K. Jin, P. Whitlock, W. Schaffer, A. Chiang, L. Vincent, M. Friedrich, K. Shido, N.R. Hackett, R.G. Crystal, S. Rafii, and B.L. Hempstead, *Neurotrophins promote revascularization by local recruitment of TrkB+ endothelial cells and systemic mobilization of hematopoietic progenitors*. J Clin Invest, 2005. **115**(3): p. 653-63.
11. Raychaudhuri, S.K., S.P. Raychaudhuri, H. Weltman, and E.M. Farber, *Effect of nerve growth factor on endothelial cell biology: proliferation and adherence molecule expression on human dermal microvascular endothelial cells*. Arch Dermatol Res, 2001. **293**(6): p. 291-5.
12. Emanuelli, C., M.B. Salis, A. Pinna, G. Graiani, L. Manni, and P. Madeddu, *Nerve growth factor promotes angiogenesis and arteriogenesis in ischemic hindlimbs*. Circulation, 2002. **106**(17): p. 2257-62.

13. Micera, A., A. Lambiase, B. Stampacchiacchiere, S. Bonini, and F. Levi-Schaffer, *Nerve growth factor and tissue repair remodeling: trkA(NGFR) and p75(NTR), two receptors one fate*. Cytokine Growth Factor Rev, 2007. **18**(3-4): p. 245-56.
14. Werner, S. and R. Grose, *Regulation of wound healing by growth factors and cytokines*. Physiol Rev, 2003. **83**(3): p. 835-70.
15. Scuri, M., L. Samsell, and G. Piedimonte, *The role of neurotrophins in inflammation and allergy*. Inflamm Allergy Drug Targets, 2010. **9**(3): p. 173-80.
16. Calabrese, F., A.C. Rossetti, G. Racagni, P. Gass, M.A. Riva, and R. Molteni, *Brain-derived neurotrophic factor: a bridge between inflammation and neuroplasticity*. Front Cell Neurosci, 2014. **8**: p. 430.
17. Beamer, B., C. Hettrich, and J. Lane, *Vascular endothelial growth factor: an essential component of angiogenesis and fracture healing*. HSS J, 2010. **6**(1): p. 85-94.
18. Johnstone, M.R., M. Sun, C.J. Taylor, R.D. Brady, B.L. Grills, J.E. Church, S.R. Shultz, and S.J. McDonald, *Gambogic amide, a selective TrkA agonist, does not improve outcomes from traumatic brain injury in mice*. Brain Inj, 2018. **32**(2): p. 257-268.
19. Grills, B.L., J.A. Schuijers, and A.R. Ward, *Topical application of nerve growth factor improves fracture healing in rats*. J Orthop Res, 1997. **15**(2): p. 235-42.
20. Arany, S., S. Koyota, and T. Sugiyama, *Nerve growth factor promotes differentiation of odontoblast-like cells*. J Cell Biochem, 2009. **106**(4): p. 539-45.
21. Cao, J., L. Wang, D.L. Lei, Y.P. Liu, Z.J. Du, and F.Z. Cui, *Local injection of nerve growth factor via a hydrogel enhances bone formation during mandibular distraction osteogenesis*. Oral Surg Oral Med Oral Pathol Oral Radiol, 2012. **113**(1): p. 48-53.
22. Wang, L., J. Cao, D.L. Lei, X.B. Cheng, Y.W. Yang, R. Hou, Y.H. Zhao, and F.Z. Cui, *Effects of nerve growth factor delivery via a gel to inferior alveolar nerve in mandibular distraction osteogenesis*. J Craniofac Surg, 2009. **20**(6): p. 2188-92.
23. Wang, L., J. Cao, D.L. Lei, X.B. Cheng, H.Z. Zhou, R. Hou, Y.H. Zhao, and F.Z. Cui, *Application of nerve growth factor by gel increases formation of bone in mandibular distraction osteogenesis in rabbits*. Br J Oral Maxillofac Surg, 2010. **48**(7): p. 515-9.
24. Wang, L., Y. Zhao, X. Cheng, Y. Yang, G. Liu, Q. Ma, H. Shang, L. Tian, and D. Lei, *Effects of locally applied nerve growth factor to the inferior alveolar nerve histology in a rabbit model of mandibular distraction osteogenesis*. Int J Oral Maxillofac Surg, 2009. **38**(1): p. 64-9.
25. Wang, L., S. Zhou, B. Liu, D. Lei, Y. Zhao, C. Lu, and A. Tan, *Locally applied nerve growth factor enhances bone consolidation in a rabbit model of mandibular distraction osteogenesis*. J Orthop Res, 2006. **24**(12): p. 2238-45.
26. Yada, M., K. Yamaguchi, and T. Tsuji, *NGF stimulates differentiation of osteoblastic MC3T3-E1 cells*. Biochem Biophys Res Commun, 1994. **205**(2): p. 1187-93.

27. Huang, E.J. and L.F. Reichardt, *Neurotrophins: roles in neuronal development and function*. Annu Rev Neurosci, 2001. **24**: p. 677-736.
28. Reichardt, L.F., *Neurotrophin-regulated signalling pathways*. Philos Trans R Soc Lond B Biol Sci, 2006. **361**(1473): p. 1545-64.
29. Bothwell, M., *Functional interactions of neurotrophins and neurotrophin receptors*. Annu Rev Neurosci, 1995. **18**: p. 223-53.
30. Barbacid, M., *The Trk family of neurotrophin receptors*. J Neurobiol, 1994. **25**(11): p. 1386-403.
31. Kilian, O., S. Hartmann, N. Dongowski, S. Karnati, E. Baumgart-Vogt, F.V. Hartel, T. Noll, R. Schnettler, and K.S. Lips, *BDNF and its TrkB receptor in human fracture healing*. Ann Anat, 2014. **196**(5): p. 286-95.
32. Ebadi, M., R.M. Bashir, M.L. Heidrick, F.M. Hamada, H.E. Refaey, A. Hamed, G. Helal, M.D. Baxi, D.R. Cerutis, and N.K. Lassi, *Neurotrophins and their receptors in nerve injury and repair*. Neurochem Int, 1997. **30**(4-5): p. 347-74.
33. Asaumi, K., T. Nakanishi, H. Asahara, H. Inoue, and M. Takigawa, *Expression of neurotrophins and their receptors (TRK) during fracture healing*. Bone, 2000. **26**(6): p. 625-33.
34. Yamashiro, T., T. Fukunaga, K. Yamashita, N. Kobashi, and T. Takano-Yamamoto, *Gene and protein expression of brain-derived neurotrophic factor and TrkB in bone and cartilage*. Bone, 2001. **28**(4): p. 404-9.
35. Aiga, A., K. Asaumi, Y.J. Lee, H. Kadota, S. Mitani, T. Ozaki, and M. Takigawa, *Expression of neurotrophins and their receptors tropomyosin-related kinases (Trk) under tension-stress during distraction osteogenesis*. Acta Med Okayama, 2006. **60**(5): p. 267-77.
36. Ida-Yonemochi, H., Y. Yamada, H. Yoshikawa, and K. Seo, *Locally Produced BDNF Promotes Sclerotic Change in Alveolar Bone after Nerve Injury*. PLoS One, 2017. **12**(1): p. e0169201.
37. Matsuda, S., T. Fujita, M. Kajiya, K. Takeda, H. Shiba, H. Kawaguchi, and H. Kurihara, *Brain-derived neurotrophic factor induces migration of endothelial cells through a TrkB-ERK-integrin alphaVbeta3-FAK cascade*. J Cell Physiol, 2012. **227**(5): p. 2123-9.
38. Lin, C.Y., S.Y. Hung, H.T. Chen, H.K. Tsou, Y.C. Fong, S.W. Wang, and C.H. Tang, *Brain-derived neurotrophic factor increases vascular endothelial growth factor expression and enhances angiogenesis in human chondrosarcoma cells*. Biochem Pharmacol, 2014. **91**(4): p. 522-33.
39. Kajiya, M., H. Shiba, T. Fujita, K. Ouhara, K. Takeda, N. Mizuno, H. Kawaguchi, M. Kitagawa, T. Takata, K. Tsuji, and H. Kurihara, *Brain-derived neurotrophic factor stimulates bone/cementum-related protein gene expression in cementoblasts*. J Biol Chem, 2008. **283**(23): p. 16259-67.

40. Nakanishi, T., K. Takahashi, C. Aoki, K. Nishikawa, T. Hattori, and S. Taniguchi, *Expression of nerve growth factor family neurotrophins in a mouse osteoblastic cell line*. *Biochem Biophys Res Commun*, 1994. **198**(3): p. 891-7.
41. Jang, S.W., X. Liu, M. Yepes, K.R. Shepherd, G.W. Miller, Y. Liu, W.D. Wilson, G. Xiao, B. Bianchi, Y.E. Sun, and K. Ye, *A selective TrkB agonist with potent neurotrophic activities by 7,8-dihydroxyflavone*. *Proc Natl Acad Sci U S A*, 2010. **107**(6): p. 2687-92.
42. Agrawal, R., E. Noble, E. Tyagi, Y. Zhuang, Z. Ying, and F. Gomez-Pinilla, *Flavonoid derivative 7,8-DHF attenuates TBI pathology via TrkB activation*. *Biochim Biophys Acta*, 2015. **1852**(5): p. 862-72.
43. Liu, X., C.B. Chan, S.W. Jang, S. Pradoldej, J. Huang, K. He, L.H. Phun, S. France, G. Xiao, Y. Jia, H.R. Luo, and K. Ye, *A synthetic 7,8-dihydroxyflavone derivative promotes neurogenesis and exhibits potent antidepressant effect*. *J Med Chem*, 2010. **53**(23): p. 8274-86.
44. Zhao, S., X. Gao, W. Dong, and J. Chen, *The Role of 7,8-Dihydroxyflavone in Preventing Dendrite Degeneration in Cortex After Moderate Traumatic Brain Injury*. *Mol Neurobiol*, 2016. **53**(3): p. 1884-95.
45. Zhao, S., A. Yu, X. Wang, X. Gao, and J. Chen, *Post-Injury Treatment of 7,8-Dihydroxyflavone Promotes Neurogenesis in the Hippocampus of the Adult Mouse*. *J Neurotrauma*, 2016. **33**(22): p. 2055-2064.
46. Gupta, V.K., Y. You, J.C. Li, A. Klistorner, and S.L. Graham, *Protective effects of 7,8-dihydroxyflavone on retinal ganglion and RGC-5 cells against excitotoxic and oxidative stress*. *J Mol Neurosci*, 2013. **49**(1): p. 96-104.
47. Chen, L., X. Gao, S. Zhao, W. Hu, and J. Chen, *The Small-Molecule TrkB Agonist 7, 8-Dihydroxyflavone Decreases Hippocampal Newborn Neuron Death After Traumatic Brain Injury*. *J Neuropathol Exp Neurol*, 2015. **74**(6): p. 557-67.
48. Devi, L. and M. Ohno, *7,8-dihydroxyflavone, a small-molecule TrkB agonist, reverses memory deficits and BACE1 elevation in a mouse model of Alzheimer's disease*. *Neuropsychopharmacology*, 2012. **37**(2): p. 434-44.
49. Castello, N.A., M.H. Nguyen, J.D. Tran, D. Cheng, K.N. Green, and F.M. LaFerla, *7,8-Dihydroxyflavone, a small molecule TrkB agonist, improves spatial memory and increases thin spine density in a mouse model of Alzheimer disease-like neuronal loss*. *PLoS One*, 2014. **9**(3): p. e91453.
50. Zeng, Y., Y. Liu, M. Wu, J. Liu, and Q. Hu, *Activation of TrkB by 7,8-dihydroxyflavone prevents fear memory defects and facilitates amygdalar synaptic plasticity in aging*. *J Alzheimers Dis*, 2012. **31**(4): p. 765-78.

51. Andero, R., N. Daviu, R.M. Escorihuela, R. Nadal, and A. Armario, *7,8-dihydroxyflavone, a TrkB receptor agonist, blocks long-term spatial memory impairment caused by immobilization stress in rats*. Hippocampus, 2012. **22**(3): p. 399-408.
52. Riemenschneider, M., S. Schwarz, S. Wagenpfeil, J. Diehl, U. Muller, H. Forstl, and A. Kurz, *A polymorphism of the brain-derived neurotrophic factor (BDNF) is associated with Alzheimer's disease in patients lacking the Apolipoprotein E epsilon4 allele*. Mol Psychiatry, 2002. **7**(7): p. 782-5.
53. Deng, F.Y., L.J. Tan, H. Shen, Y.J. Liu, Y.Z. Liu, J. Li, X.Z. Zhu, X.D. Chen, Q. Tian, M. Zhao, and H.W. Deng, *SNP rs6265 regulates protein phosphorylation and osteoblast differentiation and influences BMD in humans*. J Bone Miner Res, 2013. **28**(12): p. 2498-507.
54. Soliman, F., C.E. Glatt, K.G. Bath, L. Levita, R.M. Jones, S.S. Pattwell, D. Jing, N. Tottenham, D. Amso, L.H. Somerville, H.U. Voss, G. Glover, D.J. Ballon, C. Liston, T. Teslovich, T. Van Kempen, F.S. Lee, and B.J. Casey, *A genetic variant BDNF polymorphism alters extinction learning in both mouse and human*. Science, 2010. **327**(5967): p. 863-6.
55. Notaras, M., R. Hill, and M. van den Buuse, *A role for the BDNF gene Val66Met polymorphism in schizophrenia? A comprehensive review*. Neurosci Biobehav Rev, 2015. **51**: p. 15-30.
56. Scheller, K.J., S.J. Williams, A.J. Lawrence, B. Jarrott, and E. Djouma, *An improved method to prepare an injectable microemulsion of the galanin-receptor 3 selective antagonist, SNAP 37889, using Kolliphor((R)) HS 15*. MethodsX, 2014. **1**: p. 212-6.
57. Brady, R.D., B.L. Grills, J.E. Church, N.C. Walsh, A.C. McDonald, D.V. Agoston, M. Sun, T.J. O'Brien, S.R. Shultz, and S.J. McDonald, *Closed head experimental traumatic brain injury increases size and bone volume of callus in mice with concomitant tibial fracture*. Sci Rep, 2016. **6**: p. 34491.
58. Shultz, S.R., M. Sun, D.K. Wright, R.D. Brady, S. Liu, S. Beynon, S.F. Schmidt, A.H. Kaye, J.A. Hamilton, T.J. O'Brien, B.L. Grills, and S.J. McDonald, *Tibial fracture exacerbates traumatic brain injury outcomes and neuroinflammation in a novel mouse model of multitrauma*. J Cereb Blood Flow Metab, 2015. **35**(8): p. 1339-47.
59. Brady, R.D., B.L. Grills, T. Romano, J.D. Wark, T.J. O'Brien, S.R. Shultz, and S.J. McDonald, *Sodium selenate treatment mitigates reduction of bone volume following traumatic brain injury in rats*. J Musculoskelet Neuronal Interact, 2016. **16**(4): p. 369-376.
60. Brady, R.D., S.R. Shultz, M. Sun, T. Romano, C. van der Poel, D.K. Wright, J.D. Wark, T.J. O'Brien, B.L. Grills, and S.J. McDonald, *Experimental Traumatic Brain Injury Induces Bone Loss in Rats*. J Neurotrauma, 2016. **33**(23): p. 2154-2160.

61. Sun, M., R.D. Brady, D.K. Wright, H.A. Kim, S.R. Zhang, C.G. Sobey, M.R. Johnstone, T.J. O'Brien, B.D. Semple, S.J. McDonald, and S.R. Shultz, *Treatment with an interleukin-1 receptor antagonist mitigates neuroinflammation and brain damage after polytrauma*. *Brain Behav Immun*, 2017. **66**: p. 359-371.
62. Allan, E.H., P.W. Ho, A. Umezawa, J. Hata, F. Makishima, M.T. Gillespie, and T.J. Martin, *Differentiation potential of a mouse bone marrow stromal cell line*. *J Cell Biochem*, 2003. **90**(1): p. 158-69.
63. Allan, E.H., K.D. Hausler, T. Wei, J.H. Gooi, J.M. Quinn, B. Crimeen-Irwin, S. Pompolo, N.A. Sims, M.T. Gillespie, J.E. Onyia, and T.J. Martin, *EphrinB2 regulation by PTH and PTHrP revealed by molecular profiling in differentiating osteoblasts*. *J Bone Miner Res*, 2008. **23**(8): p. 1170-81.
64. Onan, D., E.H. Allan, J.M. Quinn, J.H. Gooi, S. Pompolo, N.A. Sims, M.T. Gillespie, and T.J. Martin, *The chemokine Cxcl1 is a novel target gene of parathyroid hormone (PTH)/PTH-related protein in committed osteoblasts*. *Endocrinology*, 2009. **150**(5): p. 2244-53.
65. Quach, J.M., E.C. Walker, E. Allan, M. Solano, A. Yokoyama, S. Kato, N.A. Sims, M.T. Gillespie, and T.J. Martin, *Zinc finger protein 467 is a novel regulator of osteoblast and adipocyte commitment*. *J Biol Chem*, 2011. **286**(6): p. 4186-98.
66. Nakashima, K., X. Zhou, G. Kunkel, Z. Zhang, J.M. Deng, R.R. Behringer, and B. de Crombrughe, *The novel zinc finger-containing transcription factor osterix is required for osteoblast differentiation and bone formation*. *Cell*, 2002. **108**(1): p. 17-29.
67. Ito, M., K. Tsurusaki, and K. Hayashi, *Peripheral QCT for the diagnosis of osteoporosis*. *Osteoporos Int*, 1997. **7 Suppl 3**: p. S120-7.
68. Ferretti, J.L., R.F. Capozza, and J.R. Zanchetta, *Mechanical validation of a tomographic (pQCT) index for noninvasive estimation of rat femur bending strength*. *Bone*, 1996. **18**(2): p. 97-102.
69. Bagi, C.M., N. Hanson, C. Andresen, R. Pero, R. Lariviere, C.H. Turner, and A. Laib, *The use of micro-CT to evaluate cortical bone geometry and strength in nude rats: correlation with mechanical testing, pQCT and DXA*. *Bone*, 2006. **38**(1): p. 136-44.
70. Anevskaa, K., J.N. Cheong, J.D. Wark, M.E. Wlodek, and T. Romano, *Maternal stress does not exacerbate long-term bone deficits in female rats born growth restricted, with differential effects on offspring bone health*. *Am J Physiol Regul Integr Comp Physiol*, 2018. **314**(2): p. R161-R170.
71. Anevskaa, K., L.A. Gallo, M. Tran, A.J. Jefferies, J.D. Wark, M.E. Wlodek, and T. Romano, *Pregnant growth restricted female rats have bone gains during late gestation which contributes to second generation adolescent and adult offspring having normal bone health*. *Bone*, 2015. **74**: p. 199-207.

72. Anevskaja, K., D. Mahizir, J.F. Briffa, A.J. Jefferies, J.D. Wark, B.L. Grills, R.D. Brady, S.J. McDonald, M.E. Wlodek, and T. Romano, *Treadmill Exercise before and during Pregnancy Improves Bone Deficits in Pregnant Growth Restricted Rats without the Exacerbated Effects of High Fat Diet*. *Nutrients*, 2019. **11**(6).
73. Anevskaja, K., J.D. Wark, M.E. Wlodek, and T. Romano, *The transgenerational effect of maternal and paternal F1 low birth weight on bone health of second and third generation offspring*. *J Dev Orig Health Dis*, 2019. **10**(2): p. 144-153.
74. Tsai, S.J., *Critical Issues in BDNF Val66Met Genetic Studies of Neuropsychiatric Disorders*. *Front Mol Neurosci*, 2018. **11**: p. 156.
75. van den Buuse, M., J.J.W. Lee, and E.J. Jaehne, *Interaction of Brain-Derived Neurotrophic Factor Val66Met genotype and history of stress in regulation of prepulse inhibition in mice*. *Schizophr Res*, 2018. **198**: p. 60-67.
76. Turner, C.H. and D.B. Burr, *Basic biomechanical measurements of bone: a tutorial*. *Bone*, 1993. **14**(4): p. 595-608.
77. Kauschke, V., M. Schneider, A. Jauch, M. Schumacher, M. Kampschulte, M. Rohnke, A. Henss, C. Bamberg, K. Trinkaus, M. Gelinsky, C. Heiss, and K.S. Lips, *Effects of a Pasty Bone Cement Containing Brain-Derived Neurotrophic Factor-Functionalized Mesoporous Bioactive Glass Particles on Metaphyseal Healing in a New Murine Osteoporotic Fracture Model*. *Int J Mol Sci*, 2018. **19**(11).
78. Doblare, M. and J.M. Garcia, *On the modelling bone tissue fracture and healing of the bone tissue*. *Acta Cient Venez*, 2003. **54**(1): p. 58-75.
79. Pilakka-Kanthikeel, S., V.S. Atluri, V. Sagar, S.K. Saxena, and M. Nair, *Targeted brain derived neurotrophic factors (BDNF) delivery across the blood-brain barrier for neuro-protection using magnetic nano carriers: an in-vitro study*. *PLoS One*, 2013. **8**(4): p. e62241.
80. Khosla, S., *Leptin-central or peripheral to the regulation of bone metabolism?* *Endocrinology*, 2002. **143**(11): p. 4161-4.
81. Upadhyay, J., O.M. Farr, and C.S. Mantzoros, *The role of leptin in regulating bone metabolism*. *Metabolism*, 2015. **64**(1): p. 105-13.
82. Camerino, C., M. Zayzafoon, M. Rymaszewski, J. Heiny, M. Rios, and P.V. Hauschka, *Central depletion of brain-derived neurotrophic factor in mice results in high bone mass and metabolic phenotype*. *Endocrinology*, 2012. **153**(11): p. 5394-405.
83. Ferguson, V.L., R.A. Ayers, T.A. Bateman, and S.J. Simske, *Bone development and age-related bone loss in male C57BL/6J mice*. *Bone*, 2003. **33**(3): p. 387-98.

84. Delahunty, K.M., L.G. Horton, H.F. Coombs, 3rd, K.L. Shultz, K.L. Svenson, M.A. Marion, M.F. Holick, W.G. Beamer, and C.J. Rosen, *Gender- and compartment-specific bone loss in C57BL/6J mice: correlation to season?* J Clin Densitom, 2009. **12**(1): p. 89-94.



## Chapter 6.

### Discussion and Future Directions

Neurotrophins and their receptors are recognised to have a broad range of biological functions in neural and non-neural tissues. Specifically, evidence suggests two neurotrophins, NGF and BDNF, have numerous roles in tissue healing processes following trauma. The key issues using the exogenous peptides, NGF and BDNF, in animal research is their 1. poor solubility 2. lack BBB penetration and 3. short half-life due to rapid degradation [1-3]. New approaches in the pharmaceutical industry have led to the development of non-peptide neurotrophin mimetics. Two non-peptide molecules developed that have shown robust neurotrophic activity are the selective agonists for either TrkA or TrkB; namely, GA and 7,8-DHF, respectively [4, 5]. In this thesis, two molecules were used to explore selective Trk activation following TBI and long bone fracture healing. Data suggests that targeting the neurotrophin receptor TrkA had no effect in acute outcomes of TBI. On the other hand, targeting TrkA and TrkB affected fracture healing, specifically altering the structure and biomechanical properties of healing callus. The major findings of this thesis, as well as the limitations and potential implications for future research will now be discussed.

#### *GA does not attenuate acute outcomes of TBI in mice*

The TrkA agonist, GA, has previously been shown to have neuroprotective properties and reduce cortical infarct size in a murine model of transient ischemic brain injury [5]. Whether GA's neuroprotective effects could be translated to a murine model of TBI had not yet been explored. The first study of this thesis used a moderate LFPI model in mice to determine the effects of GA on behavioural outcomes, neuroinflammation, apoptosis, neurite growth and synaptogenesis in the acute stages of TBI.

Behavioural deficits have been shown to occur in acute time-points following TBI in rodent models as similarly shown in this study [6-8]. It was established that GA treatment did not affect the TBI-induced changes in motor function and behaviour. TBI-induced motor deficits measured by rotarod were not lessened with GA treatment, which is likened to previous studies that report NGF treatment did not improve TBI-induced motor deficits in open-wire grid [9] and beam balance tests [10, 11]. Spatial memory measured via Y-maze, and cognition analysed via EPM and open-field were not improved with administration of GA at 72 h post-TBI. Previous studies using the Morris water maze have shown NGF treatment following TBI, reduced cognitive latencies and improved spatial memory in rodents at weeks 1 and 2 post-injury but not at days 1, 2 and 3 post-injury [9-12]. It is possible that if behavioural analysis was extended to 1- or 2-weeks post-injury, there may be an improvement in spatial memory and cognition in the GA-treated mice, which is comparable to previous studies that used NGF for treatment. Additionally, if more cognitive

sensitive tasks such as Water maze or touchscreen were performed, a larger TBI effect may have been revealed and therefore, allowed insights into the efficacy of GA on this outcome. Thus, future investigation of GA's influence on spatial memory and cognition following TBI are warranted.

Cerebral oedema following TBI is a major indicator of brain injury severity. Intranasal administration of NGF had previously been shown to reduce oedema in rats at 72 h post-TBI using a weight-drop model [13]. Brain water content was measured using the wet weight-dry weight calculation, a commonly used method to determine BBB dysfunction following TBI [14] and found that GA did not attenuate the cerebral oedema deficit seen at 72 hours post-TBI. The lack of effect of GA may be due to differing times that cerebral oedema peaks between mice and rats. It has been shown that cerebral oedema peaks in mice 3-24 h post-LFPI, and thus by measuring at 72 h post-TBI, the window was likely missed. A future investigation could analyse a more acute time-point such as 3- or 24-h post-injury for differences in cerebral oedema.

Prior studies using rat models have shown behavioural deficits, similar to the deficits seen in the current experiments are manifestations of neuroinflammation and cerebral oedema [8, 15]. Inflammatory responses that occur following TBI can lead several cells within the brain to become reactive. Astrocytes are an important cell type in neuroinflammation [16] and respond to brain injury by becoming hypertrophic and increase expression of vimentin, GFAP and LCN2 [17-19]. The other main cell types vital to the neuroinflammatory response are microglia [20]. In response to TBI, activated microglia can be identified by an increase in expression markers CD32, CD16 [21] and Iba1 [22]. In the current experiments, significant upregulation of mRNA expression of several of these neuroinflammatory genes described were observed at 72 h post-injury in the cortex and hippocampus following TBI. However, there was no difference of mRNA expression between the control and GA-treated groups. These results were different to previous rodent studies that demonstrated NGF increased protein expression of pro-inflammatory cytokines TNF- $\alpha$  and IL-1 $\beta$  during the first 72 h post-TBI [13, 23]. Possible reasons for the lack neuroinflammatory upregulation in response to GA may include that either the dose GA administered did not directly affect the neuroinflammatory response, or that the detectable changes occurred at an earlier time-point. Additionally, markers of astrogliosis and reactive microglia were analysed, and not TNF- $\alpha$  or IL-1 $\beta$ , which are pro-inflammatory cytokines formed by astrocytes and microglia [24], and these were measured in the NGF-TBI study [13].

Lastly, in early stages of TBI, neurons have been shown to begin early phase sprouting within 72 h of injury in the hippocampus and cortex with elevation in protein and mRNA expression of neurite growth markers GAP-43, synapsin, synaptophysin and agrin [25-29]. In the current experiments, GAP-43, synapsin and synaptophysin did not change mRNA expression in response to injury or GA treatment. There is a strong correlation between GAP-43 expression and

NGF in the literature [30-32], however, there is a gap in the literature for the treatment effect NGF has on the expression of early sprouting markers of neurons post-TBI. Despite the lack in changes of expression for neurite marker GAP-43 and synaptogenesis markers synapsin and synaptophysin, this thesis has further characterized the LFPI model in mice in the acute stages of TBI.

The discussion in **Chapter 3** described several feasible reasons as to why the GA treatment regimen used seemed not to attenuate the outcomes of TBI. Firstly, TrkA expression in the cortex was significantly reduced in mice following moderate-to-severe TBI, which minimised GA receptor binding and action. Systemic administration of GA has previously been shown to protect kainic acid-induced apoptosis [5], therefore GA administration prior to TBI may protect neurons from apoptosis and reduction of TrkA expression. Furthermore, the concentration of GA that was systemically delivered may not have been enough to reduce neuroinflammation, apoptosis and stimulate neurite growth. It is possible that higher doses or a prolonged treatment regimen of GA may have provided neuroprotection during TBI and future studies should explore such a regimen. A limitation associated with this experimental study was that a single acute time-point of TBI was analysed. GA has a suspected role in neuronal survival and growth, which are processes that can take up to weeks to detect following a TBI insult. Therefore, analysis of GA-treatment on TBI long-term may reveal neuroprotective effects when analysing neurogenesis and behavioural outcomes. Finally, blood and brain concentrations of GA were not determined in this study, it was assumed that based on previous studies by Jang and colleagues, that when peripherally administered, GA crosses the BBB following brain trauma [5]. A future direction could entail bio-distribution studies with radiolabel tracing of GA to confirm its movement across the BBB.

#### *GA improves murine fracture healing*

Just over twenty years ago, researchers from my lab showed that osmotic infusions of NGF delivered to rats with rib fractures improved bone healing [33], therefore, it was hypothesised that mimicking the action of NGF at its receptor using selective TrkA agonist, GA, may also improve fracture healing.

Administration of 1 mg/kg/day of GA was found to decrease total callus tissue volume, bony surface area of callus and increase bone fractional volume at 21 days post-fracture. Interestingly, total bone volume was not affected by GA treatment. Furthermore, biomechanical testing revealed that GA-treated calluses were smaller in CSA measurement, and had increased load per unit area and stiffness per unit area in 42 days fracture calluses. Peak force and stiffness were not altered by GA treatment. From these findings it was concluded that GA treatment may have enhanced fracture healing, specifically the mechanical properties of callus.

The biomechanical outcomes are identical to a previous study in my laboratory, where NGF treatment to healing rat rib fractures improved these mechanical properties of calluses at 42 days post-fracture [33]. In the same study, it was demonstrated that NGF enhanced bony content within fracture calluses at 21 days post-fracture [33]. A reduction in the overall size of callus as presented via  $\mu$ CT, in conjunction with the enhanced mechanical properties of callus suggest that GA treatment influenced bone remodelling in healing callus. The architectural layout of bone and degree of mineralisation is deemed highly important when analysing mechanical strength of healing fractures [34]. Whilst it appeared that GA did not influence the overall bone volume in calluses, there may have been a difference in bone quality, namely larger quantities of lamellar bone compared to woven bone in GA-treated calluses. Although it was not possible to histomorphometrically analyse the 42-day calluses because they were used in biomechanical assessment, it would have added to the overall results of this thesis. Future research in histomorphometric analysis of 42-day calluses could distinguish between lamellar and woven bone in healing calluses. Likewise,  $\mu$ CT analysis demonstrated bony union in all calluses at 21 days post-fracture, therefore, it is possible that mechanical testing at an earlier time-point of healing may have yielded different findings.

The limitations of this study are described in depth in **Chapter 4**. Briefly, the amount of GA used in the study was less than initially planned, namely due to the insolubility of GA and the osmotic pump requirements of delivery. Higher doses of GA, like those used in previous studies may have yielded a more profound effect on fracture healing [5]. Additionally, biomechanical analysis was performed on 42-day fracture calluses that were in advanced stages of healing. Had biomechanical analysis been performed in 21-day calluses where bony union was also present there may have been different results.

The mechanism by which GA influenced fracture healing was unknown at this point and a possible theory included indirectly via stimulation of neuronal fibres at the fracture site. Bone periosteum is densely lined with TrkA positive fibres [35] and NGF treatment has been previously shown to increase catecholamine synthesis in healing rat rib calluses [33]. Catecholamine synthesis has been directly linked to stimulate blood vessels and sensory nerve sprouting, two factors that influence fracture healing [36], through TrkA signalling in endochondral bone ossification [37]. Similarly, sensory and sympathetic nerves have been shown to positively influence fracture callus [38], and without nerve innervation calluses are larger in size and the bony matrix is highly disorganised [39-41]. Thus, GA, similarly to NGF, may have indirectly promoted fracture healing via stimulation of TrkA positive sensory and/or sympathetic fibres within the healing callus, which may have further influenced the vascularisation and ossification of the fractured bone to produce smaller calluses by 21 days. A future experiment to investigate

the effects of GA on sensory and sympathetic nerve fibres in fracture callus would be to perform immunohistochemistry on whole callus periosteum quantifying the expression of TrkA fibres by confocal microscopy or to quantify the amount of catecholamines using high performance liquid chromatography.

*GA promotes osteoblastic differentiation and mineralization in osteogenic cell line*

With evidence of GA influencing fracture healing, the next step was to identify whether this was via direct osteoblastic signalling. Kusa O cells are multi-potential, bone marrow stromal cells and were chosen for this study as they have previously been characterised as cells with osteogenic potential, which are suitable for investigating osteoblastic differentiation [42, 43]. It was hypothesised that GA would promote Kusa O differentiation into an osteoblast-like phenotype and therefore increase mineralisation. If GA could increase Kusa O osteoblast-like cells to mineralise, then perhaps GA stimulated osteoblastic cells in the *in vivo* fracture model to enhance the synthesis of mineralised matrix, thus producing mechanically stronger fractures.

The presence of TrkA receptors in Kusa O cells at 14 days were confirmed via Western blot analysis, however, the receptors were not present in undifferentiated Kusa O cells. Proliferation of Kusa O were not altered by GA treatment. Expression of alkaline phosphatase, osteonectin and DMP-1 mRNA was significantly increased by GA treatment in Kusa O cells at 14 days of differentiation. Expression of OPG and RANKL was not affected by GA treatment. Furthermore, mineralisation by Kusa O cells was markedly increased compared to non-treated cells at 21 days of incubation. Therefore, it was concluded that GA administration may act directly on osteoblasts to stimulate mineralisation.

Previous reports conclude that NGF/TrkA signalling occurs through osteoblasts during fracture healing, with TrkA receptors localised exclusively to mature osteoblasts and not osteoprogenitor cells [44-46]. Further supporting this theory, is that neither NGF nor GA appear to influence proliferation of an osteogenic cell line, which is not only consistent with the current Kusa O data, but also recently published data in MC3T3-E1 cells [47, 48]. Similarly, the data in the current experiments show that GA treatment had no effect on expression of early osteoblastic markers, yet did increase the expression of mature osteoblastic markers, which is again consistent with previous studies of NGF treatment in MC3T3-E1 cells, where there was elevated ALP [47]. More recent data has been published that demonstrated GA increased osteoblastic markers as early as 7 days, which was dissimilar to the current results, however, this previous study utilised MC3T3-E1 cells, which is a different cell line to the one used in this thesis [48]. Nevertheless, the findings from the current study suggest that GA may act on osteoblasts to stimulate mineralisation, and that this may have positively impacted long bone fracture healing in mice.

### *7,8-DHF is detrimental to healing murine tibial fractures*

Another neurotrophic factor that has been shown to have a role in fracture healing is BDNF. BDNF and its high affinity receptor, TrkB, have been localised at the site of fracture healing in human and rodent studies [45, 49, 50]. Additionally, BDNF treatment has been demonstrated to stimulate neovascularisation [49, 51, 52] and increase ossification proteins ALP and BMP-2 in mineralizing cells cementoblasts [53]. Therefore, it was hypothesised that a selective TrkB agonist, 7,8-DHF, may improve fracture healing.

Treatment of 5 mg/kg/day of 7,8-DHF in mice with tibial fractures was found to decrease total callus tissue volume and mean cross sectional area at 28 days post-fracture. Additionally, calluses treated with 7,8-DHF were biomechanically weaker with reduced peak force to failure and increased stiffness at 28 days. Given these findings it was concluded that contrary to the initial hypothesis, 7,8-DHF treatment in fact negatively impacted fracture healing in mice.

The present data whereby peripheral TrkB activation improves fracture healing was not supported by previous literature that demonstrated BDNF-functionalised cement improved fracture healing in mice with femoral fractures [54]. Through histomorphometric analysis, they found BDNF increased new bone formation at 35 days post-fracture the junction of cement and fracture [54]. While the present studies did not perform histomorphometric analysis at 28 days post-fracture, the mechanically weaker calluses seen in the 7,8-DHF treated group indicate less bony content [55].

Such opposing effects seen between these studies may have been due to the different biodistribution profiles of BDNF and 7,8-DHF, and in turn the site of TrkB activation. BDNF when peripherally delivered is unable to cross the BBB [56], whereas 7,8-DHF has been shown to readily cross the BBB [4, 57-60]. A definitive study investigating selective deletion of BDNF in brains of mice demonstrate an increase femoral length and BMD in the centrally-deleted BDNF mice compared to wildtype. Thus, it is proposed that 7,8-DHF's action on TrkB receptors centrally in the brain, overrode possible positive peripheral effects on bone to negatively impact on fracture healing. This is not the first molecule to have shown opposite central and peripheral effects on bone, with hormone leptin being a hallmark example [61, 62]. Unfortunately, biodistribution studies to confirm 7,8-DHF ability to cross the BBB were not able to be completed in the current study, however, future studies could investigate the biodistribution of 7,8-DHF in mice. Another option would be to quantify TrkB phosphorylation via Western blot analysis of brain tissue in mice treated with 7,8-DHF and comparing these results to controls.

Additionally, to my knowledge, unlike NGF and TrkA, there has been no literature reporting TrkB positive fibres in bone periosteum, and therefore, future experimentation

investigating TrkB nerve fibre distribution in bone or lining bone periosteum would add to the current literature.

#### *7,8-DHF did not affect the osteogenic cell line Kusa4b10*

A possible mechanism by which 7,8-DHF impaired fracture healing was assessed using the osteogenic cell line, Kusa4b10. Kusa4b10s are a sub-clone of Kusa O cells that have greater osteogenic potential than Kusa Os [42] and were gifted to our laboratory to assess the effect of 7,8-DHF on an osteoblast-like cells. Similar to Kusa Os, Kusa4b10s resemble an osteoblast-like phenotype when differentiated up to 14 days [42], and since our group had previously identified the expression of TrkB receptors on parent Kusa O cells, it was hypothesised that 7,8-DHF may have an effect during differentiation and mineralisation of these cells. However, 7,8-DHF did not alter expression of osteoblastic markers ALP or Runx2 at 3-, 7-, or 14-days of differentiation, suggesting a lack of effect of 7,8-DHF on osteoblasts. Supporting this finding, is a previous study that demonstrated BDNF's inability to influence ALP expression in MC3T3-E1 cells following 5 days of treatment. Overall, this finding, or lack thereof, further supports the theory that 7,8-DHF may not have directly acted at the site of fracture healing, but indirectly, potentially through central signalling.

#### *BDNF polymorphisms do not affect bone in C57BL/6 mice*

The final part of this thesis analysed the effect of BDNF (Val66Met) polymorphisms on bone metabolism. Previous evidence in Caucasian populations suggest that BDNF<sup>Met/Met</sup> polymorphic genotypes have significantly reduced BMD compared to BDNF<sup>Val/Met</sup> and BDNF<sup>Val/Val</sup> genotypes [63]. The primary aim of this study therefore was to determine if the described bone changes due to BDNF polymorphisms in humans were reflected in an established BDNF polymorphism mouse model.

To my knowledge this is the first study that investigated the change in bone content in mouse BDNF polymorphic variants; Val/Val, Val/Met, Met/Met, using pQCT. The current study found that there were no changes in the amount of femoral cortical or trabecular bone content between BDNF polymorphic variant mice. These results described above suggest that the hBDNF<sup>Val66Met</sup> mouse model, whilst good to analyse neuropsychiatric changes seen between BDNF polymorphisms, appears an inappropriate model to use to analyse bone discrepancies seen between BDNF genotypes. Although BDNF polymorphic variants seemed to have minimal effect on the total amount of cortical and trabecular bone as shown by pQCT, future  $\mu$ CT analysis or histomorphometric analysis of femora of the hBDNF<sup>Val66Met</sup> mice may show structural variations in bone. Similarly, if the power of the study was increased to reflect a larger population of mice, an effect may have been seen.

### Limitations when using animal fracture models

Whilst preclinical animal models of fracture healing; fibular and tibial fracture models, are very good at replicating the pathophysiological stages of fracture healing, there are several limitations surrounding both types of models. The bilateral fibular murine model used in chapter 4 was advantageous due to the quick and low invasiveness of the surgery and the production of two fractures per animal, however, the model produced relatively small calluses (some calluses weighing <5 mg) which made certain analyses difficult. Biomechanical analysis was tedious due to the minute size of the fibulae and there were difficulties of such small calluses for biomechanical analyses, which reduced numbers for analysis. Similarly, when it came to tissue harvesting for Western blotting or PCR, there was on occasion not enough tissue to harvest for analysis, which may be a reason the fibular fracture model is used infrequently compared to tibial and femoral murine fracture models [64]. The above-mentioned issues with the fibular fracture model was the main driving force to move to the tibial fracture model for Chapter 5, however, this model also had limitations. Stabilising the tibial fracture by using an intramedullary pin only limits transverse forces applied to the healing fracture and not rotational forces. In fact, one study investigating the rotational stiffness in mouse femoral fractures using different stabilisation tools has shown that the intramedullary pin provides no rotational stability, and only the locking plate or external fixation tool can provide stability [65]. The potential influences of rotational forces during fracture healing could be limited in future by using a locking plate fracture model, which is similarly exhibited in the femoral fracture model [64].

### Future directions regarding neurotrophins in bone

Data generated from this thesis has provided significant insight into the roles of two main neurotrophins and their receptors on fracture healing and on bone cell function. Future studies should elucidate further the roles each neurotrophin receptor has on skeletal metabolism. For example, this thesis demonstrated the TrkA agonism had a positive outcome on fracture healing, however, it would be interesting to see if TrkA antagonism is detrimental to fracture healing. Recent research has shown that using the TrkA antagonist, AR786, successfully blocked NGF activation in a rodent model of inflammatory osteoarthritis [66]. Therefore, given the data presented in this thesis a detrimental effect of fracture healing may be a possibility in osteoarthritic patients using such a treatment with a TrkA antagonist. TrkA antagonism during fracture healing would further assist in characterising the NGF and TrkA interactions in bone metabolism.

Similarly, BDNF and its receptor TrkB plays a role in bone metabolism and fracture healing. Data from this thesis proposes that BDNF may have two distinct roles in bone metabolism, dependent on if TrkB is activated centrally or peripherally, however further investigations are



required to support this proposal. Future studies should attempt to demonstrate central activation of TrkB has a negative effect on bone and peripheral activation of TrkB has a positive effect on bone. As BDNF is too large to cross into the BBB, a corresponding experiment to investigate the peripheral effects of BDNF administration on fracture healing would be to add a cohort of mice and systemically treat with BDNF peptide. Additionally, the use of TrkB antagonists such as ANA-12 [67] or other BDNF agonists such as LM22A-4 [68], which have been shown to selectively bind to TrkB and also crosses the BBB would be a likely possible valuable treatment in improving fracture healing.

### **6.1. Conclusions**

These studies demonstrated that selectively targeting neurotrophic receptor, TrkA, does not attenuate the acute outcomes of TBI. Conversely, selectively targeting TrkA and TrkB receptors respectively with GA and 7,8-DHF during long bone fracture healing had opposing effects. GA treatment had mild positive effects on fracture healing producing smaller and mechanically stronger calluses compared to controls. GA's influence on fracture healing, may be through stimulating mineralisation in osteoblasts, which was demonstrated in an osteoblastic murine cell line, Kusa O. Comparatively, 7,8-DHF had negative effects on fracture healing; producing smaller and mechanically inferior calluses compared to controls. It is proposed that 7,8-DHF may not have directly acted at the fracture site, which is supported by the lack of effect of 7,8-DHF on a murine osteogenic cell line, Kusa4b10, but instead, the reported negative outcome on fracture healing was possibly a product of central TrkB receptor activation. Furthermore, these studies demonstrate the mouse knock-in model hBDNF<sup>Val66Met</sup> may not reflect the variable BMD phenotype seen in BDNF<sup>Val66Met</sup> mutations in human populations. The results presented in this thesis demonstrate that neurotrophin signalling can influence skeletal maintenance and healing, which add clues to the puzzle for the development of possible future therapeutics targeting the stimulation of normal bone formation in reparative situations or in treatment of bone disorders such as osteoporosis.

## 6.2. References

1. Friden, P.M., L.R. Walus, P. Watson, S.R. Doctrow, J.W. Kozarich, C. Backman, H. Bergman, B. Hoffer, F. Bloom, and A.C. Granholm, *Blood-brain barrier penetration and in vivo activity of an NGF conjugate*. Science, 1993. **259**(5093): p. 373-7.
2. Angeletti, R.H., P.U. Aneletti, and R. Levi-Montalcini, *Selective accumulation of ( 125 I) labelled nerve growth factor in sympathetic ganglia*. Brain Res, 1972. **46**: p. 421-5.
3. Tria, M.A., M. Fusco, G. Vantini, and R. Mariot, *Pharmacokinetics of nerve growth factor (NGF) following different routes of administration to adult rats*. Exp Neurol, 1994. **127**(2): p. 178-83.
4. Jang, S.W., X. Liu, M. Yepes, K.R. Shepherd, G.W. Miller, Y. Liu, W.D. Wilson, G. Xiao, B. Bianchi, Y.E. Sun, and K. Ye, *A selective TrkB agonist with potent neurotrophic activities by 7,8-dihydroxyflavone*. Proc Natl Acad Sci U S A, 2010. **107**(6): p. 2687-92.
5. Jang, S.W., M. Okada, I. Sayeed, G. Xiao, D. Stein, P. Jin, and K. Ye, *Gambogic amide, a selective agonist for TrkA receptor that possesses robust neurotrophic activity, prevents neuronal cell death*. Proc Natl Acad Sci U S A, 2007. **104**(41): p. 16329-34.
6. Xiong, Y., A. Mahmood, and M. Chopp, *Animal models of traumatic brain injury*. Nat Rev Neurosci, 2013. **14**(2): p. 128-42.
7. Li, S., T. Kuroiwa, S. Ishibashi, L. Sun, S. Endo, and K. Ohno, *Transient cognitive deficits are associated with the reversible accumulation of amyloid precursor protein after mild traumatic brain injury*. Neurosci Lett, 2006. **409**(3): p. 182-6.
8. Shultz, S.R., D.F. MacFabe, K.A. Foley, R. Taylor, and D.P. Cain, *A single mild fluid percussion injury induces short-term behavioral and neuropathological changes in the Long-Evans rat: support for an animal model of concussion*. Behav Brain Res, 2011. **224**(2): p. 326-35.
9. Longhi, L., D.J. Watson, K.E. Saatman, H.J. Thompson, C. Zhang, S. Fujimoto, N. Royo, D. Castelbuono, R. Raghupathi, J.Q. Trojanowski, V.M. Lee, J.H. Wolfe, N. Stocchetti, and T.K. McIntosh, *Ex vivo gene therapy using targeted engraftment of NGF-expressing human NT2N neurons attenuates cognitive deficits following traumatic brain injury in mice*. J Neurotrauma, 2004. **21**(12): p. 1723-36.
10. Sinson, G., M. Voddi, and T.K. McIntosh, *Nerve growth factor administration attenuates cognitive but not neurobehavioral motor dysfunction or hippocampal cell loss following fluid-percussion brain injury in rats*. J Neurochem, 1995. **65**(5): p. 2209-16.
11. Dixon, C.E., P. Flinn, J. Bao, R. Venya, and R.L. Hayes, *Nerve growth factor attenuates cholinergic deficits following traumatic brain injury in rats*. Exp Neurol, 1997. **146**(2): p. 479-90.

12. Tian, L., R. Guo, X. Yue, Q. Lv, X. Ye, Z. Wang, Z. Chen, B. Wu, G. Xu, and X. Liu, *Intranasal administration of nerve growth factor ameliorate  $\beta$ -amyloid deposition after traumatic brain injury in rats*. Brain Research, 2012. **1440**: p. 47-55.
13. Lv, Q., X. Fan, G. Xu, Q. Liu, L. Tian, X. Cai, W. Sun, X. Wang, Q. Cai, Y. Bao, L. Zhou, Y. Zhang, L. Ge, R. Guo, and X. Liu, *Intranasal delivery of nerve growth factor attenuates aquaporins-4-induced edema following traumatic brain injury in rats*. Brain Res, 2013. **1493**: p. 80-9.
14. Shultz, S.R., X.L. Tan, D.K. Wright, S.J. Liu, B.D. Semple, L. Johnston, N.C. Jones, A.D. Cook, J.A. Hamilton, and T.J. O'Brien, *Granulocyte-macrophage colony-stimulating factor is neuroprotective in experimental traumatic brain injury*. J Neurotrauma, 2014. **31**(10): p. 976-83.
15. Nimmo, A.J., I. Cernak, D.L. Heath, X. Hu, C.J. Bennett, and R. Vink, *Neurogenic inflammation is associated with development of edema and functional deficits following traumatic brain injury in rats*. Neuropeptides, 2004. **38**(1): p. 40-7.
16. Myer, D.J., G.G. Gurkoff, S.M. Lee, D.A. Hovda, and M.V. Sofroniew, *Essential protective roles of reactive astrocytes in traumatic brain injury*. Brain, 2006. **129**(Pt 10): p. 2761-72.
17. Bi, F., C. Huang, J. Tong, G. Qiu, B. Huang, Q. Wu, F. Li, Z. Xu, R. Bowser, X.G. Xia, and H. Zhou, *Reactive astrocytes secrete Icn2 to promote neuron death*. Proc Natl Acad Sci U S A, 2013. **110**(10): p. 4069-74.
18. Eng, L.F. and R.S. Ghirnikar, *GFAP and astrogliosis*. Brain Pathol, 1994. **4**(3): p. 229-37.
19. Hill, S.J., E. Barbarese, and T.K. McIntosh, *Regional heterogeneity in the response of astrocytes following traumatic brain injury in the adult rat*. J Neuropathol Exp Neurol, 1996. **55**(12): p. 1221-9.
20. Streit, W.J., R.E. Mrak, and W.S. Griffin, *Microglia and neuroinflammation: a pathological perspective*. J Neuroinflammation, 2004. **1**(1): p. 14.
21. Walker, D.G. and L.F. Lue, *Immune phenotypes of microglia in human neurodegenerative disease: challenges to detecting microglial polarization in human brains*. Alzheimers Res Ther, 2015. **7**(1): p. 56.
22. Ito, D., Y. Imai, K. Ohsawa, K. Nakajima, Y. Fukuuchi, and S. Kohsaka, *Microglia-specific localisation of a novel calcium binding protein, Iba1*. Brain Res Mol Brain Res, 1998. **57**(1): p. 1-9.
23. Lv, Q., W. Lan, W. Sun, R. Ye, X. Fan, M. Ma, Q. Yin, Y. Jiang, G. Xu, J. Dai, R. Guo, and X. Liu, *Intranasal nerve growth factor attenuates tau phosphorylation in brain after traumatic brain injury in rats*. J Neurol Sci, 2014. **345**(1-2): p. 48-55.
24. Gehrman, J., Y. Matsumoto, and G.W. Kreutzberg, *Microglia: intrinsic immune effector cell of the brain*. Brain Res Brain Res Rev, 1995. **20**(3): p. 269-87.

25. Hulsebosch, C.E., D.S. DeWitt, L.W. Jenkins, and D.S. Prough, *Traumatic brain injury in rats results in increased expression of Gap-43 that correlates with behavioral recovery*. *Neurosci Lett*, 1998. **255**(2): p. 83-6.
26. Thompson, S.N., T.R. Gibson, B.M. Thompson, Y. Deng, and E.D. Hall, *Relationship of calpain-mediated proteolysis to the expression of axonal and synaptic plasticity markers following traumatic brain injury in mice*. *Exp Neurol*, 2006. **201**(1): p. 253-65.
27. Faló, M.C., T.M. Reeves, and L.L. Phillips, *Agrin expression during synaptogenesis induced by traumatic brain injury*. *J Neurotrauma*, 2008. **25**(7): p. 769-83.
28. Hall, K.D. and J. Lifshitz, *Diffuse traumatic brain injury initially attenuates and later expands activation of the rat somatosensory whisker circuit concomitant with neuroplastic responses*. *Brain Res*, 2010. **1323**: p. 161-73.
29. Ding, J.Y., C.W. Kreipke, P. Schafer, S. Schafer, S.L. Speirs, and J.A. Rafols, *Synapse loss regulated by matrix metalloproteinases in traumatic brain injury is associated with hypoxia inducible factor-1alpha expression*. *Brain Res*, 2009. **1268**: p. 125-34.
30. Yankner, B.A., L.I. Benowitz, L. Villa-Komaroff, and R.L. Neve, *Transfection of PC12 cells with the human GAP-43 gene: effects on neurite outgrowth and regeneration*. *Brain Res Mol Brain Res*, 1990. **7**(1): p. 39-44.
31. Benowitz, L.I. and A. Routtenberg, *GAP-43: an intrinsic determinant of neuronal development and plasticity*. *Trends Neurosci*, 1997. **20**(2): p. 84-91.
32. Federoff, H.J., E. Grabczyk, and M.C. Fishman, *Dual regulation of GAP-43 gene expression by nerve growth factor and glucocorticoids*. *J Biol Chem*, 1988. **263**(36): p. 19290-5.
33. Grills, B.L., J.A. Schuijers, and A.R. Ward, *Topical application of nerve growth factor improves fracture healing in rats*. *J Orthop Res*, 1997. **15**(2): p. 235-42.
34. Morgan, E.F., Z.D. Mason, K.B. Chien, A.J. Pfeiffer, G.L. Barnes, T.A. Einhorn, and L.C. Gerstenfeld, *Micro-computed tomography assessment of fracture healing: relationships among callus structure, composition, and mechanical function*. *Bone*, 2009. **44**(2): p. 335-44.
35. Castaneda-Corral, G., J.M. Jimenez-Andrade, A.P. Bloom, R.N. Taylor, W.G. Mantyh, M.J. Kaczmarek, J.R. Ghilardi, and P.W. Mantyh, *The majority of myelinated and unmyelinated sensory nerve fibers that innervate bone express the tropomyosin receptor kinase A*. *Neuroscience*, 2011. **178**: p. 196-207.
36. Beamer, B., C. Hettrich, and J. Lane, *Vascular endothelial growth factor: an essential component of angiogenesis and fracture healing*. *HSS J*, 2010. **6**(1): p. 85-94.
37. Tomlinson, R.E., Z. Li, Q. Zhang, B.C. Goh, Z. Li, D.L. Thorek, L. Rajbhandari, T.M. Brushart, L. Minichiello, F. Zhou, A. Venkatesan, and T.L. Clemens, *NGF-TrkA Signaling by Sensory*

- Nerves Coordinates the Vascularization and Ossification of Developing Endochondral Bone*. Cell Rep, 2016. **16**(10): p. 2723-35.
38. Hukkanen, M., Y.T. Konttinen, S. Santavirta, P. Paavolainen, X.H. Gu, G. Terenghi, and J.M. Polak, *Rapid proliferation of calcitonin gene-related peptide-immunoreactive nerves during healing of rat tibial fracture suggests neural involvement in bone growth and remodelling*. Neuroscience, 1993. **54**(4): p. 969-79.
  39. Hukkanen, M., Y.T. Konttinen, S. Santavirta, L. Nordsletten, J.E. Madsen, R. Almaas, A.B. Oestreicher, T. Rootwelt, and J.M. Polak, *Effect of sciatic nerve section on neural ingrowth into the rat tibial fracture callus*. Clin Orthop Relat Res, 1995(311): p. 247-57.
  40. Madsen, J.E., M. Hukkanen, A.K. Aune, I. Basran, J.F. Moller, J.M. Polak, and L. Nordsletten, *Fracture healing and callus innervation after peripheral nerve resection in rats*. Clin Orthop Relat Res, 1998(351): p. 230-40.
  41. Nordsletten, L., J.E. Madsen, R. Almaas, T. Rootwelt, J. Halse, Y.T. Konttinen, M. Hukkanen, and S. Santavirta, *The neuronal regulation of fracture healing. Effects of sciatic nerve resection in rat tibia*. Acta Orthop Scand, 1994. **65**(3): p. 299-304.
  42. Allan, E.H., P.W. Ho, A. Umezawa, J. Hata, F. Makishima, M.T. Gillespie, and T.J. Martin, *Differentiation potential of a mouse bone marrow stromal cell line*. J Cell Biochem, 2003. **90**(1): p. 158-69.
  43. Umezawa, A., T. Maruyama, K. Segawa, R.K. Shaddock, A. Waheed, and J. Hata, *Multipotent marrow stromal cell line is able to induce hematopoiesis in vivo*. J Cell Physiol, 1992. **151**(1): p. 197-205.
  44. Aiga, A., K. Asaumi, Y.J. Lee, H. Kadota, S. Mitani, T. Ozaki, and M. Takigawa, *Expression of neurotrophins and their receptors tropomyosin-related kinases (Trk) under tension-stress during distraction osteogenesis*. Acta Med Okayama, 2006. **60**(5): p. 267-77.
  45. Asaumi, K., T. Nakanishi, H. Asahara, H. Inoue, and M. Takigawa, *Expression of neurotrophins and their receptors (TRK) during fracture healing*. Bone, 2000. **26**(6): p. 625-33.
  46. Grills, B.L. and J.A. Schuijers, *Immunohistochemical localization of nerve growth factor in fractured and unfractured rat bone*. Acta Orthop Scand, 1998. **69**(4): p. 415-9.
  47. Yada, M., K. Yamaguchi, and T. Tsuji, *NGF stimulates differentiation of osteoblastic MC3T3-E1 cells*. Biochem Biophys Res Commun, 1994. **205**(2): p. 1187-93.
  48. Fioravanti, G., P.Q. Hua, and R.E. Tomlinson, *The TrkA agonist gambogic amide augments skeletal adaptation to mechanical loading through actions on sensory nerves and osteoblasts*. bioRxiv, 2020: p. 2020.08.28.272740.

49. Kilian, O., S. Hartmann, N. Dongowski, S. Karnati, E. Baumgart-Vogt, F.V. Hartel, T. Noll, R. Schnettler, and K.S. Lips, *BDNF and its TrkB receptor in human fracture healing*. *Ann Anat*, 2014. **196**(5): p. 286-95.
50. Ebadi, M., R.M. Bashir, M.L. Heidrick, F.M. Hamada, H.E. Refaey, A. Hamed, G. Helal, M.D. Baxi, D.R. Cerutis, and N.K. Lassi, *Neurotrophins and their receptors in nerve injury and repair*. *Neurochem Int*, 1997. **30**(4-5): p. 347-74.
51. Kermani, P., D. Rafii, D.K. Jin, P. Whitlock, W. Schaffer, A. Chiang, L. Vincent, M. Friedrich, K. Shido, N.R. Hackett, R.G. Crystal, S. Rafii, and B.L. Hempstead, *Neurotrophins promote revascularization by local recruitment of TrkB+ endothelial cells and systemic mobilization of hematopoietic progenitors*. *J Clin Invest*, 2005. **115**(3): p. 653-63.
52. Kermani, P. and B. Hempstead, *Brain-derived neurotrophic factor: a newly described mediator of angiogenesis*. *Trends Cardiovasc Med*, 2007. **17**(4): p. 140-3.
53. Kajiya, M., H. Shiba, T. Fujita, K. Ouhara, K. Takeda, N. Mizuno, H. Kawaguchi, M. Kitagawa, T. Takata, K. Tsuji, and H. Kurihara, *Brain-derived neurotrophic factor stimulates bone/cementum-related protein gene expression in cementoblasts*. *J Biol Chem*, 2008. **283**(23): p. 16259-67.
54. Kauschke, V., M. Schneider, A. Jauch, M. Schumacher, M. Kampschulte, M. Rohnke, A. Henss, C. Bamberg, K. Trinkaus, M. Gelinsky, C. Heiss, and K.S. Lips, *Effects of a Pasty Bone Cement Containing Brain-Derived Neurotrophic Factor-Functionalized Mesoporous Bioactive Glass Particles on Metaphyseal Healing in a New Murine Osteoporotic Fracture Model*. *Int J Mol Sci*, 2018. **19**(11).
55. Doblare, M. and J.M. Garcia, *On the modelling bone tissue fracture and healing of the bone tissue*. *Acta Cient Venez*, 2003. **54**(1): p. 58-75.
56. Pilakka-Kanthikeel, S., V.S. Atluri, V. Sagar, S.K. Saxena, and M. Nair, *Targeted brain derived neurotropic factors (BDNF) delivery across the blood-brain barrier for neuro-protection using magnetic nano carriers: an in-vitro study*. *PLoS One*, 2013. **8**(4): p. e62241.
57. Agrawal, R., E. Noble, E. Tyagi, Y. Zhuang, Z. Ying, and F. Gomez-Pinilla, *Flavonoid derivative 7,8-DHF attenuates TBI pathology via TrkB activation*. *Biochim Biophys Acta*, 2015. **1852**(5): p. 862-72.
58. Devi, L. and M. Ohno, *7,8-dihydroxyflavone, a small-molecule TrkB agonist, reverses memory deficits and BACE1 elevation in a mouse model of Alzheimer's disease*. *Neuropsychopharmacology*, 2012. **37**(2): p. 434-44.
59. Castello, N.A., M.H. Nguyen, J.D. Tran, D. Cheng, K.N. Green, and F.M. LaFerla, *7,8-Dihydroxyflavone, a small molecule TrkB agonist, improves spatial memory and increases*

- thin spine density in a mouse model of Alzheimer disease-like neuronal loss.* PLoS One, 2014. **9**(3): p. e91453.
60. Andero, R., N. Daviu, R.M. Escorihuela, R. Nadal, and A. Armario, *7,8-dihydroxyflavone, a TrkB receptor agonist, blocks long-term spatial memory impairment caused by immobilization stress in rats.* Hippocampus, 2012. **22**(3): p. 399-408.
61. Khosla, S., *Leptin-central or peripheral to the regulation of bone metabolism?* Endocrinology, 2002. **143**(11): p. 4161-4.
62. Upadhyay, J., O.M. Farr, and C.S. Mantzoros, *The role of leptin in regulating bone metabolism.* Metabolism, 2015. **64**(1): p. 105-13.
63. Deng, F.Y., L.J. Tan, H. Shen, Y.J. Liu, Y.Z. Liu, J. Li, X.Z. Zhu, X.D. Chen, Q. Tian, M. Zhao, and H.W. Deng, *SNP rs6265 regulates protein phosphorylation and osteoblast differentiation and influences BMD in humans.* J Bone Miner Res, 2013. **28**(12): p. 2498-507.
64. Qi, B., Yu, J., Zhao, Y., Zhu, D., Yu, T., *Mouse fracture models: a primer.* Int J Clin Exp Med, 2016. **9**(7): p. 12418-12429.
65. Histing, T., J.H. Holstein, P. Garcia, R. Matthys, A. Kristen, L. Claes, M.D. Menger, and T. Pohlemann, *Ex vivo analysis of rotational stiffness of different osteosynthesis techniques in mouse femur fracture.* J Orthop Res, 2009. **27**(9): p. 1152-6.
66. Nwosu, L.N., P.I. Mapp, V. Chapman, and D.A. Walsh, *Blocking the tropomyosin receptor kinase A (TrkA) receptor inhibits pain behaviour in two rat models of osteoarthritis.* Ann Rheum Dis, 2016. **75**(6): p. 1246-54.
67. Cazorla, M., J. Premont, A. Mann, N. Girard, C. Kellendonk, and D. Rognan, *Identification of a low-molecular weight TrkB antagonist with anxiolytic and antidepressant activity in mice.* J Clin Invest, 2011. **121**(5): p. 1846-57.
68. Fletcher, J.L., L.K. Dill, R.J. Wood, S. Wang, K. Robertson, S.S. Murray, A. Zamani, and B.D. Semple, *Acute treatment with TrkB agonist LM22A-4 confers neuroprotection and preserves myelin integrity in a mouse model of pediatric traumatic brain injury.* bioRxiv, 2020: p. 2020.10.01.321570.

## Appendix A

### **Composition of Alcian blue and Eosin stain**

a) Dye 1 - Alcian blue (1 %)

- 1 g Alcian blue
- 2 ml Acetic acid
- 97 ml water

b) Dye 2 – 1% alcoholic Eosin

- FRONINE Laboratory supplies
- 144 Hamilton St.
- Riverstone, NSW 2765, Australia

### **Protocol:**

Using a staining rack, submerge slides in 1% Alcian blue stain for 30 minutes.

Rinse slides for 10 seconds in 1% Acetic acid.

Rinse slides 30 seconds in distilled water.

Submerge slides in 1% alcoholic Eosin for 1 minute 30 seconds.

Rinse slides for 1 minute in distilled water.

Air dry and coverslip using DPX.

### **Composition of Tartrate-resistant acid phosphatase (TRAP) stain**

a) Acetate buffer; pH 5.0

- 0.2M sodium acetate
- 50mM L(+) tartaric acid

b) Dye 1

- 0.5 mg Naphthol AS-MX phosphate disodium salt
- 1 ml distilled H<sub>2</sub>O

c) Dye 2

- 1.1 mg Fast Red TR salt
- 1 ml distilled H<sub>2</sub>O

### **Protocol:**

Create final staining solution by mixing Fast Red and Naphthol solutions (Note: use immediately, as stain lasts for up to 1 h).

In a humid chamber add 100 µl of 0.2M acetate buffer to each section and incubate for 20 minutes at room temperature.

Add 100 µl of TRAP-reagent to each section and incubate for 2-4 h in a humid chamber at 37°C.

Rinse slides for 20 s in distilled water.

Air dry and coverslip using DPX.



## Appendix B

### Chapter 3

Publication: Johnstone M. R., Sun M., Taylor C. J., Brady R. D., Grills B. L., Church J. E., Shultz S. R., and McDonald S. J., Gambogic amide, selective TrkA agonist, does not improve outcomes from traumatic brain injury in mice. *Brain Injury*. 2018 32(2) 257-268. DOI: 10.1080/02699052.2017.1394492.

- I performed ~70% of behavioural analysis, with assistance from Dr Mujun Sun.
- I performed ~80% of the treatments administered, with assistance from Dr Mujun Sun, Dr Sandy Shultz and Dr Stuart McDonald.
- I performed all the brain water content analysis.
- I performed all the PCR analysis of the brain samples.
- I performed ~80% of the Western blot analysis, with assistance from Dr Jarrod Church and Dr Caroline Taylor.
- I wrote the first full draft of the manuscript.
- Dr Sandy Shultz performed all lateral fluid percussion injury surgeries and acute injury severity assessment.
- Dr Sandy Shultz and Dr Stuart McDonald performed post-mortem brain collection.
- Dr Sandy Shultz, Dr Stuart McDonald, Dr Brian Grills and Dr Rhys Brady assisted with data analysis and provided revision of manuscript.

Dates and persons/organisations who gave permission to include these publications are:

**Chapter 3:** Mary Ann Muller, US Journal Permissions at Taylor and Francis

6<sup>th</sup> October 2020



## Gambogic amide, a selective TrkA agonist, does not improve outcomes from traumatic brain injury in mice

Maddison R Johnstone<sup>a</sup>, Mujun Sun<sup>b</sup>, Caroline J Taylor<sup>a</sup>, Rhys D Brady<sup>a,b</sup>, Brian L Grills<sup>a</sup>, Jarrod E Church<sup>a</sup>, Sandy R Shultz<sup>b,c</sup>, and Stuart J McDonald<sup>a</sup>

<sup>a</sup>Department of Physiology, Anatomy and Microbiology, School of Life Sciences, La Trobe University, Melbourne, VIC, Australia; <sup>b</sup>Department of Medicine, The Royal Melbourne Hospital, The University of Melbourne, Parkville, VIC, Australia; <sup>c</sup>Department of Neuroscience, Central Clinical School, Monash University, Melbourne, VIC, Australia

### ABSTRACT

**Objectives:** There is evidence that treatment with nerve growth factor (NGF) may reduce neuroinflammation and apoptosis after a traumatic brain injury (TBI). NGF is thought to exert its effects via binding to either TrkA or p75 neurotrophin receptors. This study aimed to investigate the effects of a selective TrkA agonist, gambogic amide (GA), on TBI pathology and outcomes in mice following lateral fluid percussion injury.

**Methods:** Male C57BL/6 mice were given either a TBI or sham injury, and then received subcutaneous injections of either 2 mg/kg of GA or vehicle at 1, 24, and 48 h post-injury. Following behavioural studies, mice were euthanized at 72 h post-injury for analysis of neuroinflammatory, apoptotic, and neurite outgrowth markers.

**Results:** Behavioural testing revealed that GA did not mitigate motor deficits after TBI. TBI caused an increase in cortical and hippocampal expression of several markers of neuroinflammation and apoptosis compared to sham groups. GA treatment did not attenuate these increases in expression, possibly contributed to by our finding of TrkA receptor down-regulation post-TBI.

**Conclusions:** These findings suggest that GA treatment may not be suitable for attenuating TBI pathology and improving outcomes.

### ARTICLE HISTORY

Received 24 April 2017  
Revised 21 July 2017  
Accepted 2 October 2017

### KEYWORDS

Nerve growth factor; neuroinflammation; neurite growth; synaptogenesis; apoptosis; behaviour



### Introduction

Traumatic brain injury (TBI) is a form of acquired brain injury and is a leading cause of death and disability worldwide (1). While some patients with TBI recover within months of injury (2), TBI can result in chronic physical, cognitive and emotional abnormalities, and has been associated with the development of neurodegenerative diseases (3–7). The brain damage in TBI results from both the irreversible primary mechanical insult and also the activation of secondary injury mechanisms, such as neuroinflammation and apoptosis, that evolve over the hours to months after the initial impact (3,5,8). Neuroinflammation in TBI is characterized by the activation of microglia and astrocytes and release of pro-inflammatory cytokines, whereas apoptosis is a significant contributor to cell death following TBI (9,10). Several experimental TBI studies have shown that activation of neuroinflammation and apoptosis can lead to worsened cognitive capacity, emotional disturbances and motor control dysfunction (11–16), and that treatments targeting these mechanisms have potential to improve TBI outcomes (17–19).

Nerve growth factor (NGF) is a neurotrophin responsible for the growth and maintenance of target neurons in the central nervous system (CNS) (20,21). Several studies

have demonstrated that NGF exerts pro-survival responses in neurons by binding to its high-affinity receptor TrkA (22,23). Although there are currently no reported data on the therapeutic use of NGF in clinical trials for TBI, there have been promising animal studies that support the potential benefit of TrkA activation post-TBI. In experimental rodent TBI models, NGF administration has been shown to alleviate several of the deficits associated with the secondary mechanisms of TBI, including promoting neuron survival, reducing expression of inflammatory markers, and reducing cerebral oedema (15,24–29). Furthermore, NGF treatment following TBI was found to improve spatial memory of rodents during Morris water maze testing (15,28–31).

A potential issue with using NGF in the treatment of CNS injuries is the poor pharmacokinetic properties of the peptide. NGF has low blood brain barrier (BBB) penetrability and has a short elimination half-life (~2 h) following systemic administration (32–34). As such, the use of small non-peptide neurotrophic mimetics may have superior therapeutic potential. One such substance is gambogic amide (GA), a recently discovered, BBB permeable, selective high-affinity TrkA agonist (35–37). GA was

**CONTACT** Stuart J McDonald  [stuart.mcdonald@latrobe.edu.au](mailto:stuart.mcdonald@latrobe.edu.au)  Department of Physiology, Anatomy and Microbiology, La Trobe University, Health Sciences 2 building, Melbourne, VIC, Australia.

Sandy R. Shultz, Stuart J. McDonald Joint Senior Authors

Color versions of one or more of the figures in the article can be found online at [www.tandfonline.com/ibj](http://www.tandfonline.com/ibj).

© 2017 Taylor & Francis Group, LLC

found to selectively bind to TrkA and activate downstream Akt and MAPK signalling in neurons *in vitro*, resulting in the promotion of neurite outgrowth and increased resistance to glutamate-induced cell death (35). *In vivo*, systemic administration of 2 mg/kg/day of GA in mice protected neurons from kainic acid-induced apoptosis, and reduced infarct volume in a transient model of ischemic brain injury (35). No studies, however, have investigated the therapeutic potential of GA in TBI. Accordingly, the aim of the present study was to investigate the effects of GA treatment on neuroinflammation, apoptosis, neurite outgrowth, and behavioural outcomes following lateral fluid percussion injury (LFPI) in mice.

## Methods

### Subjects

Thirty C57BL/6 male mice were obtained from the Australian Animal Resource Centre (ARC, Western Australia). Mice were 12 weeks old at time of injury, and were housed individually throughout the experiment under a 12-h light/dark cycle with access to food and water *ad libitum*. All experimental procedures were approved by The Florey Institute of Neuroscience and Mental Health Animal Ethics Committee (Protocol no. 14-006 UM), were within the guidelines of the Australian code of practice for the care and use of animals for scientific purposes by the Australian National Health and Medical Research Council, and were in compliance with the ARRIVE guidelines for how to report animal experiments.

### Experimental groups

Mice were randomly assigned to receive either an LFPI ( $n = 16$ ) or a sham injury ( $n = 14$ ). One mouse died immediately post-LFPI and another mouse given LFPI was euthanized after failing to recover basic motor function after injury. To assess the effects of GA on acute TBI outcomes, mice were then randomly assigned to one of four experimental groups: sham injury + vehicle (i.e. 30% w/v of Kolliphor<sup>®</sup> HS 15 in saline; SHAM+VEH;  $n = 7$ ), sham injury + GA in vehicle (SHAM+GA;  $n = 7$ ), TBI + vehicle (TBI+VEH;  $n = 7$ ) and TBI + GA (TBI+GA;  $n = 7$ ). As GA had poor water solubility at the concentration suitable for subcutaneous injection, a vehicle consisting of 30% w/v of Kolliphor<sup>®</sup> HS 15 and saline was used to form a microemulsion of GA. Kolliphor<sup>®</sup> HS 15 (Solutol<sup>®</sup> HS 15) is a non-ionic emulsifier, a white, odourless paste that is well tolerated and commonly used as a vehicle in human and veterinary injection formulations (38–41). Subcutaneous injections of GA (2 mg/kg/day) or vehicle were made at 1-, 24- and 48-h post-injury. GA and this dosing regimen were chosen due to the previously demonstrated potent and selective neurotrophic actions of GA *in vitro*, and promising neuroprotective properties at 2 mg/kg/day following ischemic brain injury<sup>35–36</sup>. All mice were euthanized at 72 h post-injury, a time-point chosen as it would allow for acute behavioural assessments, as well as capturing a number of pathological/physiological events (e.g. oedema, apoptosis, microglia activation, astrocyte activation,

neurite outgrowth, synaptogenesis) at a single acute post-injury time-point (5,7,42,43).

### Lateral fluid percussion injury

The LFPI is a commonly used and well-validated model of TBI. LFPI and sham injury procedures were conducted using previously described standard protocols (44). Briefly, mice were anaesthetized with isoflurane and underwent a 3-mm craniotomy over the lateral parietal cortex to expose the intact dura mater of the brain. A hollow injury cap was placed over the craniotomy and was secured by dental acrylic; the mouse was removed from anaesthesia and attached to the fluid percussion device via the injury cap. At first response of hind-limb withdrawal, the fluid percussion device delivered a fluid pulse of 1–1.5 atm to the brain. Upon resumption of spontaneous breathing, the injury cap was removed and the wound sutured. Sham-injury mice underwent the identical procedures as the LFPI mice with the exception of the delivery of the fluid pulse.

### Acute injury severity

Apnoea, hind-limb withdrawal and self-righting reflex times were monitored and recorded in all mice after injury as an indicator of acute injury severity (13,43). Apnoea was defined as the time from injury to spontaneous breathing, loss of consciousness was the time from injury to a hind-limb withdrawal response to a toe pinch, and self-righting reflex was the time from injury to the return of an upright position. Apnoea was observed in LFPI mice only ( $p < 0.001$ ), and increased durations of unconsciousness ( $p < 0.001$ ) and self-righting ( $p < 0.001$ ) were observed in LFPI mice compared to sham-injured mice (Table 1). There were no significant differences in injury severity measures between vehicle- and GA-treated mice.

### Behavioural testing

Mice underwent a series of behavioural tests in rotarod, open-field, elevated plus-maze (EPM) and Y-maze over a period of 3 days beginning at 1 day post-injury.

### Rotarod

The accelerated rotarod was used at 1-, 2- and 3-days post-injury to assess sensorimotor ability (44,45). The testing apparatus consisted of rotating barrels (diameter = 3 cm) in four consecutive lanes (diameter = 5 cm) separated by walls (diameter = 10 cm; Harvard Apparatus, Holliston, TX, USA). Mice completed training one day before injury followed by

**Table 1.** Acute injury severity outcomes in mice given SHAM or TBI and assigned to a VEH or GA-treatment group.

	Apnoea (s)	Hind-limb (s)	Self-righting (s)
SHAM-VEH	0	0	75.1 ± 7.0
SHAM-GA	0	0	83.0 ± 7.3
TBI-VEH	49.9 ± 3.3 <sup>a</sup>	253.6 ± 11.4 <sup>a</sup>	439.9 ± 13.2 <sup>a</sup>
TBI-GA	56.0 ± 3.8 <sup>a</sup>	256.1 ± 9.9 <sup>a</sup>	440.9 ± 16.9 <sup>a</sup>

<sup>a</sup>TBI significantly greater than sham-injured groups,  $p < 0.001$   
VEH, vehicle; GA, gambogic amide; TBI, traumatic brain injury.

three days of consecutive trials starting day 1 post-injury. Each trial consisted of the mouse being placed on the rotating barrel, the speed was increased from 4 to 40 rpm over a period of 5 min, and the average duration of time the mouse was able to stay on the rotating barrel was recorded for each trial period (maximum time of 5 min).

#### Open-field

One day post-injury mice underwent open-field testing to assess locomotion and anxiety-like behaviour as previously described (43,44). Briefly, the testing area consisted of a 100 cm diameter circular field surrounded by a 20 cm high plastic wall, with mice were individually placed in the centre of field and allowed to explore the arena for a 5-min test period. Using EthoVision<sup>®</sup> tracking software (Noldus, Leesburg, VA, USA) behaviour was recorded and quantified with the following parameters; time spent in inner field (66 cm diameter) and total distance travelled. Time spent in the inner field was a measure of anxiety-like behaviour in mice and total distance travelled in the field was as a measure of locomotion.

#### Elevated plus-maze

At two days post-injury mice completed EPM testing to assess anxiety-like behaviour (44,46). The testing apparatus consisted of four arms (length = 30 cm, width = 6 cm) shaped in a plus. Two opposing arms (closed-arms) had 15 cm high walls bounding them and the other two opposing arms (open-arms) had no walls. Mice were placed in the centre of the EPM facing the open-arm and allowed to explore the arena for 5 min. Behaviour was recorded using an overhead camera and was quantified using EthoVision<sup>®</sup> tracking software (Noldus). Decreased amount of time spent in the open-arm equated to increased anxiety-related behaviour in mice (44). Total distance travelled was used as a measure of locomotion.

#### Y-maze

Y-maze was completed at three days post-injury to assess spatial memory (44). The Y-maze testing apparatus consisted of three arms (length = 38 cm, width = 8 cm) enclosed by 13-cm high walls shaped in a Y-shape (San Diego Instruments, San Diego, CA, USA). Unique visual cues were placed at the distal end of each arm. Mice completed a 15-min training period prior to testing. During the training period, two of the arms remained open (start arm and old arm) and one of the three arms (novel arm) was blocked by a barrier. The mouse was given a 15-min interval period between training and testing. Commencing the 5-min testing period, the novel arm of the Y-maze was unblocked and the mouse was again placed in the start arm and allowed to freely explore all three arms. Behaviour was recorded using an overhead camera and analysed using EthoVision<sup>®</sup> tracking software (Noldus). Time spent exploring the novel and total distance travelled was used as a measure of spatial memory.

#### Brain tissue collection and preparation

Anesthetized mice (4% isoflurane for 1 min) were decapitated at 72 h post-injury. Brains were removed and dissected, and the tissue was rapidly frozen in liquid nitrogen and stored at  $-80^{\circ}\text{C}$ . One piece of brain tissue (~10 mg) from the ipsilateral cortex (IC) and hippocampus (IH) was collected for RT-PCR, with an adjacent region of IC (~5mg) collected for Western blot analysis.

#### RNA extraction and RT-PCR

Samples were homogenized in 600  $\mu\text{l}$  of PureZOL<sup>™</sup> RNA isolation reagent using Precellys<sup>™</sup> 24 Bead Mill Homogenizer (Bertin Technologies, Villeurbanne, France) at  $4^{\circ}\text{C}$ , before being centrifuged at 12,000 rpm for 20 min at  $4^{\circ}\text{C}$ . Lysate from each sample was collected ready for RNA extraction. RNA was extracted using the spin protocol in Aurum<sup>™</sup> Total RNA Fatty and Fibrous Tissue Kit (Bio-Rad Laboratories Inc., Hercules, USA) according to the manufacturer's instructions. Reverse transcription was performed from 600 ng of total RNA using iScript<sup>™</sup> cDNA Synthesis Kit (Bio-Rad) according to manufacturer's instructions. PCR was performed to quantify expression of genes associated with neuroinflammation (vimentin, GFAP, LCN2, Iba1, CD31, CD16), apoptosis (caspase-3), neurite outgrowth (GAP-43) and synaptogenesis (synaptophysin, synapsin, agrin) (see Table 2 for oligonucleotide primer sequences). Glyceraldehyde 3-phosphate dehydrogenase (GAPDH) was used as an internal control gene. RT-PCR was performed using SsoFast EvaGreen Supermix (Bio-Rad) on an iQ 96-well PCR system (Bio-Rad). Each amplification reaction contained 1  $\mu\text{l}$  of cDNA (30-ng input RNA) and 300 nM of primer and was performed in triplicate. Thermal cycling conditions included initial denaturation at  $95^{\circ}\text{C}$  for 30 s, followed by 40 cycles of  $95^{\circ}\text{C}$  for 5 s and  $55^{\circ}\text{C}$  for 5 s. Melt curve analysis was performed post-cycling to confirm specificity of the amplified products. Relative quantification of genes of interest mRNA expression was determined using the  $2^{-\Delta\Delta\text{Ct}}$  method.

#### Western blot analysis

Western blotting was used to detect expression of TrkA receptors, and phosphorylated-Akt, a downstream indicator of TrkA receptor activation. IC tissue was homogenized with RIPA-EDTA buffer with added protease and phosphatase cocktail inhibitors (43). To determine sample protein concentration, Pierce<sup>™</sup> BCA<sup>™</sup> Protein Assay Kit (Pierce Biotechnology, Rockford, USA) was used and, supernatant protein concentration was mixed [3:1 (v/v) ratio] with 4  $\times$  SDS loading buffer (Bio-Rad). Samples were heated at  $95^{\circ}\text{C}$  for 5 min, centrifuged, and then stored at  $-20^{\circ}\text{C}$  for Western blot analysis. Protein (10  $\mu\text{g}$ ) was loaded into each well and protein was separated using Precast Mini-PROTEAN<sup>™</sup> TGX<sup>™</sup> gel (Bio-Rad). Protein bands were transferred onto polyvinylidene difluoride (PVDF) membranes. Primary antibodies used included the following: anti-TrkA (1:1000, Abcam, Cambridge, UK, USA), anti-Akt (1:1000, Cell Signaling Technology, Danvers, USA) and anti-

Table 2. RT-PCR oligonucleotide name and sequence (5'–3').

Oligonucleotide name	Sequence (5'–3')
mGAPDH	Sense ATGACATCAAGAAGGTGGTG
	Anti-sense CATACCAGGAAATGAGCTTG
mVimentin	Sense GGCTGCCAACCGGAACAA
	Anti-sense CGCTCCAGGGACTCGTTA
mGFAP	Sense TCCTGGAAACAGCAAAACAAG
	Anti-sense CAGCCTCAGGTGGTTTCAT
mLCN2	Sense CCCCATCTGCTCACTGTC
	Anti-sense TTTTCTGGACCGCATTG
mIba1	Sense GGATTGACAGGAGGAAAA
	Anti-sense TGGGATCATCGAGGAATTG
mCD32	Sense AATCCTGCCGTTCTACTGATC
	Anti-sense GTGTCCACGGTCTTCTTGAG
mCD16	Sense TTGGACACCCAGATGTTTACG
	Anti-sense GTCTTCTGAGCACCTGGATC
mCaspase-3	Sense TGTCATCTCGCTCTGGTACG
	Anti-sense AAATGACCCCTTCATACCA
mGAP-43	Sense AGCCTAAACAAGCCGATGTG
	Anti-sense GCAGGAGAGACAGGGTTCAG
mSynaptophysin	Sense TGCCAACAAGACGGAG
	Anti-sense GGCGGATGAGCTAACT
mSynapsin	Sense CAGCACAAACATACCTGTGG
	Anti-sense GGTCTCCAGTTACCGACA
mAgrin	Sense CTTTGATGGCGGACCTACA
	Anti-sense GTGATAGCTGAGTTGCAGGT

phosphorylated-Akt (S438, 1:1000, Cell Signaling Technology). Signal detection was developed with chemiluminescent substrate kit (Clarity™ ECL Western Blotting Substrate, Bio-Rad). Immunoreactive bands were digitally imaged using Molecular Imager™ Chemidoc™ XRS+ (Bio-Rad) and results were quantified using Image Lab™ Software (Bio-Rad). Values were normalized for protein loading using  $\beta$ -actin as a loading control.

#### Statistical analysis

Rotarod data were analysed with a mixed design analysis of variance (ANOVA) using SPSS Statistics 22.0 software (IBM, New York, USA). All other outcomes were analysed with a two-way ANOVA, with Bonferroni *post-hoc* comparisons carried out when appropriate. Statistical analyses were performed using GraphPad Prism 6 software (GraphPad Software, Inc. La Jolla, CA, USA), with significance defined as  $p < 0.05$ .

## Results

### GA does not influence acute behavioural outcomes following LFPI

Rotarod analysis revealed that TBI mice spent significantly less time on the rotarod (Figure 1A,  $p < 0.01$ ), a measure of motor function, compared to sham-injured mice. There was also a significant effect for test day, with mice spending significantly more time on the rotarod during the third day of rotarod testing (Figure 1A,  $p < 0.001$ ). There was no effect of GA treatment on rotarod performance.

In the EPM, TBI mice had significantly reduced distance travelled (Figure 1C,  $p < 0.01$ ), a measure of locomotion, compared to sham-injured mice. Mice given a TBI also displayed a trend for spending increased time in the open arm of the EPM (Figure 1C,  $p = 0.0622$ ) compared to sham-injured mice. There was no GA-treatment effect on EPM measures.

Although no injury effect was seen in the Y-maze (Figure 1B), GA-treated mice had significantly reduced distance travelled (Figure 1B,  $p < 0.05$ ) and spent significantly less time (Figure 1B,  $p < 0.01$ ) in the novel arm compared to vehicle-treated mice.

No statistically significant differences were found in the open-field (Figure 1D).

### TBI causes down-regulation of TrkA receptor

Western blot analysis of mouse IC was performed to analyse the expression of TrkA receptors and activation of pro-survival pathways phosphorylated-Akt (p-Akt). At 72 h post-TBI, TrkA receptors were down regulated in TBI groups compared to sham groups (Figure 2A,  $p < 0.001$ ). GA did not alter the expression of TrkA receptors. There was no significant GA-treatment effect on p-Akt, yet there was a trend that TBI increased p-Akt (Figure 2B,  $p = 0.07$ ).

### GA did not attenuate the increase in neuroinflammatory markers following LFPI

PCR analysis of mouse IC and IH was performed to analyse the relative fold-change in genes commonly associated with neuroinflammation: vimentin, GFAP, LCN2, Iba1, CD32 and CD16. As seen in Figure 3, mice with TBI had significantly increased mRNA expression in both the IC and IH in all of the markers of neuroinflammation (vimentin, IC,  $p < 0.001$ , Figure 3A, IH  $p < 0.05$ , Figure 3G; GFAP, IC,  $p < 0.01$ , Figure 3B, IH  $p < 0.05$ , Figure 3H; LCN2, IC,  $p < 0.05$ , Figure 3C, IH,  $p < 0.05$ ; Iba1, Figure 3I, IC,  $p < 0.01$ , Figure 3D, IH,  $p < 0.01$ , Figure 3J; CD32, IC,  $p < 0.001$ , Figure 3E, IH,  $p < 0.05$ , Figure 3K; and CD16, IC,  $p < 0.05$ , Figure 3F, IH,  $p < 0.01$ , Fig. L) at 72 h post-injury compared with sham-injured groups. There was no significant GA-treatment effect on neuroinflammatory markers. GA-treated mice had significantly increased LCN2 expression in the IH (Figure 3I,  $p < 0.05$ ) but not in the IC compared to vehicle-treated mice.

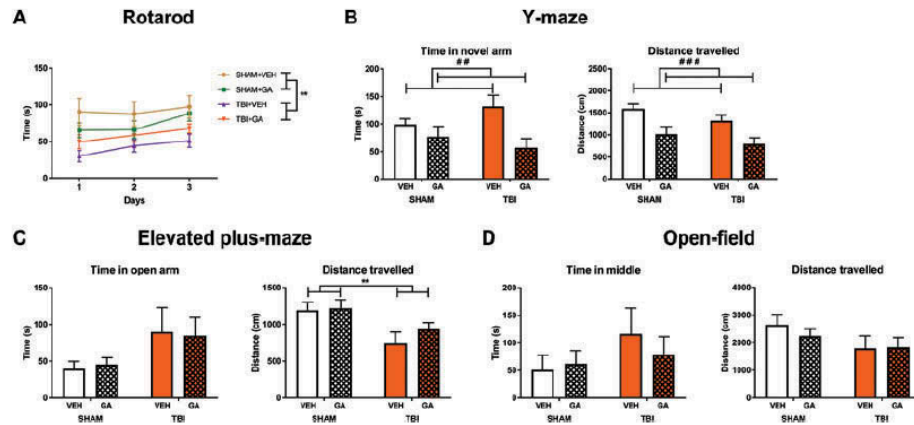


**Figure 1.** The effects of GA treatment on behavioural outcomes post-LFPI. **(A)** Rotarod testing found that LFPI groups had motor deficits compared to SHAM groups ( $p = 0.005$ ) as indicated by significantly less time spent on the rotarod during testing. GA treatment did not affect rotarod performance. **(B)** No injury effect was seen in the Y-Maze; however, mice treated with GA spent less time in the novel arm compared to vehicle-treated mice ( $p = 0.0095$ ). **(C)** There was a non-significant trend for LFPI mice spending more time in the open arm of the elevated-plus maze (EPM) compared to SHAM mice ( $p = 0.0622$ ). LFPI mice had a significant reduction in the distance travelled in the EPM ( $p = 0.0064$ ). There were no treatment effects on EPM measures. **(D)** No differences were found between groups in open-field. Data expressed as mean  $\pm$  SEM,  $n = 7$ /group. Double asterisk injury effect,  $p < 0.01$ , number sign treatment effect,  $## p < 0.01$ ;  $*** p < 0.001$ .

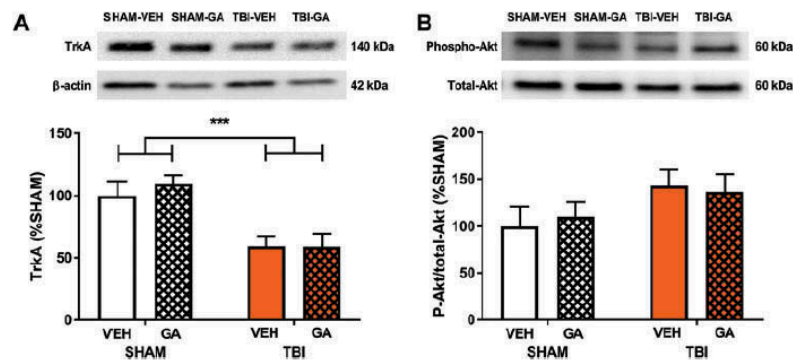


**Figure 2.** The effects of GA treatment on TrkA expression and phosphorylated-Akt activation post-LFPI. **(A)** Western blotting found LFPI caused a significant decrease in TrkA receptor expression compared to SHAM groups ( $p = 0.0001$ ). GA treatment did not affect TrkA expression. **(B)** There was a trend for LFPI to increase the pAkt/total Akt ratio compared with SHAM groups ( $p = 0.0735$ ). No differences were found following GA treatment. Data expressed as mean  $\pm$  SEM,  $n = 6$ /group. Triple asterisk injury effect,  $p < 0.001$ .

#### GA did not attenuate the increase in apoptosis marker caspase-3 following LFPI

PCR analysis of apoptotic marker; caspase-3, was assessed in mouse IC and IH. At 72 h post-injury there was an overall significant increase in caspase-3 expression in the IC (Figure 4A,  $p < 0.05$ ) and IH (Figure 4B,  $p < 0.01$ ) in mice with TBI compared to sham injury. GA did not alter expression of caspase-3.

#### Neurite sprouting and synaptogenic gene expression did not alter in response to LFPI or GA

Expression of markers associated with neurite outgrowth (GAP-43) and synaptogenesis (synaptophysin, synapsin and agrin) within the IC and IH was analysed. At 72 h post-injury, expression of GAP-43, synaptophysin and synapsin did not alter in response to TBI nor GA treatment in the IC and IH

(Figure 5A-C, E-G). Agrin mRNA expression was significantly increased in the IH (Figure 5H,  $p < 0.05$ ) of LFPI mice; however, GA treatment had no effect on agrin expression (Figure 5D, H).

#### Discussion

Previous studies have found that treatment with NGF reduced neuronal apoptosis (15,26), suppressed neuroinflammation (24,25), and improved cognitive outcomes in rodents with TBI (28,29,31). The pro-survival effects of NGF are thought to be mediated via TrkA activation (22), and TrkA activation has been shown to promote neurite outgrowth (35,47). High-affinity selective TrkA agonist, GA, has previously been shown to stimulate neurite outgrowth (36,48), prevent apoptosis of primary neurons *in vitro* (35), and through systemic

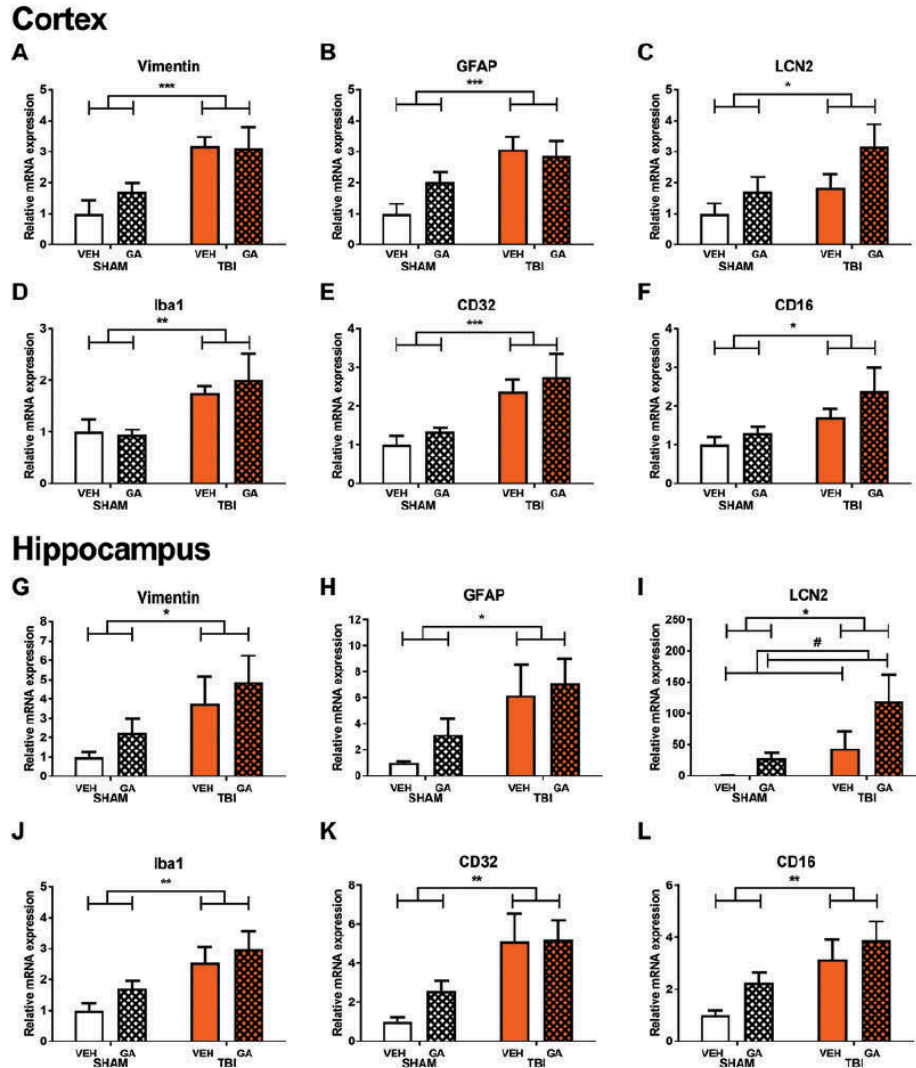


**Figure 3.** The effects of GA treatment on expression of markers of neuroinflammation post-LFPI. Cortex and hippocampus from mice with LFPI had significantly increased vimentin (A, G), GFAP (B, H), LCN2 (C, I), Iba1 (D, J), CD32 (E, K) and CD16 (F, L) at 72 h post-injury compared to sham-injured mice; however, treatment with GA did not alter the expression of these markers. LCN2 (C, I) expression was significantly increased in response to LFPI in the cortex and in the hippocampus. GA-treated groups had significantly increased LCN2 expression in the hippocampus ( $p < 0.05$ ) but not in the cortex compared to vehicle-treated groups. Data expressed as mean  $\pm$  SEM,  $n = 7$ /group. Asterix injury effect, \*  $p < 0.05$ ; \*\*  $p < 0.01$ ; \*\*\*  $p < 0.001$ .

delivery, protect neurons from kainic acid-induced apoptosis and reduce infarct volume following ischemic injury (35). Despite these findings, no studies have investigated the specific effects of GA treatment following TBI. Accordingly, in this study we used an LFPI model of TBI in mice to examine the effects of GA treatment on behavioural outcomes, neuroinflammation, apoptosis, neurite growth and synaptogenesis in the acute stages of TBI. Overall, our findings suggest that treatment with GA did not affect the TBI-induced changes in motor function, neuroinflammation or apoptosis at 72 h post-injury.

Our findings of TBI-induced motor deficits, as indicated by decreased time on the rotarod and decreased distance travelled in the EPM, are similar to findings of other experimental TBI studies (13,14,49). Treatment with GA did not attenuate motor deficits; a finding which is comparable to studies that have reported that NGF treatment did not improve post-TBI performance in an open wire grid (30), foot-fault test (50) and beam balance test (29,31).

We found that TBI did not affect novel arm preference in the Y-maze at 3 days post-injury. This lack of spatial memory deficit post-TBI may reflect the acute nature of the

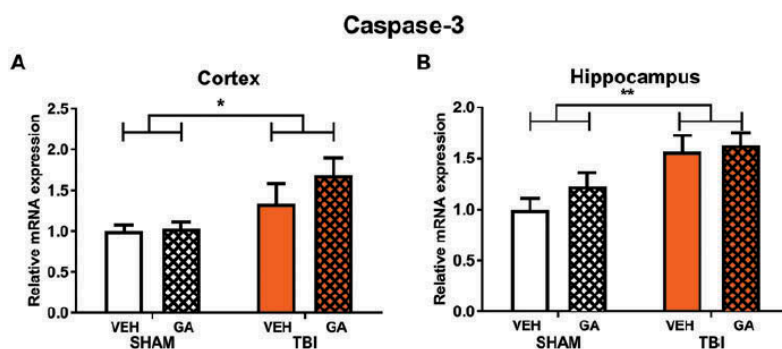


**Figure 4.** Expression of apoptosis marker caspase-3 in mouse cortex (A) and hippocampus (B) 72 h after LFPI or SHAM injury. Caspase-3 mRNA expression increased in mice with LFPI in the cortex ( $p < 0.05$ ) and hippocampus ( $p < 0.01$ ). GA treatment did not alter caspase-3 expression. Data expressed as mean  $\pm$  SEM,  $n = 7$ /group. Asterix injury effect, \*  $p < 0.05$ ; \*\*  $p < 0.01$ .

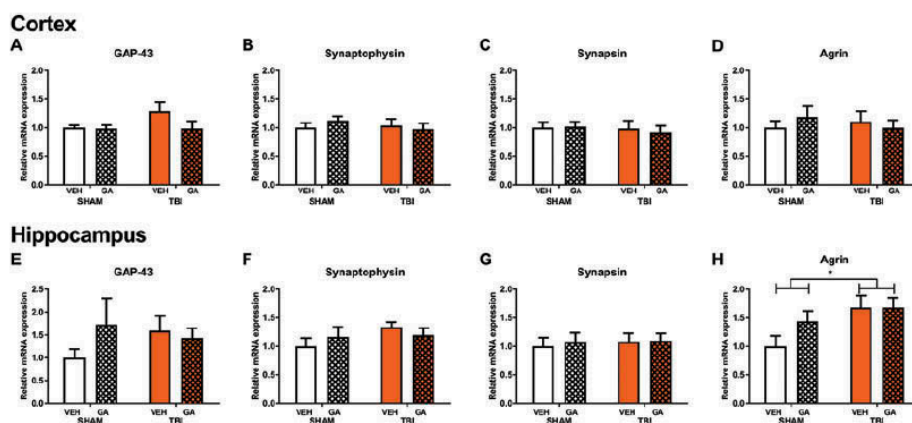


**Figure 5.** The effects of GA treatment on expression of markers of neurite sprouting and synaptogenesis post-LFPI. LFPI did not alter the mRNA expression of markers of neurite sprouting (GAP-43) and synaptogenesis (synaptophysin, synapsin) in mouse cortex (A–C) and hippocampus (E–G) at 72 h post-injury compared with sham-injured mice. Likewise, treatment with GA had no effect on the expression of neurite sprouting and synaptogenic markers compared to vehicle groups. The LFPI-injured mice had significantly increased agrin expression in the hippocampus (H), but not in the cortex (D), compared to sham-injured mice at 72 h post-injury (\* $p < 0.05$ ). GA treatment did not alter the expression of agrin compared to vehicle groups. Data expressed as mean  $\pm$  SEM,  $n = 7$ /group.

behavioural testing, with previous studies showing that neurodegeneration and hippocampal atrophy following a single LFPI in rodents takes weeks to months to fully manifest (51,52). The finding that GA-treated mice spent significantly less time in the novel arm compared to vehicle-treated mice may be contributed to by the fact that the GA-treated mice had travelled significantly less distance compared to vehicle-treated mice during Y-maze testing. However, no effects of GA treatment were observed on distance travelled and sensorimotor performance in the rotarod and open-field, which indicates that GA did not likely induce gross changes in sickness behaviour, motor ability or locomotion. As such, the possible influence of GA on spatial memory and locomotion warrants further investigation. While this is the first study to report the effects of GA on spatial memory outcomes in mice following acute TBI, several studies have investigated the effects of NGF on spatial cognition following experimental TBI (28–31). Behavioural testing during and at cessation of

NGF treatment following TBI reduced cognitive latencies and improved spatial memory in rodents at weeks 1 and 2 post-injury using the Morris water maze (28,29,31), but not at 1-, 2- and 3-days post-injury (28). Accordingly, future investigations may consider assessments on the influence of GA and NGF on spatial memory at later time-points post-injury.

Neuroinflammation is an important secondary injury mechanism that occurs after TBI (18). At 72 h post-TBI, there was an apparent increase in the neuroinflammatory response, with the increased expression of markers associated with astrocytic activation (vimentin, GFAP and LCN2) and reactive microglia (CD32, CD16 and Iba1) in the IC and IH of the TBI groups. These findings are similar to previous studies involving acute-phase analysis of brain tissue following LFPI (52–55), and provide evidence of a substantial neuroinflammatory response following LFPI in mice. Previous rodent TBI studies have shown NGF treatment to be beneficial in attenuating the cortical neuroinflammatory response by reducing



protein expression of pro-inflammatory cytokines TNF- $\alpha$  and IL-1 $\beta$  during the first 72 h post-injury (24,25). We found that GA treatment had no effect on the mRNA expression of the majority of neuroinflammatory markers compared to vehicle-treated groups (35). These findings may suggest that TrkA activation does not suppress neuroinflammation post-TBI, and that the previously reported anti-inflammatory effects of NGF post-TBI may not be mediated through TrkA signalling. Interestingly, we did however find that GA treatment increased LCN2 expression. Although increased LCN2 expression is associated with astrogliosis (56), this protein is expressed by a variety of cells, and increased expression has been previously associated with non-inflammatory processes such as angiogenesis (57), cell migration, iron transport and tissue regeneration (58,59). Furthermore, a recent study has shown that NGF treatment also increased expression of LCN2 (60). Therefore together with our finding, this may suggest that TrkA activation promotes expression of LCN2; however, further studies are required to establish this association and understand the possible impact of LCN2 up-regulation in both the uninjured and injured brain. Finally, as the neuroinflammatory response induced by TBI can persist well beyond the acute stages post-TBI, future studies may consider assessment of any effects of GA treatment at later time-points post-injury (42).

Neuronal apoptosis is another acute cellular response to TBI (61–63). Similar to other experimental TBI studies, we found that LFPI in mice increased the expression of the apoptotic marker caspase-3 at 72 h post-injury (64–66). GA treatment did not reduce expression of caspase-3 in TBI. This result was unexpected, as this treatment regime (2 mg GA/kg/day) has previously been shown to significantly reduce kainic acid-induced apoptosis in the hippocampus of mice and reduce infarct volume 24 h following ischemic injury (35). Furthermore, NGF treatment also strongly reduced caspase-3 expression following weight-drop TBI (24). Our findings suggest that GA did not prevent TBI-induced apoptosis; however, further analysis featuring multiple time-points and other measurements of apoptosis such as TUNEL-staining may provide further insight.

Neuronal and synaptic changes can begin in the hippocampus and cortex within 72 h of TBI (67). Neuronal sprouting is associated with elevations in mRNA and protein expression of GAP-43, synapsin, synaptophysin and agrin (67–71). GAP-43 is a marker of axonal cone formation during neurite sprouting (72), whereas synapsin, synaptophysin and agrin are markers of synaptogenesis (67,69,73). We report that GAP-43, synapsin and synaptophysin mRNA expression were not significantly altered in response to LFPI in the IC or IH at 72 h post-injury. This finding may be attributed to the early time-point analysed, with a previous study finding increased hippocampal synaptophysin and GAP-43 mRNA expression at 28- but not 7-days post-FPI (70). We did however find an effect of TBI on the expression of agrin, a protein associated with synaptogenesis that has similarly been shown to be up-regulated at 7 days post-FPI. Taken together, these findings suggest agrin may be a suitable marker of the early sprouting phase of synaptogenesis post-TBI (69). Finally, though several studies have shown NGF induces synaptogenesis and neurite

outgrowth (35,74–76), we observed no effect of GA treatment on markers of these processes at 72 h post-injury. These preliminary findings, together with our behavioural findings, suggest GA may not increase neurite outgrowth and synaptogenesis in the acute stages post-TBI; however, further analysis featuring multiple time-points and protein markers are required, particularly considering development and reestablishment of functioning circuits can take multiple weeks post-injury (77,78). Therefore, analysis of GA treatment on TBI long-term may reveal positive effects on neurogenesis and behavioural outcomes.

The lack of efficacy the GA observed in the current study may be attributed to the significant decrease in cortical TrkA expression observed in mice with TBI. Similarly, down-regulation of TrkB expression post-TBI has been found in several studies and hypothesized as possibly contributing to the lack of neuroprotection induced by exogenous BDNF treatment (79). Relatively few studies have investigated TrkA expression post-TBI, with the findings of these studies largely mixed (80–82). Therefore, further profiling of the temporal and regional expression patterns of TrkA expression post-TBI will provide greater insights into the potential suitability and timing of therapies targeting this signalling pathway.

Although we found no beneficial effects of GA treatment, this study does provide some novel characterization of the LFPI in mice. LFPI is most commonly used in rats (7); however, a small number of studies have recently demonstrated successful adaptation of this model to mice (44,83). One such study found that the same injury parameters used in this study produced substantial behavioural deficits, brain atrophy and astrogliosis at 3 months post-injury (44). The mortality rates (10–20%) and self-righting reflex (7–8 min) were very similar to the findings of the current study, and considered together, indicate that this TBI model is of moderate severity (44,83). It is however important to note that acute effects of this particular TBI model in mice have not been well characterized; therefore, our findings do provide some novel insights, particularly regarding the cortical and hippocampal neuroinflammatory response.

It is important to note that this study does contain limitations. Firstly, although we observed significant TBI-induced motor deficits and increased expression of several neuroinflammatory and apoptotic markers, a limitation of the single time-point approach is that we may have missed the peak activation of some processes and thus any beneficial effects of GA treatment. Although we used a dosing regimen of GA previously shown to improve outcomes following ischemic injury (35), it is possible that GA administered at higher doses or for a prolonged duration may have provided neuroprotection following TBI. As such, future studies should conduct dose-effect analyses in order to provide further insights on the efficacy of GA treatment. In addition, though we found no effects of GA treatment on behaviour and neuropathology during the first 72 h post-TBI, it is possible that GA has beneficial effects that may only be detectable at later time-points; however, it is noteworthy that several studies have shown beneficial effects of NGF during the early stages post-TBI (15,24,25,29,31,84). Furthermore, this study did not analyse brain concentrations of GA, and tissue collection at 24 h

following the final GA-treatment limited inferences that could be made on TrkA signalling; however, the work of Jang and colleagues provided strong evidence that GA does selectively activate TrkA signalling and can exert central neurotrophic effects (35). Nonetheless, additional work is needed to advance understanding of pharmacological profile and functionality of GA. Finally, due to the poor water solubility of GA, we used an emulsifying agent, Kolliphor<sup>®</sup> HS 15 (Solutol<sup>®</sup> HS 15) mixed with saline, as a vehicle to deliver GA. Solutol<sup>®</sup> HS 15 is widely used as a vehicle in veterinary and pre-clinical research; however, a recent study found preliminary evidence that Solutol<sup>®</sup> HS 15 may have neuroprotective properties, with mice treated with this vehicle found to have significantly reduced neuronal loss and infarct volume following ischemic injury (85). As such, the neuroprotective potential of GA may have been limited by the choice of vehicle; however, it is worth noting that in vehicle-treated mice we observed significant motor and pathophysiological changes induced by TBI, and that previous TBI studies using this vehicle found significant effects of treatment delivered in Solutol<sup>®</sup> HS 15 compared to vehicle alone (40,41). Future studies investigating the neuroprotective properties of GA should consider using alternative solvents. Finally, some significant GA-treatment effects were apparent in the current study, suggesting that dose of GA administered did enter the brain and exerted some behavioural and pathological effects. However, we did not determine blood and brain concentrations of GA, nor provide evidence of TrkA pathway activation. Therefore, in order to further establish a lack of GA efficacy in treating TBI, these factors should be determined in future studies. It is also important that this study should be replicated in our own and other laboratories, like all treatment studies should, to confirm the validity of the findings reported here.

## Conclusions

GA is a small, potent TrkA agonist that has previously been shown to penetrate the BBB, protect neurons from apoptosis and promote neurogenesis in the rodent brain. This study found that treatment with GA at a dose previously shown to reduce the effects of ischemic injury did not attenuate TBI-induced motor deficits, neuroinflammation or apoptosis. Future studies may consider analysis of the effects of GA at different doses or at later time-points post-injury.

## Funding

This work was supported by funding to SJM through the Understanding Disease RFA of La Trobe University and to SRS from the Australian National Health and Medical Research Council. No benefits in any form have been received or will be received from a commercial party related directly or indirectly to the content of this article.

## Author contribution statement

MRJ, BLG, SRS and SJM conceptualized and designed the experiments. SRS, MRJ, SJM and MS conducted the injury methods and administered treatments. MRJ and MS completed behavioural testing. MRJ, RDB, SJM,

JEC, CJT and MS completed post-mortem analysis. All authors contributed to the data interpretation and preparation of the manuscript.

## Declaration of interest statement

The authors report no declarations of interest.

## References

- Hyder AA, Wunderlich CA, Puvanachandra P, Gururaj G, Kobusingye OC. 2007. "The impact of traumatic brain injuries: a global perspective." *NeuroRehabilitation* 22(5): 341–53.
- Carroll LJ, Cassidy JD, Peloso PM, Borg J, von Holst H, Holm L, Paniak C, Pepin M. Injury WHOCTFoMTB.2004. "Prognosis for mild traumatic brain injury: results of the WHO Collaborating Centre Task Force on Mild Traumatic Brain Injury." *J Rehabil Med* 43: 84–105.
- Faden AI, Loane DJ. 2015. "Chronic neurodegeneration after traumatic brain injury: Alzheimer disease, chronic traumatic encephalopathy, or persistent neuroinflammation?" *Neurotherapeutics* 12 (1): 143–50. doi: 10.1007/s13311-014-0319-5.
- Rapoport MJ, McCullagh S, Shammi P, Feinstein A. 2005. "Cognitive impairment associated with major depression following mild and moderate traumatic brain injury." *J Neuropsychiatry Clin Neurosci* 17 (1): 61–65. doi: 10.1176/jnp.17.1.61.
- Blennow K, Hardy J, Zetterberg H. 2012. "The neuropathology and neurobiology of traumatic brain injury." *Neuron* 76 (5): 886–99. doi: 10.1016/j.neuron.2012.11.021.
- Ragnarsson KT. 2002. "Results of the NIH consensus conference on "rehabilitation of persons with traumatic brain injury"." *Restor Neurol Neurosci* 20(3–4): 103–08.
- Shultz SR, McDonald SJ, Vonder Haar C, Meconi A, Vink R, Van Donkelaar P, Taneja C, Iverson GL, Christie BR. 2016. "The potential for animal models to provide insight into mild traumatic brain injury: translational challenges and strategies." *Neurosci Biobehav Rev* 6: 396–414. doi: 10.1016/j.neubiorev.2016.09.014.
- Shoji H, Kaneko Y, Mabuchi T, Kibayashi K, Adachi N, Borlongan CV. 2010. "Genetic and histologic evidence implicates role of inflammation in traumatic brain injury-induced apoptosis in the rat cerebral cortex following moderate fluid percussion injury." *Neuroscience* 171 (4): 1273–82. doi: 10.1016/j.neuroscience.2010.10.018.
- Streit WJ, Mrak RE, Griffin WS. 2004. "Microglia and neuroinflammation: a pathological perspective." *J Neuroinflammation* 1 (1): 14. doi: 10.1186/1742-2094-1-14.
- Carson MJ, Thrash JC, Walter B. 2006. "The cellular response in neuroinflammation: the role of leukocytes, microglia and astrocytes in neuronal death and survival." *Clin Neurosci Res* 6 (5): 237–45. doi: 10.1016/j.cnr.2006.09.004.
- Hicks RR, Smith DH, Lowenstein DH, Saint Marie R, McIntosh TK. 1993. "Mild experimental brain injury in the rat induces cognitive deficits associated with regional neuronal loss in the hippocampus." *J Neurotrauma* 10 (4): 405–14. doi: 10.1089/neu.1993.10.405.
- Nimmo AJ, Cernak I, Heath DL, Hu X, Bennett CJ, Vink R. 2004. "Neurogenic inflammation is associated with development of edema and functional deficits following traumatic brain injury in rats." *Neuropeptides* 38 (1): 40–47. doi: 10.1016/j.npep.2003.12.003.
- Wright DK, Trezise J, Kamnaksh A, Bekdash R, Johnston LA, Ordridge R, Semple BD, Gardner AJ, Stanwell P, O'Brien TJ, et al. 2016. "Behavioral, blood, and magnetic resonance imaging biomarkers of experimental mild traumatic brain injury." *Sci Rep* 6: 28713. doi: 10.1038/srep28713.
- Xiong Y, Mahmood A, Chopp M. 2013. "Animal models of traumatic brain injury." *Nat Rev Neurosci* 14 (2): 128–42. doi: 10.1038/nrn3407.
- Sinson G, Perri BR, Trojanowski JQ, Flamm ES, McIntosh TK. 1997. "Improvement of cognitive deficits and decreased

- cholinergic neuronal cell loss and apoptotic cell death following neurotrophin infusion after experimental traumatic brain injury." *J Neurosurg* 86 (3): 511–18. doi: 10.3171/jns.1997.86.3.0511.
16. Fox GB, Fan L, Levesseur RA, Faden AI. 1998. "Sustained sensory/motor and cognitive deficits with neuronal apoptosis following controlled cortical impact brain injury in the mouse." *J Neurotrauma* 15 (8): 599–614. doi: 10.1089/neu.1998.15.599.
  17. Loane DJ, Faden AI. 2010. "Neuroprotection for traumatic brain injury: translational challenges and emerging therapeutic strategies." *Trends Pharmacol Sci* 31 (12): 596–604. doi: 10.1016/j.tips.2010.09.005.
  18. Kumar A, Loane DJ. 2012. "Neuroinflammation after traumatic brain injury: opportunities for therapeutic intervention." *Brain Behav Immun* 26 (8): 1191–201. doi: 10.1016/j.bbi.2012.06.008.
  19. Hellewell S, Semple BD, Morganti-Kossmann MC. 2016. "Therapies negating neuroinflammation after brain trauma." *Brain Res* 1640: (Pt A) 36–56. doi: 10.1016/j.brainres.2015.12.024.
  20. Levi-Montalcini R, Angeletti PU. 1968. "Nerve growth factor." *Physiol Rev* 48(3): 534–69.
  21. Levi-Montalcini R, Cohen S. 1956. "Vitro and in Vivo Effects of a Nerve Growth-Stimulating Agent Isolated from Snake Venom." *Proc Natl Acad Sci U S A* 42 (9): 695–99. doi: 10.1073/pnas.42.9.695.
  22. Yoon SO, Casaccia-Bonnel P, Carter B, Chao MV. 1998. "Competitive signaling between TrkA and p75 nerve growth factor receptors determines cell survival." *J Neurosci* 18(9): 3273–81.
  23. Reichardt LF. 2006. "Neurotrophin-regulated signalling pathways." *Philos Trans R Soc Lond B Biol Sci* 361 (1473): 1545–64. doi: 10.1098/rstb.2006.1894.
  24. Lv Q, Fan X, Xu G, Liu Q, Tian L, Cai X, Sun W, Wang X, Cai Q, Bao Y, et al. 2013. "Intranasal delivery of nerve growth factor attenuates aquaporins-4-induced edema following traumatic brain injury in rats." *Brain Res* 1493: 80–89. doi: 10.1016/j.brainres.2012.11.028.
  25. Lv Q, Lan W, Sun W, Ye R, Fan X, Ma M, Yin Q, Jiang Y, Xu G, Dai J, et al. 2014. "Intranasal nerve growth factor attenuates tau phosphorylation in brain after traumatic brain injury in rats." *Journal of the Neurological Sciences* 345 (1–2): 48–55. doi: 10.1016/j.jns.2014.06.037.
  26. Kromer LF. 1987. "Nerve growth factor treatment after brain injury prevents neuronal death." *Science* 235 (4785): 214–16. doi: 10.1126/science.3798108.
  27. Sinson G, Voddi M, McIntosh TK. 1995. "Nerve Growth Factor Administration Attenuates Cognitive but Not Neurobehavioral Motor Dysfunction or Hippocampal Cell Loss Following Fluid-Perfusion Brain Injury in Rats." *Journal of Neurochemistry* 65 (5): 2209–16. doi: 10.1046/j.1471-4159.1995.65052209.x.
  28. Tian L, Guo R, Yue X, Lv Q, Ye X, Wang Z, Chen Z, Wu B, Xu G, Liu X. 2012. "Intranasal administration of nerve growth factor ameliorate  $\beta$ -amyloid deposition after traumatic brain injury in rats." *Brain Research* 1440: 47–55. doi: 10.1016/j.brainres.2011.12.059.
  29. Dixon CE, Flinn P, Bao J, Venya R, Hayes RL. 1997. "Nerve growth factor attenuates cholinergic deficits following traumatic brain injury in rats." *Exp Neurol* 146 (2): 479–90. doi: 10.1006/exnr.1997.6557.
  30. Longhi I, Watson DJ, Saatman KE, Thompson HJ, Zhang C, Fujimoto S, Royo N, Castelbuono D, Raghupathi R, Trojanowski JQ, et al. 2004. "Ex vivo gene therapy using targeted engraftment of NGF-expressing human NT2N neurons attenuates cognitive deficits following traumatic brain injury in mice." *J Neurotrauma* 21 (12): 1723–36. doi: 10.1089/neu.2004.21.1723.
  31. Sinson G, Voddi M, McIntosh TK. 1995. "Nerve growth factor administration attenuates cognitive but not neurobehavioral motor dysfunction or hippocampal cell loss following fluid-perfusion brain injury in rats." *J Neurochem* 65 (5): 2209–16. doi: 10.1046/j.1471-4159.1995.65052209.x.
  32. Tria MA, Fusco M, Vantini G, Mariot R. 1994. "Pharmacokinetics of nerve growth factor (NGF) following different routes of administration to adult rats." *Exp Neurol* 127 (2): 178–83. doi: 10.1006/exnr.1994.1093.
  33. Friden PM, Walus LR, Watson P, Doctrow SR, Kozarich JW, Backman C, Bergman H, Hoffer B, Bloom F, Granholm AC. 1993. "Blood-brain barrier penetration and in vivo activity of an NGF conjugate." *Science* 259 (5093): 373–77. doi: 10.1126/science.8420006.
  34. Angeletti RH, Aneletti PU, Levi-Montalcini R. 1972. "Selective accumulation of (125 I) labelled nerve growth factor in sympathetic ganglia." *Brain Res* 46: 421–25. doi: 10.1016/0006-8993(72)90033-9.
  35. Jang SW, Okada M, Sayeed I, Xiao G, Stein D, Jin P, Ye K. 2007. "Gambogic amide, a selective agonist for TrkA receptor that possesses robust neurotrophic activity, prevents neuronal cell death." *Proc Natl Acad Sci U S A* 104 (41): 16329–34. doi: 10.1073/pnas.0706662104.
  36. Shen J, Yu Q. 2015. "Gambogic amide selectively upregulates TrkA expression and triggers its activation." *Pharmacol Rep* 67 (2): 217–23. doi: 10.1016/j.pharep.2014.09.002.
  37. Chan CB, Liu X, Jang SW, Hsu SI, Williams I, Kang S, Chen J, Ye K. 2009. "NGF inhibits human leukemia proliferation by down-regulating cyclin A1 expression through promoting acinus/CBP2 association." *Oncogene* 28 (43): 3825–36. doi: 10.1038/onc.2009.236.
  38. Scheller KJ, Williams SJ, Lawrence AJ, Jarrott B, Djouma E. 2014. "An improved method to prepare an injectable microemulsion of the galanin-receptor 3 selective antagonist, SNAP 37889, using Kolliphor(R) HS 15." *MethodsX* 1: 212–16. doi: 10.1016/j.mex.2014.09.003.
  39. Scheller KJ, Williams SJ, Lawrence AJ, Djouma E. 2017. "The galanin-3 receptor antagonist, SNAP 37889, suppresses alcohol drinking and morphine self-administration in mice." *Neuropharmacology* 118: 1–12. doi: 10.1016/j.neuropharm.2017.03.004.
  40. Yang Y, Salayandia VM, Thompson JF, Yang LY, Estrada EY, Yang Y. 2015. "Attenuation of acute stroke injury in rat brain by minocycline promotes blood-brain barrier remodeling and alternative microglia/macrophage activation during recovery." *J Neuroinflammation* 12: 26. doi: 10.1186/s12974-015-0245-4.
  41. Singleton RH, Yan HQ, Fellows-Mayle W, Dixon CE. 2010. "Resveratrol attenuates behavioral impairments and reduces cortical and hippocampal loss in a rat controlled cortical impact model of traumatic brain injury." *J Neurotrauma* 27 (6): 1091–99. doi: 10.1089/neu.2010.1291.
  42. Simon DW, McGeachy MJ, Bayir H, Clark RS, Loane DJ, Kochanek PM. 2017. "The far-reaching scope of neuroinflammation after traumatic brain injury." *Nat Rev Neurol* 13 (3): 171–91. doi: 10.1038/nrneurol.2017.13.
  43. Shultz SR, Sun M, Wright DK, Brady RD, Liu S, Beynon S, Schmidt SF, Kaye AH, Hamilton JA, O'Brien TJ, et al. 2015. "Tibial fracture exacerbates traumatic brain injury outcomes and neuroinflammation in a novel mouse model of multitrauma." *J Cereb Blood Flow Metab* 35 (8): 1339–47. doi: 10.1038/jcbfm.2015.56.
  44. Shultz SR, Tan XL, Wright DK, Liu SJ, Semple BD, Johnston L, Jones NC, Cook AD, Hamilton JA, O'Brien TJ. 2014. "Granulocyte-macrophage colony-stimulating factor is neuroprotective in experimental traumatic brain injury." *J Neurotrauma* 31 (10): 976–83. doi: 10.1089/neu.2013.3106.
  45. Hamm RJ, Pike BR, O'Dell DM, Lyeth BG, Jenkins LW. 1994. "The rotarod test: an evaluation of its effectiveness in assessing motor deficits following traumatic brain injury." *J Neurotrauma* 11 (2): 187–96. doi: 10.1089/neu.1994.11.187.
  46. Johnstone VP, Wright DK, Wong K, O'Brien TJ, Rajan R, Shultz SR. 2015. "Experimental Traumatic Brain Injury Results in Long-Term Recovery of Functional Responsiveness in Sensory Cortex but Persisting Structural Changes and Sensorimotor, Cognitive, and Emotional Deficits." *J Neurotrauma* 32 (17): 1333–46. doi: 10.1089/neu.2014.3785.
  47. Sofroniew MV, Howe CL, Mobley WC. 2001. "Nerve growth factor signaling, neuroprotection, and neural repair." *Annu Rev Neurosci* 24: 1217–81. doi: 10.1146/annurev.neuro.24.1.1217.

48. Shah AG, Friedman MJ, Huang S, Roberts M, Xj L, Li S. 2009. "Transcriptional dysregulation of TrkA associates with neurodegeneration in spinocerebellar ataxia type 17." *Hum Mol Genet* 18 (21): 4141–52. doi: [10.1093/hmg/ddp363](https://doi.org/10.1093/hmg/ddp363).
49. Li S, Kuroiwa T, Ishibashi S, Sun L, Endo S, Ohno K. 2006. "Transient cognitive deficits are associated with the reversible accumulation of amyloid precursor protein after mild traumatic brain injury." *Neurosci Lett* 409 (3): 182–86. doi: [10.1016/j.neulet.2006.09.054](https://doi.org/10.1016/j.neulet.2006.09.054).
50. Young J, Pionk T, Hiatt I, Geeck K, Smith JS. 2015. "Environmental enrichment aides in functional recovery following unilateral controlled cortical impact of the forelimb sensorimotor area however intranasal administration of nerve growth factor does not." *Brain Res Bull* 115: 17–22. doi: [10.1016/j.brainresbull.2015.04.003](https://doi.org/10.1016/j.brainresbull.2015.04.003).
51. Shultz SR, Wright DK, Zheng P, Stuchbery R, Liu SJ, Sashindranath M, Medcalf RL, Johnston LA, Hovens CM, Jones NC, et al. 2015. "Sodium selenate reduces hyperphosphorylated tau and improves outcomes after traumatic brain injury." *Brain* 138 (Pt 5): 1297–313. doi: [10.1093/brain/awv053](https://doi.org/10.1093/brain/awv053).
52. Bao F, Shultz SR, Hepburn JD, Omana V, Weaver LC, Cain DP, Brown A. 2012. "A CD11d monoclonal antibody treatment reduces tissue injury and improves neurological outcome after fluid percussion brain injury in rats." *J Neurotrauma* 29 (14): 2375–92. doi: [10.1089/neu.2012.2408](https://doi.org/10.1089/neu.2012.2408).
53. Shultz SR, MacFabe DF, Foley KA, Taylor R, Cain DP. 2012. "Sub-concussive brain injury in the Long-Evans rat induces acute neuroinflammation in the absence of behavioral impairments." *Behav Brain Res* 229 (1): 145–52. doi: [10.1016/j.bbr.2011.12.015](https://doi.org/10.1016/j.bbr.2011.12.015).
54. Dietrich WD, Truettner J, Zhao W, Alonso OF, Busto R, Ginsberg MD. 1999. "Sequential changes in glial fibrillary acidic protein and gene expression following parasagittal fluid-percussion brain injury in rats." *J Neurotrauma* 16 (7): 567–81. doi: [10.1089/neu.1999.16.567](https://doi.org/10.1089/neu.1999.16.567).
55. Rall JM, Matzilevich DA, Dash PK. 2003. "Comparative analysis of mRNA levels in the frontal cortex and the hippocampus in the basal state and in response to experimental brain injury." *Neuropathol Appl Neurobiol* 29 (2): 118–31. doi: [10.1046/j.1365-2990.2003.00439.x](https://doi.org/10.1046/j.1365-2990.2003.00439.x).
56. Bi F, Huang C, Tong J, Qiu G, Huang B, Wu Q, Li F, Xu Z, Bowser R, Xia XG, et al. 2013. "Reactive astrocytes secrete lcn2 to promote neuron death." *Proc Natl Acad Sci U S A* 110 (10): 4069–74. doi: [10.1073/pnas.1218497110](https://doi.org/10.1073/pnas.1218497110).
57. Wu L, Du Y, Lok J, Lo EH, Xing C. 2015. "Lipocalin-2 enhances angiogenesis in rat brain endothelial cells via reactive oxygen species and iron-dependent mechanisms." *J Neurochem* 132 (6): 622–28. doi: [10.1111/jnc.13023](https://doi.org/10.1111/jnc.13023).
58. Lee S, Jha MK, Suk K. 2015. "Lipocalin-2 in the Inflammatory Activation of Brain Astrocytes." *Crit Rev Immunol* 35 (1): 77–84. doi: [10.1615/CritRevImmunol.2015012127](https://doi.org/10.1615/CritRevImmunol.2015012127).
59. Suk K. 2016. "Lipocalin-2 as a therapeutic target for brain injury: an astrocentric perspective." *Prog Neurobiol* 144: 158–72. doi: [10.1016/j.pneurobio.2016.08.001](https://doi.org/10.1016/j.pneurobio.2016.08.001).
60. Kao TH, Peng YJ, Salter DM, Lee HS. 2015. "Nerve growth factor increases MMP9 activity in annulus fibrosus cells by upregulating lipocalin 2 expression." *Eur Spine J* 24 (9): 1959–68. doi: [10.1007/s00586-014-3675-2](https://doi.org/10.1007/s00586-014-3675-2).
61. Rink A, Fung KM, Trojanowski JQ, Lee VM, Neugebauer E, McIntosh TK. 1995. "Evidence of apoptotic cell death after experimental traumatic brain injury in the rat." *Am J Pathol* 147(6): 1575–83.
62. Raghupathi R, Graham DI, McIntosh TK. 2000. "Apoptosis after traumatic brain injury." *J Neurotrauma* 17 (10): 927–38. doi: [10.1089/neu.2000.17.927](https://doi.org/10.1089/neu.2000.17.927).
63. Conti AC, Raghupathi R, Trojanowski JQ, McIntosh TK. 1998. "Experimental brain injury induces regionally distinct apoptosis during the acute and delayed post-traumatic period." *J Neurosci* 18(15): 5663–72.
64. Yakovlev AG, Knoblach SM, Fan L, Fox GB, Goodnight R, Faden AI. 1997. "Activation of CPP32-like caspases contributes to neuronal apoptosis and neurological dysfunction after traumatic brain injury." *J Neurosci* 17(19): 7415–24.
65. Yakovlev AG, Ota K, Wang G, Movsesyan V, Bao WL, Yoshihara K, Faden AI. 2001. "Differential expression of apoptotic protease-activating factor-1 and caspase-3 genes and susceptibility to apoptosis during brain development and after traumatic brain injury." *J Neurosci* 21(19): 7439–46.
66. Beer R, Franz G, Srinivasan A, Hayes RL, Pike BR, Newcomb JK, Zhao X, Schmutzhard E, Poewe W, Kampfl A. 2000. "Temporal profile and cell subtype distribution of activated caspase-3 following experimental traumatic brain injury." *J Neurochem* 75 (3): 1264–73. doi: [10.1046/j.1471-4159.2000.0751264.x](https://doi.org/10.1046/j.1471-4159.2000.0751264.x).
67. Thompson SN, Gibson TR, Thompson BM, Deng Y, Hall ED. 2006. "Relationship of calpain-mediated proteolysis to the expression of axonal and synaptic plasticity markers following traumatic brain injury in mice." *Exp Neurol* 201 (1): 253–65. doi: [10.1016/j.expneurol.2006.04.013](https://doi.org/10.1016/j.expneurol.2006.04.013).
68. Hulsebosch CE, DeWitt DS, Jenkins LW, Prough DS. 1998. "Traumatic brain injury in rats results in increased expression of Gap-43 that correlates with behavioral recovery." *Neurosci Lett* 255 (2): 83–86. doi: [10.1016/S0304-3940\(98\)00712-5](https://doi.org/10.1016/S0304-3940(98)00712-5).
69. Faló MC, Reeves TM, Phillips LL. 2008. "Agrin expression during synaptogenesis induced by traumatic brain injury." *J Neurotrauma* 25 (7): 769–83. doi: [10.1089/neu.2008.0511](https://doi.org/10.1089/neu.2008.0511).
70. Hall KD, Lifshitz J. 2010. "Diffuse traumatic brain injury initially attenuates and later expands activation of the rat somatosensory whisker circuit concomitant with neuroplastic responses." *Brain Res* 1323: 161–73. doi: [10.1016/j.brainres.2010.01.067](https://doi.org/10.1016/j.brainres.2010.01.067).
71. Ding JY, Kreipke CW, Schafer P, Schafer S, Speirs SI, Rafols JA. 2009. "Synapse loss regulated by matrix metalloproteinases in traumatic brain injury is associated with hypoxia inducible factor-1alpha expression." *Brain Res* 1268: 125–34. doi: [10.1016/j.brainres.2009.02.060](https://doi.org/10.1016/j.brainres.2009.02.060).
72. Benowitz LI, Routtenberg A. 1997. "GAP-43: an intrinsic determinant of neuronal development and plasticity." *Trends Neurosci* 20(2): 84–91.
73. Chin LS, Li L, Ferreira A, Ks K, Greengard P. 1995. "Impairment of axonal development and of synaptogenesis in hippocampal neurons of synapsin I-deficient mice." *Proc Natl Acad Sci U S A* 92 (20): 9230–34. doi: [10.1073/pnas.92.20.9230](https://doi.org/10.1073/pnas.92.20.9230).
74. Garofalo L, Ribeiro-da-Silva A, Cuéllar AC. 1992. "Nerve growth factor-induced synaptogenesis and hypertrophy of cortical cholinergic terminals." *Proc Natl Acad Sci U S A* 89 (7): 2639–43. doi: [10.1073/pnas.89.7.2639](https://doi.org/10.1073/pnas.89.7.2639).
75. Burgos I, Cuéllar AC, Liberini P, Pioro E, Masliah E. 1995. "NGF-mediated synaptic sprouting in the cerebral cortex of lesioned primate brain." *Brain Res* 692 (1–2): 154–60. doi: [10.1016/0006-8993\(95\)00696-N](https://doi.org/10.1016/0006-8993(95)00696-N).
76. Tuszynski MH, Sang H, Yoshida K, Fh G. 1991. "Recombinant human nerve growth factor infusions prevent cholinergic neuronal degeneration in the adult primate brain." *Ann Neurol* 30 (5): 625–36. doi: [10.1002/ana.410300502](https://doi.org/10.1002/ana.410300502).
77. Wieloch T, Nikolich K. 2006. "Mechanisms of neural plasticity following brain injury." *Curr Opin Neurobiol* 16 (3): 258–64. doi: [10.1016/j.conb.2006.05.011](https://doi.org/10.1016/j.conb.2006.05.011).
78. Nudo RJ. 2003. "Adaptive plasticity in motor cortex: implications for rehabilitation after brain injury." *J Rehabil Med* 41: 7–10. doi: [10.1080/16501960310010070](https://doi.org/10.1080/16501960310010070).
79. Conte V, Raghupathi R, Watson DJ, Fujimoto S, Royo NC, Marklund N, Stocchetti N, McIntosh TK. 2008. "TrkB gene transfer does not alter hippocampal neuronal loss and cognitive deficits following traumatic brain injury in mice." *Restor Neurol Neurosci* 26(1): 45–56.
80. Oyesiku NM, Evans CO, Houston S, Darrell RS, Smith JS, Fulop ZL, Dixon CE, Stein DG. 1999. "Regional changes in the expression of neurotrophic factors and their receptors following acute traumatic brain injury in the adult rat brain." *Brain Res* 833 (2): 161–72. doi: [10.1016/S0006-8993\(99\)01501-2](https://doi.org/10.1016/S0006-8993(99)01501-2).
81. O'Dell DM, Raghupathi R, Crino PB, Eberwine JH, McIntosh TK. 2000. "Traumatic brain injury alters the molecular fingerprint of

- TUNEL-positive cortical neurons In vivo: A single-cell analysis." *J Neurosci* 20(13): 4821–28.
82. Cekic M, Johnson SJ, Bhatt VH, Stein DG. 2012. "Progesterone treatment alters neurotrophin/proneurotrophin balance and receptor expression in rats with traumatic brain injury." *Restor Neurol Neurosci* 30(2): 115–26.
83. Alder J, Fujioka W, Lifshitz J, Crockett DP, Thakker-Varia S. 2011. "Lateral fluid percussion: model of traumatic brain injury in mice." *J Vis Exp* 22(54). pii: 3063. doi:10.3791/3063.
84. Tian L, Guo R, Yue X, Lv Q, Ye X, Wang Z, Chen Z, Wu B, Xu G, Liu X. 2012. "Intranasal administration of nerve growth factor ameliorate beta-amyloid deposition after traumatic brain injury in rats." *Brain Res* 1440: 47–55. doi: 10.1016/j.brainres.2011.12.059.
85. Lin HW, Saul I, Gresia VL, Neumann JT, Dave KR, Perez-Pinzon MA. 2014. "Fatty acid methyl esters and Solutol HS 15 confer neuroprotection after focal and global cerebral ischemia." *Transl Stroke Res* 5 (1): 109–17. doi: 10.1007/s12975-013-0276-z.

## Appendix C

### Chapter 4

Publication: Johnstone M. R., Brady R. D., Schuijers J. A., Church J. E., Orr D., Quinn J. M. W., McDonald S. J., Grills B. L. The selective TrkA agonist, gambogic amide, promotes osteoblastic differentiation and improves fracture healing in mice. *Journal of Musculoskeletal and Neuronal Interactions*. 2019 19(1) 94-103. PMID: 30839307 PMCID: PMC6454248.

- I performed all the treatment administration and post-mortem fibular collections.
- I performed all the histological assessment.
- I performed ~75% of the biomechanical assessment, with assistance from Dr Stuart McDonald and Dr David Orr.
- I performed ~85% of the  $\mu$ CT analysis, with assistance from Dr Rhys Brady.
- I performed ~85% of the cell culture, with assistance from Dr Jarrod Church and Dr Julian Quinn.
- I wrote the first full draft of the manuscript.
- Dr Brian Grills performed all bilateral fibular fracture surgeries and osmotic pump insertion.
- Dr Brian Grills, Dr Stuart McDonald, Dr Johannes Schuijers assisted with data analysis and provided revision of manuscript.

Dates and persons/organisations who gave permission to include these publications are:

**Chapter 4:** Stavroula Rizou, HELIOS

2<sup>nd</sup> October 2020

## Original Article

# The selective TrkA agonist, gambogic amide, promotes osteoblastic differentiation and improves fracture healing in mice

Maddison R. Johnstone<sup>1</sup>, Rhys D. Brady<sup>1,2</sup>, Johannes A. Schuijers<sup>1</sup>, Jarrod E. Church<sup>1</sup>, David Orr<sup>1</sup>, Julian M.W. Quinn<sup>3</sup>, Stuart J. McDonald<sup>1,\*</sup>, Brian L. Grills<sup>1,\*</sup>

<sup>1</sup>Department of Physiology, Anatomy and Microbiology, School of Life Sciences, La Trobe University, Melbourne, Australia;

<sup>2</sup>Departments of Neuroscience and Medicine, Central Clinical School, Monash University, Melbourne, Australia;

<sup>3</sup>Bone Research Division, Garvan Institute of Medical Research, Darlinghurst, Australia

\* Joint Senior Authors

## Abstract

**Objectives:** To study effects of the selective TrkA agonist, gambogic amide (GA), on fracture healing in mice and on an osteoprogenitor cell line *in vitro*. **Methods:** Mice were given bilateral fibular fractures and treated for two weeks with vehicle or 1 mg/kg/day GA and euthanized at 14-, 21-, and 42-days post-fracture. Calluses were analysed by micro-computed tomography ( $\mu$ CT), three-point bending and histology. For RT-PCR analyses, Kusa O cells were treated with 0.5nM of GA or vehicle for 3, 7, and 14 days, while for mineralization assessment, cells were treated for 21 days. **Results:**  $\mu$ CT analysis found that 21-day GA-treated calluses had both decreased tissue volume ( $p < 0.05$ ) and bone surface ( $p < 0.05$ ) and increased fractional bone volume ( $p < 0.05$ ) compared to controls. Biomechanical analyses of 42-day calluses revealed that GA treatment increased stiffness per unit area by 53% ( $p < 0.01$ ) and load per unit area by 52% ( $p < 0.01$ ). GA treatment increased Kusa O gene expression of alkaline phosphatase and osteocalcin ( $p < 0.05$ ) by 14 days as well as mineralization at 21 days ( $p < 0.05$ ). **Conclusions:** GA treatment appeared to have a beneficial effect on fracture healing at 21- and 42-days post-fracture. The exact mechanism is not yet understood but may involve increased osteoblastic differentiation and matrix mineralization.

**Keywords:** Nerve Growth Factor, TrkA Agonist, Fracture Healing, Bone

## Introduction

Poor bone fracture healing is a common clinical problem that severely affects the quality of life to patients, particularly in the case of non-union (i.e., failure to join the broken bone surfaces) which frequently necessitates surgery<sup>1-3</sup>. Most fractures heal successfully within 2 months, but delayed and non-union fractures affect approximately 5-10% of all patients worldwide<sup>3,4</sup>. However, there are few non-surgical

options available to improve patient outcomes and avoid non-union. One approach for identifying novel therapeutic agents that improve healing is to investigate biological mechanisms that underlie proper fracture union; such mechanisms include re-establishment of adequate blood supply and innervation of the fracture site<sup>1,2,5,6</sup>. In particular, it is notable that both sensory and sympathetic innervation during fracture healing improves both mineral callus composition and mechanical strength<sup>6-8</sup>. Nerve sprouting rapidly increases in the periosteum and callus in early stages of fracture healing, and several studies have shown that reduced fracture site innervation result in significantly larger calluses that have low bone mineral content and are consequently mechanically weaker than calluses in appropriately innervated fractures<sup>6-11</sup>. Accordingly, non-surgical treatments for fracture healing that increase both bone formation and innervation may improve bone healing and reduce the chance of delayed union (or non-union) of fractured bone.

The authors have no conflict of interest.

Corresponding author: Brian L. Grills, Department of Physiology, Anatomy and Microbiology, La Trobe University, Melbourne, VIC, 3083, Australia  
E-mail: brian.grills@latrobe.edu.au

Edited by: G. Lyritis

Accepted 18 December 2018



Nerve growth factor (NGF) is a neurotrophin responsible for growth and maintenance of sympathetic and sensory neurons in the peripheral nervous system<sup>12</sup>, and exerts its effects via two receptors: the high-affinity/pro-growth and survival receptor TrkA, or the low-affinity/pro-apoptotic receptor, p75NTR<sup>13,14</sup>. Several studies in rodents have identified a beneficial role for NGF treatment in fracture healing and distraction osteogenesis, showing that topical administration of NGF increased sympathetic neurite outgrowth, accelerated the transition of immature woven bone to mature lamellar bone, increased mineralised bone within healing callus and improved mechanical properties of fractures<sup>15-19</sup>. Additionally, during fracture healing, both NGF and TrkA have been detected in skeletal cells, which include bone-forming osteoblasts and osteoprogenitor cells (precursor cells of osteoblasts) as well as cartilage-forming chondrocytes<sup>20-22</sup>. Osteoblastic MC3T3-E1 cells in an *in vitro* study also responded to NGF treatment with increased migration and greater osteoblastic differentiation, indicated by expression of alkaline phosphatase (ALP) and type 1 collagen<sup>23</sup>. Taken together, these findings suggest that in addition to promoting re-innervation of the fracture site, NGF may directly promote bone formation and this may enhance fracture healing.

While NGF has shown promise in pre-clinical studies, it shows poor pharmacokinetic properties, which severely limit its potential as a therapeutic agent. NGF is susceptible to proteolytic degradation and has a short elimination half-life (~2 h) following systemic administration<sup>24-26</sup>. Therefore, use of small, non-peptide neurotrophic mimetics may be a superior approach. Gambogic amide (GA) is a non-peptide molecule that has been shown to have selective high affinity for TrkA receptors and is tolerated *in vivo*<sup>27-29</sup>. Systemic administration of 2 mg/kg/day of GA in mice selectively induced TrkA activation in hippocampal neurons, reduced infarct size in a model of ischemic stroke and increased neurite outgrowth in PC12 cells<sup>27-30</sup>. However, to date, no studies have investigated the potential of GA treatment on fracture healing. Accordingly, we investigated the effects of GA on the structural and mechanical features of healing fractures in mice, and on osteoprogenitor cell differentiation and mineralization *in vitro*.

## Methods

### Animals

Eighty C57BL/6 male mice were used throughout this work and were supplied by the La Trobe University animal breeding facility. Mice were sixteen weeks of age at time of experimentation, were housed in groups of 4-5 during the experiment under a 12 h light/dark cycle and had access to food and water *ad libitum*. All experimental procedures were approved by the La Trobe University Animal Ethics Committee (AEC-13-03 and AEC 15-73), were within the guidelines of the Australian code of practice for the care and use of animals for scientific purposes by the Australian National

Health and Medical Research Council, and in compliance with the ARRIVE guidelines for how to report animal experiments.

### Experimental groups

All mice received bilateral fibular fractures. To assess the effects of GA (1 mg/kg/day) on fracture healing, mice were randomly assigned to receive DMSO-vehicle (controls) or GA treatment. Treatment was subcutaneously delivered via mini-osmotic pumps at a rate of 0.25  $\mu$ l/h for 14 days. It has been previously shown that intraperitoneal injections of GA at doses ranging from 0.35-4 mg/kg/day resulted in increased TrkA phosphorylation in both central<sup>29,31</sup> and peripheral<sup>32</sup> neural tissues. We found that the maximum possible soluble dose of GA suitable for osmotic pump delivery was 1 mg/kg/day. Animals from treated and control groups were euthanized via carbon dioxide asphyxiation at 14-, 21-, or 42-days post-fracture.

### Bilateral fibular fractures and pump insertion

Bilateral fibular fractures were conducted using previously described standard protocols<sup>33,34</sup>. In brief, under isoflurane anaesthesia, a 5 mm skin incision was made over the fibula. Using microtenotomy scissors, mice received a bilateral transverse and non-comminuted fibular fracture at the midpoint of the fibula approximately 12 mm proximal to the calcaneal tuberosity. Skin incisions were closed using skin glue (3M™ Vetbond™ Tissue Adhesive, St. Paul, MN, USA). Immediately post-fracture, a 10 mm incision was made on the dorsal surface of mice in between the scapulae. Mini-osmotic pumps (ALZET® Model 1002, DURECT Corporation, CA, USA) were then subcutaneously inserted and incisions were closed using Reflex wound clips.

### Micro-computed tomography ( $\mu$ CT)

Fractured fibulae (8-11/group) were immersed in fixative (4% paraformaldehyde in 0.1 M sodium cacodylate buffer) for 48 h and then stored in 10% sucrose in 0.1 M sodium cacodylate buffer at 4°C until use. Scanning of fibulae was performed using SKYSCAN 1076 *in vivo* X-ray micro-computed tomography (Bruker-microCT) in 70% ethanol with acquisition parameters of 9  $\mu$ m voxel resolution, 0.5 mm aluminium filter, 48 kV voltage, 100  $\mu$ A current, 2,400 ms exposure, rotation 0.5° across 180°, frame averaging of 1. Images were reconstructed using NRecon (V1.6.3.1) with the following parameters: smoothing factor, 1; ring artefacts, 6; beam-hardening correction; 35%; pixel defect mask, 5%; C.S rotation, 0; and misalignment compensation, <3. Images were realigned and orientated using Dataviewer (V1.4.4) to obtain transaxial datasets for calluses. Analysis of the transaxial datasets was performed using CTAn (V1.11.8.0) and the region of interest (ROI) was identified as a 2 mm longitudinal region of callus (i.e. 1 mm proximal and distal to the fracture line of the callus); the border of the callus was manually traced. Thresholds used for parameter quantification were determined using



the automatic “otsu” algorithm within CTAn and visual examination of unreconstructed x-ray images. A grayscale adaptive threshold of 42-255 was used for structural analysis of calluses 14-, 21- and 42-day post-fracture. 2D and 3D data, and 3D models were generated, and the following parameters were used for structural analysis of callus: total callus volume (TV); new mineralized tissue (BV), bone fractional volume (BV/TV) and bone surface (BS).

#### *Biomechanical assessment of fracture calluses*

A three-point mechanical bending test was used to assess the effects of GA on the mechanical properties of 42-day calluses as described previously<sup>34</sup>. Briefly, whole fibulae with intact callus (18-20 fibulae/group) that were dissected at autopsy were stored in silicone oil at -20°C. On the day of assessment, samples were equilibrated to room temperature for 1 h. Each fibula was mounted onto the three-point bending apparatus with the callus lying centrally under the fulcrum; this ensured peak stress was applied directly in an anterior-posterior direction to the centre of each callus. A 10 N force transducer descended at a constant rate of 1.67 mm/sec and loaded each callus. Load and deflection data were recorded continuously, which plotted an x-y (load-displacement) graph. Biomechanically disrupted fracture callus ends were imprinted onto dental wax and magnified images were taken of each imprint using Leica DFC420 light microscope (Leica Microsystems Ltd., Heerbrugg, Switzerland) connected to Leica IM50 imaging software (Leica). Cross-sectional areas were obtained for each callus by averaging the total area values traced with software Leica Qwin V3 Standard (Leica). Differences in peak force to failure, load per unit area, stiffness and stiffness per unit area were calculated from the deflection data.

#### *Histology*

$\mu$ CT scanned calluses were processed in LR White Resin Hard Grade Acrylic (London Resin Company, Reading, UK). Sections of un-decalcified calluses, 5  $\mu$ m thick, were made longitudinally at the mid-point of the callus using a Leica RM 2155 Rotary Microtome (Leica Microsystems, Nussloch, Germany). Sections (4 per callus, 4-7 calluses/group) were histochemically stained to detect tartrate-resistant acid phosphatase (TRAP; a universal cytochemical marker for osteoclasts). Sections of callus were viewed and photographed under a Leica DFC420 light microscope (Leica). To identify whether GA treatment influenced bone resorption during fracture healing, the percentage of TRAP was measured as the total area of callus stained positive for TRAP activity divided by total callus area using Leica Qwin software (Leica) as previously described<sup>35</sup>.

#### *Cell culture*

Kusa O cells were derived from multi-potential bone marrow stromal cells<sup>36</sup> and have previously been

characterised as cells with osteogenic potential suitable for investigations on osteoblastic differentiation<sup>37</sup>. Cells were cultured in  $\alpha$ -MEM (Gibco® Life Technologies™, Auckland, NZ), supplemented with 10% Australian Premium Foetal Bovine Serum (FBS) (Australian Ethical Biologicals Pty. Ltd., Coburg, AU), and used between passages 11-19. All cultures were maintained in an incubator at 37°C in 5% CO<sub>2</sub> and 95% O<sub>2</sub>. For proliferation studies, cells were subcultured at a density of 3000 cells/ml in  $\alpha$ -MEM supplemented with 10% FBS ( $\alpha$ -MEM+10% FBS) for 3 h, after which medium was aspirated and replaced with  $\alpha$ -MEM+2% FBS. Cells were treated with various concentrations of GA (0.05nM, 0.1nM, 0.5nM, 1nM, 5nM, 10nM, 50nM, 100nM, 500nM, 1 $\mu$ M, 5 $\mu$ M, 10 $\mu$ M) for 72 h, negative control was  $\alpha$ -MEM only and positive controls was  $\alpha$ -MEM+10% FBS,  $\alpha$ -MEM + 100 ng/ml IGF (Life Technologies™, Scoresby, AU). Cell proliferation (n=4/group) was measured using CellTiter 96® AQ<sub>ueous</sub> One Solution Cell Proliferation Assay kit (Promega Corporation, Madison, USA) as per manufacturer's instructions with absorbance read at 490 nm. Data was normalized to controls. For studies that required Kusa O cell differentiation, including Western blotting, RT-PCR and mineralization studies, cells were subcultured at a density of 3000 cells/ml in  $\alpha$ -MEM + 10% FBS for 3 days, after which medium was aspirated and replaced with osteoblastic differentiation medium, which contained  $\alpha$ -MEM+10% FBS supplemented with 50  $\mu$ g/ml ascorbate and 10mM  $\beta$ -glycerophosphate<sup>37,38</sup>. Medium was replenished three days a week.

#### *Western blotting*

Lysate was isolated from undifferentiated Kusa O cells and 14 days differentiated (ascorbate/glycerophosphate exposed) Kusa O cells to analyse TrkA expression (n=6/group). Mouse brain lysates (n=2) were used as a positive control for TrkA. Briefly, cells were washed three times in PBS and then lysed in RIPA-EDTA buffer (150mM NaCl, 1% Triton X, 0.5% sodium deoxycholate, 0.1% SDS, 50mM Tris, 0.5mM EDTA) with added protease and phosphatase cocktail inhibitors. Protein sample concentration was determined using Pierce™ BCA™ Protein Assay Kit (Pierce Biotechnology, Rockford, USA), supernatant protein concentration was mixed [1:1 (v/v) ratio] with Laemmli x2 loading buffer. Samples were boiled for 5 min, centrifuged, and then stored at -20°C. Protein (10  $\mu$ g) was loaded into each well and protein was separated using Precast Mini-PROTEAN® TGX™ gel (Bio-Rad Laboratories Inc., Hercules, USA). Protein bands were transferred onto polyvinylidene difluoride (PVDF) membranes. The membrane was probed with anti-TrkA (1:1000, Abcam, Waterloo, NSW). Signal detection was developed with chemiluminescence (Immuno-Star™ HRP kit, Bio-Rad Laboratories Inc., Hercules, USA). Immunoreactive bands were digitally imaged using Molecular Imager® Chemidoc™ XRS+ (Bio-Rad) and results were quantified using Image Lab™ Software (Bio-Rad). Values were normalised for protein loading using  $\alpha$ -tubulin as a loading control.

### Real-time Polymerase Chain Reaction (RT-PCR)

Kusa O cells were daily cultured in osteoblastic differentiation media and treated with 0.5nM of GA or vehicle for 3, 7, and 14 days (n=5-8/group). Total RNA was prepared using PureZOL™ (Bio-Rad Laboratories Inc., Hercules, USA). RT-PCR was performed as described previously<sup>39,40</sup>. Briefly, reverse transcription was performed from 1 µg of total RNA using iScript™ cDNA Synthesis Kit (Bio-Rad). β-actin was used as an internal control gene. PCR was performed in triplicate using SsoFast™ EvaGreen® Supermix (Bio-Rad) and specific oligonucleotide primers (Table 1) on an iQ 96-well PCR system (Bio-Rad). Each amplification reaction contained 1 µl of cDNA and 300nM of primer. Thermal cycling conditions included initial denaturation at 95°C for 30 s, followed by 40 cycles of 95°C for 5 s and 55°C for 5 s. Melt curve analysis was performed post-cycling to confirm specificity of the amplified products. Relative quantification of genes of interest mRNA expression was determined using the 2<sup>-ΔΔCt</sup> method.

### Mineralization analysis

Kusa O cells were cultured in osteoblastic differentiating medium and treated with 0.5nM of GA or vehicle daily (n= 4/group) for 21 days<sup>37,41</sup>. For mineralization area analysis, Kusa O cells were washed three times in PBS, fixed in ice cold 70% ETOH for 30 min, and then stained with 0.5% Alizarin Red stain (pH 4.2) for 30 min. Cells were then washed five times in PBS and scanned images were taken. Mineralized areas were quantified using ImageJ software (National Institutes of Health, Bethesda, USA).

### Statistical analysis

All outcomes were analysed using GraphPad Prism 6 software (GraphPad Software, Inc., La Jolla, USA). All data was subject to Shapiro-Wilk normality tests. All animal data outcomes and *in vitro* mineralization analysis were analysed with Mann-Whitney U tests. *In vitro* proliferation assays were analysed using regular one-way ANOVA. RT-PCR was analysed with a two-way ANOVA. Bonferroni *post-hoc* comparisons were carried out when appropriate. In all analyses, statistical significance was defined as  $p < 0.05$ .

## Results

There were no apparent behavioural changes, side effects, or changes in the weight gain pattern of GA treatment in mice.

### µCT

Representative µCT reconstructions of longitudinal mid-point hemi-calluses are shown in Figure 1(a-f). Bony union was reached in all calluses by 21 days in both the GA-treated and control groups. For all µCT parameters, no effects of GA were found at either 14- or 42-days post-fracture. In contrast, analyses revealed that calluses from 21-day GA-treated mice

**Table 1.** Oligonucleotide name and sequence (5'-3') used in Real-Time PCR.

Oligonucleotide name	Sequence (5'-3')
mBeta actin	Sense - GCTGTGCTATGTTGCTCTAG
	Anti-sense - CGCTGCTTGCCAATAGTG
mOsterix	Sense - TATGCTCCGACCTCCTCAAC
	Anti-sense - AATAAGATTGGGAAGCAGA AAG
mRunx2	Sense - AGCAACAGCAACAACAGCAG
	Anti-sense - GTAATCTGACTCTGTCTTG
mAlkaline phosphatase	Sense - AAACCCAGACACAAGCATTCC
	Anti-sense - TCCACCAGCAAGAAGAAGCC
mOsteocalcin	Sense - TCTCTGACCTCACAGATCCC
	Anti-sense - TACCTTATTGCCCTCTGCTTG
mDMP-1	Sense - CGCCGATAAGGAGGATGATG
	Anti-sense - GTGTGGTGTCTGTGGAGTC
mRANKL	Sense - ATCAGAAGACAGCACTCACT
	Anti-sense - ATCTAGGACATCCATGCTAATGT
mOsteoprotegrin	Sense - TGACCACTCTTATACGGACAG
	Anti-sense - GCCCTTCTCACACTCAC

(Figure 1g-j) had significantly reduced tissue volume (Figure 1g;  $p < 0.05$ ) which suggested a smaller callus. The measured bone surface in calluses (Figure 1j;  $p < 0.05$ ) was also lower compared to 21-day vehicle-treated mice, which suggested more consolidated bone was present in these calluses. Consistent with these observations, at 21 days post-fracture, calluses from GA-treated mice also showed increased BV/TV, i.e. bone volume fraction corrected for tissue volume (Figure 1i;  $p < 0.05$ ) compared to vehicle-treated mice.

### Biomechanical analyses

A three-point bending test was used to assess the biomechanical properties of 42-day fibular calluses. The average cross-sectional area of the fracture callus at its breaking point was significantly smaller in samples from GA-treated mice (36%, Table 2,  $p < 0.001$ ) compared to vehicle-treated mice. Calluses from GA-treated mice showed and increased load per unit area (52%) and stiffness per unit area (53%) (Table 2,  $p < 0.01$ ) compared to vehicle-treated mice. However, the peak force to failure and stiffness of calluses were not significantly different between vehicle-treated and GA-treated mice.

### Histological assessment

A TRAP histochemical stain was used to assess osteoclastic density on the bone surface in calluses at 14, and 21 days post-fracture. Quantitative assessment revealed less dense TRAP histochemical staining; this was calculated as the proportion of TRAP staining/total callus surface area, in 21-day calluses compared to 14-day calluses ( $p < 0.01$ ). No

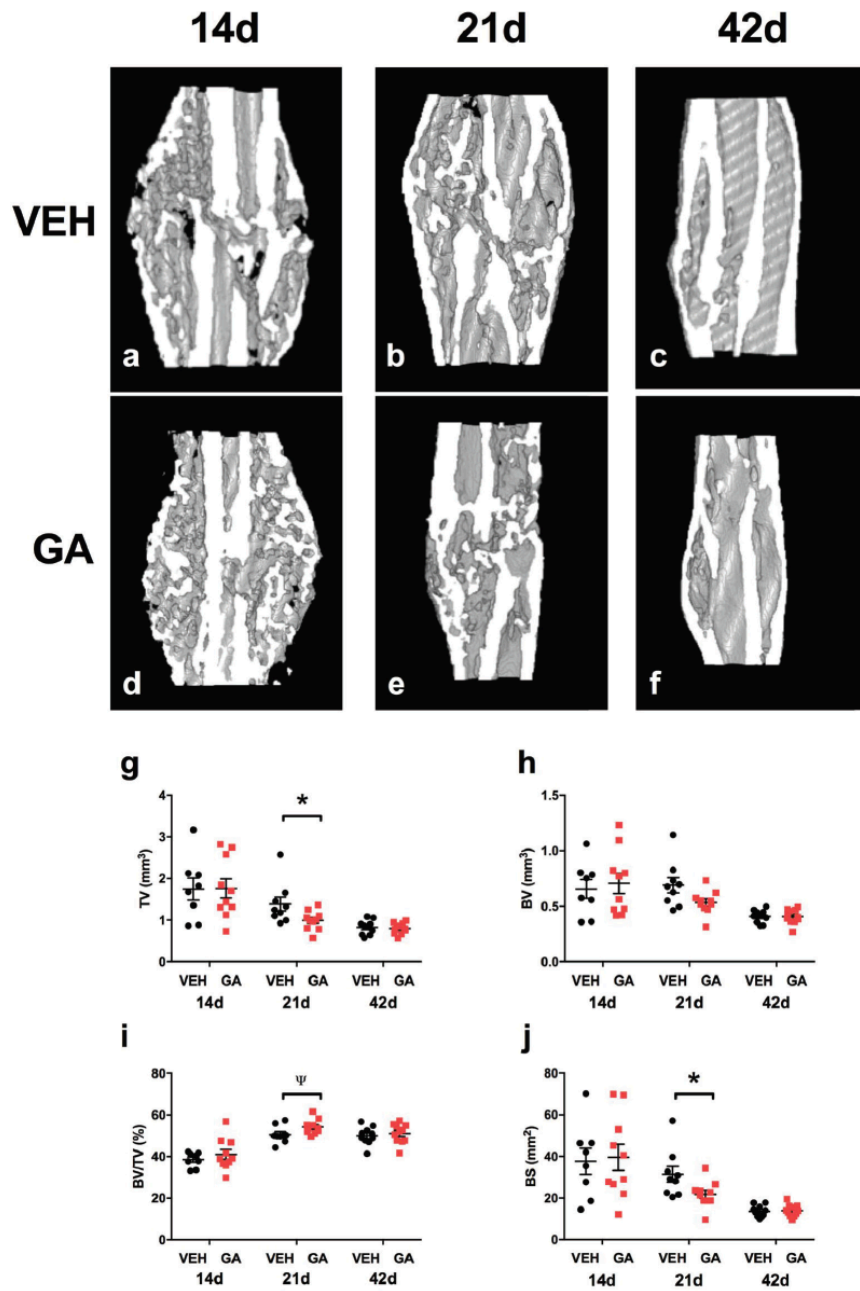


**Figure 1.** The effects of GA treatment on callus structural parameters using  $\mu$ CT. Longitudinal mid-point images representative of  $\mu$ CT reconstructions of hemi-calluses (a-f).  $\mu$ CT analysis found that GA-treated decreased callus tissue volume (g; TV) and bone surface area (j; BS) at 21 days post-fracture ( $*p < 0.05$ ) compared to vehicle-treated mice. There was a trend that GA increased bone fractional volume of calluses (i;  $\Psi p = 0.05$ ) compared to vehicle-treated mice. No differences were seen at 14-, and 42-days post-fracture between GA-treated and vehicle-treated mice. Bars are mean  $\pm$  SEM,  $n = 8-11$ /group.

**Table 2.** Mechanical properties of control and GA-treated calluses at 42 days post-fracture.

Treatment	Peak Force (N)	Stiffness (x 10 <sup>4</sup> Nm <sup>2</sup> )	CSA (x 10 <sup>-7</sup> m <sup>2</sup> )	LPA (x 10 <sup>7</sup> Nm <sup>-2</sup> )	SPA (x 10 <sup>9</sup> Nm <sup>-2</sup> )
Vehicle (n = 20) Mean ± SEM	3.92 ± 0.20	5.41 ± 0.30	5.22 ± 0.30	1.45 ± 0.13	4.15 ± 0.63
GA (n = 17) Mean ± SEM	3.76 ± 0.28	5.09 ± 0.38	3.59 ± 0.28	2.72 ± 0.43	8.63 ± 1.53
p-value	0.39	0.38	< 0.001	< 0.01	< 0.01

CSA, cross sectional area; LPA, load per unit area; SPA, stiffness per unit area. Values are means ± SEM.

differences in the percentage of TRAP staining in calluses were found between GA-treated and vehicle-treated mice, both at 14- and 21-days post-fracture (Results not shown).

#### Cell culture

Western blot analysis of high-affinity receptor, TrkA, was assessed in undifferentiated Kusa O cells and 14 day differentiated Kusa O cells. TrkA receptor protein expression was absent in undifferentiated Kusa O cells, however, TrkA expression was detected in 14 day differentiated Kusa O cells (Figure 2a). Proliferation assays were used to assess GA influence on Kusa O cell proliferation. At 72 h following treatment, Kusa O cell proliferation was not affected in response to daily GA-treatment ranging from 0 to 100nM. However, daily GA-treatment ranging from 500nM to 10µM significantly reduced Kusa O cell proliferation (Figure 2b,  $p < 0.001$ ) suggesting toxic effects at these doses.

#### RT-PCR

A pilot study on the effect of GA treatments on Kusa O differentiation *in vitro* revealed that a daily GA dose of 0.5nM appeared to increase expression of osteoblast-associated genes to a greater extent than for GA doses ranging from 1-10nM (data not shown). As such, a dose 0.5nM of GA was chosen for all further *in vitro* studies.

Kusa O cells differentiated and treated daily with 0.5nM of GA for 3, 7, and 14 days were analysed for expression of genes associated with early osteoblasts (osterix and runx2; data not shown), mature osteoblasts (ALP and osteocalcin; Figure 2c,d), osteocytes (DMP-1; Figure 2e) and osteoclastogenesis (OPG and RANKL; Figure 2f,g). Significant main effects of time and treatment, as well as an interaction were present for Kusa O expression of ALP, osteocalcin and DMP. Post-hoc analysis revealed that daily GA treatment increased the expression of ALP (Figure 2c;  $p < 0.01$ ), osteocalcin (Figure 2d;  $p < 0.01$ ) and DMP-1 (Figure 2e;  $p < 0.0001$ ) in 14-day, but not 3- and 7-day differentiated Kusa O cells compared to vehicle-treated Kusa O cells. Daily GA treatment did not influence expression of either osterix or runx2 (Data not shown). Gene expression of markers associated with osteoclastogenesis, OPG and RANKL, in Kusa O cells did not alter at 3, 7, and 14 days of differentiating or in response to daily GA treatment (Figure 2f,g).

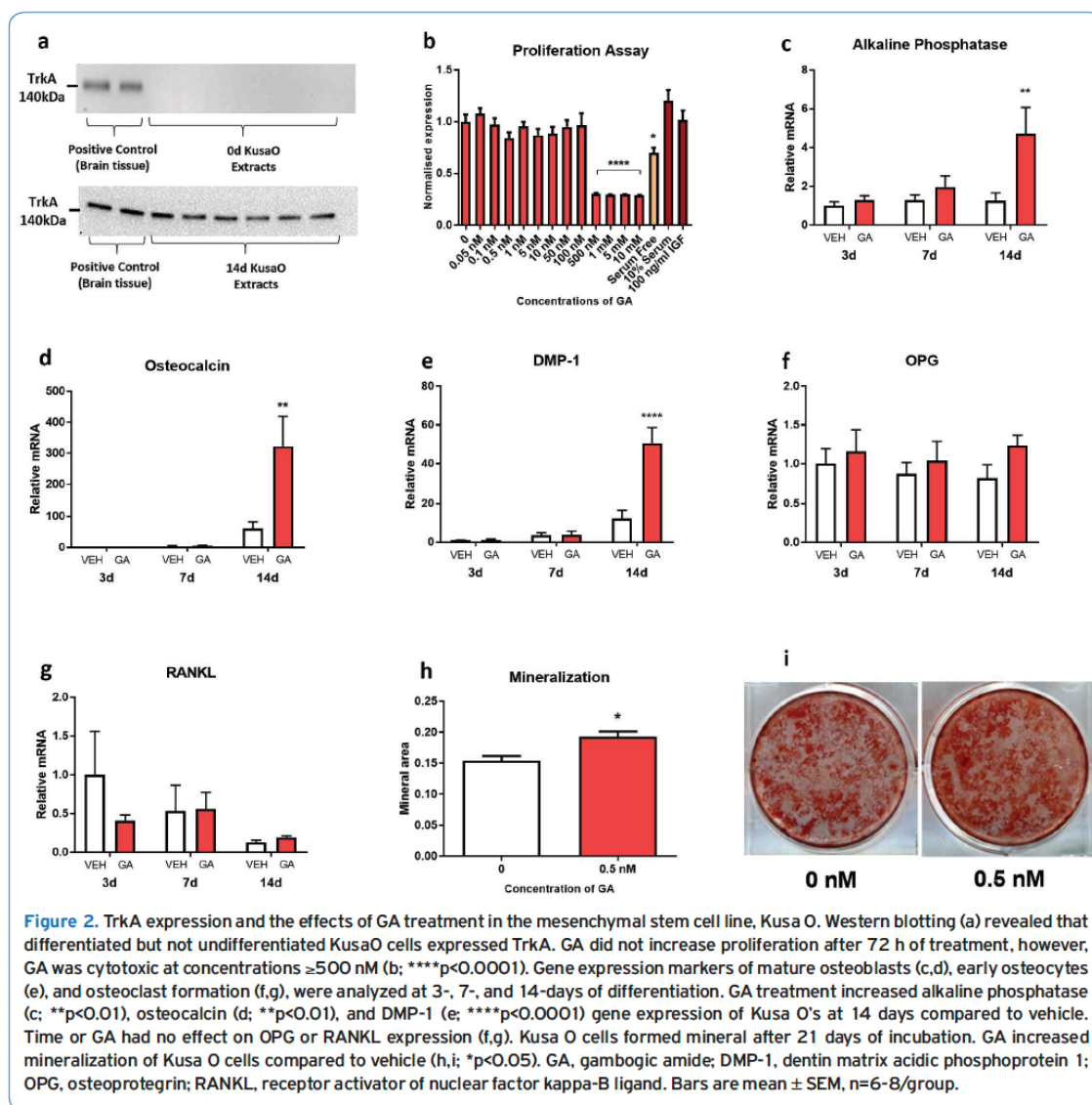
#### Mineralization in vitro

Kusa O cells formed mineralised matrix during 21 days of incubation with ascorbate and  $\beta$ -glycerophosphate. Daily treatment of 0.5nM of GA increased mineralization area in Kusa O cells compared to control cultures (Figure 2h,i;  $p < 0.05$ ). There was no mineralisation evident in negative control cultures that employed undifferentiated Kusa O cells.

#### Discussion

In this study, we analysed the influence of GA, a small molecule TrkA receptor agonist during fracture healing of murine fibulae and found strong evidence that suggests GA acts in a similar manner to previously reported actions of NGF on fracture healing. GA treatment resulted in fracture calluses that were smaller in size and mechanically stronger per unit area. We showed that systemic treatment with 1 mg/kg/day GA delivered for 14 days to mice with fibular fractures decreased tissue volume of callus at 21 days post-fracture and increased the mechanical properties; load per unit area and stiffness per unit area of fractures at 42 days. Additionally, GA increased mRNA expression of markers associated with osteoblastic and osteocytic differentiation. Consistent with a direct action of GA on osteoblasts, we also found that osteoblastic differentiation and *in vitro* mineralisation was increased in osteoprogenitor Kusa O cells. Our data therefore suggests that GA, like NGF, may promote fracture healing through promoting both osteoprogenitor differentiation and mineralisation.

$\mu$ CT analysis was used to determine the influence of GA on bone content of calluses at various stages during fracture healing. Of the three time-points analysed; 14, 21, and 42 days after fracture, we found significant differences in callus architecture only in the 21-day group. At 21 days post-fracture, while there was no change in the amount of bone volume, calluses of GA-treated mice had overall reduced tissue volume and elevated bone fractional volume in comparison to mice treated with vehicle, which suggests that GA treatment influenced bone remodelling of healing fractures. This finding is similar to that previously reported with NGF treatment in rats with rib fractures; where after 14 days with NGF treatment, fractured bone had smaller calluses at 21 days post-fracture<sup>15</sup>, with enhanced bony content within



calluses compared to vehicle-treated fractures. It is unclear whether this smaller callus trait reflected a change in cartilage formation or endochondral bone formation, however it would be consistent with a more rapid maturation of the fracture site. Several other studies involving distraction osteogenesis have also reported that NGF treatment enhanced both bone formation and callus development during the consolidation phase (28 days) of healing compared to vehicle-treated calluses<sup>16,18,19</sup>. One possible mechanism by which GA, like NGF, resulted in smaller calluses is likely through the stimulation of

nerve growth in and around the fracture site. The periosteum of bone is densely lined with TrkA positive nerve fibres<sup>42</sup>. NGF treatment increased nerve growth and activity in healing rat rib calluses by upregulating catecholamine synthesis<sup>15</sup>, which has been directly linked to stimulate both blood vessel and sensory nerve sprouting through TrkA signalling in developing endochondral bone<sup>43</sup>. Innervation of bone is important for angiogenesis and bone formation, which are two factors that mediate both ossification<sup>43</sup> and fracture healing rate<sup>44</sup>. It has been documented that both sensory

and sympathetic nerves within callus contribute positively in regard to fracture callus remodelling<sup>9</sup>, with numerous studies reporting that removal of sensory and sympathetic neural input results in the formation of larger, disorganised fracture calluses<sup>6-8</sup>. GA, similarly to NGF, may have indirectly facilitated fracture healing by stimulating sensory and sympathetic nerve growth within the callus via TrkA, which in turn may have assisted in co-ordinating vascularisation and ossification of fractured bone to produce smaller calluses by 21 days.

Whilst our  $\mu$ CT data showed no differences in either tissue or bone volume of calluses by 42 days post-fracture, fracture sites from mice treated with GA had increased stiffness per unit area and load per unit area compared to vehicle-treated mice. These outcomes are identical to a previous study in our lab where NGF treatment to healing rat rib fractures improved these mechanical properties of calluses at 42 days post-fracture<sup>15</sup>. Nonetheless, it is important to note that GA treatment in the current study, as well as NGF treatment in the previous study<sup>15</sup>, did not alter the mechanical properties of peak force to failure and stiffness. Mechanical strength of healing fractures is highly dependent on callus structure and degree of mineralization<sup>45</sup>, and whilst there may not be an overall difference in the amount of bone present, there may be a difference in the quality of bone present in the callus. Our findings may indicate that there may have been a higher portion of mature, mechanically stronger lamellar bone than immature woven bone in the calluses of the GA-treated mice compared to vehicle-treated mice at 42 days, however, we were unable to distinguish the two types of bone in our  $\mu$ CT analysis. We postulate that this may explain why there was no difference in the amount of bone in calluses between treatments at 42 days via  $\mu$ CT analysis, despite the fact that biomechanically, the calluses of the GA-treated group were stronger per unit area compared to controls. Furthermore,  $\mu$ CT findings indicated that when compared to 21 days post-fracture, calluses at 42 days were at a substantially more advanced stage of healing in both vehicle and GA-treated groups; as such, it is possible that mechanical testing at an earlier time-point of healing (i.e. when healing was less advanced and the structural effects of GA treatment were apparent) may have yielded different findings.

Given the aforementioned findings of reduced callus size and enhanced mechanical properties, it was apparent that GA treatment caused changes to callus remodelling. TRAP staining was used to assess whether GA treatment influenced osteoclastic cell density during fracture healing, but we observed no differences in this parameter. This suggests that GA may have not influenced remodelling through bone resorption and is consistent with our *in vitro* data that showed that GA does not affect gene expression of osteoblastic OPG or RANKL, factors which together regulate osteoclastic formation and activity. Our results are supported by a recent study that reported TRAP staining density and osteoclastic number was not affected during endochondral ossification of TrkA-variant mouse pups, whereas bone formation was severely impacted, which was presumably due to the

lack of NGF-TrkA signalling<sup>43</sup>. Additionally, other studies using immunofluorescence analysis did not find TrkA on osteoclasts, nor was this receptor found on osteoclastic precursors in callus tissue during fracture healing<sup>20,21</sup>. Therefore, it appears from our data that GA may not influence remodelling of calluses via osteoclastic activity and is more likely to affect bone mass in callus through promotion of osteoblastic differentiation and bone mineralisation.

To determine whether GA exerted an effect on osteoblasts and mineralisation, we utilised Kusa O cells, a murine, multi-potential bone marrow stromal cell line<sup>36</sup>. Undifferentiated Kusa O cells (day 0) do not contain mature osteoblasts and display a phenotype that is osteoprogenitor-like<sup>37,41</sup>. However, by 14 days of differentiation, Kusa O cells contain many mature osteoblasts<sup>37,41</sup>. Through Western blotting analysis we found that the osteoblast-like Kusa O cells expressed TrkA receptors, but the undifferentiated Kusa O cells did not, which suggests that TrkA activation is more likely to occur in osteoblasts rather than osteoprogenitors in bone. This data is supported by previous reports using *in vivo* rodent models, which localised TrkA receptors in mature osteoblasts and not pre-osteoblasts during fracture healing<sup>20-22</sup> and suggests that TrkA signalling may be conducted via mature osteoblastic populations in bone. NGF does not influence proliferation of the murine osteoblastic precursor cell line, MC3T3-E1<sup>23</sup>, which is consistent with our Kusa O data. Additionally, in Kusa O cells we found that GA did not influence gene expression of markers associated with early osteoblasts maturation, i.e., osterix and runx2, however, GA did increase the gene expression of markers of mature osteoblasts, namely ALP and osteocalcin, as well as the osteocytic marker, DMP-1, as well as matrix mineralisation<sup>46,47</sup>. Again, this is consistent with earlier studies of NGF treatment in MC3T3-E1 cells which increased ALP levels *in vitro*<sup>23</sup>. Furthermore, both NGF and TrkA receptor have been localised in osteoblasts during bone healing<sup>20-22</sup> and NGF has been shown to be important during bone formation by directly stimulating osteoblasts to synthesize bone<sup>17,23,43</sup>.

Our findings provide evidence that GA treatment stimulated osteoblastic differentiation and mineralisation *in vitro* and improved fracture callus strength *in vivo*. The improvement in callus strength may have been, in part, due to the direct action of GA on osteoblasts, however, the possible direct action of GA on stimulating local nerves around the callus, cannot be dismissed, and this may have also contributed to improving fracture healing.

This study had some limitations. Firstly, although our findings indicate that GA had mild, positive effects on fracture healing. Due to solubility issues with osmotic pump delivery, our study was limited to use of a dosing regimen of 1 mg/kg/day. It is possible that higher doses of GA may have a more profound effect on fracture healing. Previous studies have utilised doses up to 4 mg/kg/day of GA using intraperitoneal injection<sup>29</sup>, however osmotic pump delivery was chosen to ensure constant systemic delivery of GA. In addition, our *in vitro* findings indicate that GA may increase osteoblastic differentiation and mineralization, however quantification of

other osteoblast-associated markers and additional time-points of mineralization analysis in future studies are likely to provide further insights.

## Conclusions

Our study showed that systemic administration of GA at 1 mg/kg/day for 14 days via mini-osmotic pumps in mice that were given fibular fractures had mild positive effects on fracture healing. GA treatment resulted in smaller fracture calluses with some enhancement of mechanical properties, without any detrimental side effects to the animals. Additionally, *in vitro* analysis implied that GA may act directly on osteoblasts to stimulate mineralisation. These results complement previous research and the concept that neurotrophin signalling can influence skeletal maintenance and healing.

## Acknowledgements

*This project was funded through the Department of Physiology, Anatomy and Microbiology at La Trobe University. No benefits in any form have been received or will be received from a commercial party related directly or indirectly to the content of this article. We would like to acknowledge laboratory technician Karen Griggs for her assistance throughout these experiments.*

## References

- Hak DJ, Fitzpatrick D, Bishop JA, Marsh JL, Tilp S, Schnettler R, et al. Delayed union and nonunions: epidemiology, clinical issues, and financial aspects. *Injury* 2014;45(Suppl.2):S3-7.
- Gomez-Barrena E, Rosset P, Lozano D, Stanovici J, Ernthaller C, and Gerbhard F. Bone fracture healing: cell therapy in delayed unions and nonunions. *Bone* 2015;70:93-101.
- Mills LA, Simpson AH. The relative incidence of fracture non-union in the Scottish population (5.17 million): a 5-year epidemiological study. *BMJ Open* 2013;3(2).
- Zura R, Xiong Z, Einhorn T, Watson JT, Ostrum RF, Prayson MJ, et al. Epidemiology of Fracture Nonunion in 18 Human Bones. *JAMA Surg* 2016;151(11):e162775.
- Brinker MR, O'Connor DP. The Biological Basis for Nonunions. *JBJS Rev* 2016;4(6).
- Madsen JE, Hukkanen M, Aune AK, Basran I, Moller JF, Polak JM, et al. Fracture healing and callus innervation after peripheral nerve resection in rats. *Clin Orthop Relat Res* 1998;(351):230-40.
- Hukkanen M, Konttinen YT, Santavirta S, Nordsletten L, Madsen JE, Almaas R, et al. Effect of sciatic nerve section on neural ingrowth into the rat tibial fracture callus. *Clin Orthop Relat Res* 1995;(311):247-57.
- Nordsletten L, Madsen JE, Almaas R, Rootwelt T, Halse J, Konttinen YT, et al. The neuronal regulation of fracture healing. Effects of sciatic nerve resection in rat tibia. *Acta Orthop Scand* 1994;65(3):299-304.
- Hukkanen M, Konttinen YT, Santavirta S, Paavolainen P, Gu XH, Terenghi G, et al. Rapid proliferation of calcitonin gene-related peptide-immunoreactive nerves during healing of rat tibial fracture suggests neural involvement in bone growth and remodelling. *Neuroscience* 1993; 54(4):969-79.
- Li J, Ahmad T, Spetea M, Ahmed M, Kreicbergs A. Bone reinnervation after fracture: a study in the rat. *J Bone Miner Res* 2001;16(8):1505-10.
- Li J, Kreicbergs A, Bergstrom J, Stark A, Ahmed M. Site-specific CGRP innervation coincides with bone formation during fracture healing and modeling: A study in rat angulated tibia. *J Orthop Res* 2007;25(9):1204-12.
- Levi-Montalcini R, Angeletti PU. Nerve growth factor. *Physiol Rev* 1968;48(3):534-69.
- Micera A, Lambiase A, Stampachiacchiere B, Bonini S, Levi-Schaffer F. Nerve growth factor and tissue repair remodeling: trkA(NGFR) and p75(NTR), two receptors one fate. *Cytokine Growth Factor Rev* 2007;18(3-4):245-56.
- Reichardt LF. Neurotrophin-regulated signalling pathways. *Philos Trans R Soc Lond B Biol Sci* 2006; 361(1473):1545-64.
- Grills BL, Schuijers JA, Ward AR. Topical application of nerve growth factor improves fracture healing in rats. *J Orthop Res* 1997;15(2):235-42.
- Cao J, Wang L, Lei DL, Liu YP, Du ZJ, Cui FZ. Local injection of nerve growth factor via a hydrogel enhances bone formation during mandibular distraction osteogenesis. *Oral Surg Oral Med Oral Pathol Oral Radiol* 2012;113(1):48-53.
- Wang L, Cao J, Lei DL, Cheng XB, Zhou HZ, Hou R, et al. Application of nerve growth factor by gel increases formation of bone in mandibular distraction osteogenesis in rabbits. *Br J Oral Maxillofac Surg* 2010;48(7):515-9.
- Wang L, Zhou S, Liu B, Lei D, Zhao Y, Lu C, et al. Locally applied nerve growth factor enhances bone consolidation in a rabbit model of mandibular distraction osteogenesis. *J Orthop Res* 2006;24(12):2238-45.
- Letic-Gavrilovic A, Piattelli A, Abe K. Nerve growth factor beta(NGF beta) delivery via a collagen/hydroxyapatite (Col/HAp) composite and its effects on new bone ingrowth. *J Mater Sci Mater Med* 2003;14(2):95-102.
- Asaumi K, Nakanishi T, Asahara H, Inoue H, Takigawa M. Expression of neurotrophins and their receptors (TRK) during fracture healing. *Bone* 2000;26(6):625-33.
- Grills BL, Schuijers JA. Immunohistochemical localization of nerve growth factor in fractured and unfractured rat bone. *Acta Orthop Scand* 1998;69(4):415-9.
- Aiga A, Asaumi K, Lee YJ, Kadota H, Mitani S, Ozaki T, et al. Expression of neurotrophins and their receptors tropomyosin-related kinases (Trk) under tension-stress during distraction osteogenesis. *Acta Med Okayama* 2006;60(5):267-77.
- Yada M, Yamaguchi K, Tsuji T. NGF stimulates differentiation of osteoblastic MC3T3-E1 cells. *Biochem Biophys Res Commun* 1994;205(2):1187-93.
- Friden PM, Walus LR, Watson P, Doctrow SR, Kozarich

- JW, Backman C, et al. Blood-brain barrier penetration and *in vivo* activity of an NGF conjugate. *Science* 1993;259(5093):373-7.
25. Tria MA, Fusco M, Vantini G, Mariot R. Pharmacokinetics of nerve growth factor (NGF) following different routes of administration to adult rats. *Exp Neurol* 1994; 127(2):178-83.
  26. Angeletti RH, Aneletti PU, Levi-Montalcini R. Selective accumulation of (125 I) labelled nerve growth factor in sympathetic ganglia. *Brain Res* 1972;46:421-5.
  27. Jang SW, Okada M, Sayeed I, Xiao G, Stein D, Jin P, et al. Gambogic amide, a selective agonist for TrkA receptor that possesses robust neurotrophic activity, prevents neuronal cell death. *Proc Natl Acad Sci U S A* 2007; 104(41):16329-34.
  28. Chan CB, Liu X, Jang SW, Hsu SI, Williams I, Kang S, et al. NGF inhibits human leukemia proliferation by downregulating cyclin A1 expression through promoting acinus/CtBP2 association. *Oncogene* 2009; 28(43):3825-36.
  29. Shen JY, Yu QS, Gambogic amide selectively upregulates TrkA expression and triggers its activation. *Pharmacological Reports* 2015;67(2):217-223.
  30. Shah AG, Friedman MJ, Huang S, Roberts M, Li XJ, Li S. Transcriptional dysregulation of TrkA associates with neurodegeneration in spinocerebellar ataxia type 17. *Hum Mol Genet* 2009;18(21): 4141-52.
  31. Chan CB, Liu X, Jang SW, Hsu SI, Williams I, Kang S, et al. NGF inhibits human leukemia proliferation by downregulating cyclin A1 expression through promoting acinus/CtBP2 association. *Oncogene* 2009; 28(43):3825-3836.
  32. Ezkurdia N, Raurell I, Rodriguez S, Gonzalez A, Esteban R, Genesca J, et al. Inhibition of Neuronal Apoptosis and Axonal Regression Ameliorates Sympathetic Atrophy and Hemodynamic Alterations in Portal Hypertensive Rats. *Plos One* 2014;9(1).
  33. Kellum E, Starr H, Arounleut P, Immel D, Fulzele S, Wenger K, et al. Myostatin (GDF-8) deficiency increases fracture callus size, Sox-5 expression, and callus bone volume. *Bone* 2009;44(1):17-23.
  34. Brady RD, Grills BL, Schuijers JA, Ward AR, Tonkin BA, Walsh NC, et al. Thymosin beta4 administration enhances fracture healing in mice. *J Orthop Res* 2014; 32(10):1277-82.
  35. Brady RD, Grills BL, Church JE, Walsh NC, McDonald AC, Agoston DV, et al. Closed head experimental traumatic brain injury increases size and bone volume of callus in mice with concomitant tibial fracture. *Sci Rep* 2016;6:34491.
  36. Umezawa A, Maruyama T, Segawa K, Shadduck RK, Waheed A, Hata J, Multipotent marrow stromal cell line is able to induce hematopoiesis *in vivo*. *J Cell Physiol* 1992;151(1):197-205.
  37. Allan EH, Ho PW, Umezawa A, Hata J, Makishima F, Gillespie MT, et al. Differentiation potential of a mouse bone marrow stromal cell line. *J Cell Biochem* 2003;90(1):158-69.
  38. Allan EH, Hausler KD, Wei T, Gooi JH, Quinn JM, Crimeen-Irwin B, et al. EphrinB2 regulation by PTH and PTHrP revealed by molecular profiling in differentiating osteoblasts. *J Bone Miner Res* 2008;23(8):1170-81.
  39. Wright DK, Liu S, van der Poel C, McDonald SJ, Brady RD, Taylor L, et al. Traumatic Brain Injury Results in Cellular, Structural and Functional Changes Resembling Motor Neuron Disease. *Cereb Cortex* 2017;27(9):4503-4515.
  40. McDonald SJ, Dooley PC, McDonald AC, Schuijers JA, Ward AR et al. Transient expression of myofibroblast-like cells in rat rib fracture callus. *Acta Orthop* 2012; 83(1):93-8.
  41. Nakamura A, Ly C, Cipetic M, Sims NA, Vieusseux J, Kartsogiannis V, et al. Osteoclast inhibitory lectin (OCIL) inhibits osteoblast differentiation and function *in vitro*. *Bone* 2007;40(2):305-15.
  42. Castaneda-Corral G, Jimenez-Andrade JM, Bloom AP, Taylor RN, Mantyh WG, Kaczmarek MJ, et al. The majority of myelinated and unmyelinated sensory nerve fibers that innervate bone express the tropomyosin receptor kinase A. *Neuroscience* 2011;178:196-207.
  43. Tomlinson RE, Li Z, Zhang Q, Goh BC, Li Z, Thorek DL, et al. NGF-TrkA Signaling by Sensory Nerves Coordinates the Vascularization and Ossification of Developing Endochondral Bone. *Cell Rep* 2016;16(10):2723-35.
  44. Beamer B, Hettrich C, Lane J. Vascular endothelial growth factor: an essential component of angiogenesis and fracture healing. *HSS J* 2010; 6(1):85-94.
  45. Morgan EF, Mason ZD, Chien KB, Pfeiffer AJ, Barnes GL, Einhorn TA, et al. Micro-computed tomography assessment of fracture healing: relationships among callus structure, composition, and mechanical function. *Bone* 2009; 44(2):335-44.
  46. Zhou H, Choong P, McCarthy R, Chou ST, Martin TJ, Ng KW. *In situ* hybridization to show sequential expression of osteoblast gene markers during bone formation *in vivo*. *J Bone Miner Res* 1994;9(9):1489-99.
  47. Day TF, Guo X, Garrett-Beal L, Yang Y. Wnt/beta-catenin signaling in mesenchymal progenitors controls osteoblast and chondrocyte differentiation during vertebrate skeletogenesis. *Dev Cell* 2005;8(5):739-50.



## Appendix D

### Chapter 5

Publication: Johnstone M. R., Brady R. D., Church J. E., Orr D., McDonald S. J., Grills B. L. The TrkB agonist, 7,8-dihydroxyflavone, impairs fracture healing in mice. *Journal of Musculoskeletal and Neuronal Interactions*. Accepted for publication 9<sup>th</sup> November 2020.

- I performed 95% of the unilateral tibia fracture surgeries, with assistance from Dr Rhys Brady.
- I performed all the post-mortem tibial collections.
- I performed ~50% of the cell culture, with assistance from Dr Jarrod Church.
- I performed all the  $\mu$ CT analysis and RT-PCR analysis.
- I performed ~80% of biomechanical assessment, with assistance from Dr Stuart McDonald and Dr David Orr.
- I performed ~70% of the pQCT, with assistance from Dr Kristina Anevskaa.
- I performed post-mortem femoral collections, from corpses prepared by Dr Emily Jaehne and Samuel Hogart.
- I wrote the first full draft of the manuscript.
- Dr Brian Grills, Dr Stuart McDonald, Dr Rhys Brady and Dr Jarrod Church assisted with data analysis and provided revision of manuscript.

## Appendix E

### *Injectable microemulsion of 1 mg/ml 7, 8-dihydroxyflavone*

#### Components:

- a) 7, 8-dihydroxyflavone  
Abcam plc  
330 Cambridge Science Park  
Cambridge, CB4 0FL  
United Kingdom
- b) 30% (w/v) Kolliphor® HS 15  
Sigma-Alrich Pty. Ltd.  
12 Anella Avenue  
Castle Hill, NSW 2154  
Australia
- c) 0.01M sodium phosphate buffer (pH 7.4)  
Add 40.44 ml 0.2M disodium phosphate ( $\text{Na}_2\text{HPO}_4$ ) and 9.5 ml 0.2M monosodium phosphate ( $\text{NaH}_2\text{PO}_4$ ) to 50.06 ml distilled water to create 0.2M sodium phosphate buffer. Dilute to create 0.01M sodium phosphate buffer and pH to 7.4 using either sodium hydroxide (base) or phosphoric acid (acid).

#### Protocol (for 20 mg 7,8-dihydroxyflavone):

Weigh out 6 g of Kolliphor® HS 15 (it has a consistency like Vaseline, so warm it up in a 50 ml falcon tube to make it softer) and place it into a glass pestle and mortar.

Weigh out 20 mg of 7,8-dihydroxyflavone and place it on top on the Kolliphor® HS 15 in the mortar.

Using a pestle, mix well until all visible particles are dissolved.

Using a spatula transfer into falcon tube.

Gradually add 14 ml of 0.01M sodium phosphate buffer and vortex.

Once suspension is made, let it sit for 20 min to allow bubbles to disappear.

Load syringes and inject animals.

- Note: to create vehicle, use the same methods but exclude the 7,8-dihydroxyflavone.
- Note: Microemulsion can be frozen into aliquots at -20 degrees.